

Department of Biology
Unit of Biochemistry
University of Fribourg (Switzerland)

**Igo1 and Igo2:
Central controllers of nutrient–regulated gene expression in quiescent yeast cells**

THESIS

presented to the Faculty of Science of the University of Fribourg (Switzerland)
in consideration of the award of the academic grade of *Doctor rerum naturalium*

by

Xuan Luo

from

Changsha, China

Thesis No: 1757

UniPrint

2012

Accepted by the Faculty of Science of the University of Fribourg (Switzerland) upon the recommendation of Prof. Robbie Loewith and Prof. Andreas Conzelmann (President of the jury: Prof. Louis-Félix Bersier).

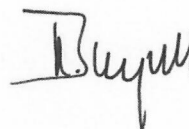
Fribourg, the 15th June 2012

Thesis supervisor



Prof. Claudio De Virgilio

Dean



Prof. Rolf Ingold

Table of Contents

Résumé	i
Summary	1
Chapter I. Introduction	3
I. 1 Characteristics of quiescence (G_0) program	3
I. 1. 1 Cell cycle arrest in quiescent cells	4
I. 1. 2 Metabolism in quiescent cells	5
I. 1. 3 Transcriptional regulation in quiescent cells	6
I. 1. 4 Translational regulation in quiescent cells	7
I. 2 Signaling pathways regulating quiescence (G_0) program	8
I. 2. 1 PKA negatively regulates G_0 entry	8
I. 2. 2 Negative regulator of quiescence entry: TORC1	14
I. 2. 3 The Pho85 signaling pathway: negative regulator of G_0 entry	22
I. 3 Rim15 and G_0 entry	24
I. 3. 1 Rim15 is negatively regulated by PKA, TORC1 and the Pho80-Pho85 cyclin-CDK complex	25
I. 3. 2 Rim15 regulates distal readouts that are essential for G_0 program initiation	28
I. 4 Post-transcriptional regulation: mRNA decay pathways	28
I. 4. 1 Subcellular localization of mRNA decay: P bodies	31
I. 4. 2 Stress granules: storage sites of mRNPs that may reenter into translation	32
I. 5 Igo1/2 regulate G_0-specific RNA stability	34
I. 5. 1 The Rim15 substrates Igo1/2 protect G_0 -specific mRNAs from degradation by the 5'-3' decay pathway	34
I. 5. 2 Igo1 homologues ARPP-19 and Ensa inhibit PP2A ^{Cdc55}	37

Chapter II. Igo1 localization	39
II. 1 GFP-tagged Igo1 variants behave as their non-tagged counterparts	40
II. 2 Nuclear accumulation of Igo1 upon rapamycin treatment depends on phosphorylation of Igo1 at Ser⁶⁴ by Rim15	41
II. 3 Igo1^{S64D}-GFP is constitutively enriched in the nucleus and does not dynamically change its localization during rapamycin treatment	44
II. 4 Igo1^{S105A}-GFP remains cytoplasmic upon rapamycin treatment.....	45
II. 5 Igo1^{S105D}-GFP oscillates between the nucleus and the cytoplasm upon rapamycin treatment	46
II. 6 Igo1-NLS-GFP is not functional, but Igo1-NES-GFP is functional	47
II. 6. 1 NLS and NES are targeting sequences essential for the nuclear import or export of cargo proteins	47
II. 6. 2 Igo1-NLS-GFP and Igo1-NES-GFP mainly localize in the nucleus and cytoplasm, respectively	49
II. 6. 3 Igo1 fulfills its function in the cytoplasm	51
II. 7 Igo1-GFP is cytoplasmic in the importin mutant <i>kap123Δ</i>, which displays a normal <i>HSP26-lacZ</i> expression upon rapamycin treatment.....	54
II. 8 Discussion	56
II. 8. 1 Igo1 localization is dynamic upon TORC1 inactivation	56
II. 8. 2 Igo1 fulfills at least one of its functions in the cytoplasm	57
II. 8. 3 Igo1 phosphorylation status	57
II. 8. 4 Working model	58
Chapter III. Igo1/2 target mRNA decapping factors.....	61
III. 1 Screening for mutants that suppress the defect in <i>HSP26</i> expression in <i>igo1Δ igo2Δ</i> mutant cells.....	61
III. 2 Loss of proteins involved in the 5'-3' mRNA decay suppresses the defect of an <i>igo1Δ igo2Δ</i> mutant in <i>HSP26</i> expression following rapamycin treatment	66
III. 2. 1 Loss of Ccr4 and Dhh1 suppresses the defect of an <i>igo1Δ igo2Δ</i> mutant in <i>HSP26</i> expression following rapamycin treatment	66
III. 2. 2 Loss of Pat1 suppresses the defect of an <i>igo1Δ igo2Δ</i> mutant in <i>HSP26</i> expression following rapamycin treatment	68

III. 2. 3 Loss of Lsm1 and Lsm6 fully suppresses the defect of an <i>igo1Δ igo2Δ</i> mutant in rapamycin-induced <i>HSP26</i> expression at the mRNA level, but only partially at protein level	71
III. 3 Discussion	73
Chapter IV. Genetic screen for multicopy suppressors of <i>igo1Δ igo2Δ</i> defects	77
IV. 1 Genetic screen procedure for multicopy suppressors of <i>igo1Δ igo2Δ</i> defects	77
IV. 2 <i>GIS3</i>, <i>ZDS1</i> or <i>WHI2</i> suppresses the defect of <i>igo1Δ igo2Δ</i> and <i>rim15Δ</i> cells in <i>HSP26</i> expression following rapamycin-treatment or glucose limitation	82
IV. 2. 1 Overexpression of <i>GIS3</i> fully suppresses the defect of <i>igo1Δ igo2Δ</i> and <i>rim15Δ</i> cells in rapamycin-induced <i>HSP26</i> expression at both the mRNA and protein levels	82
IV. 2. 2 Overexpression of <i>ZDS1</i> fully suppresses the defect of <i>igo1Δ igo2Δ</i> and <i>rim15Δ</i> cells in rapamycin-induced <i>HSP26</i> expression at both the mRNA and protein levels	86
IV. 2. 3 Overexpression of <i>WHI2</i> partially suppresses the defect of an <i>igo1Δ igo2Δ</i> and a <i>rim15Δ</i> mutant in rapamycin-induced <i>HSP26</i> expression at both the mRNA and protein levels	89
IV. 3 Analyses of <i>Gis3</i> as a suppressor of the defect of <i>igo1Δ igo2Δ</i> and <i>rim15Δ</i> mutant cells in <i>HSP26</i> expression	90
IV. 3. 1 <i>Gis3</i> mainly and constitutively localizes in the nucleus	90
IV. 3. 2 <i>Gis3</i> is new physical interactor of PP2A ^{Cdc55}	92
IV. 3. 2. 1 <i>Gis3</i> -TAP purification identifies subunits of PP2A ^{Cdc55} as physical interactors	92
IV. 3. 2. 2 <i>Gis3</i> interacts with PP2A ^{Cdc55} subunits in a yeast two-hybrid system	94
IV. 3. 2. 3 <i>Gis3</i> coimmunoprecipitates with Cdc55 <i>in vivo</i>	98
IV. 4 Discussion.....	99
IV. 4. 1 Overexpression of <i>ZDS1</i> and <i>WHI2</i> fully or partially suppress, respectively, respectively the defect of <i>igo1Δ igo2Δ</i> and <i>rim15Δ</i> cells in <i>HSP26</i> expression.....	100
IV. 4. 2 <i>Gis3</i> : potential inhibitor of PP2A ^{Cdc55}	100
IV. 4. 3 Working model	101
Chapter V. Concluding remarks	105
V. 1 <i>Igo1</i> may play a role in promoter regulation	107
V. 2 <i>Igo1</i> may interact directly or indirectly with G₀ specific mRNA	107

V. 3 Igo1 may channel G₀-specific mRNPs to P bodies and stress granules under glucose deprivation conditions 108

V. 4 The Igo1 target PP2A^{Cdc55} may play a role in mRNA stability 108

V. 5 Igo1: a role in mitotic entry? 109

Material and Methods..... 111

Abbreviation 121

Appendix 1: Gis3 physical interactors (271 proteins identified from Gis3-TAP purification)... 122

Appendix 2: Initiation of the TORC1-regulated G₀ program requires Igo1/2, which license specific mRNAs to evade degradation via the 5'-3' mRNA decay pathway 129

Appendix 3: Initiation of the yeast G₀ program requires Igo1 and Igo2, which antagonize activation of decapping of specific nutrient-regulated mRNAs 133

References 155

Summary

Eukaryotic cell proliferation is controlled by different growth factors and the availability of essential nutrients. In their absence, cells cease mitotic division and enter a reversible nonproliferating state, known as quiescent or G_0 state. In yeast *Saccharomyces cerevisiae*, PKA, TORC1 and the Pho80-Pho85 cyclin-CDK complex all negatively regulate G_0 entry in response to different nutrient availability by sequestering inactive Rim15 in the cytoplasm. Following starvation, dephosphorylated Rim15 translocates into the nucleus, where it activates the G_0 program at both the transcriptional and posttranscriptional level. While the transcription activation occurs by direct or indirect activation of Msn2/4 and Gis1, Rim15 phosphorylates Igo1/2 to protect the corresponding G_0 -specific mRNAs from the 5'-3' decay pathway. To better understand the role of Igo1/2 in the regulation of the G_0 entry, I studied the localization of Igo1 following rapamycin-induced TORC1 inactivation, and performed two genetic screens to identify new genetic interactors of *IGO1* and *IGO2*.

In a first part, I analyzed the localization of GFP-tagged wild-type Igo1 and Igo1 variants, which are nonphosphorylatable by Rim15, or which carry phosphomimetic residues instead. These studies revealed that Igo1 accumulates transiently in the nucleus following rapamycin treatment in a Rim15-dependent manner. The implications of these findings are discussed in Chapter II.

In a second part, I performed a genetic screen with the knockout collection of viable non-essential gene deletion mutants to identify mutations that suppress the defect of an *igo1Δ igo2Δ* mutant in *HSP26* gene expression in cells entering G_0 . Interestingly, we found the deletion of *DHH1*, *PAT1*, *LSM1* or *LSM6*, which encode decapping activators of 5'-3' decay pathway, suppresses the defect of *igo1Δ igo2Δ* cells in *HSP26* expression. This study, which is presented in Chapter III, suggests that Igo1/2 likely play a key role in the protection of *HSP26* mRNA by antagonizing decapping activators, such as Dhh1 and/or Pat1.

In a third part, which is presented in Chapter IV, a screen to identify multicopy suppressors of the defects of *igo1Δ igo2Δ* cells in *HSP26* expression was performed. I obtained 3 candidates, namely *GIS3*, *ZDS1* and *WHI2*, which when overexpressed suppress the defect of *igo1Δ igo2Δ* cells in rapamycin- and glucose-limitation-induced *HSP26* expression. We observed that the poorly characterized Gis3 protein is mainly and constitutively localized in the nucleus and does not significantly change in localization following rapamycin-induced TORC1 inactivation. A TAP-tag analysis revealed that Gis3 physically interacts with different subunits of the phosphatase PP2A, including the scaffold protein Tpd3, the regulatory subunit Cdc55 and both catalytic subunits Pph21 and Pph22. This suggests that Gis3 may be a new regulator of PP2A^{Cdc55} in regulating G₀ gene expression. As it has been reported that the α -endosulfine ARPP-19 and Ensa, the Igo1 homologues, also inhibit PP2A-B55 δ in higher eukaryotes, we propose that Gis3 and Igo1/2 belong to two parallel branches that inhibit PP2A^{Cdc55} to fully activate the G₀ program. Zds1 may favor G₀-specific transcription by inhibition of PP2A and/or PKA, which in turn negatively regulates Msn2. Whi2 may regulate G₀-specific transcription by activating directly the transcription factor Msn2. Thus, this study reveals a new role of PP2A^{Cdc55} as a key regulator of the G₀ program in yeast and provides a basis for the rectification of the distal effectors that play a role in setting up this program.

Taken together, the parallel approaches outlined in this thesis not only shed light on the regulation of Igo1 localization by Rim15, but also revealed new aspects of Igo1/2 function in inhibition of decapping activators of the 5'-3' decay pathway, and identified Gis3 as a new regulator of the quiescence program in yeast, which may play a role in the regulation of PP2A^{Cdc55}.

Chapter I. Introduction

Eukaryotic cell proliferation is controlled by different growth factors and the availability of essential nutrients. In their absence, cells cease mitotic division and enter a reversible nonproliferating state, known as quiescent or G_0 state. The entry into such resting states is typically accompanied by a dramatic decrease in the overall growth rate and an increased level of environmental stress resistance. The distinct physiological, biochemical and morphological traits of G_0 cells allows cell survival for very long time periods when essential nutrients are imitated and resume growth of proliferation upon refeeding (Lillie and Pringle, 1980). The knowledge of quiescence regulation provides insightful information about the control of two of the most fundamental aspects of eukaryotic cell biology: cell proliferation and long-term cell survival. As there are related processes in higher eukaryotes, this information may also help to develop new therapies against human cell proliferation disorders, such as cancer (Dazert and Hall, 2011). Like all microorganisms, yeast *Saccharomyces cerevisiae* cells spend most of their natural lifetime in these quiescent states. The advantages of a small genome and amenability to genetic manipulation have made *S. cerevisiae* a powerful model system for analyzing many eukaryotic processes, notably, the regulatory mechanisms of entry into, survival during and exit from quiescence. The following introduction will comprise the characteristics of quiescence (G_0) program and its regulation by different signaling pathways, the role of the G_0 master regulator Rim15 and its substrates Igo1/2. The outline of the characteristics of quiescence (G_0) program and its regulation by different signaling pathways are based on a recent review (De Virgilio, 2012).

I. 1 Characteristics of quiescence (G_0) program

Starvation is one of the most common stresses encountered by living organisms. When starved for carbon, nitrogen, phosphate or sulfur, *S. cerevisiae* cells enter the reversible nondividing quiescent state. Our current knowledge about quiescent state is based on the observation of several distinct adaptive phases of growth prior to entry into G_0 phase when yeast cells are grown in glucose-containing rich medium such as YPD. The first of these phases starts when about half of the glucose has been consumed, at which time point cells start to synthesize the reserve carbohydrate glycogen (Lillie and Pringle, 1980). This earliest sign of G_0 entry is then followed by a critical phase for stress resistance, characterized by

specific transcriptional changes and the synthesis of trehalose before and following glucose exhaustion, respectively (Werner-Washburne et al., 1993). When glucose is depleted, cells enter the diauxic shift phase, where they transiently reduce their growth rate to adapt their metabolism to the subsequent respiratory growth on nonfermentable carbon sources, such as ethanol and acetate that are produced by glycolysis. At this stage, cells induce the transcription of genes whose products are involved in respiration, antioxidant defense, fatty acid metabolism, and glyoxylate cycle reactions (Costa and Moradas-Ferreira, 2001; Jamieson, 1992).

In response to starvation, cells initiate a quiescent program that has distinct characteristics in cell cycle, metabolism, transcription and translation.

I. 1. 1 Cell cycle arrest in quiescent cells

Cells that are nutritionally deprived of nitrogen, sulfur, phosphate, and carbon sources arrest at START A within the G_1 phase of the cell cycle. Functioning of RAS/cAMP pathway is required for the progress through START A, which precedes START B, which corresponds to the stage at which pheromone-treated cells arrest. G_1 cyclin Cln3 associated cyclin-dependent protein kinase (CDK) p34^{Cdc28} activity is required for setting the size threshold at which cells pass through START B, where cells are committed to a new round of division (Hartwell, 1974; Sherlock and Rosamond, 1993). However, impaired proper $G_{1/0}$ arrest in starved auxotrophic mutants that are deprived for essential nutrient such as leucine and uracil, likely results in shortening of life span (Boer et al., 2008; Saldanha et al., 2004). These observations indicate that cell cycle arrest at START A and entry into the G_0 phase appear to be tightly regulated and are not simple consequences of growth arrest. Surprisingly, it has been observed that cells are able to enter the G_0 phase not only through the G_1 phase, but also through S, G2 and M phases of the cell cycle (Laporte et al., 2011; Wei et al., 1993).

I. 1. 2 Metabolism in quiescent cells

Starvation for various nutrients such as carbon sources, ammonia, sulfate, or phosphate cause cells to trigger multiple metabolic changes, including the accumulation of the reserve carbohydrate glycogen and trehalose, which are among the most studied metabolic changes.

When cells are grown in batch cultures, the major intracellular reserve carbohydrate glycogen starts to be synthesized when half of the glucose has been consumed and peaks at the beginning of the diauxic shift phase. This reserve carbohydrate is accumulated in the cytoplasm and, as a result of macroautophagy also in the vacuole. The synthesis of highly branched mature glycogen is catalyzed successively by the glucogenins Gly1/2, glycogen synthases Gsy1/2 and the branching enzyme Glc3. Following the diauxic shift, glycogen stores are then utilized for the synthesis of the nonreducing disaccharid trehalose (Francois and Parrou, 2001). Following the subsequent growth phase on non-fermentable carbon sources, glycogen is synthesized again, which serves as a reserve for extended periods of starvation. The glycogen stored in the cytoplasm and the vacuole is mobilized by the debranching enzyme Ddb1 and the glycogen phosphorylase Gph1 or the vacuolar glucoamylase Sga1, respectively (for review, see (Wilson et al., 2010)).

The nonreducing disaccharide trehalose is thought to contribute to the tolerance of thermal, osmotic, oxidative and ethanol stress (Pereira et al., 2001). It is involved as well in preventing aggregation of denatured proteins (Singer and Lindquist, 1998). When cells are subjected to glucose limitation, it is synthesized during the diauxic shift and the following growth phase on non-fermentable carbon source. The accumulated trehalose is progressively degraded once glycogen stores are depleted. The two-step biosynthesis of trehalose requires α , α -trehalose-phosphate synthase complex, which consists of trehalose-6-phosphate synthase Tps1, trehalose-6-phosphate phosphatase Tps2 and their regulatory proteins Tps3 and Tsl1 (Bell et al., 1992; De Virgilio et al., 1993; Vuorio et al., 1993). Following refeeding of quiescent cells, trehalose is rapidly mobilized mainly by trehalase Nth1-mediated hydrolysis (Shi et al., 2010).

I. 1. 3 Transcriptional regulation in quiescent cells

Transcriptional reprogramming takes place to adapt cells to environmental transitions, during diauxic shift, postdiauxic shift, and stationary phases (DeRisi et al., 1997; Gasch et al., 2000; Klosinska et al., 2011; Radonjic et al., 2005). This reprogramming process involves various signaling pathways, including TORC1 and PKA pathways (see details in further sections) and is regulated by different mechanisms, which are described in detail below.

When cells encounter nutrient limitation, the down-regulation of ribosome biogenesis is fine-tuned by coordinated regulation of all three RNA polymerases (i.e. RNA Pol I, II and III) (reviewed in (Lempiainen and Shore, 2009)). (1) When cells enter the stationary phase, the decrease of mRNA levels transcribed by RNA Pol II is regulated in a DNA topoisomerase I (Top1)-dependent manner (Choder, 1991). (2) Moreover, following entry into stationary phase, the levels of *TATA*-box *binding protein* (TBP) and several TBP-associated factors (TAF_{II}s, especially TAF_{II}145), which form the transcription factor TFIID, decreases dramatically (Walker et al., 1997). On the contrary, the stress-specific RNA Pol II subunit Rpb4, whose level increases following entry into stationary phase, is required for G₀-specific transcription and for stress survival by increasing its association with other subunits of RNA Pol II (Choder, 1993; Choder and Young, 1993). (3) Furthermore, the evolutionarily conserved CTD of Rpb1 the largest subunit of RNA Pol II, which contains 25-52 tandem copies of a heptapeptide sequence (consensus Y-S-P-T-S-P-S) (Corden, 1990), is involved in stationary phase transcription regulation (Carlson, 1997). Cells with CTD-truncated Rpb1 fail to enter normal stationary phase (Howard et al., 2002). Phosphorylation of the CTD repeat at specific sites is indicative of active RNA Pol II. In the process of transcription initiation TFIID kinase phosphorylates CTD heptad repeats at Ser⁵. During transcription elongation, Ser² of CTD heptad repeats is phosphorylated by Ctk1/Ctk2/Ctk3-composed CTDK1 (Dahmus, 1996; Komarnitsky et al., 2000). A Ctk1 kinase dead mutant shows impaired CTD Ser² phosphorylation and exhibited delayed growth when this mutant enters stationary phase (Borggreffe et al., 2002; Ostapenko and Solomon, 2005). (4) Furthermore, the RNA Pol II CTD plays a role in the regulation of the entry into and the survival during the stationary phase, by serving as flexible binding scaffold for numerous nuclear factors, For instance, the cyclin-dependent kinase Cdk8 (Srb10), cyclin partner CycC (Srb11) and Med 12 (Srb8), Med13 (Srb9) form a stoichiometric Mediator regulatory module, which has been proposed to

negatively regulate the function of RNA Pol II by phosphorylating CTD (Borggreffe et al., 2002). When cells enter the diauxic growth phase, Cdk8 (Srb10) and CycC (Srb11) are depleted, while the transcription of nutrient deprivation-induced genes is derepressed in a Srb10 point mutant. The results indicate that the physical loss of the Srb10 CDK and CycC from the RNA Pol II holoenzyme is essential for quiescence entry in response of nutrient starvation (Holstege et al., 1998). Moreover, *srb9Δ*, *srb1Δ* and *srb11Δ* mutants exhibit decreased viability following an extended period of nutrient deprivation, indicating that the Mediator plays a role in surviving periods of prolonged starvation (Chang et al., 2001).

I. 1. 4 Translational regulation in quiescent cells

Upon entry into quiescent state, the down-regulation of ribosomal protein (RP) and translation factor gene expression and the repression of translation initiation result in about 300-fold decrease in protein synthesis rates (DeRisi et al., 1997; Fuge et al., 1994; Ju and Warner, 1994). While the translation of 95% of proteins synthesized in exponential phase is shut down following entry of cells into stationary phase (Boucherie, 1985), the translation remains active in stationary phase for numerous starvation-induced mRNAs, such as *HSP26* mRNAs and mRNAs of the *SNO* and *SNZ* families, which are involved in the synthesis of pyridoxine/vitamin B6 (Dickson and Brown, 1998; Padilla et al., 1998). This remaining translational capacity is necessary for the survival of cells in extended period of starvation (Paz and Choder, 2001).

Nutrient availability signals impinge on the α -subunit of the eukaryotic translation initiation factor 2 (eIF2 α). Its phosphorylation status regulates the rate of translation initiation. The translation initiation process commences by the transfer of methionyl-tRNA^{Met} together with GTP by eIF2 α in a ternary complex (TC) to form the 40S ribosomal subunit. Phosphorylation of eIF2 α -Ser⁵¹ inhibits the formation of TC, and consequently, the subsequent translation initiation steps (Hinnebusch, 2005). The phosphorylation status of eIF2 α -Ser⁵¹ is regulated by the eIF2 α kinase Gcn2 and eIF2 α -phosphatases (eIF2 α -PPs) (*i.e.* type I protein phosphatase (PP1) Glc7 and the type 2A protein phosphatase (PP2A)-related Sit4) (Cherkasova et al., 2010; Wek et al., 1992). Gcn2 activation is regulated by several mechanisms that including the following ones: (1) uncharged tRNAs, which accumulate

during amino acid starvation, bind to the C-terminal histidyl-tRNA synthetase-related domain of Gcn2, which leads to its activation (Hinnebusch, 2005); (2) dephosphorylation of the inhibitory Ser⁵⁷⁷ residue by the Tap42-associated Sit4 phosphatase (Cherkasova and Hinnebusch, 2003); and (3) the autophosphorylation of Thr⁸⁸² and Thr⁸⁸⁷ in the Gcn2 activation loop, which is required for full kinase activity (Romano et al., 1998). Furthermore, Gcn2 activation appears to be stimulated by Snf1, a kinase responsible for the activation of glucose-repressed genes, when cells grow on low glucose levels. Snf1 promotes autophosphorylation of Gcn2 Thr⁸⁸² and/or inhibits eIF2 α -PPs Glc7 and Sit4 (Cherkasova et al., 2010). Of note, the Tap42/Sit4 PP2A-like phosphatase formation is negatively regulated by target of rapamycin complex 1 (TORC1) (Di Como and Arndt, 1996; Jiang and Broach, 1999). Taken together, the protein kinases Gcn2, Snf1 and TORC1 are involved in the translation initiation regulation in response to nutrient starvation.

I. 2 Signaling pathways regulating quiescence (G₀) program

Limitation for nitrogen, sulfur, phosphate, and carbon sources causes yeast cells to arrest in quiescent state. The sensing of nutrient availability and the reprogramming for quiescent state adaptation is tightly regulated by at least 3 signaling pathways, namely the PKA, TORC1 and Pho85 pathways.

I. 2. 1 PKA negatively regulates G₀ entry

The highly conserved cyclic AMP (cAMP)-dependent protein kinase A (PKA) pathway in the yeast *S. cerevisiae* plays a major role in the control of ribosome biogenesis, stress responses and metabolism, in response to nutrient availability, in particular glucose and related fermentable sugars such as sucrose. The heterotetrameric PKA complex consists of two catalytic subunits encoded by *TPK1*, *TPK2* or *TPK3*, and two regulatory Bcy1 subunits, which inhibit the activity of the catalytic subunits. In presence of cAMP, Bcy1 binds to cAMP and dissociates from the complex as a homodimer, releasing the two catalytic subunits as active monomers to phosphorylate distinct target proteins (Ptacek et al., 2005; Robertson and Fink, 1998; Toda et al., 1985). The current knowledge of how the intracellular and

extracellular nutrient signals impinge on PKA, and how the downstream effectors achieve their function, will be discussed in the following paragraphs.

PKA senses glucose availability and intracellular acidification

Two parallel pathways relaying intracellular and extracellular nutrient signals converge on adenylate cyclase Cdc35, which counterbalances the effect of phosphodiesterase Pde1/2 on intracellular cAMP level to regulate PKA function (Fig. 1). The GTP-bound forms of Ras1 and Ras2 proteins directly activate the adenylate cyclase Cdc35. The Ras-GTP/ Ras-GDP ratio is negatively regulated by the *GTPase-activating proteins* (GAP) Ira1/2, which are regulated by the intracellular acidification (Tanaka et al., 1989; Tanaka et al., 1990). On the other hand, the Ras GTP level is positively regulated by the *guanine nucleotide exchange factors* (GEF) Cdc25 and Sdc25 (Broek et al., 1987; Colombo et al., 1998; Thevelein and de Winde, 1999). Following glucose refeeding of starved cells, the intracellular cAMP increases only transiently. This transient increase likely results from a feedback inhibition of cAMP synthesis via the hyperphosphorylation of Cdc25. This hyperphosphorylation results in its dissociation from Ras and activation of cAMP hydrolysis by Pde1/2 (Gross et al., 1992; Hu et al., 2010; Ma et al., 1999). The Ras-GTP level increase in response to glucose appears to be dependent on intracellular phosphorylation of glucose and regulation of Cdc25 and Ira1/2 (Colombo et al., 2004; Gross et al., 1999; Rolland et al., 2001). However, the molecular mechanism by which glucose causes Ras-GTP levels increase remains elusive.

In parallel of Ras1/2, a *G-protein-coupled receptor* (GPCR) senses the extracellular nutrient signal (in particular glucose and sucrose) and subsequently activates PKA via Cdc35 stimulation. This GPCR system is composed of the seven-transmembrane receptor Gpr1, the small GTP-binding protein Gpa2, its GAP Rgs2 and the G β -subunit Asc1. The Gpr1-Gpa2 GPCR system plays an important role in transient cAMP synthesis activated by glucose (Thevelein and de Winde, 1999). As Gpr1-Gpa2 are dispensable for growth and entry into quiescence (Sherlock and Rosamond, 1993), compared to the Cdc25/Ras/Cdc35 branch, this GPCR system plays a minor role in regulation of G₀ entry.

In addition to its major regulator cAMP, PKA is controlled by several other mechanisms. For instance, PKA autophosphorylates its regulatory subunit Bcy1 at Ser¹⁴⁵, to destabilize it (Kuret et al., 1988). In addition, following entry into stationary phase, Bcy1 increases 8- to 9- fold compared to exponential phase (Werner-Washburne et al., 1991). Furthermore, Bcy1 relocates from the nucleus to the cytoplasm in this condition (Griffioen et al., 2000). This evidence indicates that PKA activity is temporally and spatially regulated. Moreover, in response to starvation, kelch repeat-containing proteins Gpb1 and Gpb2 have been found interacting with Gpa2 to bypass adenylate cyclase to affect PKA (Peeters et al., 2006; Peeters et al., 2007). Recent evidence suggests that Gpb1/2 stimulate Bcy1 phosphorylation at an unknown site, as a consequence, promoting inhibition of PKA function (Budhwar et al., 2010).

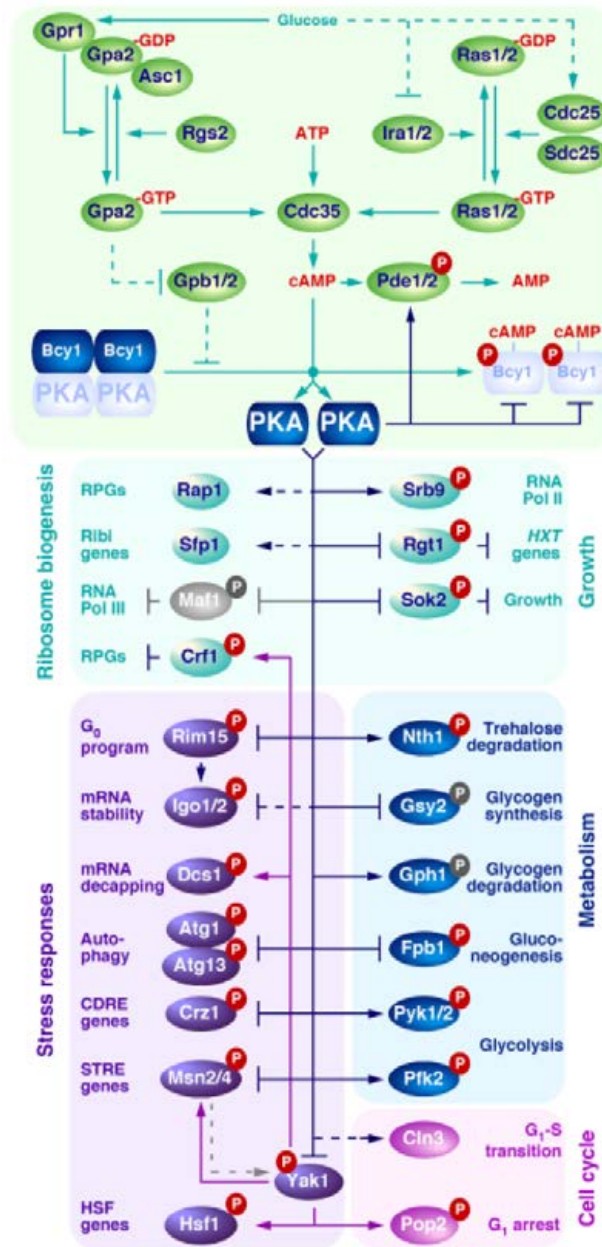


Fig. 1 Diagram of PKA-signaling pathway (De Virgilio, 2012)

PKA integrates intracellular and extracellular nutrient signals via the Cdc25/Ras/Cdc35 branch and the Gpr1-Gap2 GPCR system, respectively. PKA promotes growth by positive regulation of expression of ribosomal protein genes (RPGs), rDNA genes, and ribosome biogenesis (Ribi) genes and by inhibiting transcription repressors of growth-related genes. In parallel, PKA inhibits stress response, couples growth to G₁-S progression and regulates metabolic changes according to glucose availability.

PKA positively regulates growth through its downstream effectors

PKA regulates growth on one hand by favoring the expression of the translational machinery, via activating expression of *ribosome protein* (RP) genes, *ribosome biogenesis* (Ribi) genes, rDNA genes, which encode proteins involved in ribosome assembly and rRNA processing (Chen and Powers, 2006). On the other hand, PKA inhibits stress response and regulates metabolism prior to and following diauxic shift.

PKA promotes ribosome biogenesis by numerous processes. For the activation of RP genes, PKA activates the transcription regulator Rap1 (Klein and Struhl, 1994; Neuman-Silberberg et al., 1995) to recruit transcription activators Fhl1 and Ifh1 to RP gene promoters (Wade et al., 2004), which activate the transcription of corresponding genes (Martin et al., 2004; Rudra et al., 2005; Schawalder et al., 2004). In addition, recent evidence indicates that Rap1 promotes binding of the high-mobility group protein Hmo1 to rDNA and RP genes promoters to favor their Fhl1-Ifh1-dependent transcription (Hall et al., 2006). PKA promotes as well RP and Ribi gene expression likely by positively regulating nuclear localization of the transcription factor Sfp1 (Budovskaya et al., 2005; Cipollina et al., 2008a; Cipollina et al., 2008b; Marion et al., 2004). Moreover, PKA may exclude nuclear localization of RNA Pol III repressor Maf1 by phosphorylation, as a consequence favoring 5S rDNA and tRNA transcription (Moir et al., 2006). However, this has been challenged by a recent study (Huber et al., 2009). In parallel of promoting ribosome biogenesis, PKA also controls growth by other different means. For instance, PKA regulates RNA Pol II-mediated transcription elongation via the Spt4/Spt5 elongation factor (Howard et al., 2003). By phosphorylation events, the Mediator subunit Srb9 is controlled directly by PKA (Chang et al., 2004). PKA also inhibits the transcriptional repressor Sok2 via phosphorylation (Shenhar and Kassir, 2001; Ward et al., 1995). PKA phosphorylates the glucose transporter-like Snf3 and Rgt2 proteins target Rtg1, to remove this repressor from *hexose transporter* (HXT) gene promoters, and thereby activates expression of the corresponding genes (Kim and Johnston, 2006). Finally, PKA couples growth and cell cycle progression control via its positive regulation of Cln3 protein levels and Cln3-Cdc28 kinase activity (Hall et al., 1998).

In addition to its role in promoting growth, PKA inhibits stress response through regulation of different downstream effectors. Yak1 is one of these PKA regulated downstream effectors for stress response suppression. Yak1 is a substrate of PKA (Budovskaya et al., 2005; Zappacosta et al., 2002), PKA-dependent phosphorylation on Ser²⁹⁵ and two minor sites inhibits nuclear localization of Yak1 (Lee et al., 2011). PKA inhibition in diauxic cells leads to the activation of Yak1, which in turn, achieves its numerous functions in the nucleus. For instance, Bcy1 is phosphorylated on its N-terminal domain by Yak1, leading to its cytoplasmic localization (Griffioen et al., 2001; Werner-Washburne et al., 1991). Moreover, Yak1 phosphorylates Pop2/Caf1 at Thr⁹⁷, the phosphorylation of which is required for proper G₁ arrest in response to glucose deprivation (Moriya et al., 2001). Yak1 also phosphorylates the m⁷-GpppX pyrophosphatase Dcs1 (Malys et al., 2004), and the RP gene transcription corepressor Crf1 (Martin et al., 2004; Zhao et al., 2006). The stress-responsive transcription factors, Hsf1 and Msn2 are phosphorylated as well by Yak1 (Lee et al., 2008). The Zn²⁺-finger transcription factor Msn2 is also directly phosphorylated by PKA in its nuclear localization signal (NLS) and in its nuclear export signal (NES) to inhibit the nuclear import and likely promote nuclear export of Msn2, respectively (Garreau et al., 2000; Gorner et al., 1998; Gorner et al., 2002). When PKA is inhibited in glucose limited cells, the expression of the Msn2/4 transcription factor-dependent genes is also regulated via additional factors such as the protein kinase Rim15 and its direct substrates Igo1/2. This will be detailed below. Furthermore, PKA negatively regulates stress response by inhibiting the nuclear import of another Zn²⁺-finger transcription factor Crz1 via phosphorylation (Mazur et al., 1995). Crz1 drives the expression of calcineurin-dependent genes, whose products are important for the stress response (Kafadar and Cyert, 2004; Yoshimoto et al., 2002). Finally, PKA inhibits autophagy by its phosphorylation of Atg1 and Atg13, as a consequence, inhibits their association with preautophagosomal structure (PAS), the putative site for autophagosome formation (Budovskaya et al., 2005; Budovskaya et al., 2004; Stephan et al., 2009).

In parallel to its role in promoting ribosome biogenesis and stress response inhibition, PKA also inhibits several carbohydrate metabolic changes in glucose-deprived cells by inhibition of trehalose and glycogen synthesis, gluconeogenesis and induction of glycogenesis. PKA inhibits trehalose accumulation in glucose-limited cells via neutral trehalase Nth1 activation in a 14-3-3-dependent manner (Panni et al., 2008; Wera et al., 1999). PKA-mediated inhibition of the glycogen phosphorylase Gph1 and activation the glycogen synthase

Gsy2 contributes to PKA-dependent inhibition of glycogen accumulation (Hardy and Roach, 1993; Lin et al., 1996). PKA activates the glycolytic 6-phosphofructo-2-kinase Pfk2 (Dihazi et al., 2003; Vaseghi et al., 2001) and pyruvate kinases Pyk1/2 (Cytrynska et al., 2001; Galello et al., 2010; Portela et al., 2002; Portela et al., 2006), while gluconeogenesis is antagonized by PKA via its inhibition of glucogenic fructose-1, 6-bisphosphatase Fpb1 (Gancedo et al., 1983; Rittenhouse et al., 1987).

I. 2. 2 Negative regulator of quiescence entry: TORC1

In response to nutrient availability, another major signaling pathway involving highly conserved *target of rapamycin* (TOR) proteins, also plays a key role in cell growth regulation. Initially identified by mutations that confer rapamycin resistance to yeast *S. cerevisiae*, the two TOR paralogues, Tor1 and Tor2 are targets of rapamycin, a lipophilic macrolide with immune-suppressive property produced by *Streptomyces hygroscopicus* (Heitman et al., 1991). The molecular basis of these findings has been further clarified by the identification of two multiprotein complexes (TORC1 and TORC2) (Loewith et al., 2002). Only TORC1 is sensitive to rapamycin in complex with the peptidyl-prolyl isomerase Fpr1 (FKBP12 in mammals) (Loewith et al., 2002). In yeast *S. cerevisiae*, TORC1 consists of Lst8, Kog1, Tco89 and either Tor1 or Tor2 (Loewith and Hall, 2011; Loewith et al., 2002; Reinke et al., 2004; Wedaman et al., 2003). When bound to Fpr1-rapamycin complex, TOR kinases activity in TORC1 is inhibited. TORC1 inhibition consequently triggers numerous downstream events, such as inhibition of ribosome biogenesis and the translation machinery, gene transcription adaptation, sorting and turnover of nutrient permeases, induction of autophagy, G₁ cell cycle arrest and entry into quiescence (reviewed in (De Virgilio, 2012; De Virgilio and Loewith, 2006; Loewith and Hall, 2011)) (Fig. 2).

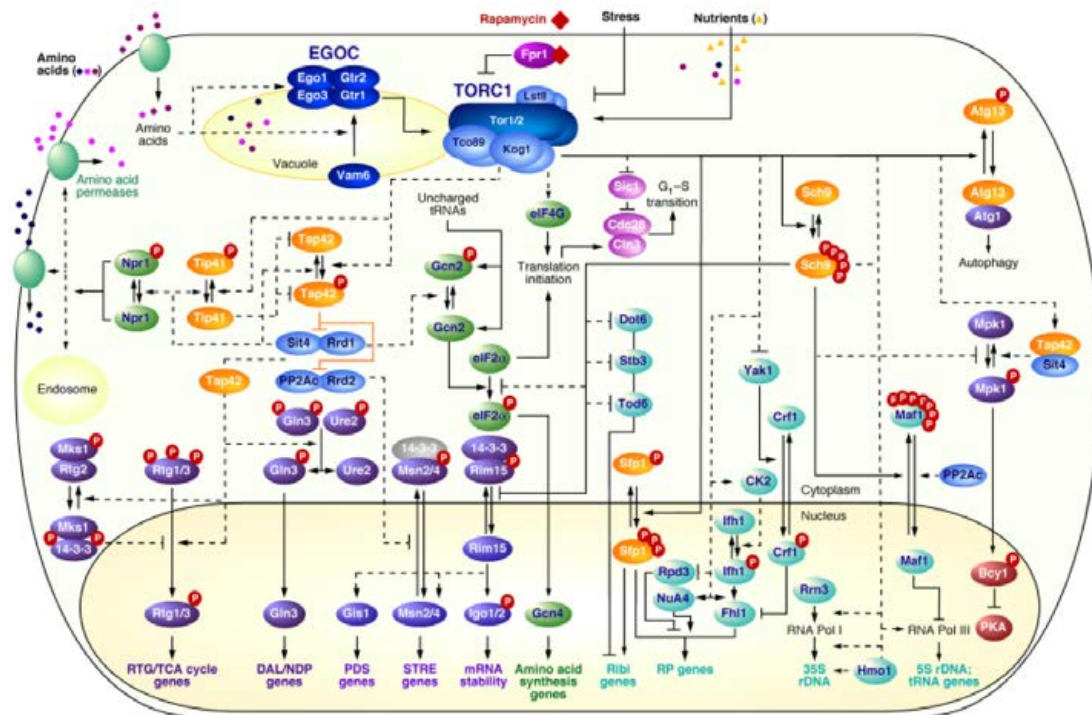


Fig. 2 TORC1 signaling pathway (De Virgilio, 2012)

Upstream of TORC1, cytoplasmic and/or intravacuolar amino acids may influence the activity of Vam6, which regulates the nucleotide-binding status of the small GTPase Gtr1. As part of the EGO complex (EGOC; dark blue), Gtr1-GTP binds to and somehow activates TORC1. Rapamycin specifically inhibits TORC1 when in complex with the peptidyl-prolyl isomerase Fpr1. TORC1 propagates signals mainly via its proximal effectors protein kinase Sch9 and the catalytic subunits of the type 2A protein phosphatases (PP2Ac) Pph21 and Pph22 or the related Sit4 protein phosphatase when associated with Tap42 and Rrd2 or Rrd1, respectively. In turn, proximal effectors act through distal effectors to promote cell growth by stimulating expression of the translation machinery (turquoise proteins), translation initiation and permease sorting (green proteins), and inhibiting stress responses (violet proteins).

TORC1 senses nitrogen, intracellular and extracellular amino acid availability

The transfer from good to poor-quality carbon or nitrogen sources, starvation for carbon or nitrogen, as well as exposure to noxious stresses induce highly similar cellular responses as that induced by a rapamycin treatment. This suggests that Tor integrates environmental nutrient signals (see review (De Virgilio and Loewith, 2006)). This assumption is further confirmed by the observation of similar transcription profiles of yeast cells exposed to rapamycin, nutrient starvation and noxious stress (Gasch and Werner-Washburne, 2002; Hardwick et al., 1999; Komeili and O'Shea, 2000; Shamji et al., 2000). Consistently, the direct substrate Sch9 of TORC1 is dephosphorylated when cells are treated with rapamycin or starved for carbon, nitrogen, phosphate, amino acid and various stresses (Binda et al., 2009; Urban et al., 2007). Additionally, intracellular amino acids also play a role in TORC1 activity regulation. For instance, TOCR1 is strongly activated by treatment with the translation elongation inhibitor cycloheximide, which likely increases the intracellular pool of free amino acids (Beugnet et al., 2003; Binda et al., 2009; Urban et al., 2007). In particular, it has been demonstrated in mammalian cells that leucine regulates mTORC1 by controlling the ability of Rheb-GTP to activate mTORC1 (Avruch et al., 2009). These observations indicate that TORC1 senses the quality and quantity of nutrients.

How TORC1 senses nutrient availability has been further clarified by the identification of the EGO (*e*xit from rapamycin-induced *g*rowth arrest) protein complex (EGOC). The evolutionarily conserved EGO complex, which contains Ego1 (LAMTOR1/p18 in mammals), Ego3 (LAMTOR2/p14 in mammals), Gtr1 (RagA and B in mammals) and Gtr2 (RagC and D in mammals), colocalizes with TORC1 mainly at the vacuolar membrane (lysosomal membrane in mammals) (Araki et al., 2005; Berchtold and Walther, 2009; Binda et al., 2009; Gao and Kaiser, 2006; Kogan et al., 2010; Reinke et al., 2004; Sancak et al., 2008; Sturgill et al., 2008). Furthermore, a crystal structure study of Gtr1/Gtr2 (RagA/RagC in mammals) has revealed that both N-terminal GTPase domains and hetero-dimerization are important for their interaction with Kog1 (Raptor in mammals) (Gong et al., 2011). EGOC has been proposed to function upstream of TORC1 to mediate amino acid signaling (Dubouloz et al., 2005). In addition, it is also reported in *Drosophila* and mammalian cells that the Rag GTPase functions upstream of TORC1 to mediate amino signals (Kim et al., 2008; Sancak et al., 2008). Gtr1 and Gtr2 are two small GTPases. When Gtr1 in its GTP-

bound form and Gtr2 in its GDP-bound form, they interact with and activate TORC1. Moreover, constitutively active Gtr1^{GTP} strongly interacts with TORC1, as a consequence, rendering TORC1 partially resistant to leucine deprivation, while Gtr1^{GDP} confers low TORC1 activity. The Gtr1 guanine nucleotide loading status involves the guanine nucleotide exchange factor (GEF) Vam6 (Binda et al., 2009).

Recent evidence shed light on mechanisms by which amino acids signals impinge on EGO. The leucyl-tRNA synthetase (LeuRS) Cdc60 has been reported to interact with the Rag GTPase Gtr1, but not Gtr2 of the EGO in a leucine-dependent manner. Mediated by the nonessential amino acid-editing domain CP1 of Cdc60, the interaction between Cdc60 and Gtr1 is necessary and sufficient for TORC1 activation by leucine (Bonfils et al., 2012). Surprisingly, in mammalian cells, it has been reported that LeuRS regulates TORC1 by direct binding to GTP-bound RagD (mammalian homologue of Gtr2) in an amino acid-dependent manner, and acting as a GAP of RagD (Han et al., 2012). The discrepancy between the findings in yeast and mammalian cells may be explained by the following scenarios. In yeast, although LeuRS binds exclusively to Gtr1, it may facilitate hydrolysis of GTP in Gtr2 through its close proximity to Gtr2. Similarly, in mammalian cells, LeuRS may protect the GTP-bound form of RagB from hydrolysis, despite its exclusive binding to RagD-GTP (Segev and Hay, 2012). In parallel, it has been also proposed that in mammalian cells, accumulation of amino acids inside the lysosomal lumen activates vacuolar H(+)-adenosine triphosphatase ATPases (v-ATPases), which transmit the signal to the Rag GTPases. Active Rag GTPases physically recruit mTORC1 to the lysosomal surface, the site of mTORC1 activation by Rheb (Zoncu et al., 2011).

Finally, negative regulators of TORC1 have been recently described. When cells are exposed to amino acids starvation, TORC1 activity is inhibited via the function of Npr2/Npr3 (Neklesa and Davis, 2009), which are subunits of the conserved vacuolar membrane-localized SEA complex (Dokudovskaya et al., 2011). Moreover, Rho1 GTPase has been reported to downregulate TORC1 and to disrupt its membrane association by direct binding to Kog1 in response to rapamycin and caffeine treatments (Yan et al., 2012).

TORC1 positively regulates growth through its downstream effectors

Under favorable growth conditions, TORC1 signals mainly via two proximal effectors (Huber et al., 2009). Firstly, the mammalian S6 kinase (S6K) orthologue, the AGC kinase Sch9 is a direct substrate of TORC1. TORC1-dependent phosphorylation at five to six C-terminal serine and threonine residues is required for Sch9 activity (Urban et al., 2007). Secondly, under favorable nutrient conditions, TORC1 phosphorylates Tap42, which forms protein complexes with PP2A catalytic subunits (PP2Ac) Pph21/Pph22 or the PP2A-related Sit4 protein phosphatase when associated with the peptidyl-prolyl *cis/trans*-isomerases Rrd2 or Rrd1, respectively (Di Como and Arndt, 1996; Jiang and Broach, 1999; Zheng and Jiang, 2005). While Tap42 association with Tip41 is decreased in these conditions, when TORC1 is inactivated, Tap42 becomes dephosphorylated, leading to its increased association with Tip41 (Jacinto et al., 2001). Consequently, the PP2A-Rrd2 or Sit4-Rrd1 heterodimer is released from the PP2A-Tap42-Rrd2 or Sit4-Tap42-Rrd1 complexes (Duvel and Broach, 2004; Duvel et al., 2003; Van Hoof et al., 2005; Yan et al., 2006; Zheng and Jiang, 2005). These inhibited proximal effectors then propagate the signals to TORC1 distal readouts to promote ribosome biogenesis, general translation and negatively regulates stress responses.

TORC1 promotes ribosome biogenesis

Under favorable environmental conditions, TORC1 promotes growth via regulation of expression and assembly of the translation machinery, which is required for the RNA Pol I-mediated transcription of 35S rDNA tandem repeats, RNA Pol II-mediated RP/Ribi gene transcription and RNA Pol III-mediated tRNAs gene transcription (Cardenas et al., 1999; Hardwick et al., 1999; Lee et al., 2012; Lempiainen and Shore, 2009; Powers and Walter, 1999; Zaragoza et al., 1998).

Similar to stationary phase, rapamycin treatment causes a decrease in the amount of initiation competent Rrn3-RNA Pol I complex, suggesting that TORC1 may promote the stabilization of the Rrn3-RNA Pol I complex (Claypool et al., 2004). It has been further demonstrated that TORC1 promotes the recruitment of RNA Pol I to the rDNA locus primarily via Sch9 (Huber et al., 2009). However, Sch9 does not impinge on the Rrn3-RNA Pol I interaction (Huber et al., 2009). This may require direct association of Tor1 with 35S

rDNA promoter (Li et al., 2006). Moreover, TORC1 controls rDNA transcription, through the binding of RNA Pol I transcription factor Hmo1 to rDNA promoters (Berger et al., 2007).

TORC1 promotes RNA Pol II-mediated RP genes transcription via regulation of Ihf1-Fhl1 complex formation (Martin et al., 2004; Rudra et al., 2005; Schawalder et al., 2004; Wade et al., 2004). Moreover, under optimal growth conditions, TORC1 directly phosphorylates the Split Zn-finger transcription factor Sfp1, which is consequently localized to the nucleus and bound to RP and possibly RiBi gene promoters to stimulate their expression (Lempiainen et al., 2009; Loewith and Hall, 2011; Marion et al., 2004). Via Sch9-mediated phosphorylation, TORC1 inhibits transcription repressors Stb3 and paralogues Dot6/Tod6, which repress RiBi and RP gene transcription by recruiting the Rpd3 histone deacetylase complex to *r*ibosomal *R*NA *p*rocessing *e*lement (RRPE) and RNA *p*olymerase *A* and *C* (PAC) elements (Freckleton et al., 2009; Humphrey et al., 2004; Liko et al., 2007; Lippman and Broach, 2009). Furthermore, active TORC1 promotes the specific recruitment of the catalytic subunit Esa1 of the histone H4 (NuA4) histone acetylase complex to the RP gene promoters (Reid et al., 2000). TORC1 inactivation in response to nutrient depletion or rapamycin treatment favors the recruitment of the Rpd3-Sin3 histone deacetylase complex to the RP promoters (Humphrey et al., 2004; Rohde and Cardenas, 2003).

TORC1 regulates RNA Pol III via Sch9-mediated phosphorylation of its conserved repressor, Maf1. Under favorable growth conditions, TORC1 promotes Maf1 phosphorylation by Sch9 and antagonizes Maf1 dephosphorylation by inhibiting the PP2A and PP2A-like phosphatases activity. Highly phosphorylated Maf1 is thus shuttled out of the nucleus, consequently RNA Pol III-dependent transcription is derepressed (Huber et al., 2009; Oficjalska-Pham et al., 2006; Roberts et al., 2006). It has been reported recently that, in response to nutrient limitation or rapamycin treatment, the LAMMER kinase Kns1 is hyperphosphorylated and accumulated in the nucleus to promote the phosphorylation of the RNA Pol III subunit Rpc53 by GSK-3 kinase Mck1. Together with another Pol III subunit Rpc11, phosphorylated Rpc53 promotes the dephosphorylation of Maf1 and consequently the RNA Pol III-dependent transcription is inhibited (Lee et al., 2012).

Rapamycin-induced inactivation of TORC1 triggers rapid extensive turnover of the existing ribosomes, indicating TORC1 affects the degradation of mature ribosomes in

addition to its major role in promoting ribosome biogenesis at the transcriptional level (Pestov and Shcherbik, 2012).

TORC1 promotes translation initiation

TORC1 promotes translation initiation in part by positive regulation of the α -subunit of the translation initiation factor eIF2 (eIF2 α) via both the Sch9 and Tap42-associated phosphatases branches (Cherkasova and Hinnebusch, 2003; Urban et al., 2007). When TORC1 is active, it inhibits the Tap42-PPase-dependent dephosphorylation of Ser⁵⁷⁷ and activation of the eIF2 α kinase Gcn2 (Cherkasova and Hinnebusch, 2003). In parallel, the inhibition of eIF2 α phosphorylation is mediated by Sch9, yet the underlying mechanism remains elusive (Urban et al., 2007). However, in addition to eIF2 α , TORC1 targets as well 5' cap-binding protein eIF4E and eIF4E-binding protein Eap1 (Berset et al., 1998; Cosentino et al., 2000).

TORC1 inhibits stress responses

In addition to stimulating growth, TORC1 suppresses various stress responses mainly via the inhibition of its downstream effector Tap42-PPase.

Upon nitrogen limitation, TORC1 prevents transcription of nitrogen-catabolite repression (NCR) sensitive genes of the nitrogen discrimination pathway by inhibition of the GATA transcription factor Gln3 (by favoring its association with the cytoplasmic protein Ure2) and Gat1 (by favoring its association with another unidentified cytoplasmic anchor protein). Phosphorylation and cytoplasmic retention of Gln3/Gat1 are positively regulated by TORC1 via its inhibition of Tap42-PPase Sit4 and PP2Ac (Beck and Hall, 1999; Bertram et al., 2000; Cardenas et al., 1999; Georis et al., 2011; Hardwick et al., 1999). Recent findings show that Sit4 and Pph21/22-Tpd3-Cdc55/Rts1 requirements for NCR-sensitive and rapamycin-induced nuclear Gat1 localization markedly differ from those of Gln3 (Tate et al., 2010; Tate et al., 2009). Moreover, the regulation of Gln3/Gat1 may vary in different genetic

background assayed (Georis et al., 2009). These observations indicate that TORC1 regulation of GATA factors localization and NCR-sensitive transcription might be more complicated than initially described.

TORC1 also plays an important role in the regulation of another heterodimeric transcription factor complex Rtg1-Rtg3, which activates *retrograde* (RTG) pathway and *tricarboxylic acid* (TCA) cycle genes whose products are required for glutamate/glutamine homeostasis (Reviewed in (Liu and Butow, 2006)). The nuclear accumulation of Rtg1/Rtg3, as well as expression of their target genes, is induced by addition of rapamycin, indicating TORC1 is a negative regulator of Rtg1/Rtg3-regulated genes (Komeili et al., 2000). Moreover, TORC1 represses the transcription of Rtg1/Rtg3-regulated genes presumably via its inhibition of Tap42-PPase (Duvel et al., 2003). Cytoplasmic protein Mks1 negatively regulates the RTG pathway by promoting the phosphorylation of Rtg3p and inhibiting the nuclear translocation of Rtg1/Rtg3 (Dilova et al., 2004; Sekito et al., 2002). Direct association between TORC1 and Mks1 (Breitkreutz et al., 2010) suggests that TORC1 may play a much more direct role in regulating this pathway.

The stress-responsive Zn²⁺-finger transcription factors Msn2/Msn4 are another distal targets of TORC1 (Beck and Hall, 1999). TORC1 inhibits Msn2/Msn4-dependent expression of carbon-source-regulated genes via its regulation of the Tap42-PPase branch (Santhanam et al., 2004). This regulation may (Beck and Hall, 1999) or may not (Santhanam et al., 2004) require the binding of Msn2/Msn4 to the cytoplasmic 14-3-3 proteins Bmh1/2. The regulation of TORC1 also impinges on Msn2/Msn4 through Sch9 to sequester Rim15 to the cytoplasm in association with Bmh2 (Pedruzzi et al., 2003; Reinders et al., 1998; Wanke et al., 2005).

In addition, inhibition of TORC1 also accelerates the decay of mRNAs of genes that are transcriptionally repressed following TORC1 inactivation (Albig and Decker, 2001). This will be discussed in detail below.

TORC1 also directly and indirectly inhibits autophagy (Funakoshi et al., 1997; Kamada et al., 2000; Kamada et al., 2010; Yorimitsu et al., 2009). TORC1 directly phosphorylates Atg13 at multiple serine (Ser) residues, reducing its affinity to Atg1. Consequently, Atg1 remains inactive, autophagy is thus inhibited (Kamada et al., 2000;

Kamada et al., 2010). Moreover, TORC1 indirectly inhibits autophagy via the Tap42-PPase branch (Yorimitsu et al., 2009).

Finally, under poor growth conditions, high-affinity membrane permeases are targeted to degradation, while low-affinity permeases are sorted to the membrane to facilitate uptake of a wide range of poor quality nutrients (See a review, (Loewith and Hall, 2011)). Via the Tap42-PPase target Npr1, TORC1 regulates the sorting of diverse nutrient permeases, such as turnover of the tryptophan permease Tat2 (Beck and Hall, 1999; Schmidt et al., 1998) and membrane sorting of the general amino acid permease Gap1 (De Craene et al., 2001). Several nutrient and cation permeases have been identified as rapamycin-sensitive phosphoproteins (Huber et al., 2009; Soulard et al., 2010), indicating these permeases might be direct substrates of Npr1. For instance, α -arrestin Aly2 has been recently identified as a Npr1 substrate, which regulates intracellular trafficking of Gap1 in response of nutrient availability (O'Donnell et al., 2010). In addition, TORC1-Npr1 negative kinase signaling cascade antagonizes endocytosis mediated by an ubiquitin ligase adaptor Art1 via N-terminal phosphorylation of Art1. This modification of Art1 prevents its translocation to the plasma membrane (PM). As a consequence, the Art1-dependent targeting of the Rsp5 ubiquitin ligase to the specific PM cargoes and the subsequent endocytosis is inhibited (MacGurn et al., 2011).

I. 2. 3 The Pho85 signaling pathway: negative regulator of G₀ entry

While the carbon and nitrogen source availability is sensed by PKA and TORC1, respectively, the regulatory mechanisms in response to phosphate starvation remains still poorly understood. The yeast cyclin-dependent kinase (CDK) Pho85 plays an important role in regulation of the phosphate starvation responses (See reviews, (Carroll and O'Shea, 2002; Huang et al., 2007)). In association with a family of 10 cyclins, Pho85 is directed to perform distinct roles in cell growth and division (Measday et al., 1997). When inorganic phosphate is abundant, the Pho80–Pho85 kinase is active, phosphorylating and inactivating the transcription factor Pho4. As a result, Pho4 is exported out of the nucleus, the transcription of genes involved in the response to phosphate starvation (PHO genes) is therefore inhibited (Kaffman et al., 1994; O'Neill et al., 1996). When inorganic phosphate becomes scarce, the CDK inhibitor Pho81 binds to Pho80-Pho85 complex, allowing dephosphorylated Pho4 to be

translocated into the nucleus to active the transcription of PHO genes (Komeili and O'Shea, 2000).

In addition to inhibition of phosphate starvation responses, Pho85 also negatively regulates a number of glucose-limitation induced genes (Carroll et al., 2001; Nishizawa et al., 2004; Timblin and Bergman, 1997). Pho80-Pho85 cyclin-CDK complex antagonizes the expression of glucose-limitation induced genes in part via its phosphorylation and consequently cytoplasmic sequestration of Rim15 (Wanke et al., 2005). Moreover, Pho80-Pho85 cyclin-CDK complex also phosphorylates and causes rapid nuclear exclusion of Crz1, which is involved in activation of calcineurin-dependent responses (Sopko et al., 2006; Stathopoulos and Cyert, 1997). In addition, when associated to cyclin Pcl8/10, Pho85 inhibits the glycogen synthesis, presumably via its phosphorylation of 2 carboxyl-terminal serines of Gsy2 (Huang et al., 1998; Wilson et al., 1999).

I. 3 Rim15 and G₀ entry

As stated above, PKA, TORC1 and the Pho80-Pho85 cyclin-CDK complex all negatively regulate G₀ entry in response of different nutrients. Their signaling pathways converge by different means on Rim15, a protein kinase that positively regulates G₀ entry (De Virgilio, 2012; Pedruzzi et al., 2003; Smets et al., 2010; Wanke et al., 2005).

Rim15 is serine/threonine kinase that is distantly related to the conserved *nuclear Dbf2-related* NDR family and large tumor suppressor serine/threonine kinase subclass of the protein kinase A, G, and C (AGC) class of kinases (Cameroni et al., 2004). Rim15 contains the N-terminal PAS and C₂HC-type zinc finger domains, the central protein kinase domain and a C-terminal receiver domain. The insert of 188 amino acids between the protein kinase subdomains VII and VIII of Rim15 is a unique feature shared by the NDR and the AGC kinases (Tamaskovic et al., 2003) (Fig. 3).

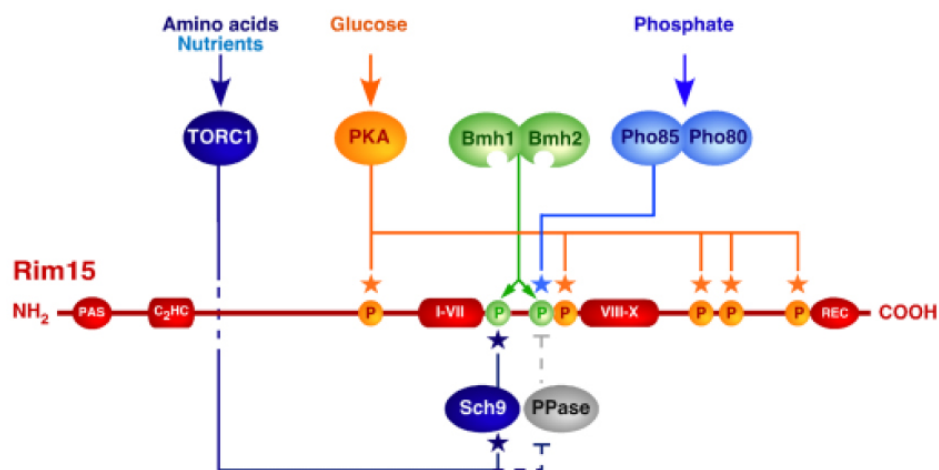


Fig. 3 Rim15 structure and nutrient signal integration (De Virgilio, 2012)

Rim15 function is regulated by at least four nutrient-regulated protein kinases TORC1 and its target Sch9, PKA and Pho80-Pho85 cyclin-CDK complex via direct phosphorylation events, as well as presumably by a protein phosphatase (PPase) inhibited by TORC1. See below for details of underlying mechanisms.

I. 3. 1 Rim15 is negatively regulated by PKA, TORC1 and the Pho80-Pho85 cyclin-CDK complex

Initially identified in a screen for mutations that cause reduced expression of the early meiosis gene *IME2* (Su and Mitchell, 1993), Rim15 has been then independently identified as a physical interactor of trehalose-6-phosphate synthase (Tps1) (Reinders et al., 1998), which initiated the understanding of its role as a positive regulator of the G₀ program initiation and the regulation of its function (Fig. 4).

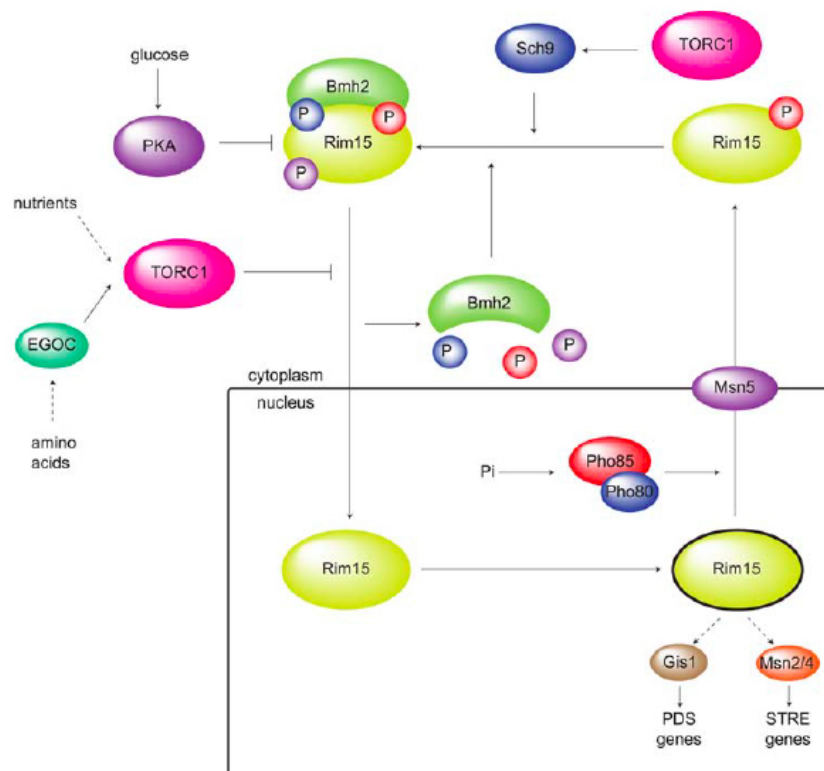


Fig. 4 The Rim15 protein kinase acts as a nutritional integrator in *S. cerevisiae* (Smets et al., 2010)

Rim15 is regulated by at least four nutrient signaling protein kinases. In response to glucose, PKA directly phosphorylates and thereby inactivates the kinase activity of Rim15. Pho80-Pho85 cyclin-CDK complex phosphorylates Rim15 at Thr¹⁰⁷⁵ to promote its association with 14-3-3 protein Bmh2 for its cytoplasmic retention. Active TORC1 and Sch9 also promote cytoplasmic sequestration of Rim15 by favoring phosphorylation at Ser¹⁰⁶¹ by Sch9 and maintaining phosphorylation at Thr¹⁰⁷⁵ via inhibiting a yet unidentified protein phosphatase. Inactivation of TORC1 and Sch9 results in the nuclear translocation of Rim15 where it activates the expression of Msn2/4- and Gis1-dependent genes. Rim15 is subject to autophosphorylation, which apparently stimulates Msn5-mediated nuclear export.

Rim15 is required for entry into G₀ phase and its function is negatively regulated by PKA

The deletion of *RIM15* impairs different G₀ program traits, such as trehalose and glycogen accumulation, thermotolerance, stationary phase survival, proper G₀ arrest and the transcription of G₀-specific genes. This suggests that Rim15 is required for proper G₀ program initiation (Reinders et al., 1998). Notably, the deletion of *RIM15* rescues the growth defect of *cdc35^{ts}* and *tpk1 tpk2 tpk3* mutants, while *RIM15* overexpression suppresses the defect of trehalose accumulation, *SSA3-lacZ* induction and thermotolerance in a *bcy1-1* mutant, in which PKA is constitutively active. Consistently, *RIM15* overexpression exacerbates the temperature-sensitive growth defect of a *cdc35-10* mutant. These findings indicate that Rim15 functions downstream of PKA and is inhibited by PKA (Reinders et al., 1998). Furthermore, it has been demonstrated that Rim15 kinase activity is inhibited by PKA via its phosphorylation at five Ser residues (*i.e.* Ser⁷⁰⁹, Ser¹⁰⁹⁴, Ser¹⁴¹⁶, Ser¹⁴⁶³ and Ser¹⁶⁶¹) (Reinders et al., 1998).

Rim15 is required for rapamycin-induced G₀ entry and its function is negatively regulated by TORC1

Further studies have shown that G₀ traits are also impaired in *rim15Δ* cells following rapamycin-induced TORC1 inactivation, indicating that TORC1 prevents induction of Rim15-dependent G₀ entry (Pedruzzi et al., 2003). Interestingly, in *pka yak1Δ* cells, accumulation of G₀-specific mRNAs (*i.e.* *SSA3*, *HSP12*, and *HSP26*) is induced by rapamycin treatment. This accumulation strongly depends on the presence of Rim15, as *pka rim15Δ* cells fail to accumulate these G₀-specific mRNAs. This suggests that TORC1 negatively controls Rim15 function via a PKA-independent mechanism. The deletion of *SIT4* does not significantly alter the level of Rim15-dependent G₀-specific mRNAs, while Sit4-dependent rapamycin-inducible *DAL5* and *PUT1* mRNAs accumulation is not Rim15-dependent. These observations suggest that TORC1 regulation of Rim15 is independent of its downstream proximal effector Sit4. Curiously, *pph21Δ pph22Δ* double deletion increases the basal level of G₀ transcripts following rapamycin treatment, indicating that the PP2Ac may play a role in inhibition of the G₀ program initiation (Pedruzzi et al., 2003). Further studies showed that

TORC1 regulates Rim15 subcellular localization via two processes: (i) TORC1 substrate Sch9 mediates the phosphorylation at the Ser¹⁰⁶¹ residue of Rim15 and (ii) The TORC1 inhibits a phosphatase (possibly Tap42-PPase), which target the Thr¹⁰⁷⁵ residue of Rim15. The phosphorylation at both Ser¹⁰⁶¹ and Thr¹⁰⁷⁵ residues of Rim15 favors its cytoplasmic sequestration by association with 14-3-3 protein Bmh2 (Pedruzzi et al., 2003; Wanke et al., 2008; Wanke et al., 2005) (Fig. 4).

Pho80-Pho85 cyclin-CDK complex negatively regulates Rim15

In parallel of TORC1, the Pho80-Pho85 cyclin-CDK complex has also been found to regulate Rim15 function through direct phosphorylation, and as consequence, promoting Rim15 cytoplasmic retention via its association with Bmh2 (Wanke et al., 2005) (Fig. 4).

The Thr¹⁰⁷⁵ residue has been found to be crucial for the binding of Bmh2 to Rim15. Depletion of Bmh1/2 results in nuclear accumulation of Rim15. These data suggests that the Pho80-Pho85 complex promotes Rim15 cytoplasmic retention by phosphorylation of Rim15 at Thr¹⁰⁷⁵ thereby favoring its association with Bmh2 in exponentially growing cells. Finally, the kinase activity of Rim15 has been found to be critical for its nuclear export in a karyopherin Msn5-dependent manner (Wanke et al., 2005).

Taken together, Rim15 is regulated by TORC1 via Sch9, PKA and the Pho80-Pho85 cyclin-CDK complex. Under starvation conditions, inhibition of these kinases leads to dephosphorylation of Rim15, promoting release from with Bhm2 and nuclear accumulation. In the nucleus, Rim15 undergoes autophosphorylation allowing its nuclear export via karyoporin Msn5. Nuclear Rim15 triggers the activation of the expression of Msn2/4- and Gis1-dependent stress response genes, the underlying mechanisms of which is still poorly understood (See reviews (De Virgilio, 2012; Smets et al., 2010)) (Fig. 4).

I. 3. 2 Rim15 regulates distal readouts that are essential for G₀ program initiation

Previous studies in the lab have identified several distal readouts of Rim15 that regulate the G₀ program initiation (Cameroni et al., 2004; Pedruzzi et al., 2000; Pedruzzi et al., 2003).

The transcription factor Gis1 has been identified as a dosage-dependent suppressor of the defect of *rim15Δ* cells in nutrient limitation-induced expression of G₀-specific *SSA3* gene (Pedruzzi et al., 2000). This suggests that Gis1 may function downstream of Rim15. Similarly to Gis1, which activates transcription of *post-diauxic shift* (PDS) elements containing genes, Msn2/4 may also activate G₀-specific genes via their binding to *stress response elements* (STREs) containing genes (Pedruzzi 2000). Furthermore, a genome wide transcriptional profiling study showed that the 73% of Gis1-dependent genes and 40% of Msn2/4-dependent genes are regulated by Rim15 at the diauxic shift (Cameroni et al., 2004). These data indicate that Gis1, Msn2 and Msn4 may all act downstream of Rim15 to activate the G₀ program.

I. 4 Post-transcriptional regulation: mRNA decay pathways

As summarized above, Rim15 functions to activate the transcription of G₀-specific genes following glucose-limitation or rapamycin treatment. Regulation of mRNA decay also plays an important role in the control of gene expression. Interestingly, inhibition of TORC1 accelerates the decay of mRNAs of genes that are transcriptionally repressed following TORC1 inactivation (Albig and Decker, 2001). In parallel, mRNAs of genes induced during the initiation of G₀ program have to be protected from degradation. This suggests that G₀ mRNAs are also subjected to post-transcriptional regulation.

Most mRNAs undergo decay by the deadenylation-dependent pathway (See review (Balagopal et al., 2012; Garneau et al., 2007)) (Fig. 5). In this mRNA decay pathway, shortening of the 3' poly(A) tail (deadenylation) is the first and often rate-limiting step (Decker and Parker, 1993; Muhlrud et al., 1994). Two deadenylation complexes contribute to this biphasic deadenylation step: (1) the Pan2/Pan3 deadenylase initiates a partial removal of the poly(A) tail (Brown and Sachs, 1998); and (2) the deadenylation is completed by the

Ccr4-Not complex that contains Ccr4 and Caf1, the main two deadenylases required for the removal of the remaining oligo(A) tail (see review, (Miller and Reese, 2012)).

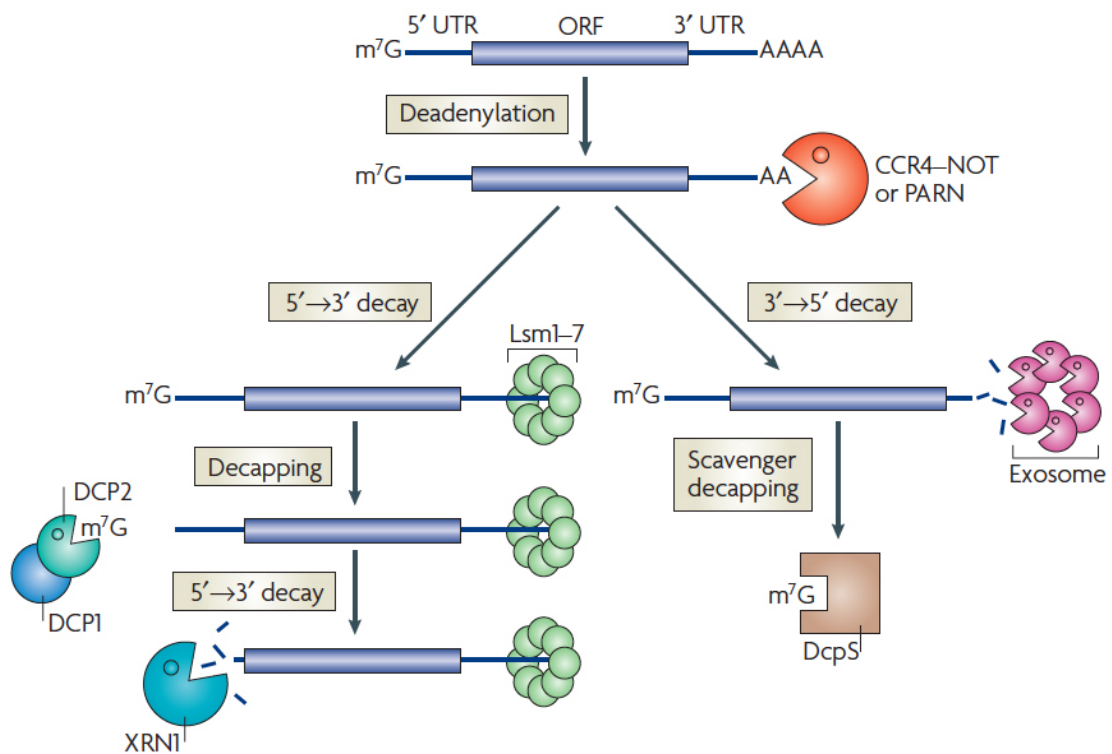


Fig. 5 Deadenylation-dependent mRNA decay (Garneau et al., 2007)

Most mRNAs undergo decay by the deadenylation-dependent pathway. The poly(A) tail is removed by a deadenylase activity, shown here as either Ccr4-NOT or PARN (Pan2/3 complex). Following deadenylation, two mechanisms can degrade the mRNA: either decapping followed by 5'-3' decay or 3'-5' decay. In the decapping pathway, the Lsm1-7 complex associates with the 3' end of the mRNA transcript and induces decapping by the Dcp1-Dcp2 complex. This leaves the mRNA susceptible to decay by the 5'-3' exonuclease Xrn1. Alternatively, the deadenylated mRNA can be degraded in the 3'-5' direction by the cytoplasmic exosome, with the remaining cap structure being hydrolyzed by the scavenger-decapping enzyme DcpS.

Once deadenylated, the unprotected 3'-end of the mRNA can potentially undergo 3'-5' degradation catalyzed by the cytoplasmic exosome. Following 3'-5' decay, the 5' cap structure on the remaining oligomer is hydrolyzed by the scavenger decapping pyrophosphatase Dcs1 (Liu et al., 2002). In *S. cerevisiae*, however, deadenylation is primarily followed by the removal of the 5'-m⁷G-cap (decapping) and a 5'-3' decay catalyzed by the cytoplasmic exonuclease Xrn1 (Balagopal et al., 2012). In this 5'-3' decay pathway, the removal of the 5'-cap is a highly regulated step that is catalyzed by the dimeric decapping enzyme Dcp1/Dcp2. Dcp2, the catalytic subunit of the decapping enzyme, recognizes and binds to mRNA and Dcp1 is required for increasing the catalytic rate by changing the conformation of Dcp2 (Deshmukh et al., 2008; Floor et al., 2008; Floor et al., 2010; Steiger et al., 2003).

Numerous decapping activators are required for the maximal activity of the decapping enzyme Dcp1/2. These decapping enhancers act by multiple mechanisms (Nissan et al., 2010). Edc1-3 proteins enhance decapping by their interaction with the Dcp1/2 complex. Proline-rich proteins Edc1 and Edc2 recognize and bind Dcp1 to enhance both mRNA substrate binding and the catalytic decapping by Dcp2. Edc3, in contrast to Edc1 and Edc2, binds directly to Dcp2 to enhance decapping (Balagopal et al., 2012). Dhh1, a DEAD-box RNA helicase, plays a significant role in the general mRNA decay pathway but does not affect the decay of non-translating mRNA *in vivo* (Coller et al., 2001; Fischer and Weis, 2002). Dhh1 is therefore likely to promote decapping by repressing translation inhibition (Coller and Parker, 2005; Nissan et al., 2010). Pat1 enhances decapping activity via both activation of the decapping enzyme and repression of translation initiation (Nissan et al., 2010). In addition, as Pat1 physically interacts with Dcp1/2 and multiple decapping activators, it may serve as a scaffold to recruit components of the decapping complex (Marnef and Standart, 2010; Nissan et al., 2010). In association with Pat1, the heptameric Lsm1-7 complex binds to the 3' end of deadenylated mRNAs via the C-terminal part of Lsm1 (Chowdhury et al., 2012) and promotes decapping (Tharun et al., 2000; Tharun and Parker, 2001). Finally, decapped mRNA is rapidly and processively hydrolyzed by the major cytoplasmic 5'-3' exonuclease Xrn1 (Jinek et al., 2011).

I. 4. 1 Subcellular localization of mRNA decay: P bodies

In eukaryotes, mRNA decapping and 5' to 3' degradation has been proposed to occur in discrete cytoplasmic foci, termed processing bodies (P bodies) (Sheth and Parker, 2003), which strongly increases in numbers and size following exposure to environmental stresses, such as glucose deprivation (Eulalio et al., 2007; Parker and Sheth, 2007). Surprisingly, following rapamycin treatment, no increase in size and number of P bodies are observed (Talarek 2010, Ramachandra 2011).

The complete protein composition of P bodies is not yet determined. To date, it is known that P bodies contain a conserved core of proteins that consists of the mRNA decapping machinery described above and non-translating mRNAs (Eulalio et al., 2007; Parker and Sheth, 2007). A recent study of ultrastructural organization of P bodies in human cells revealed that P bodies are huge ribonucleoprotein complexes localized in the close proximity of mitochondria and ribosomes. They comprise at least two distinct compartments: a dense core where decay enzymes accumulate and peripheral protrusions where p54 (Dhh1 homologue) and ribosomes are localized (Cougot et al., 2012). Moreover, the anchoring of p54 at the periphery appears to be required for P bodies maintenance (Cougot et al., 2012). The presence of P bodies in close vicinity of ribosomes may explain the observation that mRNAs undergo co-translational 5'-3' decay (Hu et al., 2009).

The mechanisms, by which stresses induce P body formation remain to be clarified. Two recent studies showed that following glucose deprivation Ste20 and PKA phosphorylate Dcp2 and Pat1, respectively. While the phosphorylation of the former is required for its recruitment to P bodies (Yoon et al., 2010), the phosphorylation of the latter strongly reduces the formation of P bodies (Ramachandran et al., 2011).

I. 4. 2 Stress granules: storage sites of mRNPs that may reenter into translation

Another type of cytoplasmic foci termed stress granules has been observed in all eukaryotes following stress, such as glucose starvation in yeast or arsenite treatment in mammalian cells (Buchan and Parker, 2009). Stress granules have been first observed in mammalian cells as cytoplasmic foci that form when translation initiation rates decrease during a stress response (Kedersha et al., 2005). Stress granules typically contain poly(A)+mRNA, 40S ribosomal subunits, eIF4E, eIF4G, eIF4A, eIF4B, *poly(A)-binding protein* (Pabp), eIF3, and eIF2, although the composition can vary depending on different stresses (Buchan and Parker 2009). The equivalent of stress granules in yeast, are referred to as EGP-bodies (for containing eIF4E, eIF4G and Pab1). They are observed in cells subjected to glucose starvation (Hoyle et al., 2007).

It appears that stress granules assembly is dependent on P-body formation, whereas P-body assembly is independent of stress granule formation (Buchan et al., 2008). This suggests that stress granules primarily form from mRNPs in preexisting P bodies. Once in P bodies, mRNAs are targeted by yet elusive mechanisms, to be degraded or to be stored subsequently in stress granules before returning to translation. This suggestion is supported by a recent study, which showed that a subset of translationally repressed transcripts of about 400 genes, can be reactivated for translation upon glucose re-addition in the absence of new transcription (Arribere et al., 2011).

The interaction of stress granules with P bodies provides evidence for an mRNA cycle. A model published recently tries to summarize this mRNA cycle between polysomes, P bodies and stress granules following exposure to stress (Fig. 6). Under favorable growth conditions, translation of housekeeping genes occurs normally on polysomes (1). Following exposure to environmental stress, such as glucose limitation, translation initiation of these housekeeping genes is inhibited. The corresponding mRNAs either undergo cotranslational decay (2) or following ribosomes disassembly, factors of the 5'-3' decay machinery are recruited (3). The mRNPs aggregate or not into P bodies (4) to either be degraded (5) or stored. The mRNPs that escape decay are subjected to remodeling as a result of which disassembly of factors of the 5'-3' decay machinery and the assembly of translation initiation machinery form stress granules (6). When conditions become suitable for growth, mRNAs reenter translation (7). Stress-induced mRNAs maybe incorporated into this mRNA cycle in P

bodies or stress granules (8), but are protected from degradation by some yet to be elucidated mechanisms (Buchan and Parker, 2009).

Taken together, this model suggest that mRNPs within P bodies can be remodeled and then accumulate within stress granules. This implies an important role of P bodies for mRNA sorting, which determines whether an mRNA is stored, is degraded, or returns to translation (Buchan and Parker, 2009).

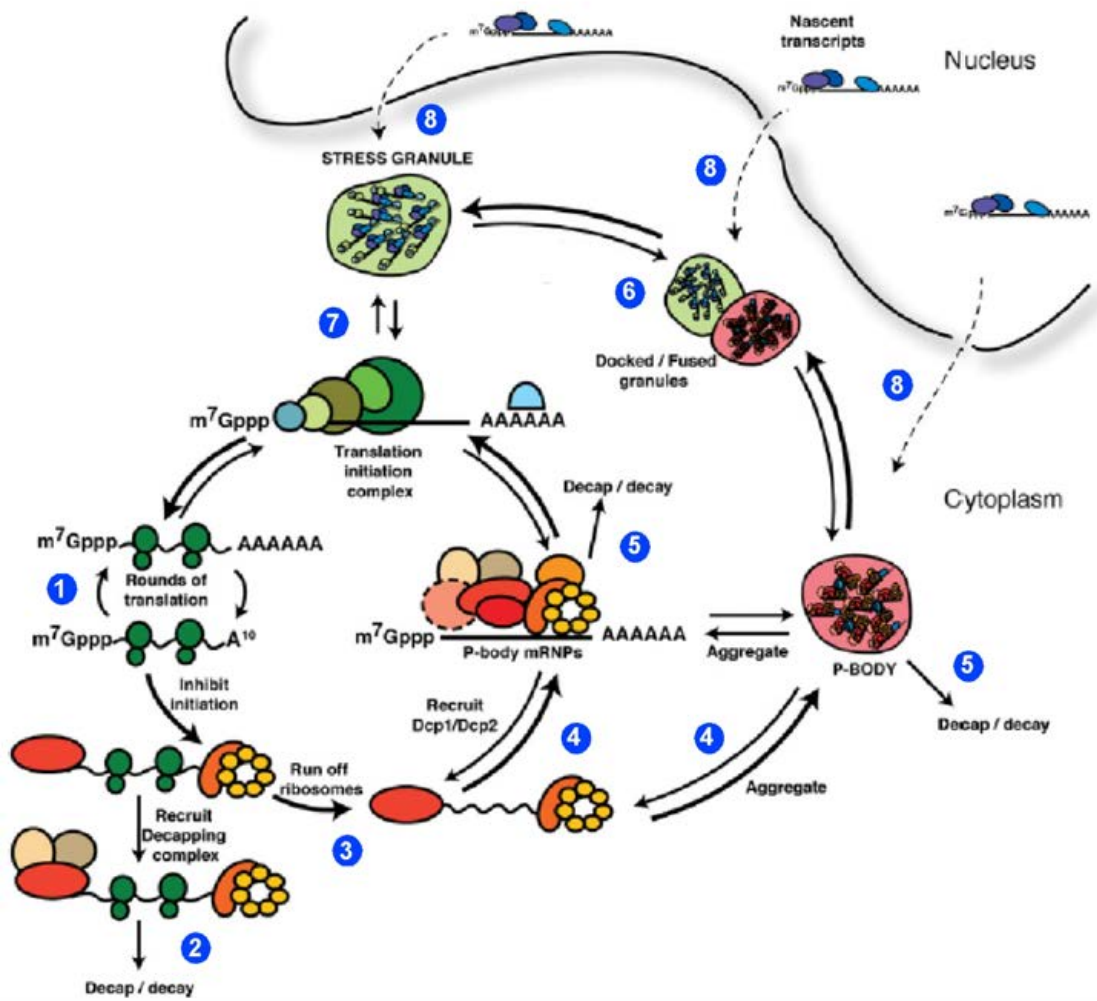


Fig. 6 Model integrating stress granules, and P-Bodies, into an mRNP cycle (Adapted from (Buchan and Parker, 2009))

A speculative model for mRNP transitions, particularly during stress. Following exposure to stress, translating mRNP could be targeted to co-translational decay, or assembly with 5'-3' decay machinery into P bodies before being channeled to stress granules for subsequent reentry into translation. Dashed arrows indicate possible destination of exported nascent transcripts. Bold arrows are thought to be the main route in the mRNA cycle under stress conditions.

I. 5 Igo1/2 regulate G₀-specific RNA stability

I. 5. 1 The Rim15 substrates Igo1/2 protect G₀-specific mRNAs from degradation by the 5'-3' decay pathway

In our attempt to elucidate the regulation of G₀ entry by Rim15, we identify Igo1 as direct substrate of Rim15 by using the proteome chip array technology (Ptacek et al., 2005). In *S. cerevisiae*, the paralogue of Igo1, Igo2 shares 58% of homology with Igo1 (Talarek et al., 2010). Both Igo1/2 belong to the conserved family of α -endosulfine proteins (Dulubova et al., 2001) (Fig. 7). Small (16-20 kDa) proteins of the α -endosulfine family in higher eukaryotes, such as the cAMP-regulated phosphoprotein-19 (ARPP-19) and α -endosulfine (Ensa), have been identified: ARPP-19 is a major substrate of PKA in brain tissue (Girault et al., 1990), while α -endosulfine was originally identified as an endogenous ligand of sulfonylurea receptors that are coupled to ATP-dependent potassium channels in the pancreas (Virsolvy-Vergine et al., 1992). They are involved in diverse biological processes, including insulin secretion (Bataille et al., 1999), oocyte meiotic maturation (Von Stetina et al., 2008), neurodegeneration (Woods et al., 2007) and axon growth (Irwin et al., 2002). Interestingly, in a nerve growth factor (NGF)-dependent manner, ARPP-19 binds to a region in the 3'-end of GAP-43 mRNA. This binding is important for stabilizing this mRNA in a PKA-dependent manner (Irwin et al., 2002).

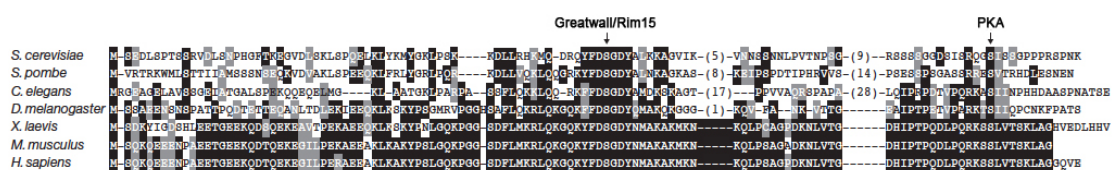


Fig. 7 *S. cerevisiae* Igo1 and Igo2 belong to the conserved family of α -endosulfine proteins (Adapted from (Mochida and Hunt, 2012))

Sequence alignment of the Ensa subfamily from yeast to human. Greatwall/Rim15 and PKA phosphorylation sites are indicated with arrows.

Our study further demonstrated that Igo1 is activated by Rim15 by phosphorylation at the conserved Ser⁶⁴ (Talarek et al., 2010). Like Rim15, Igo1/2 are required for the proper control of the expression of a subset of G₀-specific genes (e.g. *HSP26*) following rapamycin-induced TORC1 inactivation and for proper chronological life span following G₀ entry. Importantly, Igo1 physically interacts with Dhh1, Pbp1, Pbp4 and Lsm12, which are all involved in regulating mRNA stability. Dhh1, a DEAD-box RNA helicase, is a decapping activator in the 5'-3' decay pathway (Coller and Parker, 2005). Pbp1, via its interaction with Poly(A) binding proteins Pab1, and the Pbp1 binding protein Pbp4 are involved in the regulation of mRNA polyadenylation (Mangus et al., 1998; Mangus et al., 2004a; Mangus et al., 2004b). Lsm12, a physical interactor of Pbp1 and Pbp4 (Fleischer et al., 2006), likely binds the 3' untranslated region (UTR) of mRNAs (Albrecht and Lengauer, 2004). Interestingly, the interaction between Igo1 and these partners is strongly increased following rapamycin treatment. However, none of these interactions is dependent on the presence of mRNAs. The rapamycin-induced interaction between Igo1 and Dhh1 and Lsm12 is dependent on the phosphorylation at Ser⁶⁴. This suggests that following TORC1 inactivation, mRNPs containing at least Igo1/2, Pbp1 and Pbp4 are formed. Moreover, the phosphorylation of Igo1 by Rim15 subsequently leads to the recruitment of Dhh1 and Lsm12 to these mRNPs. These data prompted us to speculate that Igo1/2 may play a role in stabilizing the substantial subset of rapamycin-induced, Igo1/2-dependent mRNA species. This assumption was confirmed by the fact that the half-life of total poly(A)+ RNAs is significantly reduced in *igo1Δ igo2Δ* cells compared to wild type cells when both are treated with rapamycin. In line with this result, loss of Igo1/2 reduce the half-life of a specific *HSP26-lacZ* mRNA by 65% in rapamycin-treated cells. Furthermore, loss of Dhh1 and Ccr4, which represent activator of decapping and the deadenylase in the 5'-3' mRNA decay pathway, respectively, suppress the defect of *igo1Δ igo2Δ* cells, but not that of *rim15Δ* cells in expression of G₀-specific gene *HSP26* at both the mRNA and protein levels. This suggests that Igo1/2 may prevent degradation of mRNAs via the 5'-3' mRNA decay pathway. Interestingly, loss of the 5'-3' exonuclease Xrn1 in *igo1Δ igo2Δ* cells leads to the accumulation of *HSP26* mRNA in P bodies that are not translated. In addition, as the colocalization between Igo1 and P bodies decreases during glucose exhaustion, the colocalization of Igo1 and stress granules increase (Talarek et al., 2010). These data suggest that Igo1 may escort *HSP26* mRNA from P bodies to stress granules.

Taken together, Igo1/2 is phosphorylated by Rim15 at Ser⁶⁴ and therefore activated. Active Igo1/2 bind to the P body component Dhh1 to shelter G₀-specific mRNA from degradation and subsequently channel them towards stress granules for subsequent translation. However, the molecular mechanisms of Igo1/2 function remain to be elucidated.

I. 5. 2 Igo1 homologues ARPP-19 and Ensa inhibit PP2A^{Cdc55}

Recent studies in *Xenopus* shed light on at least one of the molecular functions of the Igo1 homologues ARPP-19 and Ensa (Gharbi-Ayachi et al., 2010; Mochida et al., 2010).

In *Xenopus* egg extracts, M phase kinase Gwl (Rim15 homologue) is activated in mitosis by phosphorylation and is essential for both mitotic entry and maintenance (Yu et al., 2006). Gwl apparently promotes mitosis by inactivating PP2A-B55 δ (Castilho et al., 2009; Vigneron et al., 2009). Although Gwl binds directly to PP2A-B55 δ (Vigneron et al., 2009), substantial phosphorylation of the components of PP2A-B55 δ is not detectable *in vitro*. Gwl is therefore suspected to act by phosphorylating and activating some unidentified PP2A-B55 δ -specific inhibitor protein (Mochida et al., 2010).

A KESTREL (kinase substrate tracking and elucidation) method allowed the identification of Gwl substrates (Mochida et al., 2010). The two Igo1/2 homologues, ARPP-19 and Ensa, which belongs to the α -endosulfine protein family, were identified as substrates of Gwl. ARPP-19 and Ensa have been demonstrated to inhibit the phosphatase activity of PP2A-B55 δ *in vitro*. As a result, phosphorylation of mitotic phospho-targets may be maintained *in vivo* which is important to promote mitotic entry. The inhibitory activity of ARPP-19 and Ensa on PP2A-B55 δ is dependent on the phosphorylation at their conserved Ser⁶⁷ by Gwl (Mochida et al., 2010), which corresponds to the site at which Rim15 phosphorylates Igo1/2 in yeast. Another study also independently demonstrated that activated Gwl phosphorylates both ARPP-19 and Ensa, which interacts with and inhibits PP2A. However, only the inhibition of PP2A by ARPP-19 can promote mitotic entry in *Xenopus* egg extracts (Gharbi-Ayachi et al., 2010).

Although it is not yet clear whether Gwl kinase itself may also inhibit directly PP2A (Mochida et al., 2010; Vigneron et al., 2009), these data clearly established an inhibitory role of the substrates of Gwl, *i.e.* ARPP-19 and Ensa on PP2A phosphatase.

PP2A Phosphatase in yeast and its regulation

The yeast *protein serine/threonine phosphatase 2A* (PP2A) is a multifunctional enzyme whose trimeric form consists of a scaffolding A subunit, a catalytic C subunit, and one of two regulatory B subunits, namely Cdc55 and Rts1 (Jiang, 2006). The A subunit Tpd3 is the structural subunit that serves as a scaffold to accommodate the other two subunits. The C subunits are the catalytic subunit Pph21 or Pph22, which, in complex with the A subunit, form the dimeric core enzyme. Each of these two catalytic subunits contributes approximately half of the PP2A activity in the cell (Ronne et al., 1991; Sneddon et al., 1990). The B subunit Cdc55 or Rts1 are the regulatory subunits that dictate the substrate specificity and intracellular localization of the AC dimeric core enzyme (Cohen, 1989). Numerous studies showed that PP2A plays roles in cell morphology and cell cycle regulation (Evans and Stark, 1997; Lin and Arndt, 1995; Sneddon et al., 1990).

As introduced earlier, *pph21Δ pph22Δ* double deletion increases the basal level of G₀ transcripts following rapamycin treatment, indicating that the PP2A may play a role in inhibition of G₀ program initiation (Pedruzzi et al., 2003). Moreover, by analogy with the results obtained in metazoans, we could speculate that in yeast cells subjected to rapamycin treatment or glucose limitation, once Igo1/2 is activated by Rim15, they may inhibit PP2A to thereby allowing the activation of downstream effectors that promote G₀ entry. This suggests that the inhibition role of α -endosulfines on PP2A^{Cdc55} form may be conserved throughout evolution.

Taken together, the Rim15 substrates Igo1/2 play a role in inhibiting the degradation of G₀ specific mRNAs by the 5'-3' decay pathway. In addition, Igo1/2 may also promote TORC1 controlled G₀ entry by inhibiting PP2A^{Cdc55}. My thesis research aimed at exploring the roles of Igo1/2 in controlling gene expression during initiation of the G₀ program and elucidating the underlying mechanisms. A particularly appealing model posits that Igo1/2 regulate gene expression via inhibition of PP2A.

Chapter II. Igo1 localization

Previous studies showed that the nuclear localization of the Rim15 kinase is antagonized by TORC1 and the Pho80-Pho85 cyclin-CDK through (Albrecht and Lengauer, 2004) phosphorylation of the 14-3-3-binding site in Rim15. Inactivation of either TORC1 or Pho80-Pho85 causes dephosphorylation of critical residues within the 14-3-3-binding site in Rim15, thus enabling nuclear import of Rim15 and induction of the Rim15-dependent G₀ program (Pedruzzi et al., 2003; Wanke et al., 2005). Our most recent studies demonstrated that Rim15 phosphorylates its direct substrate Igo1 at a conserved serine residue (*i.e.* Ser⁶⁴), and that Igo1 accumulates in the nucleus following glucose limitation (Talarek et al., 2010). These results suggest that Rim15 may play a role in Igo1 localization. In addition, Igo1 harbors a putative PKA phosphorylation site present at Ser¹⁰⁵, which appears to be conserved (Talarek et al., 2010). Mutation of this serine to a non-phosphorylatable alanine does not significantly affect the function of Igo1 *in vivo* (Cameroni, unpublished data). Thus, the role of PKA in regulating Igo1 function remains enigmatic.

In order to better understand whether and how Igo1 localization maybe regulated by Rim15 and/or by PKA, the functionality and localization of GFP-tagged Igo1 variants, which are nonphosphorylatable at either the Rim15 or PKA phosphorylation sites, or which carry phosphomimetic residues instead, were analyzed prior to and following rapamycin treatment.

Furthermore, to address the question in which subcellular compartment Igo1 fulfills its main function, we fused a well-characterized yeast nuclear localization signal (NLS) or a nuclear export signal (NES) to Igo1-GFP so that Igo1-GFP constitutively localized in the nucleus or the cytoplasm, respectively. The functionality of these Igo1 variants with restricted localization was then assessed.

II. 1 GFP-tagged Igo1 variants behave as their non-tagged counterparts

To analyze the localization of Igo1-GFP variants and their regulation by Rim15 and/or PKA, we constructed by homologous recombination centrometric plasmids expressing, under the endogenous *IGO1* promoter, GFP-tagged wild type *IGO1*, *IGO1^{S64A}* and *IGO1^{S105A}*, which are non-phosphorylatable by Rim15 and PKA, respectively, as well as the phosphomimetic variants *IGO1^{S64D}* and *IGO1^{S105D}*. The functionality of GFP-tagged Igo1 variants was assessed quantitatively by analyzing their capacity to complement the defect of an *igo1Δ igo2Δ* mutant. To this end, we measured the expression of the bacterial β -galactosidase-encoding *lacZ* gene under the control of the yeast *HSP26* promoter that is specifically induced upon rapamycin treatment in an Igo1/2-dependent manner (Fig. 8).

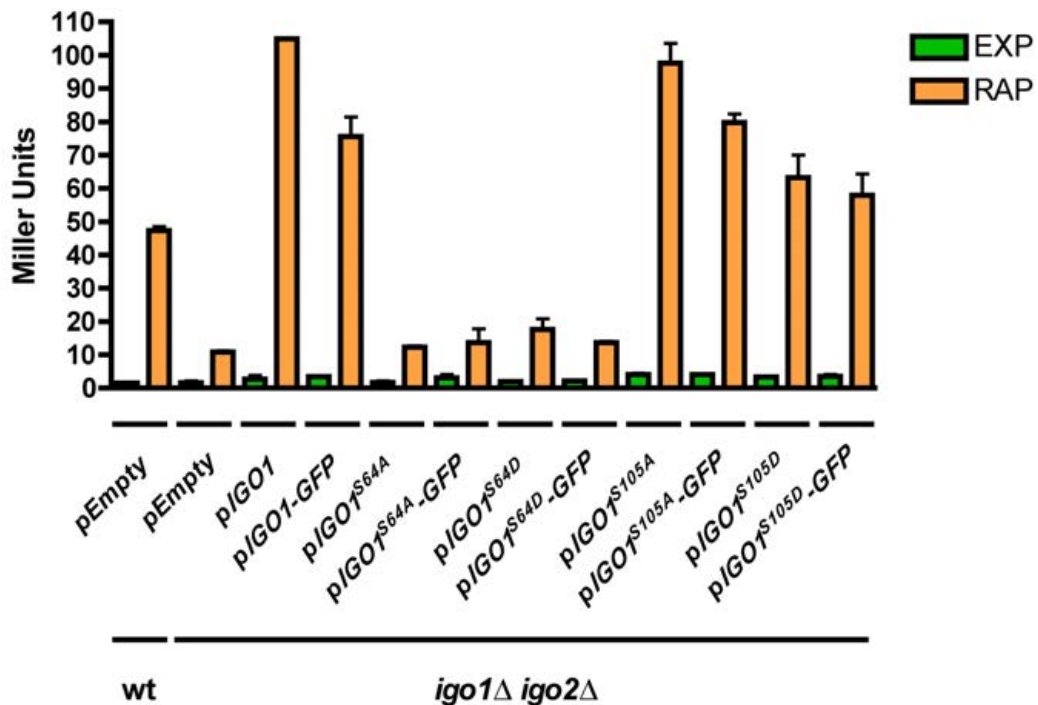


Fig. 8 Complementation of an *igo1Δ igo2Δ* mutant by the GFP-tagged Igo1 variants

Wild type or *igo1Δ igo2Δ* strains were cotransformed with indicated Igo1 variants and the *HSP26-lacZ* reporter. β -galactosidase activities (expressed in Miller units) were measured to monitor the expression of an *HSP26-lacZ* fusion gene in exponentially growing cells prior to (EXP) or following rapamycin treatment (RAP; 0.2 $\mu\text{g ml}^{-1}$; 6 hr). Data are reported as averages ($n = 3$), with standard deviations (SDs) indicated by the lines above each bar. Relevant genotypes are indicated.

During exponential growth, all strains showed a basal level of β -galactosidase activity. Following treatment of cells for 6 hr with rapamycin, β -galactosidase activity increased 50-fold in wild-type cells, but only 10-fold in *igo1 Δ igo2 Δ* mutant cells. The latter defect was complemented by expression of wild-type Igo1, Igo1^{S105A} and Igo1^{S105D}, but not by expression of Igo1^{S64A} and Igo1^{S64D}. The GFP-tagged versions of Igo1, Igo1^{S64A}, Igo1^{S64D}, Igo1^{S105A} and Igo1^{S105D} behaved as their non-tagged counterparts in this assay. These constructions are therefore suitable for localization analyses.

II. 2 Nuclear accumulation of Igo1-GFP upon rapamycin treatment depends on phosphorylation of Igo1-GFP at Ser⁶⁴ by Rim15

In order to assess the regulation of Igo1 localization by Rim15, we analyzed by fluorescence microscopy the subcellular localization of Igo1-GFP fusion protein in an *igo1 Δ* or an *igo1 Δ rim15 Δ* mutant as well as the localization of Igo1^{S64A}-GFP in an *igo1 Δ* mutant both prior to and following rapamycin treatment.

During exponential growth (*igo1 Δ* background), Igo1-GFP and Igo1^{S64A}-GFP had a diffuse localization in both the cytoplasm and the nucleus. Remarkably, similarly to previous observations where Igo1 accumulated in the nucleus upon glucose exhaustion (Talarek et al., 2010), Igo1 accumulated in the nucleus in cells that were treated for 3 hr with rapamycin (Fig. 9). To quantitatively determine the nuclear Igo1-GFP signal over time of the rapamycin treatment, images were taken at time point 0, 30 min, 60 min, 120 min and 180 min following rapamycin addition. The relative nuclear Igo1-GFP signal was quantified by comparison of the fluorescence intensity in the nucleus versus the one in the cytoplasm (Fig. 10A). The Igo1-GFP nuclear signal steadily increased until 3 hours after the treatment, whereas Igo1-GFP in *igo1 Δ rim15 Δ* mutant cells or Igo1^{S64A}-GFP in *igo1 Δ* mutant cells failed to do so (Fig. 9). To rule out the possibility that Igo1-GFP nuclear accumulation might be due to protein expression increase, Igo1-GFP protein levels in each strain at different time point was assessed by western blot. The total Igo1 protein level stayed constant during the three hours rapamycin treatment in all strains (Fig. 10B). To check whether Igo1-GFP forms cytoplasmic dots, like it does following glucose exhaustion (Talarek et al., 2010), we looked at Igo1-GFP localization in rapamycin-treated cells following a longer rapamycin treatment (up to 6 hr).

Instead of forming cytoplasmic dots, the Igo1-GFP nuclear signal peaked at 3 hr rapamycin treatment and it then decreased, before it increased again in the nucleus (data not shown).

These results indicate that the nuclear accumulation of Igo1 protein upon rapamycin treatment depends on the phosphorylation by Rim15 at the Ser⁶⁴ in Igo1.

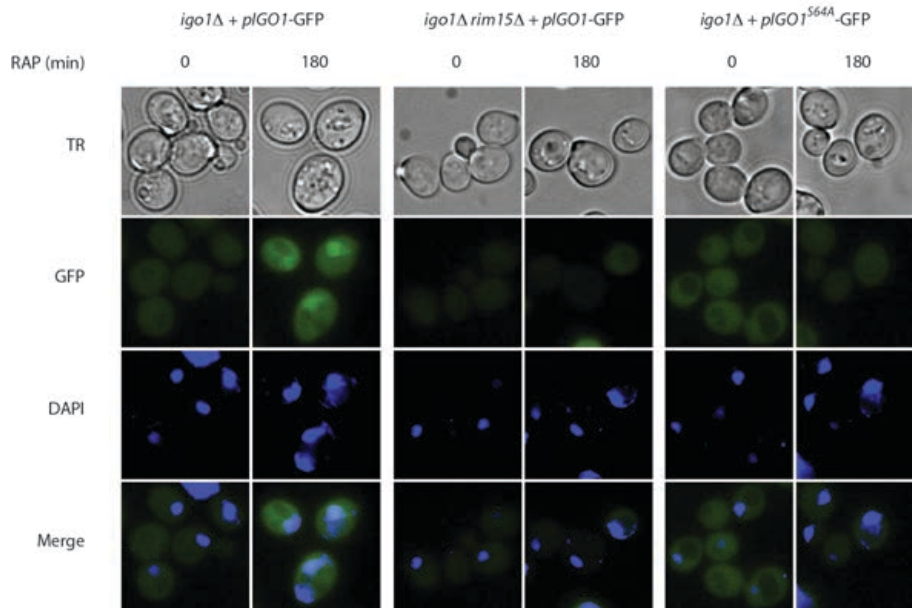


Fig. 9 Nuclear Igo1 localization upon rapamycin treatment is dependent on Rim15-mediated phosphorylation of Ser⁶⁴

igo1Δ or *igo1Δ rim15Δ* cells expressing Igo1-GFP or Igo1^{S64A}-GFP were analyzed prior to (EXP) or following rapamycin treatment (RAP; 0.2 μg ml⁻¹; 3 hr) and analyzed by fluorescence microscopy.

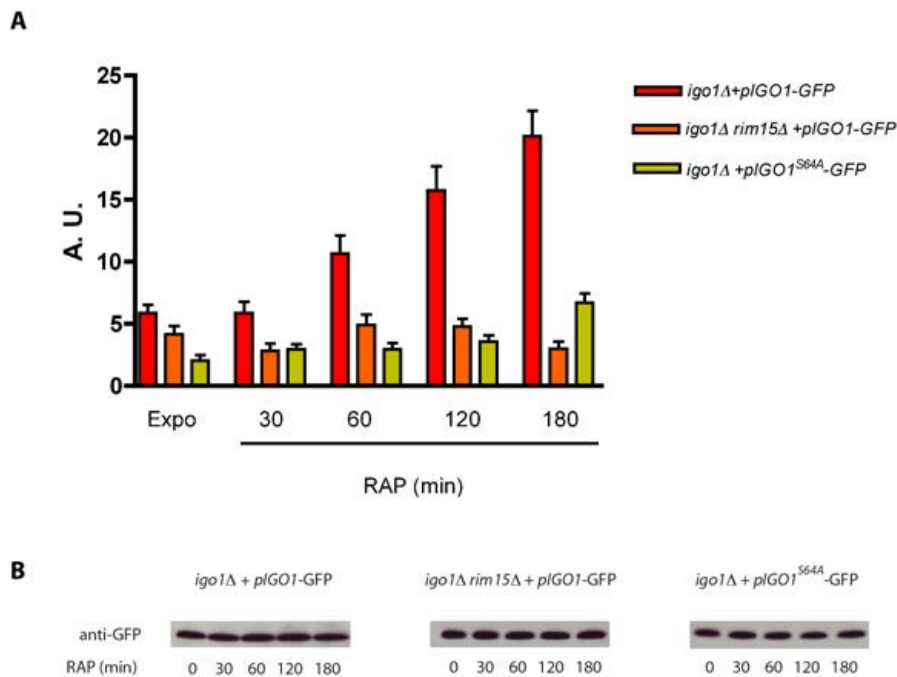


Fig. 10 Quantification of the nuclear signal of the GFP-tagged Igo1 variants

A. Relative level of nuclear Igo1-GFP (in Fig. 9 and not shown) was quantified by comparison of the fluorescence intensity per unit area in the nucleus versus cytoplasm, expressed in arbitrary units (A. U.). DNA was stained with 4', 6'-diamidino 2-phenylindole (DAPI). 50 cells of each condition were analyzed.

B. Whole cell protein extracts were analyzed by SDS-PAGE, and immunoblots were probed with anti-GFP antibodies. Same amount of total protein was loaded for each time point.

II. 3 Igo1^{S64D}-GFP is constitutively enriched in the nucleus and does not dynamically change its localization during rapamycin treatment

It was shown in the functionality test in Fig. 8 that both Igo1^{S64D} and Igo1^{S64D}-GFP failed to complement the defect of the *igo1Δ igo2Δ* mutant in *HSP26-lacZ* expression, although the serine to aspartate mutation is supposed to phosphomimic the Rim15 phosphorylation site. We also analyzed the localization of Igo1^{S64D}-GFP in an *igo1Δ rim15Δ* mutant. The nuclear Igo1^{S64D}-GFP signal was quantified as described in Fig. 10, on images taken prior to or after 30 min, 60 min, 120 min and 180 min of rapamycin addition. Compared to the Igo1^{S64A}-GFP that does not accumulate in the nucleus in response to the rapamycin treatment, the Igo1^{S64D}-GFP constantly localizes in the nucleus prior to or through out 3 hr of rapamycin treatment. However, the signal is only about half as intensive as the one of the nuclear Igo1-GFP after 3 hr of rapamycin treatment (Fig. 11).

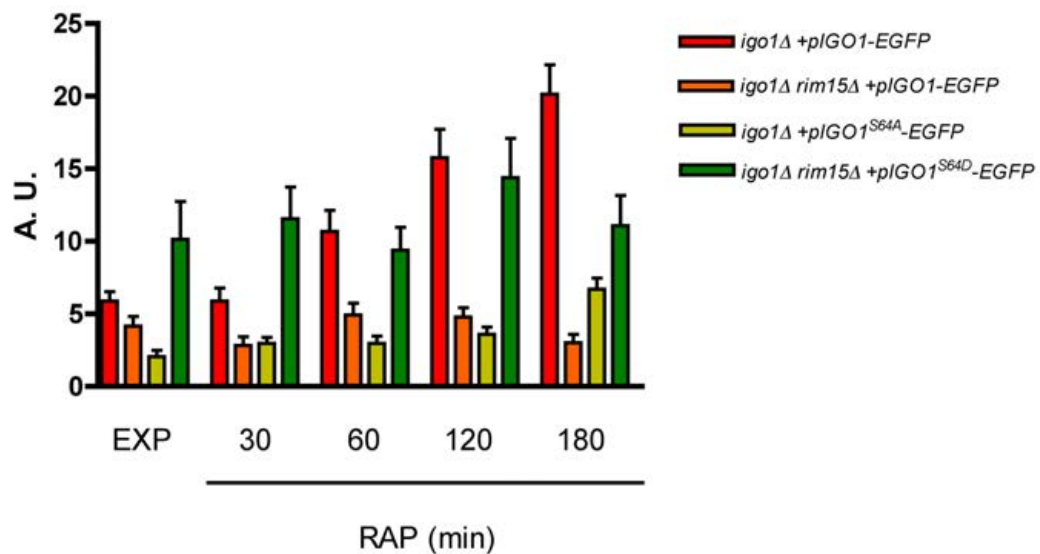


Fig. 11 Quantification of nuclear signal of Igo1^{S64D}-GFP
Relative levels of nuclear signal were quantified as described in Fig. 3.

Given that Igo1^{S64D}-GFP was not able to complement the defect of *igo1Δ igo2Δ* in *HSP26-lacZ* expression (Fig. 8), our hypothesis is that although Igo1^{S64D}-GFP is found enriched in the nucleus, it is probably either not properly functional, or may carry out an important function in the cytoplasm (see below)!

II. 4 Igo1^{S105A}-GFP remains cytoplasmic upon rapamycin treatment

As Igo1 contains a conserved PKA phosphorylation site at Ser¹⁰⁵, we assessed whether the phosphorylation at Ser¹⁰⁵ affects the localization of Igo1. This question was addressed by analyzing the localization (by fluorescence microscopy) of the PKA non-phosphorylatable Igo1^{S105A}-GFP in an *igo1Δ* mutant prior to and following a rapamycin treatment. The nuclear Igo1^{S105A}-GFP signal was quantified as described in Fig. 10, on images taken prior to or after 30 min, 60 min, 120 min and 180 min of rapamycin addition.

Although Igo1^{S105A}-GFP was able to complement the defect of an *igo1Δ igo2Δ* mutant (Fig. 8), this mutated form of Igo1 failed to accumulate in the nucleus in response to rapamycin treatment either in the presence or absence of Rim15 (Fig. 12).

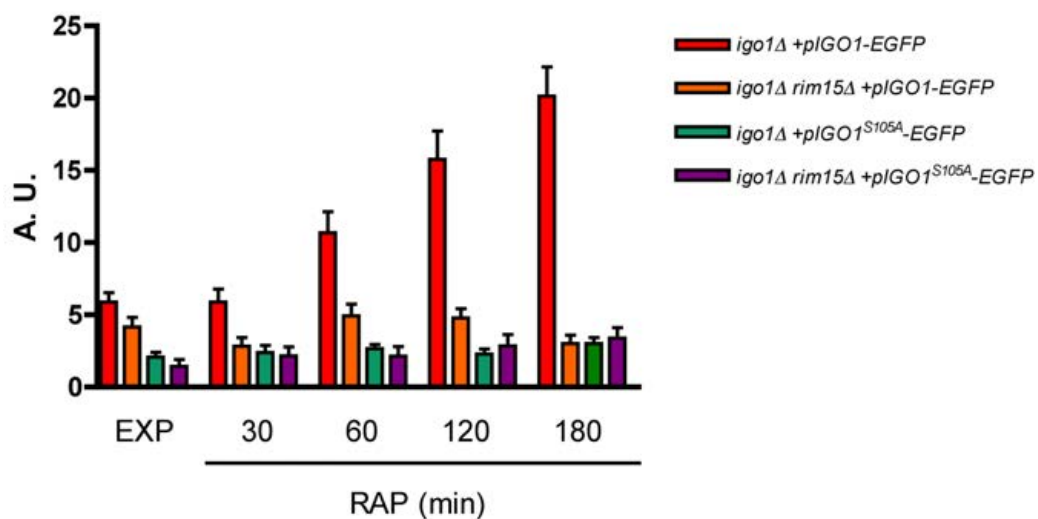


Fig. 12 Quantification of nuclear signal of Igo1^{S105A}-GFP
Relative levels of nuclear signal were quantified as described in Fig. 10.

Given that Igo1^{S105A}-GFP is able to complement the defect of *igo1Δ igo2Δ* (shown in Fig. 8), these data suggest that the nuclear accumulation of Igo1 is not required to ensure proper expression of *HSP26-lacZ* in rapamycin treated cells.

II. 5 Igo1^{S105D}-GFP oscillates between the nucleus and the cytoplasm upon rapamycin treatment

As we observed that the Igo1^{S105A}-GFP (nonphosphorylatable by PKA) remained cytoplasmic following rapamycin treatment, yet fulfilled its function normally (Fig. 8 and Fig. 11), we next assessed the behavior of the PKA phosphomimetic Igo1^{S105D}-GFP.

In an *igo1Δ* mutant, the Igo1^{S105D}-GFP nuclear signal appeared to oscillate to some extent during the 3 hr of the rapamycin treatment. The pattern of nuclear Igo1^{S105D}-GFP signal in an *igo1Δ rim15Δ* mutant was similar to that in an *igo1Δ* mutant, but the amplitude was higher than that in an *igo1Δ* mutant (Fig. 13).

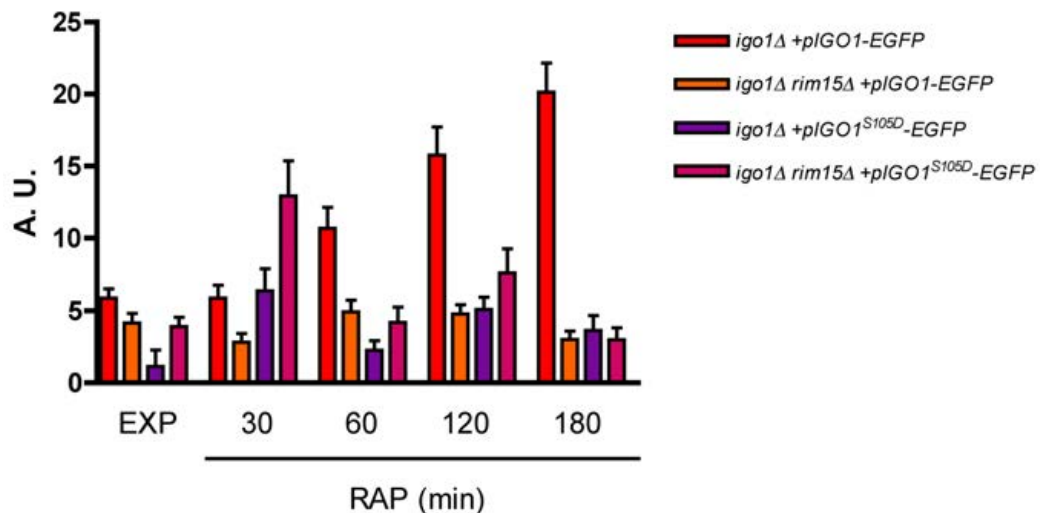


Fig. 13 Quantification of nuclear signal of Igo1^{S105D}-GFP
Relative levels of nuclear signal were quantified as described in Fig. 10.

One interpretation of these data is that the functional Igo1^{S105D}-GFP may shuttle at a greater pace between the nucleus and the cytoplasm upon rapamycin treatment. The corresponding functional implications remain elusive, though.

II. 6 Igo1-NLS-GFP is not functional, but Igo1-NES-GFP is functional

Given the previous results showing that the non-functional Igo1^{S64A} (non phosphorylatable by Rim15) did not accumulate in the nucleus of rapamycin-treated cells, and that the functional Igo1^{S105A} (non phosphorylatable by PKA) remained cytoplasmic in rapamycin-treated cells (Fig. 8, 9 and 12), this prompted us to test whether Igo1 function is required in the nucleus or in the cytoplasm.

To address this question, we took advantage of the well-characterized yeast Prp20 NLS (Hahn et al., 2008) or Prp40 NES (Murphy et al., 2004) (abbreviated as NLS and NES for the sake of simplicity) (c.f. material and methods) to target Igo1-GFP constitutively to the nucleus and cytoplasm, respectively. The localization and the functionality of these variants were then assessed. The corresponding nonfunctional forms of NLS and NES (abbreviated as NLSm and NESm, abrogating NLS and NES function) (c.f. material and methods) were also fused to Igo1-GFP, to ensure that the simple fusion of the NLS or the NES did not affect Igo1-GFP function. To rule out the possibility that Igo2 could interfere with the Igo1-NLS-GFP or Igo1-NES-GFP, the following experiments were performed in an *igo1Δ igo2Δ* mutant (See page 49).

II. 6. 1 NLS and NES are targeting sequences essential for the nuclear import or export of cargo proteins

Proteins destined for transport into the nucleus contain amino acid targeting sequences called nuclear localization signals (NLSs). The classical NLS (cNLS) consists of either one (monopartite) or two (bipartite) stretches of basic amino acids.

In the cytoplasm, cargo containing a cNLS is recognized by importin α , importin β then mediates interactions with the nuclear pore during translocation (Fried and Kutay, 2003; Lange et al., 2007) (Fig. 14). Hahn and colleagues have described that the yeast Prp20 protein contains a bipartite cNLS and the protein was identified as an authentic yeast cNLS cargo. Nuclear import of Prp20 was strongly affected when Lys¹⁹ and Lys²⁰ were mutated to threonine. We fused Prp20-NLS to Igo1-GFP to target Igo1-GFP constitutively to the nucleus.

The corresponding NLS carrying the K19T K20T mutations was used as a negative control.

Cells containing leucine-rich NES sequences are recognized by Crm1p/Xpo1, which mediates the nuclear export of protein cargos through the nuclear pore complex together with RanGTP (Allen et al., 2000; Fornerod et al., 1997; Stade et al., 1997) (Fig. 14). Murphy and colleagues demonstrated that mutation of the Leu³⁴⁰, Leu³⁴⁴ and Leu³⁴⁷ to alanines in the NES of Prp40 caused statistically significant nuclear accumulation of Prp40. The Prp-40NES was fused in this study to Igo1-GFP, to render Igo1-GFP constitutively cytoplasmic. The corresponding NES carrying the L340A, L344A and L347A mutations was used as a negative control.

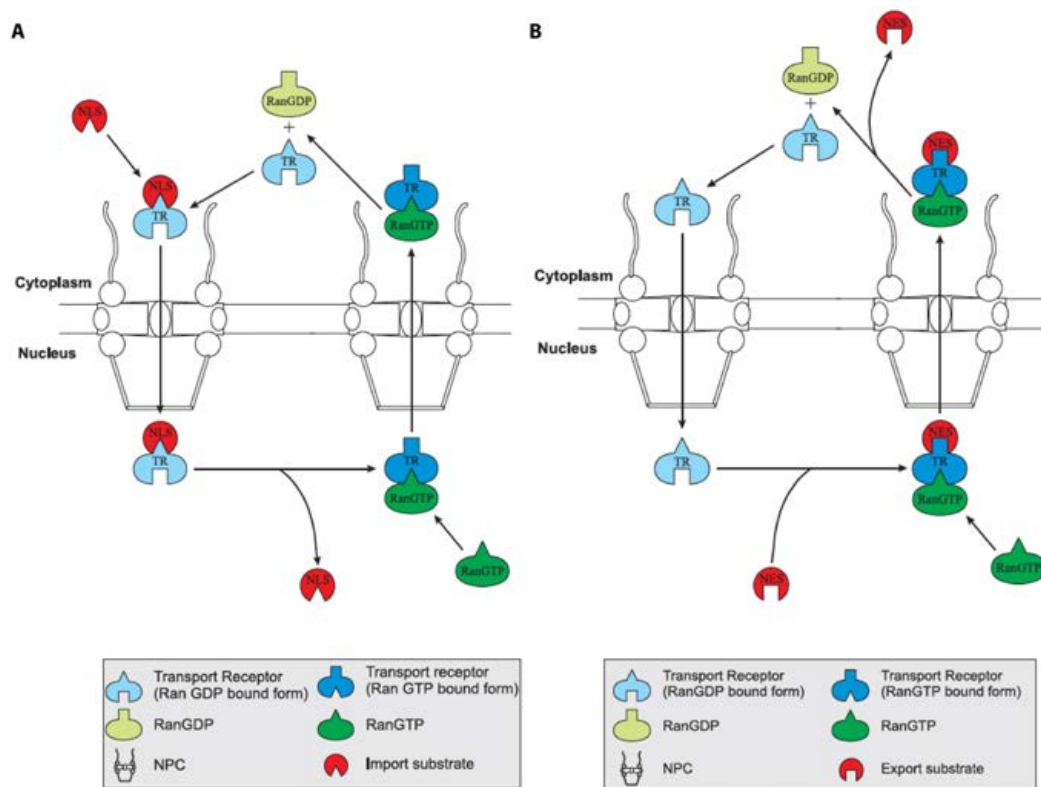


Fig. 14 Nuclear import and export (Allen et al., 2000)

A. Nuclear import. A schematic representation of nuclear import through the NPC. The transport receptor and import substrate containing NLS form a complex in the cytoplasm where RanGTP levels are low (Importin α and β are not shown separately for simplicity). This complex is translocated through the NPC. Nuclear RanGTP induces the dissociation of the import cargo from its receptor (and, in some cases, dissociation of the receptor from the NPC). The transport receptor is recycled to the nucleus, probably as a complex with RanGTP.

B. Nuclear export. A schematic representation of nuclear export through the NPC. The transport receptor and export substrate containing NES form a complex in the nucleus with RanGTP. This complex is exported from the nucleus and dissociated in the cytoplasm by hydrolysis of Ran-bound GTP to GDP. This releases the export substrate and the transport receptor is recycled into the nucleus.

II. 6. 2 Igo1-NLS-GFP and Igo1-NES-GFP mainly localize in the nucleus and cytoplasm, respectively

To elucidate the location where Igo1 fulfills its main function, the localization of Igo1-NLS-GFP and Igo1-NES-GFP and their mutated NLS and NES forms were analyzed in an *igo1Δ igo2Δ* mutant prior to and following rapamycin treatment using fluorescence microscopy.

As expected, during exponential growth, Igo1-NLS-GFP localized predominantly in the nucleus, and Igo1-NES-GFP appeared to be excluded to a great extent from the nucleus. The Igo1-GFP variants carrying the non-functional NLS_m and NES_m showed a similar localization pattern as Igo1-GFP (*i.e.* a diffuse localization in both the cytoplasm and the nucleus). Following a three hours rapamycin treatment, Igo1-GFP accumulated in the nucleus, whereas this nuclear accumulation seemed stronger in the case of Igo1-NLS-GFP. In contrast, the Igo1-NES-GFP signal did not significantly change and still appeared to be mainly excluded from the nucleus. Both variants carrying the non-functional NLS_m and NES_m behaved as the Igo1-GFP upon the rapamycin treatment. The total Igo1 protein levels stayed constant and comparable during the 3 hours rapamycin treatment in all strains, meaning the observation was not dependent on a change in expression level of these Igo1-GFP variants (Fig. 15).

The microscopy data show that the Igo1-NLS-GFP and Igo1-NES-GFP and their mutated forms exhibit the expected localization prior to or following rapamycin treatment.

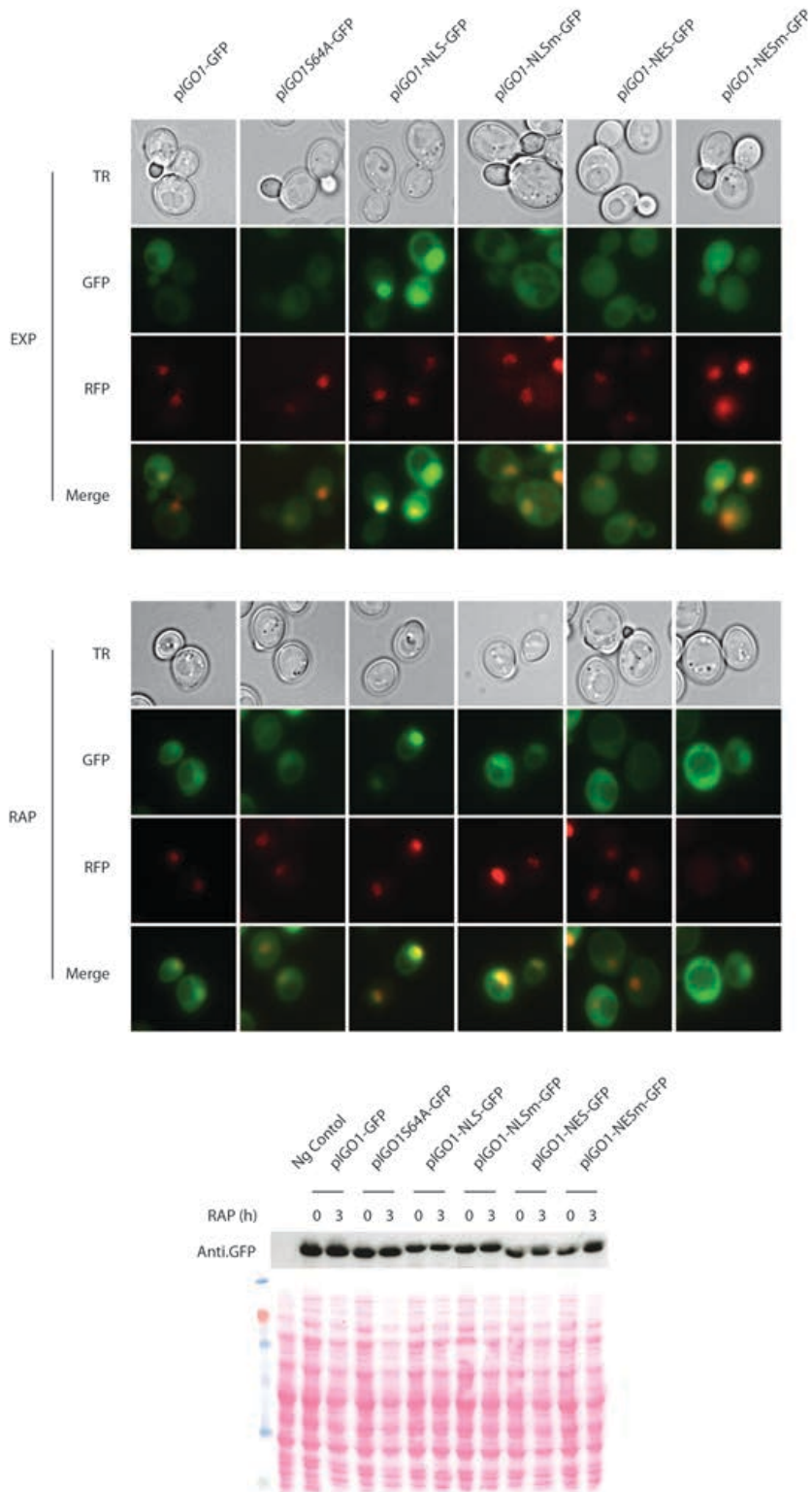


Fig. 15 Localization of Igo1-NLS(m)-GFP, Igo1-NES(m)-GFP in an *igo1Δ igo2Δ* mutant prior to and following rapamycin treatment

The indicated strains expressing the nuclear marker *HHF2*-RFP and different variants of Igo1, were harvested prior to (EXP) or following rapamycin treatment (RAP; $0.2 \mu\text{g ml}^{-1}$; 3 hr) and analyzed by fluorescence microscopy. Whole cell protein extracts were analyzed by SDS-PAGE, and immunoblots were probed with anti-GFP antibodies. Ponceau S staining of the membranes prior to immunoblot analysis served as loading control.

II. 6. 3 Igo1 fulfills its function in the cytoplasm

To test the functionality of Igo1-NLS-GFP, Igo1-NES-GFP and their mutated forms, the capacity of these constructions to complement the defect of an *igo1Δ igo2Δ* mutant was analyzed with a β -galactosidase assay by measuring the expression of the chimeric *HSP26-lacZ* gene prior to and following rapamycin treatment.

Upon rapamycin treatment, Igo1-NLS-GFP could only slightly complement the defect of an *igo1Δ igo2Δ* mutant, whereas Igo1-GFP fused with NLSm was able to complement the defect. These results suggest that the constitutive nuclear localization of Igo1 causes a severe loss of its function. Intriguingly, the defect of an *igo1Δ igo2Δ* mutant can be fully complemented by the Igo1-NES-GFP. The mutated NES did not affect the function of Igo1-GFP. These observations indicate that the mainly cytoplasmic Igo1 fusion protein was able to fulfill its function upon rapamycin treatment (Fig. 16).

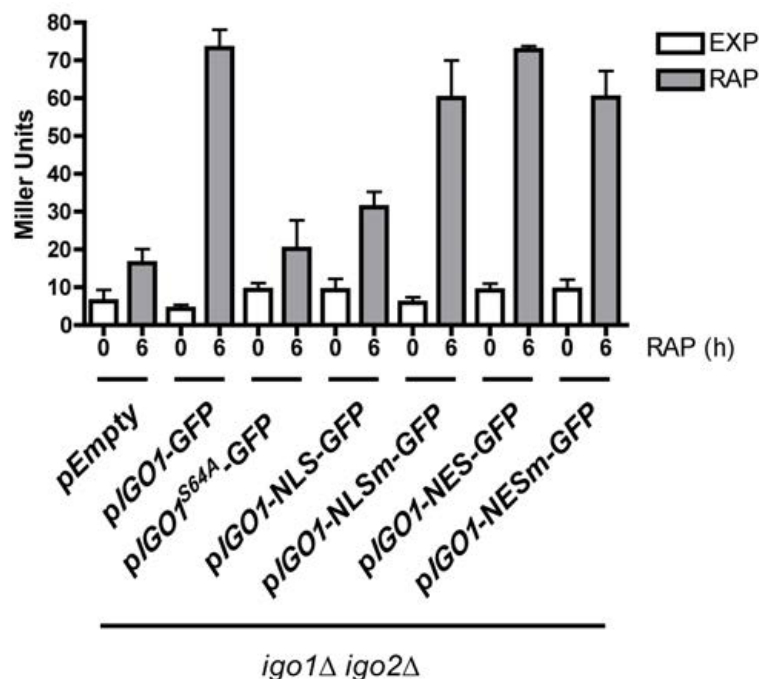


Fig. 16 NLS-fused Igo1-GFP is not functional, while Igo1-NES-GFP, Igo1-NLSm-GFP and Igo1-NESm-GFP are fully functional

Complementation analysis of Igo1-GFP variants in an *igo1Δ igo2Δ* mutant. β -galactosidase activities (expressed in Miller units) were measured to monitor the expression of an *HSP26-lacZ* fusion gene in exponentially growing cells prior to (EXP) or following rapamycin treatment (RAP; 0.2 $\mu\text{g ml}^{-1}$; 6 hr). Data are reported as averages ($n = 3$), with standard deviations (SDs) indicated by the lines above each bar. Relevant genotypes are indicated.

We confirmed these results independently by monitoring the expression of the endogenous *HSP26* gene in various strains by northern blot and western blot analyses (Fig. 17). The results were comparable to the expression pattern of the *HSP26-lacZ* reporter gene shown in Fig. 16.

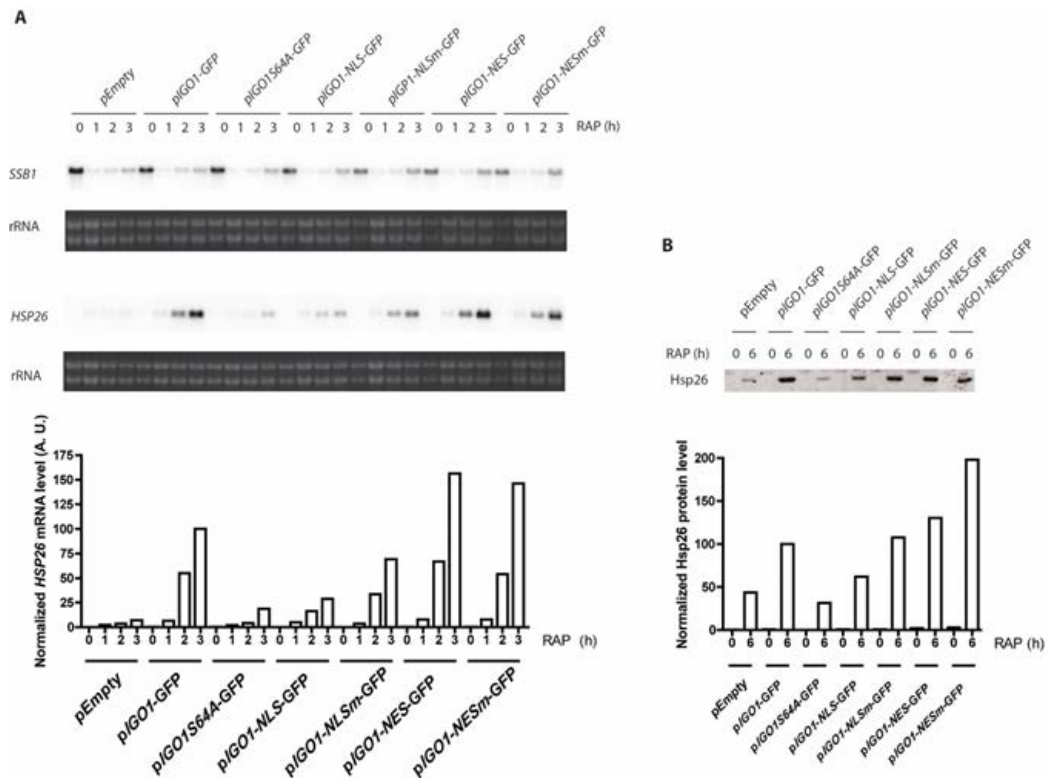


Fig. 17 *HSP26* mRNA and Hsp26 protein levels in *igo1Δ igo2Δ* mutant cells expressing Igo1-NLS-GFP, Igo1-NLSm-GFP, Igo1-NES-GFP and Igo1-NESm-GFP

A. *HSP26* and *SSB1* mRNAs levels were analyzed by northern blot analysis in an *igo1Δ igo2Δ* strain expressing the indicated constructs. Exponentially growing cells were treated for 1 hr, 2 hr, and 3 hr with rapamycin. The decrease in *SSB1* transcript levels was used as internal control for rapamycin function. All samples were run on the same gel (identical exposure time). The bar graph shows the relative levels of *HSP26* mRNA per rRNA (Arbitrarily set to 100 for *igo1Δ igo2Δ* expressing *pIGO1-GFP* after 3h of rapamycin treatment).

B. Whole cell protein extracts from the same strains in Fig. 10A were harvested prior to (EXP) or following rapamycin treatment (RAP; $0.2 \mu\text{g ml}^{-1}$; 6hr), analyzed by SDS-PAGE, and probed with anti-GFP. Same amount of total protein was loaded for each sample. The bar graph shows the relative levels of Hsp26 protein or phosphorylated-Igo1 variant proteins per total protein (Arbitrarily set to 100 for *igo1Δ igo2Δ* expressing *pIGO1-GFP* after 6 hr of rapamycin treatment).

As it has been suggested by previous studies that Igo1 is phosphorylated by Rim15 at its Ser⁶⁴, which is required for its function, we tested the corresponding phosphorylation status of different Igo1-GFP variants that have either nuclear or cytoplasmic localization by employing a PhosTag™ SDS-PAGE gel technique. Surprisingly, the NES-fused Igo1-GFP was phosphorylated to the same level as that of Igo1-GFP, whereas Igo1-NLS-GFP appeared to be somewhat less phosphorylated.

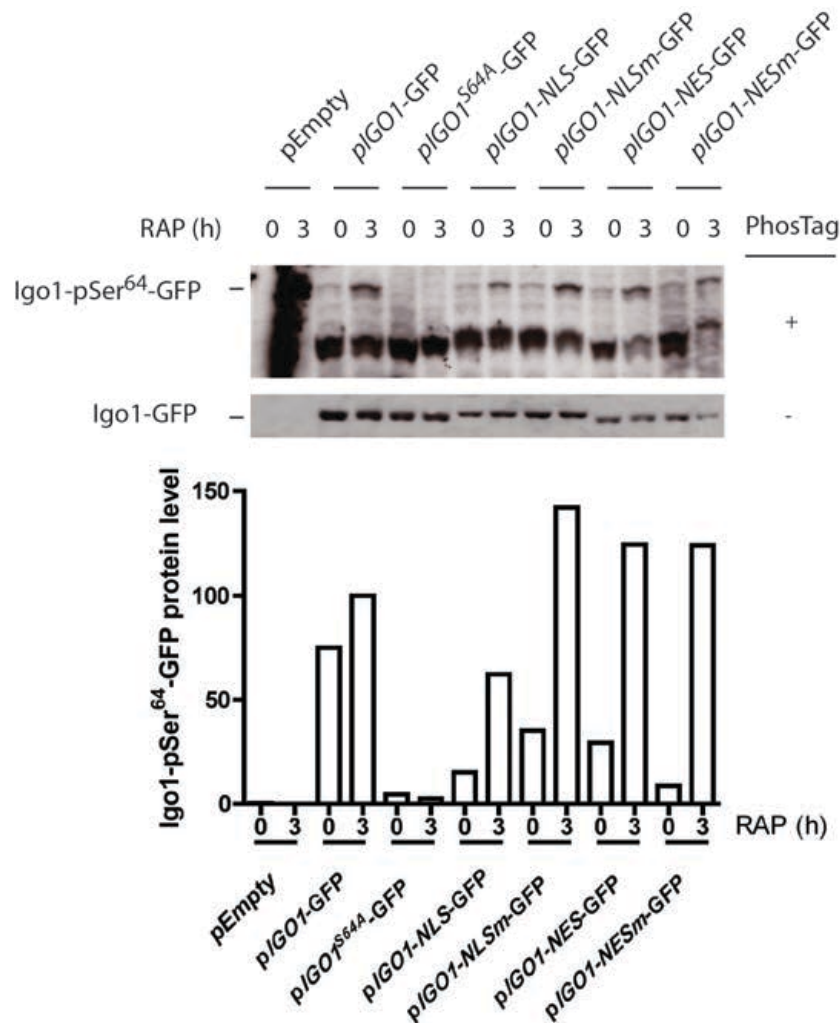


Fig. 18 Phosphorylation status of Ser⁶⁴ within different Igo1-GFP variants

Whole cell protein extracts from *igo1Δ igo2Δ* cells expressing Igo1-GFP variants were harvested prior to (EXP) or following rapamycin treatment (RAP; 0.2 μg ml⁻¹; 3hr), were analyzed by SDS-PAGE with or without 25 μM PhosTag™, and probed with anti-GFP. Ponceau S staining of the membranes prior to immunoblot analysis served as loading control. Additional controls indicate that the upper band (Igo1-pSer⁶⁴-GFP) corresponds to the phosphorylated form of Igo1 at Ser⁶⁴ (data not shown). Bar graphs show the relative levels of Igo1-pSer⁶⁴ per total protein (Arbitrarily set to 100 for *igo1Δ igo2Δ* expressing pIGO1-GFP after 3 hr of rapamycin treatment).

As shown in Fig. 15, 16, 17 and 18, upon rapamycin treatment, the defect of an *igo1Δ igo2Δ* mutant can be complemented by the expression of the constitutively cytoplasmic-localized Igo1-NES-GFP, which is phosphorylated at Ser⁶⁴. These data indicate that the presence of Igo1 in the cytoplasm is essential for fulfilling its function upon TORC1 inactivation by rapamycin treatment.

II. 7 Igo1-GFP is cytoplasmic in the importin mutant *kap123Δ*, which displays a normal *HSP26-lacZ* expression upon rapamycin treatment

In yeast, there are 20 well-characterized karyopherins, also known as importins/exportins. To reinforce our argument about Igo1 fulfilling its function in the cytoplasm, we checked first the localization of Igo1-GFP in different importin and exportin mutants available in our lab (Table 1).

Importin mutants	<i>kap123Δ</i>
	<i>nmd5Δ</i>
	<i>gsp2Δ</i>
	<i>kap122Δ</i>
	<i>gsp1^{ts}</i>
	<i>pse1^{ts}</i>
Exportin mutants	<i>msn5Δ</i>
	<i>sxm1Δ</i>
	<i>los1Δ</i>
	<i>xpo1^{ts}</i>

Table 1. Importin and exportin mutants used to study Igo1-GFP localization

Indicated importin and exportin mutants expressing Igo1-GFP were analyzed prior to (EXP) or following rapamycin treatment (RAP; 0.2 $\mu\text{g ml}^{-1}$; 3 hr) and analyzed by fluorescence microscopy.

Among various importin and exportin mutants, *kap123Δ* and *pse1^{ts}* showed cytoplasmic Igo1-GFP localization upon rapamycin treatment, suggesting that Kap123 and Pse1 may play a role in Igo1 nuclear import. The temperature sensitive *pse1^{ts}* strain was unsuitable for a functionality assay by monitoring *HSP26-lacZ* expression, since our reporter gene *HSP26-lacZ* is induced at the non-permissive temperature independently of rapamycin treatment. We therefore assessed *HSP26-lacZ* expression only in *kap123Δ* cells upon rapamycin treatment to evaluate its capacity of proper *HSP26-lacZ* expression. Our data showed that *kap123Δ* mutant cells were able to properly enter into G₀ phase, as the level of *HSP26-lacZ* expression was comparable to that in wild type cells after 6 hr rapamycin treatment (Fig. 19).

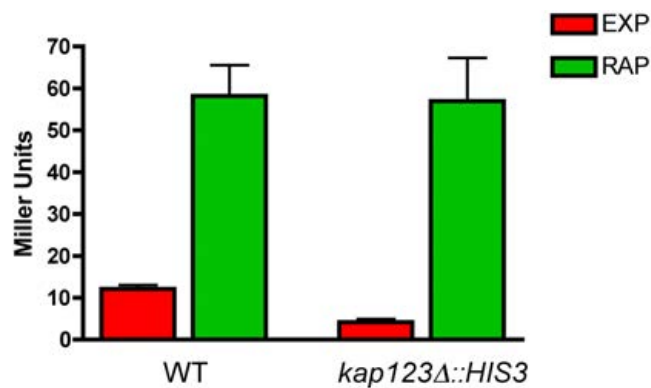


Fig. 19 Importin mutant *kap123Δ* properly induces *HSP26-lacZ* expression upon rapamycin treatment
β-galactosidase activities (expressed in Miller units) were measured to monitor the expression of an *HSP26-lacZ* fusion gene in exponentially growing cells prior to (EXP) or following rapamycin treatment (RAP; 0.2 μg ml⁻¹; 6 hr). Data are reported as averages (n = 3), with standard deviations (SDs) indicated by the lines above each bar. Relevant genotypes are indicated.

These results further corroborate the idea that Igo1 fulfills at least one of its functions in the cytoplasm.

II. 8 Discussion

II. 8. 1 Igo1 localization is dynamic upon TORC1 inactivation

To determine whether Igo1 localization is Rim15- and/or PKA-dependent following a rapamycin treatment, we constructed Igo1-GFP and GFP-tagged Igo1 variants, which are nonphosphorylatable at either the Rim15 or PKA phosphorylation sites (Ser⁶⁴ and Ser¹⁰⁵, respectively), or which carry phosphomimetic residues instead, and analyzed their localization prior to and following rapamycin treatment. We observed three categories of Igo localization patterns. (i) Igo1-GFP and Igo1^{S105D}-GFP appeared to oscillate between the nucleus and the cytoplasm during rapamycin treatment (Fig. 9, 13 and data not shown). (ii) Igo1^{S64D}-GFP was constitutively enriched in the nucleus (Fig. 11). (iii) Igo1^{S64A}-GFP and Igo1^{S105A}-GFP remained cytoplasmic even during rapamycin treatment (Fig. 10 and 12). This indicates that the phosphorylation/dephosphorylation balance on Ser⁶⁴ and Ser¹⁰⁵ is required for the dynamic localization of Igo1 upon TORC1 inactivation, which is in line with our previous results with glucose-limited cells (Talarek et al., 2010).

Following glucose-depletion, Igo1-GFP accumulates in the nucleus, but then nuclear Igo1-GFP signal decreases and, subsequently, Igo1 forms cytoplasmic dots that successively colocalize with P bodies and SGs (Talarek et al., 2010). Surprisingly, in rapamycin-treated cells (up to 6 hr), no cytoplasmic dots were observed. This is in line with the observation that P bodies and SGs do not form upon rapamycin treatment (Ramachandran and Herman, 2011).

As we observed that Igo1-GFP mislocalized in *kap123Δ* mutant cells, our data suggested that Kap123 is at least one of the importins that is involved in Igo1 nuclear import. It is known that Kap123 interacts with Gsp1 (RanGTPase, cf. Fig. 14) (Schlenstedt et al., 1997). Interestingly, Gsp1 was found as Igo1 physical interactor by Igo1-Myc pull-down coupled mass spectrometry (MS) analysis (Jaquenoud, unpublished data). These data support the idea that Igo1 nuclear import is Kap123/Gsp1-mediated.

II. 8. 2 Igo1 fulfills at least one of its functions in the cytoplasm

We observed that Igo1-GFP accumulated in the nucleus following rapamycin treatment, whereas Igo1^{S64A}-GFP remained in the cytoplasm and was not functional (Fig. 8, 9 and 10). On the other hand, Igo1^{S105A}-GFP, Igo1-NES-GFP and Igo1-GFP in *kap123Δ* displayed cytoplasmic localization upon rapamycin treatment, but were functional in our assays (Fig. 8, 12, 14, 15, 19 and data not shown). These data support the hypothesis that Igo1 has an important functional role in the cytoplasm. Notably, we cannot rule out that NES-fused Igo1-GFP might be able to temporarily transit through the nucleus before being transported to the cytoplasm via the recognition of the NES as depicted in Fig. 14. Similarly, we cannot rule out that Igo1-NLS-GFP temporarily transits through cytoplasm. Thus, Igo1 may in principle play both a role within the nucleus, as well as in the cytoplasm. Conceivably, Igo1 may function in transcriptional control, as well as in posttranscriptional control of *HSP26*, as already suggested earlier (Talarek et al., 2010).

II. 8. 3 Igo1 phosphorylation status

Although Igo1-GFP accumulates in nucleus upon rapamycin treatment, our data show that the presence of Igo1 in cytoplasm is essential for at least one of its function (Fig. 8, 9, 12, 14 and 19). It remains elusive why Igo1 accumulates in the nucleus following rapamycin treatment. Our previous results demonstrated that Rim15 accumulates in the nucleus of rapamycin-treated cells, where it becomes active. Active Rim15 induces the G₀ program, phosphorylates Igo1 and initiates an autophosphorylation process. The latter event accelerates Msn5-mediated nuclear export of Rim15 (Pedruzzi et al., 2003; Talarek et al., 2010; Wanke et al., 2005). If the hypothesis that Igo1 is phosphorylated by Rim15 in the nucleus is correct, we would expect Igo1-NLS-GFP to be more phosphorylated than Igo1-NES-GFP. To our surprise, the NLS-fused Igo1-GFP appeared somewhat less phosphorylated than Igo1-NES-GFP and Igo1-GFP. Two reasons may explain this finding. First, Rim15 may be activated in the cytoplasm or remain active in the cytoplasm following its export from the nucleus in TORC1-inactivated cells. Alternatively, following phosphorylation by Rim15, Igo1 binds to its partners and G₀ specific mRNAs to form mRNPs that are then exported out of the

nucleus. The pool of Igo1 that remains in the nucleus may be subjected to dephosphorylation by nuclear phosphatase(s).

II. 8. 4 Working model

To summarize our results, we propose the following model. In exponentially growing cells, (1) Igo1 is phosphorylated by PKA at Ser¹⁰⁵, and Igo1 localization is equilibrated between the nucleus and cytoplasm. Igo1 nuclear import might be Kap123-dependent. Following rapamycin treatment, (2) Rim15 becomes active and phosphorylates nuclear Igo1. Phosphorylation at Ser⁶⁴ and Ser¹⁰⁵ would slow down Igo1 nuclear export, consequently Igo1 accumulates in the nucleus. (3) Dephosphorylation of Ser¹⁰⁵ of nuclear Igo1, may favor export of Igo1-pSer⁶⁴ to the cytoplasm (Fig. 20).

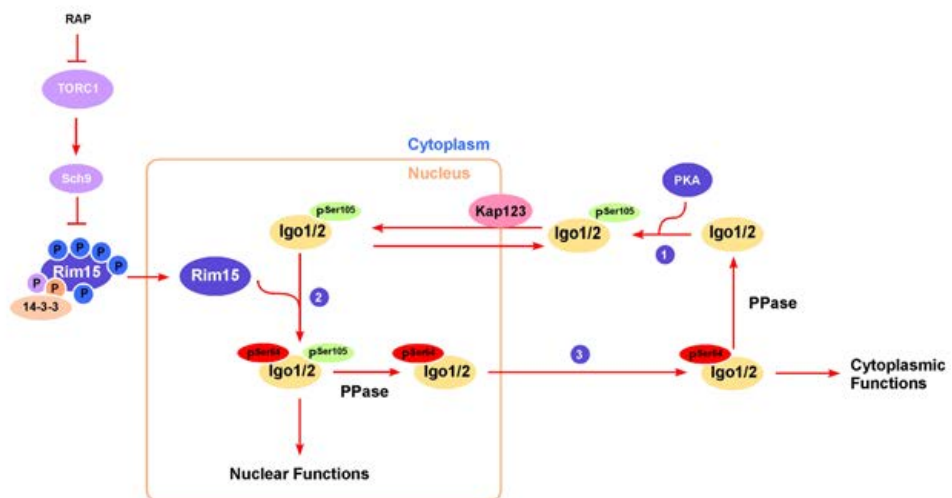


Fig. 20 Model depicting Igo1 localization and phosphorylation status upon rapamycin treatment

We propose the following experiments to test this model.

To track protein movement in live cells, a green-to-red photoconvertible fluorescent protein, namely EosFP has been developed (Wiedenmann et al., 2004). Briefly, EosFP emits green fluorescence that changes to red fluorescence upon irradiation at approximately 400 nm. This is due to a photo-induced modification involving a break in the peptide backbone close to the chromophore. We could use an EosFP-tagged Igo1 variant to further confirm that Igo1 shuttles between nucleus and cytoplasm following rapamycin treatment. By photoconverting cytoplasmic and nuclear Igo1-EosFP from green to red in rapamycin-treated cells for 2 and 3 hr respectively, the movement of red signal would reveal whether Igo1 is imported into or exported out of nucleus respectively.

To answer the question how Igo1 shuttles upon rapamycin treatment, at least two points could be addressed. As there is no cNLS or NES found in Igo1's sequence, it would be interesting to identify the non-canonical NLS or NES in Igo1 by performing random mutagenesis on the *IGO1* ORF. PCR products could be cloned into a plasmid allowing C-terminal GFP-tagging. The different *IGO1-GFP* alleles that express a full length protein would be kept. Amino acids that are responsible for proper localization of Igo1-GFP could be then identified by screening for mislocalized allele(s) upon rapamycin treatment. Another possibility is that Igo1 would need its partner(s) to be translocated into and/or out of the nucleus upon rapamycin treatment. In this regard, it would be interesting to test whether Igo1 loses its nuclear localization upon rapamycin treatment, in mutants of genes whose products have been identified as physical interactors of Igo1 upon rapamycin treatment (*i.e.* *PBP1*, *PBP4*, *LSM12* and *DHHL*) (Talarek et al., 2010).

To further consolidate that the shuttling is essential for Igo1 function, the anchor away method (Haruki et al., 2008) could be used to tether Igo1 at the plasma membrane, then the expression of *HSP26* mRNA and Hsp26 protein prior to and following rapamycin addition could be assessed. This method is based on the heterodimerization of the human FKBP12 to the FRB domain of human mTOR that occurs in the presence of rapamycin. When the endogenous plasma membrane protein Pma1 and Igo1 are fused to FKBP12 and FRB-GFP respectively, rapamycin-induced interaction of FKBP12 and FRB would consequently tether Igo1 at the plasma membrane. The experiment should be performed in a haploid *igo2Δ* mutant

in order to rule out the possibility that endogenous Igo1 and/or Igo2 forms homo-/hetero-dimers with Igo1-FRB-GFP.

The initial hypothesis that Igo1 accumulates in nucleus either prior to or following phosphorylation by Rim15 could be addressed by the following experiment: a kinase assay could be performed on bacterially-purified Igo1 or Igo1^{S64A} with nuclear or cytoplasmic subcellular fractions obtained from exponentially growing and rapamycin-treated wild type or kinase-inactive *RIM15* cells. Subcellular fractions could be obtained by differential centrifugation as described previously (Kaldis et al., 1998). The phosphorylation status of Igo1 would reveal in which subcellular compartment Igo1 is phosphorylated by Rim15. Furthermore, the phosphorylation status of Igo1 Ser⁶⁴ in a *kap123Δ* mutant would provide additional information to indicate where Igo1 is phosphorylated by Rim15.

Chapter III. Igo1/2 target mRNA decapping factors

Our previous studies identified Igo1 and Igo2 as direct targets of Rim15. The phosphorylation of Igo1/2 by Rim15 is key for proper posttranscriptional stabilization of mRNAs of Msn2/4 and Gis1-dependent genes during initiation of the G₀ program (Talarek et al., 2010). To further clarify how Igo1/2 protect these transcripts from degradation, we performed a genome-wide screen to identify mutations that suppress the defect of an *igo1Δ igo2Δ* mutant in *HSP26* gene expression in cells entering G₀.

III. 1 Screening for mutants that suppress the defect in *HSP26* expression in *igo1Δ igo2Δ* mutant cells

To carry out a genome-wide screen for *igo1Δ igo2Δ* mutant suppressors, we used a new yeast enhanced variant of the mCherry monomeric red fluorescent protein (yEmRFP) (Keppler-Ross et al., 2008) that confers a purple color to colonies when it is expressed. We constructed a *HSP26*-yEmRFP reporter where the ORF of this variant was put under the control of the *HSP26* promoter. Consequently cells that properly initiated the G₀ program formed purple colonies after 5 days of growth on SD medium. As expected, *rim15Δ* and *igo1Δ igo2Δ* cells formed white colonies (Fig. 21).

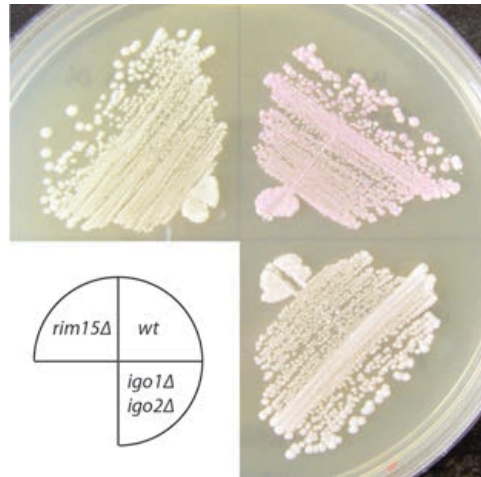


Fig. 21 *HSP26*-yEmRFP reporter expression in wild-type, *rim15Δ* and *igo1Δ igo2Δ* cells

Wild-type, *rim15Δ* and *igo1Δ igo2Δ* cells were transformed with *HSP26*-yEmRFP reporter plasmid, patched on SD-medium plates, and grown for 5 days at 30°C. Expression of yEmRFP under the control of *HSP26* promoter confers to cells a purple color.

An *igo1Δ igo2Δ* query strain derived from the strain Y7092 from the C. Boone lab collection (Tong and Boone, 2007), containing the *HSP26*-yEmRFP reporter plasmid, was crossed with the Euroscarf collection of 4,857 viable non-essential gene deletion mutants. The resulting triple mutants that were able to express *HSP26*-yEmRFP, as indicated by the fact that they formed purple colonies, were selected (Fig. 22). The primary screen yielded 384 candidates.

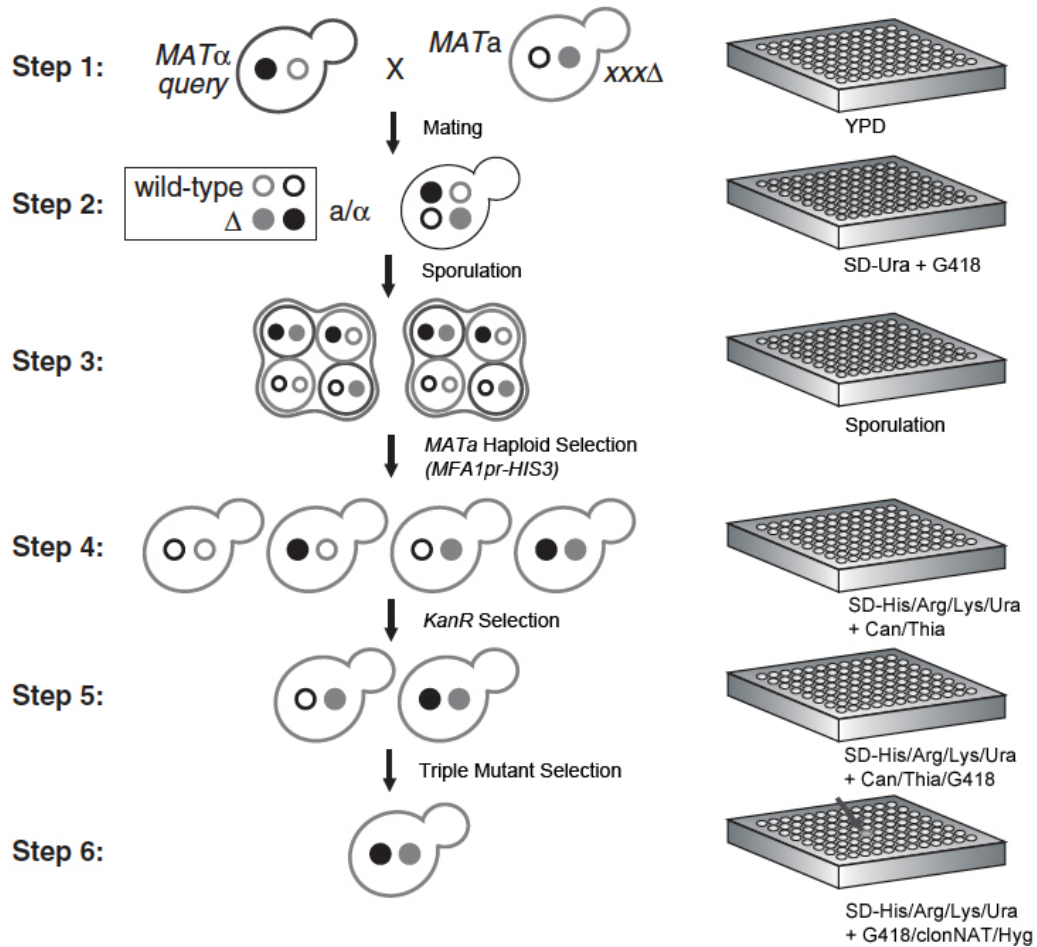


Fig. 22 Suppressor screen illustration (Adapted from (Tong and Boone, 2007))

The query strain $igo1\Delta::Nat$ $igo2\Delta::Hph$ (double deletions and reporter plasmid represented by closed black circles) derived from Y7092 strain from C. Boone lab collection, harboring the $HSP26$ -yEmRFP reporter, was crossed with the Euroscarf knockout (KO) collection (gene deletion represented by closed gray circles). The resulting diploids were selected on SD-Ura + G418 medium, before being subjected to sporulation on plate for 10 days. Spores germination were conducted on SD-His/Arg/Lys/Ura + canavanine (Can) + thialysin (Thia) medium to select for $MATa$ haploid cells. $MATa$ G418-resistant haploid cells were selected on SD-His/Arg/Lys/Ura + Can/Thia/G418 plates. Final $MATa$ G418-, nourseothricin-(Nat), hygromycin-(Hyg) resistant triple mutants were selected by two successive replica-pinning on SD-His/Arg/Lys/Ura + Can/Thia/G418/ClonNAT/Hyg medium (c.f. Materials and Methods for further details).

We hypothesized that Rim15 activates the transcription of Msn2/4- and Gis1-dependent genes by an unknown mechanism, and in parallel, the posttranscriptional stabilization of the very same mRNAs are ensured by Rim15-phosphorylated Igo1/2. We therefore anticipated that we would find suppressor mutants that affect either transcription or posttranscriptional mRNA stability of Msn2/4- and Gis1-dependent genes. We expected that genes encoding proteins involved in posttranscriptional mRNA regulation should suppress the defect of the *HSP26* expression in *igo1Δ igo2Δ* cells, but not in *rim15Δ* cells. Thus, the 384 candidate mutants were subjected to a secondary screen, *i.e.* the mutants were crossed with an *igo1Δ igo2Δ* mutant and a *rim15Δ* mutant harboring the *HSP26*-yEmRFP reporter. We found three classes of mutants:

(i) 4 candidate mutations suppressing the *HSP26*-yEmRFP expression defect in both *rim15Δ* and *igo1Δ igo2Δ* cells (Fig. 23B). The corresponding proteins very likely play a role in transcriptional regulation.

(ii) 5 candidate mutations that suppressed the defect in *HSP26*-yEmRFP expression in *igo1Δ igo2Δ* mutants, but not in *rim15Δ* mutants (Fig. 23A). The corresponding proteins very likely play a role in posttranscriptional mRNA stability regulation.

(iii) 375 Candidate mutations that could not suppress the defect in *HSP26*-yEmRFP expression neither in an *igo1Δ igo2Δ* mutant, nor in a *rim15Δ* mutant. These candidate mutations were therefore discarded.

We retained for further analyses the five candidate mutations (*i.e.* *ccr4Δ*, *dhh1Δ*, *lsm1Δ*, *lsm6Δ* and *pat1Δ*) from the category ii.

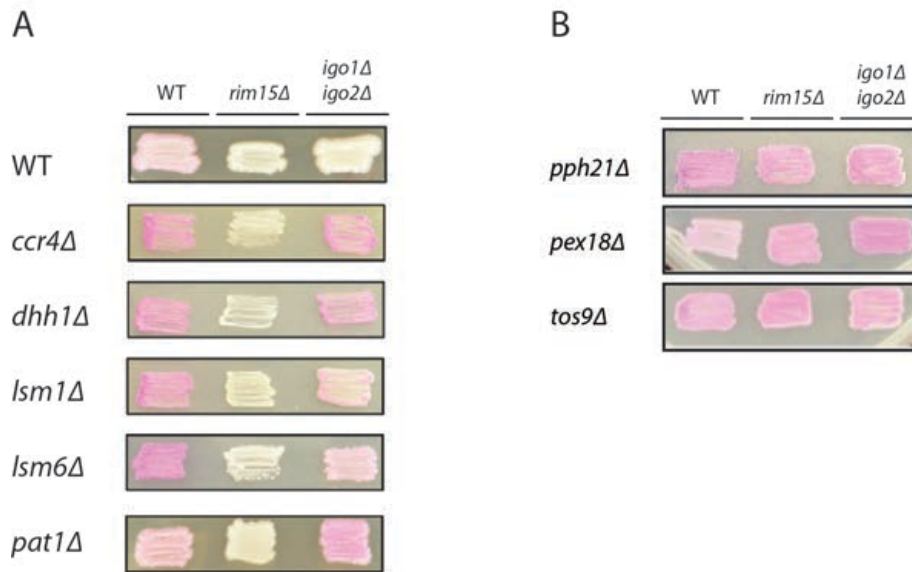


Fig. 23 Mutations suppressing the defect in *HSP26*-yEmRFP expression in *igo1Δ igo2Δ* mutants, but not in *rim15Δ* mutants (A) and in both *rim15Δ* and *igo1Δ igo2Δ* cells (B)

Strains with indicated genotypes were constructed by crosses between the single knock-out strains from Euroscarf collection and isogenic wild-type, *rim15Δ* or *igo1Δ igo2Δ* cells, transformed with *HSP26*-yEmRFP reporter plasmid, patched on SD-medium plates, and grown for 5 days at 30°C. Expression of yEmRFP under the control of *HSP26* promoter confers to cells a purple color.

In agreement with our previous findings (Talarek et al., 2010), *ccr4Δ* or *dhh1Δ* were identified in our screen. Both mutations prevent the mRNA degradation at an early step of the 5'-3' mRNA decay pathway (Parker and Sheth, 2007). Intriguingly, all the three additional newly identified suppressor mutations (*i.e.* *lsm1Δ*, *lsm6Δ* and *pat1Δ*) disrupt genes encoding constituents of the Lsm/Pat1 complex that activates mRNA decapping after deadenylation. These results suggest that the mRNA decapping pathway targets *HSP26* mRNA in the absence of Igo1/2.

The 5'- 3' mRNA decay pathway is the main mRNA decay pathway in yeast. It occurs in the cytoplasm, and starts with the trimming of poly(A) tails (Decker and Parker, 1993; Hsu and Stevens, 1993; Muhlrud et al., 1995). Then, mRNA decapping is thought to take place in three consecutive steps: (i) recruitment to the corresponding oligoadenylated mRNAs of Dhh1 and Pat1, which serve as a scaffold that binds both deadenylation and decapping enzymes (Coller et al., 2001; Nissan et al., 2010; Pilkington and Parker, 2008); (ii) Pat1-mediated loading of the Lsm1-7 complex onto oligoadenylated mRNAs (Bonnerot et al., 2000; Bouveret et al., 2000; Nissan et al., 2010; Tharun et al., 2000); and (iii) 5'-decapping by the decapping enzymes Dcp1/2 (Dunckley and Parker, 1999).

III. 2 Loss of proteins involved in the 5'-3' mRNA decay suppresses the defect of an *igo1Δ igo2Δ* mutant in *HSP26* expression following rapamycin treatment

To confirm that the suppression of the defect of an *igo1Δ igo2Δ* mutant by candidate mutants in the aforementioned experiments was not reporter-dependent, we measured the endogenous *HSP26* mRNA and Hsp26 protein levels in rapamycin-treated wild-type, *rim15Δ*, *igo1Δ igo2Δ* and in *CCR4*-, *DHH1*-, *PAT1*-, *LSM1*- or *LSM6*-deficient wild-type, *rim15Δ* and *igo1Δ igo2Δ* cells.

III. 2. 1 Loss of Ccr4 and Dhh1 suppresses the defect of an *igo1Δ igo2Δ* mutant in *HSP26* expression following rapamycin treatment

Loss of Dhh1 or Ccr4 led to higher expression of *HSP26* (at both the mRNA and protein levels) than in wild-type cells following rapamycin-induced TORC1 inactivation. As expected, loss of Dhh1 or Ccr4 suppressed the defect of *igo1Δ igo2Δ* cells but not that of *rim15Δ* cells in *HSP26* expression (at both the mRNA and protein levels) following rapamycin treatment (Fig. 24 and 25).

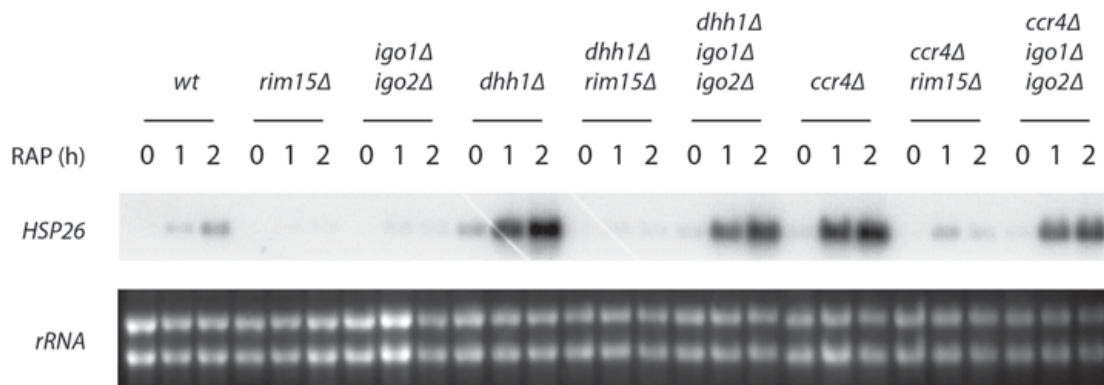


Fig. 24 Loss of Ccr4 and Dhh1 suppresses the defect of *igo1Δ igo2Δ* cells, but not that of *rim15Δ* cells in rapamycin-induced *HSP26* mRNA accumulation

Northern blot analyses of *HSP26* mRNAs were done with exponentially growing strains with indicated genotypes, treated (1 hr and 2 hr) or not (0 hr) with rapamycin (RAP; 0.2 $\mu\text{g ml}^{-1}$). All samples were run on the same gel (identical exposure time).

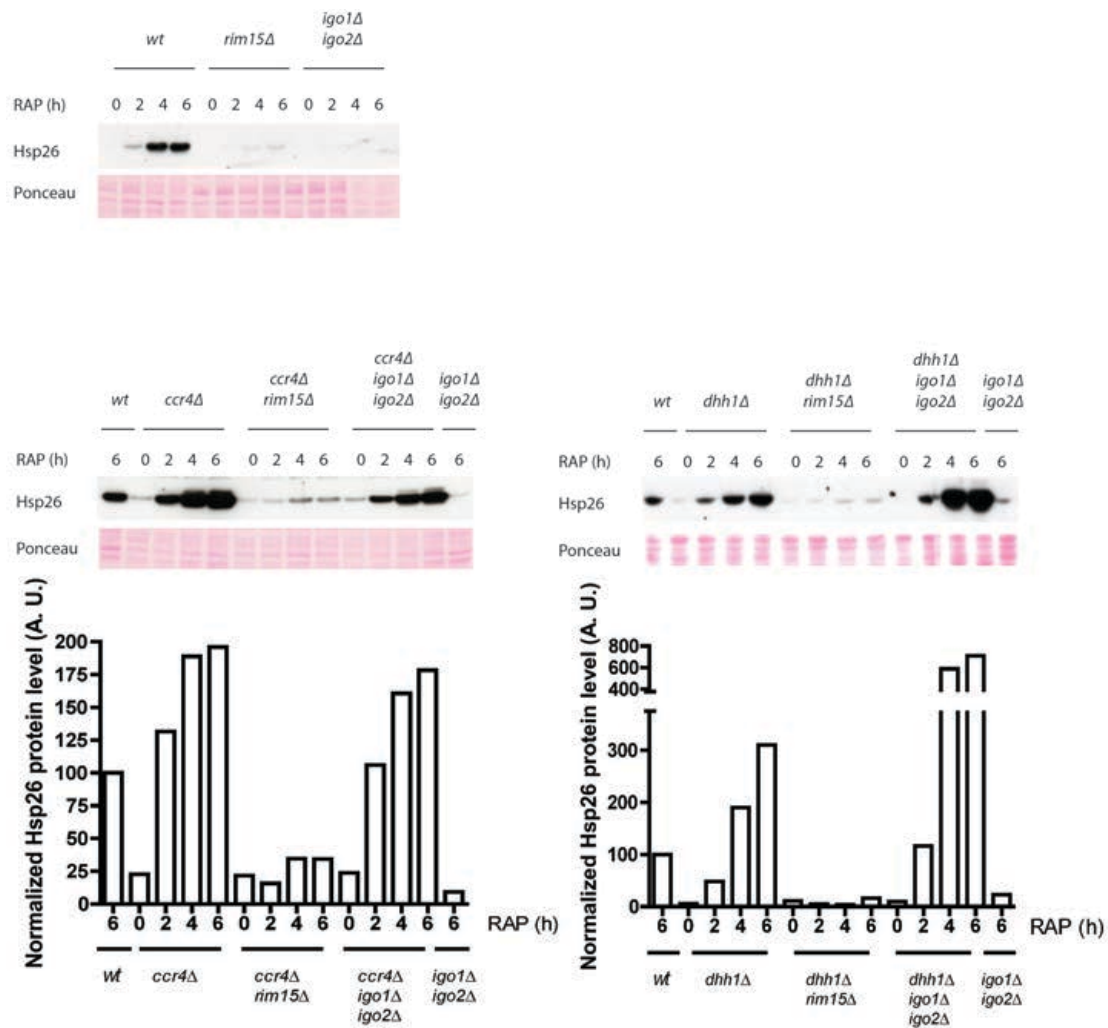


Fig. 25 Loss of Ccr4 and Dhh1 suppresses the defect of *igo1Δ igo2Δ* mutant cells, but not that of *rim15Δ* cells in rapamycin-induced Hsp26 protein expression

Whole cell protein extracts from indicated cells were harvested prior to (EXP) or following rapamycin treatment (RAP; 0.2 $\mu\text{g ml}^{-1}$; 2, 4 or 6 hr), analyzed by SDS-PAGE, and probed with anti-Hsp26 antibodies. Ponceau S staining of the membranes prior to immunoblot analysis served as loading control. Bar graphs show the relative levels of Hsp26 protein per total protein (Arbitrarily set to 100 for wild-type cells following 6 hr of rapamycin treatment).

These results are consistent with our previous findings, which showed that deletion of *CCR4* and *DHH1* suppresses the defect of rapamycin-treated *igo1Δ igo2Δ* cells in *HSP26* expression (Talarek et al., 2010).

III. 2. 2 Loss of Pat1 suppresses the defect of an *igo1Δ igo2Δ* mutant in *HSP26* expression following rapamycin treatment

We further analyzed whether loss of Pat1 also suppresses the defect of *igo1Δ igo2Δ* cells but not that of *rim15Δ* cells following rapamycin-induced TORC1 inactivation. To this end, we measured *HSP26* mRNA and Hsp26 protein levels in rapamycin-treated wild-type, *rim15Δ*, *igo1Δ igo2Δ*, *pat1Δ* cells and in *PAT1*-deficient *rim15Δ* and *igo1Δ igo2Δ* mutants.

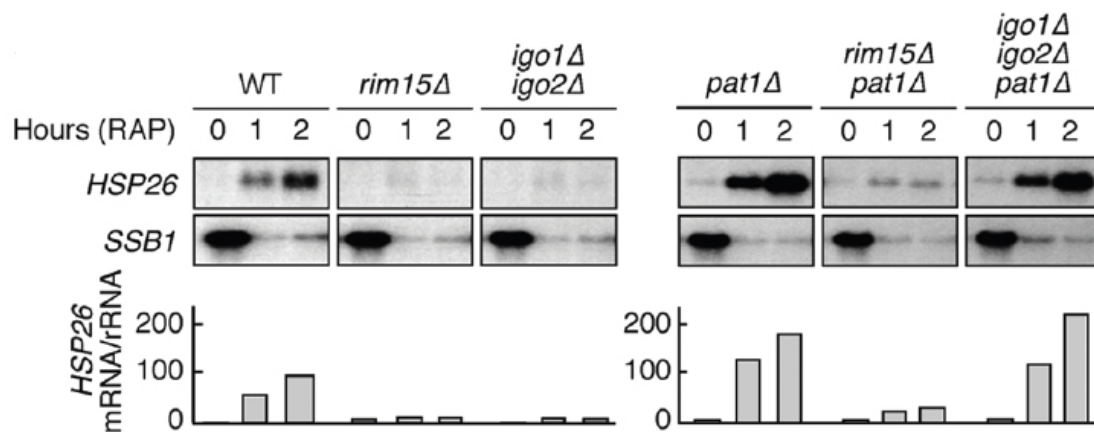


Fig. 26 Loss of Pat1 suppresses the defect of *igo1Δ igo2Δ* cells, but not that of *rim15Δ* cells in rapamycin-induced *HSP26* mRNA accumulation

Northern blot analyses of *HSP26* and *SSB1* mRNAs were done with exponentially growing strains with indicated genotypes, treated (1 hr and 2 hr) or not (0 hr) with rapamycin (RAP; 0.2 $\mu\text{g ml}^{-1}$). The decrease in *SSB1* transcript levels was used as internal control for rapamycin function. All samples were run on the same gel (identical exposure time) Bar graph show the relative levels of *HSP26* mRNA per rRNA (Arbitrarily set to 100 for wild-type cells after 2 hr of rapamycin treatment).

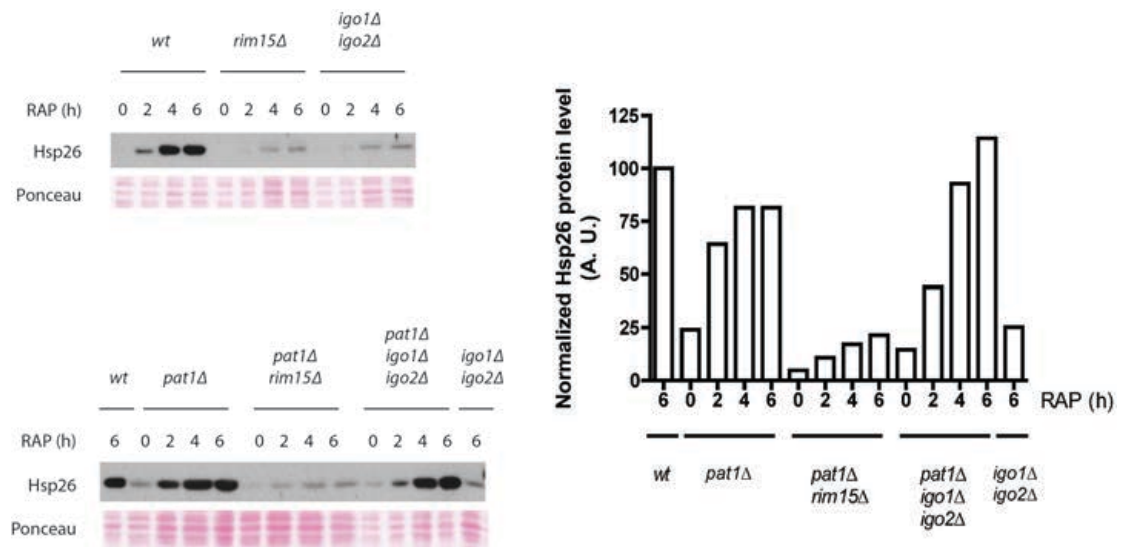


Fig. 27 Loss of Pat1 fully suppresses the defect of *igo1Δ igo2Δ* cells, but not that of *rim15Δ* cells in rapamycin-induced Hsp26 protein expression

Whole cell protein extracts from indicated cells were harvested prior to (EXP) or following rapamycin treatment (RAP; $0.2 \mu\text{g ml}^{-1}$; 2, 4 or 6 hr), were analyzed by SDS-PAGE, and probed with anti-Hsp26 antibodies. Ponceau S staining of the membranes prior to immunoblot analysis served as loading control. Bar graphs show the relative levels of Hsp26 protein per total protein (Arbitrarily set to 100 for wild-type cells after 6 hr of rapamycin treatment).

In line with the results of our screen shown in Fig. 23A, we found that *PAT1* deletion led to a higher *HSP26* mRNA levels in rapamycin treated cells. However, the corresponding Hsp26 protein levels were similar between wild-type and *pat1Δ* cells. Loss of Pat1 was sufficient to fully suppress the defect of *igo1Δ igo2Δ* cells, but not that of *rim15Δ* cells in *HSP26* mRNA and Hsp26 protein expression following rapamycin treatment (Fig. 26 and 27).

To confirm that the suppression of the defect of *igo1Δ igo2Δ* cells in rapamycin-induced *HSP26* expression was indeed due to the loss of *PAT1*, a complementation assay was performed. A wild-type copy of *PAT1* was expressed from a centromeric YCplac33-*PAT1* plasmid in *pat1Δ*, *pat1Δ rim15Δ* and *pat1Δ igo1Δ igo2Δ* cells carrying the *HSP26*-yEmRFP reporter. As expected, while colonies formed from *pat1Δ igo1Δ igo2Δ* cells harboring a control plasmid remained purple, *pat1Δ igo1Δ igo2Δ* cells, harboring a plasmid that expresses *PAT1* formed white colonies. These results confirm that the suppression of the defect of *igo1Δ igo2Δ* cells in *HSP26* expression is indeed due to the deletion of *PAT1* (Fig. 28).

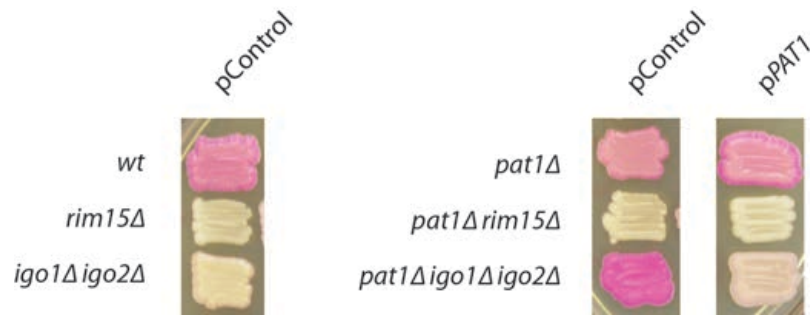


Fig. 28 Expression of *PAT1* from its own promoter restores the defect in *HSP26*-yEmRFP expression in *pat1Δ igo1Δ igo2Δ* cells

Indicated strains were cotransformed with a centromeric empty YCplac33 plasmid (pControl) or YCplac33-*PAT1* (p*PAT1*), and the *HSP26*-yEmRFP reporter. Transformants were patched on SD selective medium plates, and grown for 5 days at 30°C. Expression of yEmRFP under the control of *HSP26* promoter confers to cells a purple color.

One can conclude from Figs. 26, 27 and Fig. 28, that loss of Pat1 enables *igo1Δ igo2Δ* cells, but not *rim15Δ* cells to regain their ability to express *HSP26* (both at mRNA and Hsp26 protein levels) following rapamycin-induced TORC1 inactivation.

III. 2. 3 Loss of Lsm1 and Lsm6 fully suppresses the defect of an *igo1Δ igo2Δ* mutant in rapamycin-induced *HSP26* expression at the mRNA level, but only partially at protein level

Following a two-hour rapamycin treatment, *lsm1Δ* cells accumulated 4 times more *HSP26* mRNA than wild-type cells, while *HSP26* mRNA levels were similar between wild-type and *lsm6Δ* cells. Loss of Lsm1 or Lsm6 in *rim15Δ* and *igo1Δ igo2Δ* cells led to the accumulation of the same amount of *HSP26* mRNA as in wild-type cells. This suggests that loss of Lsm1 or Lsm6 restores the expression of *HSP26* in *rim15Δ* and *igo1Δ igo2Δ* mutants at the mRNA level (Fig. 29). Following a 6 hr rapamycin treatment, *lsm1Δ* cells accumulated 3 times more Hsp26 protein than wild-type cells, while Hsp26 protein level was similar between wild-type and *lsm6Δ* cells. However, *lsm1Δ rim15Δ* or *lsm6Δ rim15Δ* mutant cells did not accumulate Hsp26 protein. *lsm1Δ igo1Δ igo2Δ* accumulated two times less Hsp26 protein than wild-type cells, while *lsm6Δ igo1Δ igo2Δ* cells failed to accumulate Hsp26 protein (Fig. 30). These results suggest that *HSP26* mRNAs are not at all or less well translated in *LSM1/6*-deficient *rim15Δ* or *igo1Δ igo2Δ* cells, respectively, when compared to wild-type cells.

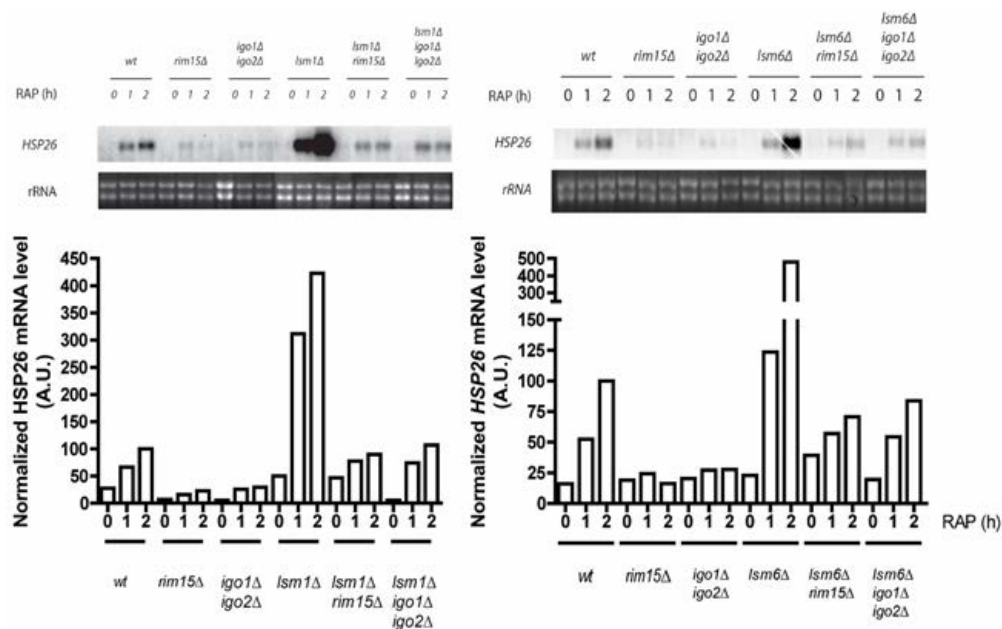


Fig. 29 Loss of Lsm1 and Lsm6 suppresses the defect of *rim15Δ* and *igo1Δ igo2Δ* cells in rapamycin-induced *HSP26* mRNA expression

Northern blot analyses of *HSP26* and *SSB1* mRNAs were done with exponentially growing indicated strains, treated (1 hr and 2 hr) or not (0 hr) with rapamycin (RAP; 0.2 $\mu\text{g ml}^{-1}$). The decrease in *SSB1* transcript levels was used as internal control for rapamycin function. All samples were run on the same gel (identical exposure time) Bar graph show the relative levels of *HSP26* mRNA per rRNA (Arbitrarily set to 100 for wild-type cells after 2 hr of rapamycin treatment).

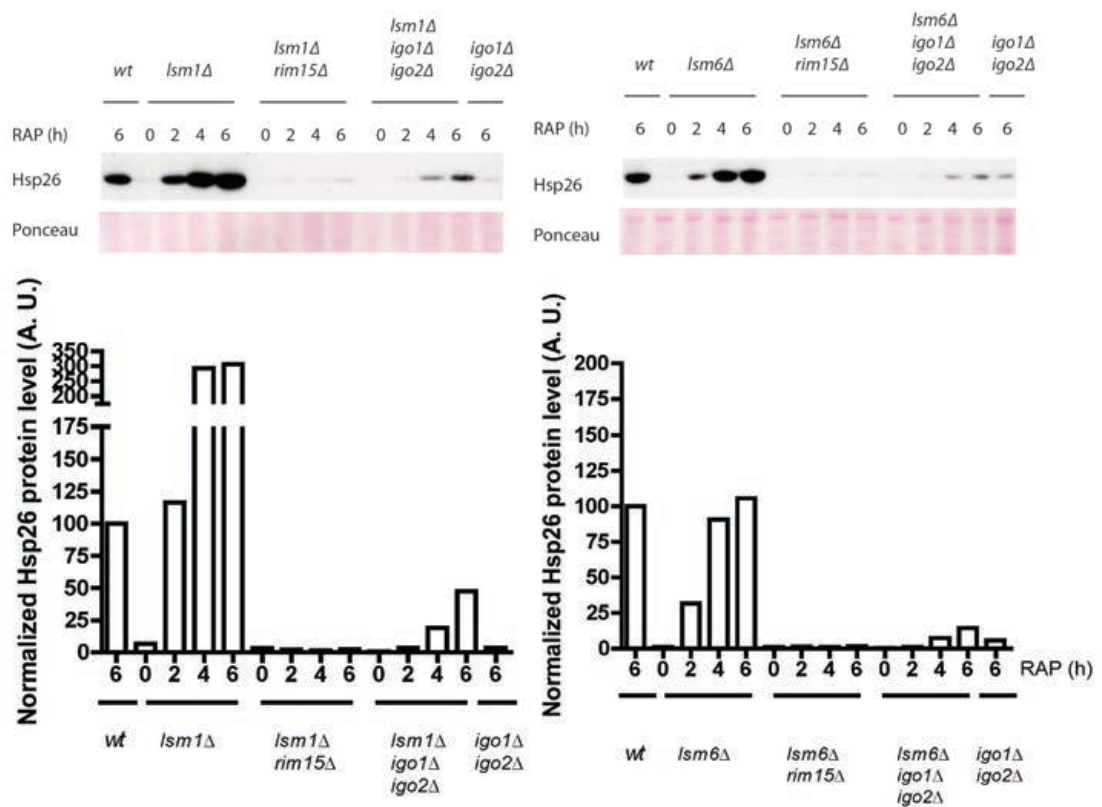


Fig. 30 Loss of Lsm1 and Lsm6 partially suppresses the defect of *igo1Δ igo2Δ* cells, but not that of *rim15Δ* cells in rapamycin-induced Hsp26 protein expression

Whole cell protein extracts from indicated cells were harvested prior to (EXP) or following rapamycin treatment (RAP; $0.2 \mu\text{g ml}^{-1}$; 2, 4 or 6 hr), were analyzed by SDS-PAGE, and probed with anti-Hsp26 antibodies. Ponceau S staining of the membranes prior to immunoblot analysis served as loading control. Bar graphs show the relative levels of Hsp26 protein per total protein (Arbitrarily set to 100 for wild-type cells after 6 hr of rapamycin treatment).

These results indicate that loss of Lsm1 and Lsm6 suppressed the defect of *igo1Δ igo2Δ* mutants in *HSP26* expression at the mRNA level, but only to a minor extent at the protein level.

III. 3 Discussion

We screened the haploid KO collection to identify suppressors of the defect of an *igo1Δ igo2Δ* mutant in *HSP26* expression. We obtained five mutations (*i.e.* *dhh1Δ*, *ccr4Δ*, *pat1Δ*, *lsm1Δ* and *lsm6Δ*) whose corresponding genes code for proteins involved in 5'-3' mRNA decay pathway (Fig. 23A). In agreement with our previous findings (Talarek et al., 2010), loss of Dhh1 or Ccr4 suppressed the defect in *HSP26* expression (both at mRNA and protein levels) in *igo1Δ igo2Δ* cells, but not in *rim15Δ* cells (Fig. 24 and 25). Our genetic data show that deletion of genes whose products are involved in the decapping step of 5'-3' mRNA decay (*i.e.* Pat1, Dhh1, Lsm1 and Lsm6) suppresses the defect of *igo1Δ igo2Δ* mutants. Intriguingly, while loss of Dhh1 or Pat1 suppresses the defect of *igo1Δ igo2Δ* cells in *HSP26* expression at both the mRNA and protein levels (Fig. 24, 25, 26 and 27), loss of Lsm1 or Lsm6 suppresses the defect of *igo1Δ igo2Δ* cells in *HSP26* expression at the mRNA level, but only to a lower extent at the protein level (Fig. 29 and 30). These results suggest that the mRNA decapping pathway targets *HSP26* mRNA in the absence of Igo1/2. However, Dhh1/Pat1 and Lsm1/Lsm6 appear to play different roles in decapping and/or translation activation of *HSP26* mRNA.

Dhh1, a DEAD-box RNA helicase, is thought to act as an enhancer of decapping at an early step of mRNA degradation (Coller et al., 2001; Fischer and Weis, 2002). Pat1 has been proposed to be a scaffold that binds proteins involved in early (Dhh1-dependent) and late (heteroheptameric complex Lsm1-7-dependent) steps of mRNA decapping. Lsm1 and Lsm6 belong to the Lsm1-7 complex, recruitment of which to oligoadenylated mRNAs has been proposed to be required for a final activation of the Dcp1/Dcp2 enzyme *in vivo* (Nissan et al., 2010).

Loss of Lsm1 and Lsm6 suppressed the defect of *igo1Δ igo2Δ* mutants in *HSP26* expression at the mRNA level, but only slightly at the protein level (Fig. 29 and 30). In this context, we expected that loss of the other subunits of the Lsm1-7 complex may also suppresses the defect of *igo1Δ igo2Δ* cells in *HSP26* expression. As the subunits Lsm2-5 of this complex are essential, we could not find them in the screen. However, loss of the non-essential Lsm7 subunit did not suppress the defect of *igo1Δ igo2Δ* cells in *HSP26*-yEmRFP expression in the primary screen. We also confirmed this result by analyzing *HSP26*-yEmRFP

expression in *lsm7Δ igo1Δ igo2Δ* cells (data not shown). Thus, loss of Lsm7 has a different impact than loss of Lsm1 or Lsm6. Interestingly, loss of Xrn1 suppresses the defect of *igo1Δ igo2Δ* cells in *HSP26* expression at the mRNA level, but not at the protein level. Xrn1 is the 5'-3' exonuclease that is involved in the last step of 5'-3' mRNA decay pathway. Accordingly, we proposed earlier that in *xrn1Δ igo1Δ igo2Δ* cells, decapped *HSP26* mRNAs are entrapped in P bodies and thus fail to be translated into proteins (Talarek et al., 2010). The suppression of the defect of *HSP26* expression in *LSM1*- or *LSM6*-deficient *igo1Δ igo2Δ* cells is reminiscent of the phenotype of *xrn1Δ igo1Δ igo2Δ* cells. Therefore we hypothesize that in *LSM1*- or *LSM6*-deficient *igo1Δ igo2Δ* cells, mRNAs may be entrapped to some extent as well in P bodies and thus fail to be translated into protein.

Based on our genetic data and the fact that Igo1 interacts with Dhh1 *in vivo*, we propose the following model. In the absence of Igo1/2, Pat1 and Dhh1 initiate a process, at the end of which quiescence-specific mRNAs are recruited into P bodies where they can be degraded (1). In *igo1Δ igo2Δ* mutants, loss of Pat1 or Dhh1 may deviate mRNAs from entering into this process and allow them to be delivered to ribosomes for translation. Loss of Lsm1/6 proteins, in contrast, cannot prevent the recruitment of quiescence-specific mRNAs into P bodies in *igo1Δ igo2Δ* cells, but may interfere with their proper decapping once they reside in P bodies. As a consequence, the corresponding mRNAs are expected to mainly accumulate, likely in a state prior to decapping, within P bodies (2). The observed partial suppression by loss of Lsm1/6 of the defect in rapamycin-induced Hsp26 protein expression in *igo1Δ igo2Δ* cells (Fig. 31) may be explained if some of the corresponding mRNAs may be able to escape from P bodies. In the presence of Igo1/2, Pat1 and Dhh1 are inhibited (3) and quiescent-specific mRNAs are therefore able to be translated (4).

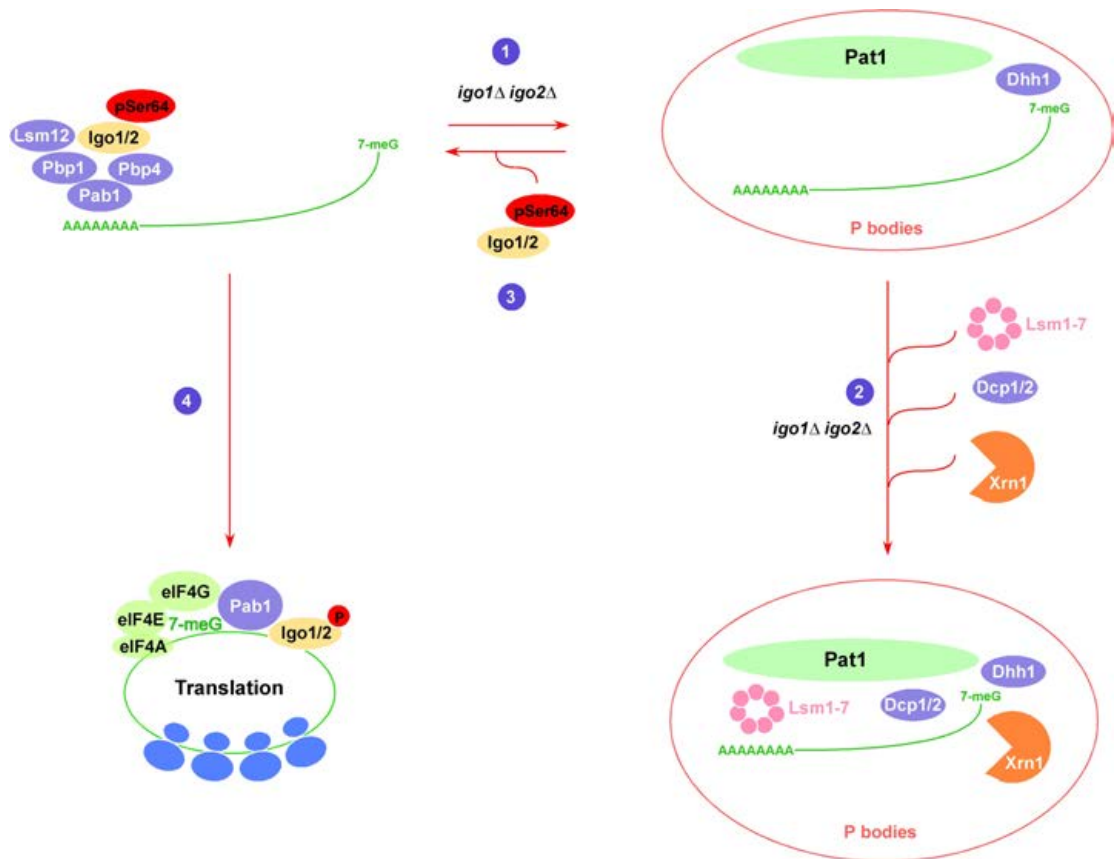


Fig. 31 Model depicting Igo1/2 antagonizing mRNA decapping activators Dhh1 and/or Pat1

This model makes several predictions that are testable in the future. For instance, we expect that capped *HSP26* mRNAs should accumulate in P-bodies in glucose-depleted *igo1Δ igo2Δ lsm1Δ* and *igo1Δ igo2Δ lsm6Δ* strains. Colocalization analyses of *HSP26* mRNAs and P body marker proteins in glucose-depleted *lsm1Δ igo1Δ igo2Δ* and *lsm6Δ igo1Δ igo2Δ* cells could further confirm our hypothesis.

The second predication is that Igo1/2 play a role in inhibition of decapping activation. This hypothesis could be experimentally addressed by performing an *in vivo* decapping assay described previously (Blewett et al., 2011). Rapamycin-induced *HSP26* mRNAs in wild-type cells are mainly subjected to translation, while in rapamycin-treated *igo1Δ igo2Δ* cells, *HSP26* mRNAs are decapped and subsequently degraded in P bodies. The transient nature of decapped mRNAs in *igo1Δ igo2Δ* mutants renders their quantification really challenging. However, in absence of the 5'-3' exonuclease Xrn1, decapped mRNAs are no longer degraded, and should therefore be detectable. If our model is correct, we should thus expect more decapped *HSP26* mRNAs in an *igo1Δ igo2Δ xrn1Δ* mutant than in an *xrn1Δ* mutant.

Furthermore, we hypothesize that Igo1/2 inhibits decapping activation by antagonizing the decapping activator Dhh1 and/or Pat1. Future studies should focus on structural and functional aspect of the interaction between Igo1/2 and both Pat1 and Dhh1 to address the mechanisms that control the mRNA decay of specific G₀-induced mRNAs. An *in vitro* binding assay of Dhh1 or Pat1 with Igo1 would be necessary to prove that Igo1 interacts directly with Dhh1 or Pat1. Moreover, it would be interesting to identify constitutively active *DHH1* or *PAT1* alleles that phenocopy loss of Igo1 and Igo2 when expressed in *dhh1Δ* or *pat1Δ* mutant, respectively. If the interaction between Igo1 and constitutive active *DHH1* or *PAT1* alleles were abrogated, it would suggest that the binding of Igo1 to Dhh1 or Pat1 may block their function as decapping activators. In addition, to test whether Igo1 inhibits the ATPase activity of Dhh1, a Dhh1 ATPase activity assay has been developed in our lab. However, the addition of bacterially purified Igo1 did not alter the ATPase activity of Dhh1. We could further test whether Igo1 purified from wild-type and *rim15Δ* cells prior to and following rapamycin treatment would affect Dhh1 ATPase activity. The test could also be performed in presence or absence of mRNA to determine whether the inhibition of Dhh1 ATPase activity by Igo1 is mRNA-dependent.

In order to find additional genetic interactors of *IGO1/2*, we also performed a synthetic lethal (SL) screen where we crossed an *igo1Δ igo2Δ* mutant with the non-essential KO collection. Surprisingly, all triple mutants were able to grow, and hence no SL interactions were found. It may be possible to find, however, mutations that exhibit synthetic effect with *igo1Δ igo2Δ* when assayed under different conditions. For instance, we may in the future assess whether any *igo1Δ igo2Δ yfgΔ* mutant has a defect in survival of stationary phase. Instead of looking for SL mutants that had impaired growth on plate, we should have screened for the capacity of triple mutants to survive on plate following 15 days of growth. Finally, our *igo1Δ igo2Δ* suppressor screen could be completed by screening the *ts* mutant collection of essential genes (Li et al., 2011). This approach could reveal essential genes whose products are negatively regulated by Igo1. To this end, a new reporter should be constructed by cloning the ORF of yEmRFP under the control of the promoter of a G₀ specific genes that is not affected by heat shock.

Chapter IV. Genetic screen for multicopy suppressors of *igo1Δ igo2Δ* defects

We previously described the identification of gene deletions that suppress the defect of *igo1Δ igo2Δ* cells in the expression of G₀-specific genes. The products of these genes appear to be negative regulators of the expression of G₀-specific genes. To further elucidate the cellular function of Igo1/2, we conducted a genetic screen for multicopy suppressors of the defect of *igo1Δ igo2Δ* cells in expression of G₀-specific genes. We anticipated that the suppressors would be positive regulators of G₀ program. These regulators could be downstream of Igo1/2, or belong to a pathway that acts parallel to the Rim15-Igo1/2 cascade.

IV. 1 Genetic screen procedure for multicopy suppressors of *igo1Δ igo2Δ* defects

To perform the genetic screen for multicopy suppressors, we used a library of multicopy plasmids, where yeast genomic DNA fragments were cloned downstream of the regulatable *GAL1* promoter. The complexity of the library is 5×10^7 (Ramer et al., 1992). An *igo1Δ igo2Δ* query strain harboring the *HSP26*-yEmRFP reporter plasmid was transformed with this library and plated on galactose-containing selective medium. 7×10^7 transformants were obtained. A library of this complexity contains enough clones to represent fusion of GAL1p at every base in the yeast genome (Ramer et al., 1992).

To verify that the suppression of the defect in *igo1Δ igo2Δ* mutant cells in *HSP26* expression was indeed due to the overexpression of genes from library plasmids upon galactose induction, candidate clones were restreaked on either galactose- or glucose-containing medium to select those that remained purple on galactose-containing medium, but turned white on glucose-containing medium. The candidate clones that had turned white on glucose-containing medium were restreaked on galactose-containing medium to select for those that turned purple again. 41 candidate suppressors were kept.

A secondary screen was then performed to remove additional false positives. Each library plasmid of the 41 candidate clones was isolated, and retransformed into *igo1Δ igo2Δ* cells to confirm that the suppression observed in the primary screen was dependent on genes expressed from the library plasmids (Fig. 32).

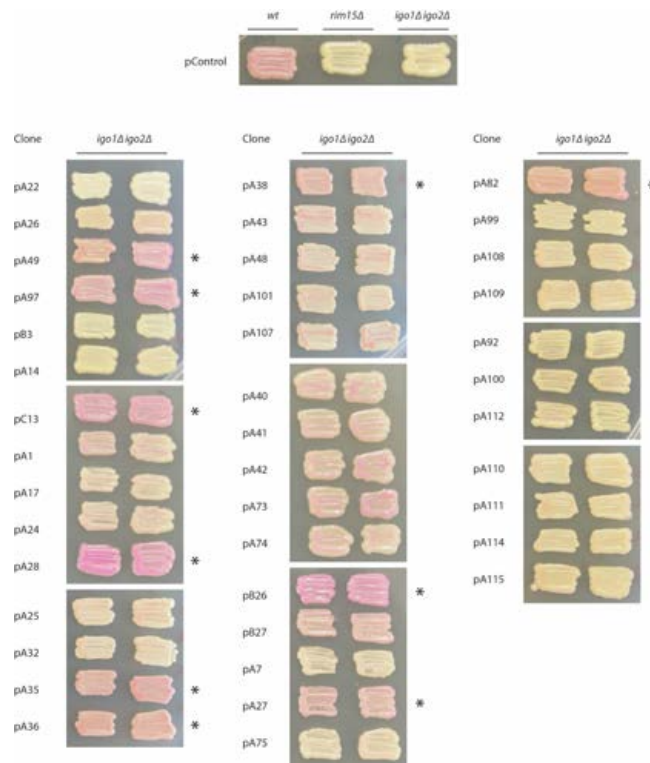


Fig. 32 Suppression of the defect of *igo1Δ igo2Δ* mutant cells in *HSP26*-yEmRFP expression by overexpression of genes from library plasmids

Library plasmids isolated from candidate clones were re-transformed into *igo1Δ igo2Δ* mutant cells coexpressing the *HSP26*-yEmRFP reporter. Control vector and the *HSP26*-yEmRFP reporter plasmid were also cotransformed into wild-type, *rim15Δ* and *igo1Δ igo2Δ* cells (top panel). Transformants were restreaked on galactose-containing selective medium and grown for 5 days at 30°C. Asterisks (*) indicate clones that were selected for sequencing.

Ten candidates were kept from the secondary screen (Fig. 32). The corresponding plasmids were sent for sequencing. Figure 33 indicates what genomic fragments were cloned downstream of the *GALI* promoter. Genes responsible for suppressing the defect in *igo1Δ igo2Δ* mutant cells in *HSP26* expression when overexpressed were likely immediately downstream of the *GALI* promoter.

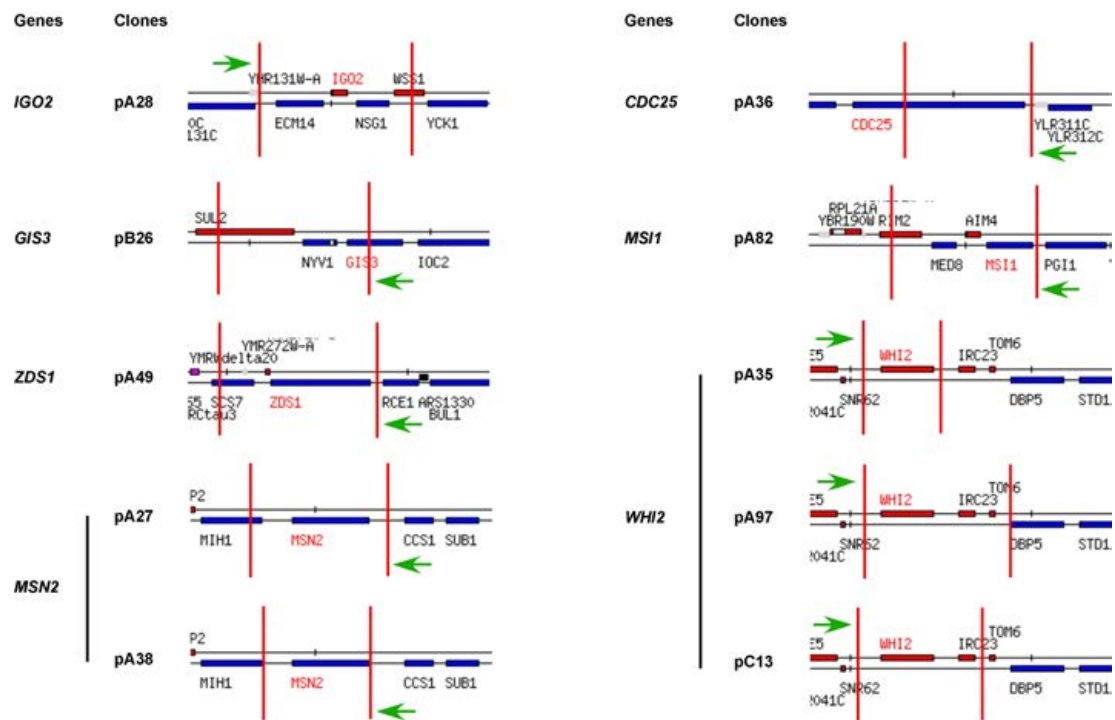


Fig. 33 Schematic representation of the genomic fragments present in plasmids that suppress the defect of *igo1Δ igo2Δ* cells in *HSP26*-yEmRFP expression in Fig. 32

Red vertical lines delimitate the sequence cloned in the original library plasmids. Arrows indicates the position and orientation of the *GAL1* promoter.

The *IGO2* ORF from the plasmid pA28 complemented the defect of *igo1Δ igo2Δ* mutant cells in *HSP26* expression, which indicates that our screen was well suited to identify new *igo1Δ igo2Δ* phenotype suppressors. The three independent fragments in pA35, pA97 and pC13 all contained the ORF of *WHI2*. The two independent fragments in pA27 and p38 contained the ORFs of *MSN2*. *ZDS1* and *MSI1* were the ORFs right downstream of the *GAL1* promoter in the fragments in pA49 and pA82, respectively. Only the 227 amino acids of the carboxyl-terminal part of Gis3 and the first 1108 amino acids of Cdc25 are expressed from pB26 and pA36 plasmids, respectively. Notably, our screen was not saturated judging from the following observations: (1) the same genomic fragment was not isolated twice for *WHI2* and *MSN2*; (2) we found *GIS3*, *ZDS1*, *IGO2*, *MSI1* and *CDC25* only once; and we did not find Igo1.

The regulation of the expression of Igo1/2-dependent G_0 -specific genes has been studied on glucose-containing medium, which is the preferred carbon source. To rule out the possibility that the suppression of the *igo1Δ igo2Δ* phenotype observed here, was galactose-

dependent, the ORF of each candidate was cloned under the control of a tetracycline-inducible *tetO₇* promoter and fused to a N-terminal His₆-HA₃ tag. As a plasmid containing the *IGO1* ORF under the control of the *tetO₇* promoter was available, we used it as a positive control. The suppression of the defect of *igo1Δ igo2Δ* cells in *HSP26-yEmRFP* was then tested on glucose-containing medium with or without doxycycline (Fig. 34). We expected that on doxycycline-containing medium, colonies would turn purple, while on doxycycline-free medium colonies should remain white.

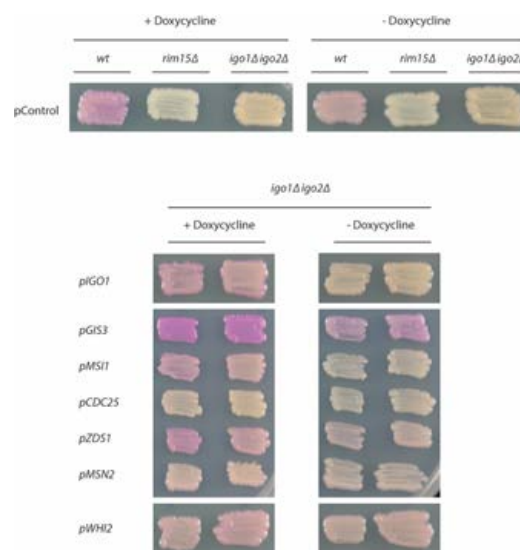


Fig. 34 Suppression of the defect of *igo1Δ igo2Δ* cells in *HSP26-yEmRFP* expression by overexpression of candidate genes under the control of the tetracyclin-inducible *tetO₇* promoter

Plasmids containing full-length candidate genes under the control of a tetracyclin-inducible *tetO₇* promoter and the *HSP26-yEmRFP* reporter were cotransformed into *igo1Δ igo2Δ* cells. Transformants were restreaked on glucose containing selective medium with or w/o doxycycline ($5\mu\text{g ml}^{-1}$) and grown for 5 days at 30°C .

As expected, overexpression of *IGO1* complemented the defect of *igo1Δ igo2Δ* cells in *HSP26-yEmRFP* expression after 5 days growth on plates with doxycycline. Colonies formed from cells harboring *ptetO₇-GIS3* plasmid turned dark purple on doxycycline-containing medium, while they were purple on doxycycline-free medium. Previous experiments using this *tetO₇* promoter suggested to us that in the absence of doxycycline, this promoter is leaky. Hence, potentially, the small amount of Gis3 produced in the absence of doxycycline was sufficient to suppress the defect of *igo1Δ igo2Δ* cells in *HSP26-yEmRFP* expression. Colonies formed from cells harboring *ptetO₇-ZDS1*, *WHI2* and *MS11* plasmids turned purple on doxycycline-containing medium, while they were light purple on

doxycycline-free medium. These results suggest that *GIS3* is a strong suppressor of the defect of *igo1Δ igo2Δ* cells in *HSP26-yEmRFP* expression, while *ZDS1*, *WHI2* and *MSI1* suppress the defect of *igo1Δ igo2Δ* cells in *HSP26-yEmRF* expression to a lower extent. Colonies formed from cells harboring the *ptetO₇-CDC25* plasmid stayed white on doxycycline-containing medium, indicating that overexpression of full length *CDC25* could not suppress the defect of *igo1Δ igo2Δ* cells in *HSP26-yEmRFP* expression. Colonies formed from cells harboring the *ptetO₇-MSN2* plasmid stayed white on doxycycline-containing medium, indicating that the suppression of the defect of *igo1Δ igo2Δ* cells in *HSP26-yEmRFP* expression might be dependent on galactose-induced *MSN2* overexpression. The latter two candidates genes were therefore not studied further.

Gis3 was initially identified as a multicopy suppressor of the Gal- phenotype of *snf1 mig1 srb8/10/11* cells (Balciunas and Ronne, 1999). Of interest, *ZDS1* and *GIS3* were also found as multicopy suppressors of the conditional growth defect of *las24-1 (kog1)* (Araki et al., 2005). *Gis3* has no assigned function to date, and no homologue in higher eukaryotes has been identified yet. *Zds1* was found to be involved in maintaining the PP2A regulatory subunit *Cdc55* in the cytoplasm where it promotes mitotic entry (Rossio and Yoshida, 2011). Additionally, it has been demonstrated that overexpression of *Zds1* leads to increased cytoplasmic localization of the PKA regulatory subunit *Bcy1* (Griffioen et al., 2001). *Whi2* was found to be required for full activation of the general stress response, possibly by promoting *Msn2* dephosphorylation (Kaida et al., 2002). *Msi1*, the subunit of chromatin assembly factor I (CAF-1) has a CAF1-independent role as a negative regulator of the RAS/cAMP pathway via sequestration of the *Npr1* kinase (Johnston et al., 2001; Ruggieri et al., 1989). In the following paragraphs, we focus our analyses on *Gis3*, *Zds1* and *Whi2*.

IV. 2 *GIS3*, *ZDS1* or *WHI2* suppresses the defect of *igo1Δ igo2Δ* and *rim15Δ* cells in *HSP26* expression following rapamycin-treatment or glucose limitation

We hypothesized that Rim15 activates the transcription of Msn2/4- and Gis1-dependent genes, and the posttranscriptional stabilization of the very same mRNAs are ensured by Rim15-phosphorylated Igo1/2 (Talarek et al., 2010). We anticipated that the multicopy suppressors of *igo1Δ igo2Δ* phenotype would affect either transcription or posttranscriptional mRNA stability. To test this hypothesis, we measured the *HSP26* mRNA and Hsp26 protein levels in wild-type, *rim15Δ* and *igo1Δ igo2Δ* cells overexpressing candidate suppressors following rapamycin treatment or glucose limitation (following growth in batch cultures for 48 hr).

IV. 2. 1 Overexpression of *GIS3* fully suppresses the defect of *igo1Δ igo2Δ* and *rim15Δ* cells in rapamycin-induced *HSP26* expression at both the mRNA and protein levels

Following a two-hour rapamycin-treatment, wild-type, *rim15Δ* and *igo1Δ igo2Δ* cells carrying *ptetO₇-GIS3* plasmid accumulated 1.5-, 1.2- and 1.15-fold higher *HSP26* mRNAs levels, respectively, than wild-type cells carrying a control vector when incubated on doxycycline-containing medium. When doxycycline was omitted, wild-type, *rim15Δ* and *igo1Δ igo2Δ* cells carrying the *ptetO₇-GIS3* plasmid accumulated 2 times more *HSP26* mRNAs than wild-type cells carrying a control vector (Fig. 35). These data suggest that overexpression of *GIS3* fully suppresses the defect of *rim15Δ* and *igo1Δ igo2Δ* cells in rapamycin-induced *HSP26* mRNA accumulation, and that in the absence of doxycycline, the leaky *tetO₇* promoter drives the production of a small amount of Gis3 (see below for details), which is sufficient to suppress the defect of *rim15Δ* and *igo1Δ igo2Δ* cells in rapamycin-induced *HSP26* mRNA accumulation. Surprisingly, the suppression in doxycycline-free (repressing condition) cells is even somewhat higher than in doxycycline-treated (derepressing condition) cells following rapamycin treatment. This may be explained by the difference of amount of Gis3 in these two conditions.

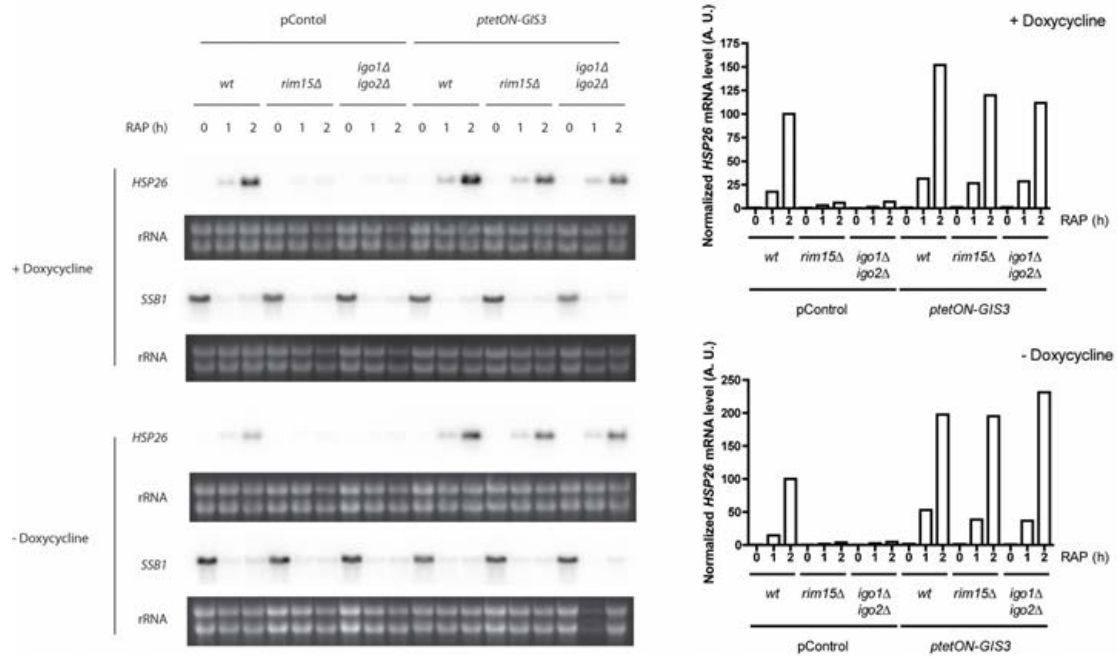


Fig. 35 Overexpression of *GIS3* suppresses the defect of both *igo1Δ igo2Δ* and *rim15Δ* cells in *HSP26* mRNA accumulation following rapamycin treatment

Northern blot analyses of *HSP26* and *SSB1* mRNAs were performed with exponentially growing strains with indicated genotypes incubated with or w/o doxycycline ($5 \mu\text{g ml}^{-1}$) for 4 hr, treated (1 hr and 2 hr) or not (0 hr) with rapamycin (RAP; $0.2 \mu\text{g ml}^{-1}$). The decrease in *SSB1* transcript levels was used as internal control for rapamycin function. All samples were run on the same gel (identical exposure time). Bar graphs show the relative levels of *HSP26* mRNA per rRNA (Arbitrarily set to 100 for wild-type cells carrying an empty vector after 2 hr of rapamycin treatment).

We next analyzed the suppression of the defect of *rim15Δ* and *igo1Δ igo2Δ* cells by *GIS3* overexpression at the Hsp26 protein level. Following a 6-hour rapamycin-treatment, wild-type, *rim15Δ* and *igo1Δ igo2Δ* cells carrying the *ptetO₇-GIS3* plasmid accumulated the same level of Hsp26 protein as wild-type cells carrying a control vector incubated with or without doxycycline (Fig. 36). These observations indicate that following a 6-hour rapamycin treatment, the expression of *GIS3* suppresses the defect of *rim15Δ* and *igo1Δ igo2Δ* cells in Hsp26 protein expression.

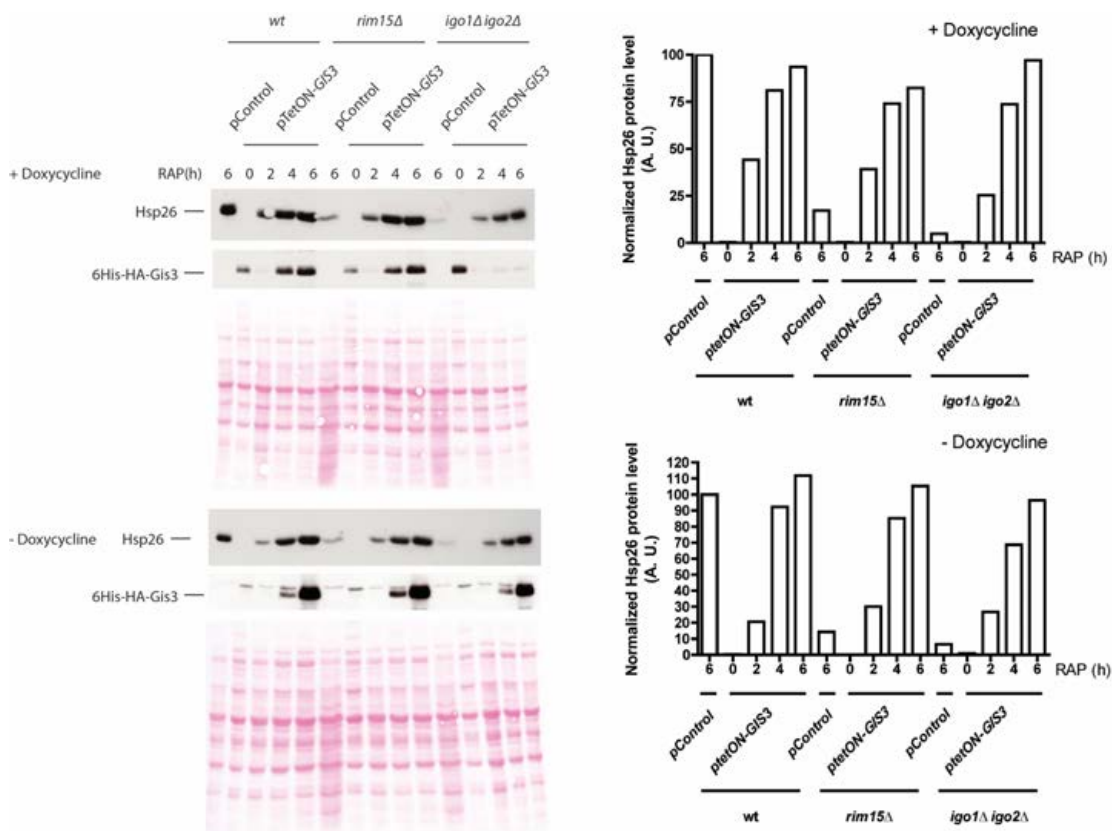


Fig. 36 Overexpression of *GIS3* suppresses the defect of both *igo1Δ igo2Δ* and *rim15Δ* cells in Hsp26 protein expression following rapamycin treatment

Whole cell protein extracts from indicated cells treated for 4 hr with or w/o doxycycline ($5\mu\text{g ml}^{-1}$), were harvested prior to (RAP; 0 hr) or following rapamycin treatment (RAP; $0.2\mu\text{g ml}^{-1}$; 2, 4 or 6 hr), were analyzed by SDS-PAGE, and probed with anti-Hsp26 and anti-HA antibodies. Ponceau S staining of the membranes prior to immunoblot analysis served as loading control. Bar graphs show the relative levels of Hsp26 protein per total protein (arbitrarily set to 100 for 6-hour rapamycin-treated wild-type cells carrying empty vector).

In parallel to the analysis of the Hsp26 protein levels, the levels of His₆-HA₃-Gis3 were also assessed in the different strains, with or without doxycycline induction. In cells treated with doxycycline, His₆-HA₃-Gis3 was expressed prior to rapamycin treatment. Following rapamycin treatment, we observed a transient decrease of doxycycline-induced Gis3 in wild-type, *rim15Δ*, *igo1Δ igo2Δ* cells (Gis3 could be visualized with longer exposure times in 6-hour rapamycin treated *igo1Δ igo2Δ* samples under these conditions). Although Gis3 protein levels were very low in 2 hr rapamycin-treated cells (Fig. 36), they were apparently sufficient to suppress the defect of *rim15Δ* and *igo1Δ igo2Δ* cells in accumulating normal *HSP26* mRNA levels in these cells (Fig. 35). In the absence of doxycycline, Gis3 protein levels showed a similar profile as in doxycycline-treated cells in all these strains (*i.e.* wild-type, *rim15Δ*, *igo1Δ igo2Δ* cells) (Fig. 36). This confirms our suspicion that the small amount of Gis3 produced in the absence of doxycycline was sufficient to suppress the defect of *igo1Δ igo2Δ* cells in *HSP26* expression at both the mRNA levels and the protein levels.

Similarly to the situation in rapamycin-treated cells, overexpression of *GIS3* suppressed the defect of *HSP26* expression at both the mRNA and protein levels in *rim15Δ* and *igo1Δ igo2Δ* cells that were subjected to glucose limitation (*i.e.* grown to saturation for 24 and 48 hr). Without doxycycline, the suppression of the *HSP26* expression defect of *rim15Δ* and *igo1Δ igo2Δ* cells by the apparently leaky *ptetO₇-GIS3* plasmid occurs to a lower extent (Fig. 37). Again, the amount of Gis3 detected in the extracts from cells not treated with doxycycline and grown for 24 and 48 hr in both culture was very low.

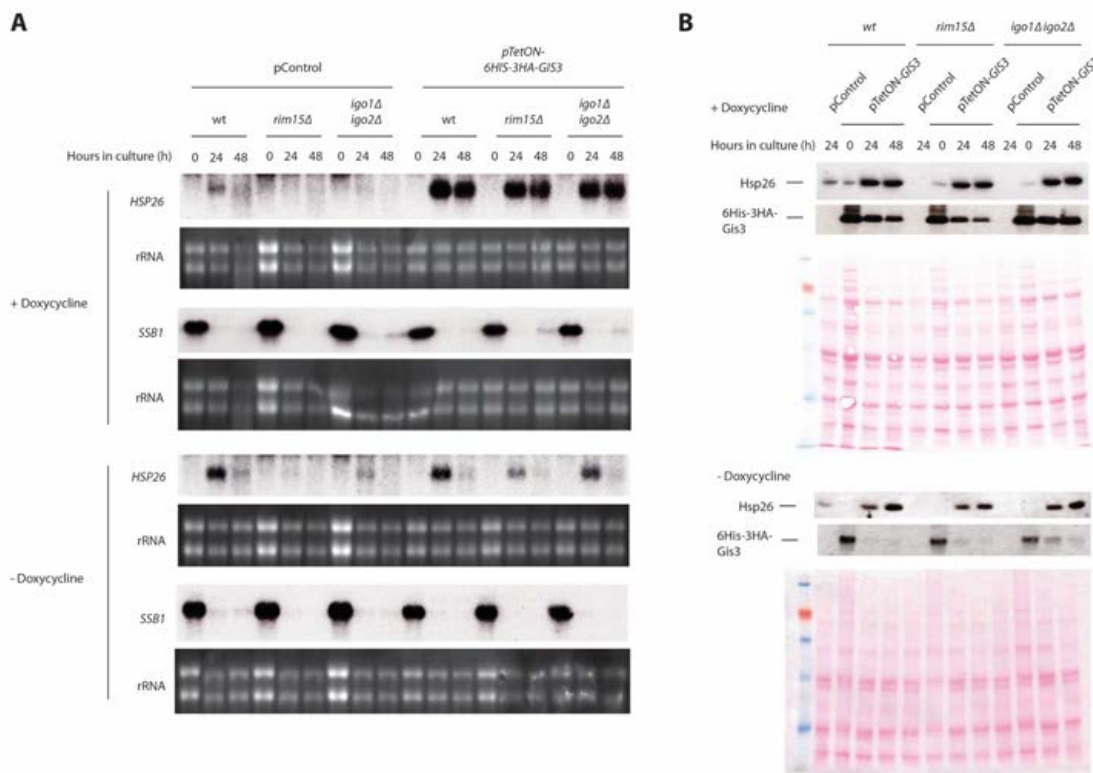


Fig. 37 Overexpression of *GIS3* suppresses the defect of both *igo1Δ igo2Δ* and *rim15Δ* cells in *HSP26* mRNA accumulation (A) and Hsp26 protein expression (B) following glucose limitation
 Strains with indicated genotypes induced 4 hr with or w/o doxycycline prior to exponential phase were harvested at exponential phase (0) and 24 hr and 48 hr after the exponential phase. Cells were treated as described in Fig. 27 for northern blot analysis, and as in Fig. 28 for western blot analysis.

We conclude that *GIS3* is a *bona fide* suppressor of the defect of *rim15Δ* and *igo1Δ igo2Δ* cells in *HSP26* expression at both the mRNA and protein level following rapamycin treatment and glucose limitation.

IV. 2. 2 Overexpression of *ZDS1* fully suppresses the defect of *igo1Δ igo2Δ* and *rim15Δ* cells in rapamycin-induced *HSP26* expression at both the mRNA and protein levels

Following a two-hour rapamycin-treatment, doxycycline-incubated wild-type, *rim15Δ* and *igo1Δ igo2Δ* cells carrying the *ptetO₇-ZDS1* plasmid accumulated 1.5 times more *HSP26* mRNAs than wild-type cells carrying a control vector (Fig. 38). When doxycycline was omitted, *rim15Δ* and *igo1Δ igo2Δ* cells carrying the *ptetO₇-ZDS1* plasmid did not accumulate *HSP26* mRNA under the same conditions (data not shown).

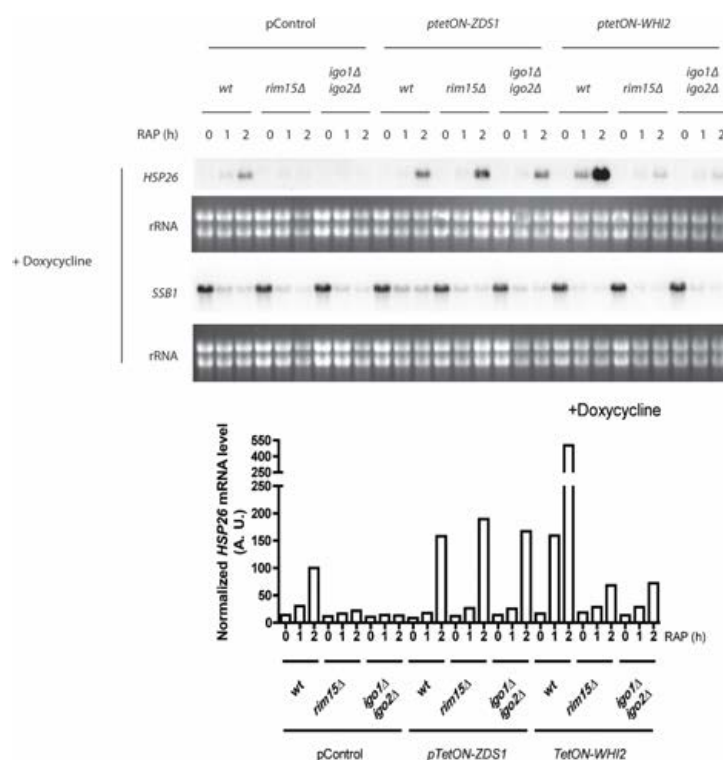


Fig. 38 Overexpression of *ZDS1* fully suppresses the defect of both *igo1Δ igo2Δ* and *rim15Δ* cells in *HSP26* mRNA expression following rapamycin treatment. Overexpression of *WHI2* partially suppresses the defect of both *rim15Δ* and *igo1Δ igo2Δ* cells in *HSP26* mRNA expression following rapamycin treatment
Northern blot analyses of *HSP26* and *SSB1* mRNAs were performed with exponentially growing strains with indicated genotypes incubated with doxycycline ($5 \mu\text{g ml}^{-1}$) for 4 hr, prior to (0 hr) or following rapamycin treatment (RAP; $0.2 \mu\text{g ml}^{-1}$) for 1 hr and 2 hr. The decrease in *SSB1* transcript levels was used as internal control for rapamycin function. All samples were run on the same gel (identical exposure time). Bar graphs show the relative levels of *HSP26* mRNA per rRNA (arbitrarily set to 100 for wild-type cells carrying empty vector after 2 hr of rapamycin treatment).

Following a 6-hour rapamycin-treatment, the Hsp26 protein levels were similar in doxycycline-incubated wild-type, *rim15Δ* and *igo1Δ igo2Δ* cells carrying the *ptetO₇-ZDS1* plasmid (Fig. 39). Following a 6-hour rapamycin-treatment, when doxycycline was omitted, *rim15Δ* and *igo1Δ igo2Δ* cells carrying the *ptetO₇-ZDS1* plasmid did not accumulate Hsp26 protein (data not shown).

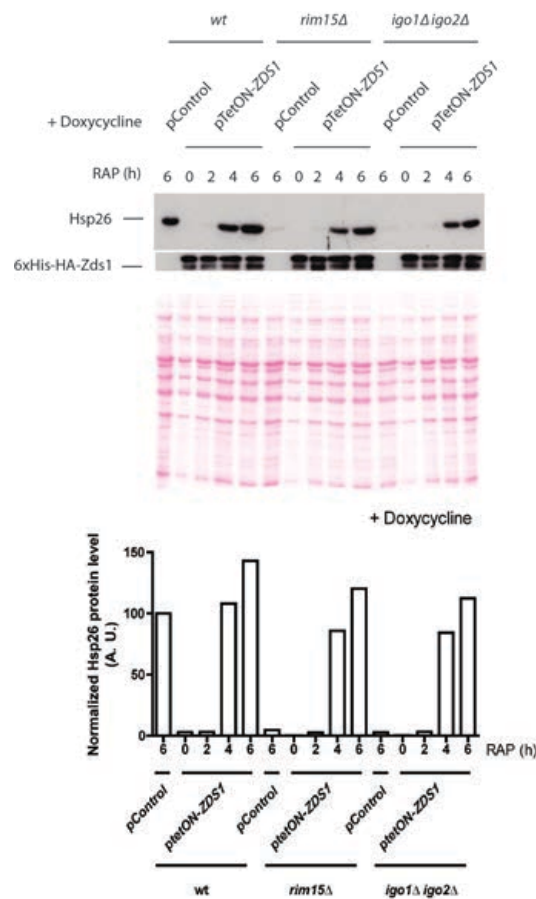


Fig. 39 Overexpression of *ZDS1* suppresses the defect of both *igo1Δ igo2Δ* and *rim15Δ* cells in Hsp26 protein expression upon rapamycin treatment

Whole cell protein extracts from indicated cells treated for 4 hr with doxycycline ($5\mu\text{g ml}^{-1}$), were harvested prior to (RAP; 0 hr) or following rapamycin treatment (RAP; $0.2\mu\text{g ml}^{-1}$; 2, 4 or 6 hr), were analyzed by SDS-PAGE, and probed with anti-Hsp26 antibodies. Ponceau S staining of the membranes prior to immunoblot analysis served as loading control.

These data show that overexpression of *ZDS1* suppresses the defect of *rim15Δ* and *igo1Δ igo2Δ* cells in rapamycin-induced *HSP26* expression at both the mRNA and protein levels.

IV. 2. 3 Overexpression of *WHI2* partially suppresses the defect of an *igo1Δ igo2Δ* and a *rim15Δ* mutant in rapamycin-induced *HSP26* expression at both the mRNA and protein levels

Following a two-hour rapamycin-treatment, wild-type cells carrying the *ptetO₇-WHI2* plasmid accumulated 5.5 times more *HSP26* mRNAs than wild-type cells carrying a control vector incubated with doxycycline (Fig. 38). *rim15Δ* and *igo1Δ igo2Δ* cells carrying the *ptetO₇-WHI2* plasmid accumulated two times less *HSP26* mRNA than wild-type cells carrying a control vector (Fig. 38). Following a two-hour rapamycin-treatment, when doxycycline was omitted, *rim15Δ* and *igo1Δ igo2Δ* cells carrying the *ptetO₇-WHI2* plasmid did not accumulate *HSP26* mRNA (data not shown).

Following two-hours of rapamycin-treatment, the Hsp26 protein level in doxycycline-incubated *rim15Δ* and *igo1Δ igo2Δ* cells carrying the *ptetO₇-WHI2* plasmid was respectively 50% and 30% of that in wild-type cells carrying a control vector (Fig. 40).

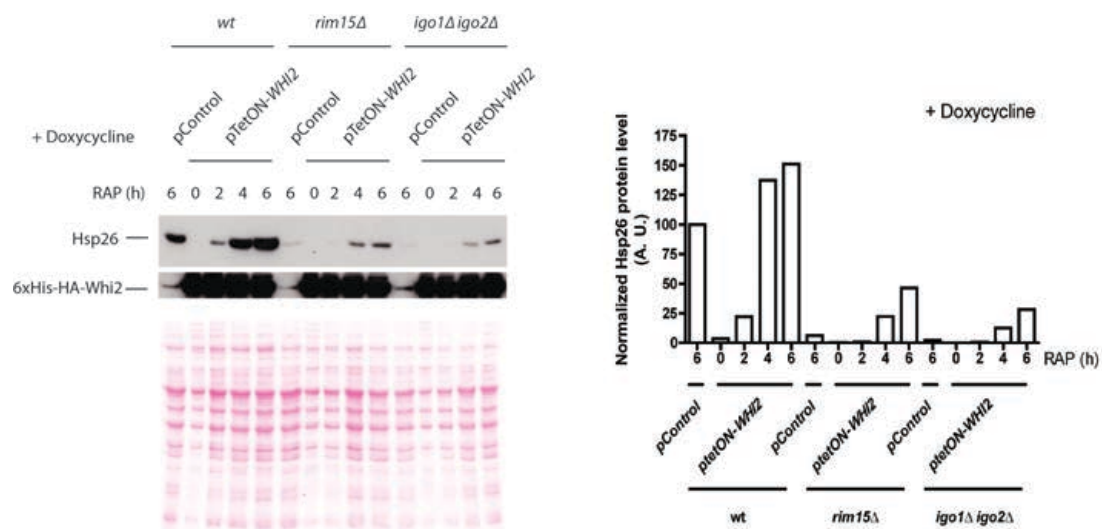


Fig. 40 Overexpression of *WHI2* partially suppresses the defect of both *igo1Δ igo2Δ* and *rim15Δ* cells in Hsp26 protein expression upon rapamycin treatment

Samples were processed as described as in Fig 39.

These results show that overexpression of *WHI2* only partially suppresses the defect of a *rim15Δ* and an *igo1Δ igo2Δ* mutant in rapamycin-induced *HSP26* expression at both the mRNA and protein levels.

IV. 3 Analyses of Gis3 as a suppressor of the defect of *igo1Δ igo2Δ* and *rim15Δ* mutant cells in *HSP26* expression

We decided to further explore the role of Gis3, a protein with unknown function, which when overexpressed, strongly suppresses of the defect of *rim15Δ* and *igo1Δ igo2Δ* cells in *HSP26* expression. To further elucidate the function of Gis3 and gain insight into the mechanism of the suppression, we aimed at analyzing its localization and identifying its physical partners.

IV. 3. 1 Gis3 mainly and constitutively localizes in the nucleus

We showed earlier that rapamycin treatment leads to nuclear accumulation of Rim15 and Igo1. To determine whether Gis3 localization changes following rapamycin treatment, Gis3-GFP was observed under the microscope in exponentially growing cells prior to and following rapamycin treatment. To this end, a N-terminally GFP-tagged *GIS3* ORF under the control of its endogenous promoter was cloned into a centromeric plasmid, and then transformed into a *gis3Δ* mutant expressing *HHF2*-RFP as a nuclear marker. We observed that Gis3-GFP mainly colocalized with Hhf2-RFP in exponentially growing cells prior to and following a 3-hour rapamycin treatment. These results suggest that Gis3 is mainly localized in the nucleus, and does not change its localization following rapamycin treatment. GFP-Gis3 protein levels were assessed by immunoblot of total protein extracts under each condition. The total GFP-Gis3 protein level stayed constant prior to and following a 3-hour rapamycin treatment (Fig. 41). This Gis3-GFP construction still needs to be tested for its capacity, when overexpressed, to suppress the defect of *igo1Δ igo2Δ* cells in *HSP26* expression.

These results suggest that Gis3 achieves its function mainly in nucleus.

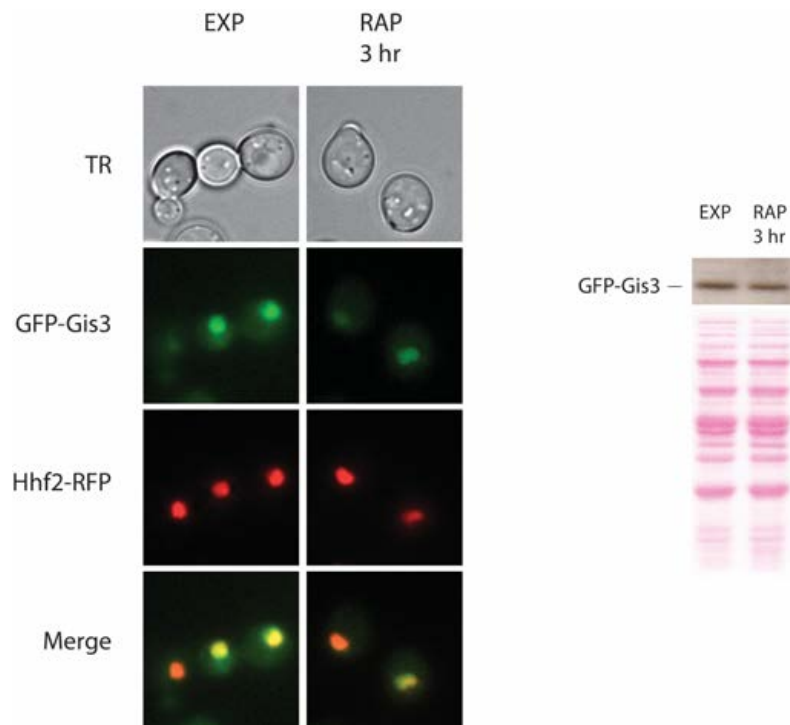


Fig. 41 GFP-Gis3 localizes in the nucleus in exponentially growing and 3 hr rapamycin-treated cells
gis3Δ mutant cells expressing the nuclear marker *HHF2*-RFP and GFP-tagged Gis3 from the endogenous promoter, were harvested prior to (EXP) or following rapamycin treatment (RAP; 0.2 $\mu\text{g ml}^{-1}$; 3 hr) and observed by fluorescence microscopy. Whole cell protein extracts were analyzed by SDS-PAGE, and immunoblots were probed with anti-GFP antibodies. Ponceau S staining of the membranes prior to immunoblot analysis served as loading control.

IV. 3. 2 Gis3 is new physical interactor of PP2A^{Cdc55}

IV. 3. 2. 1 Gis3-TAP purification identifies subunits of PP2A^{Cdc55} as physical interactors

To further elucidate the role of Gis3, we purified His₆-HA₃-Protein A TAP tagged Gis3 and Pah1 (unrelated protein) from rapamycin-treated cells and identified co-precipitating proteins using tandem *mass spectrometry* (MS) (Fig. 42). Proteins that specifically bound to Gis3 included different subunits of the phosphatase PP2A, namely the scaffold protein Tpd3, the regulatory Cdc55 protein and both catalytic Pph21 and Pph22 subunits (Table. 2). This suggests that Gis3 is a new physical interactor of PP2A^{Cdc55}. These Gis3 interactors are of special interest, as deletion of *PPH21* suppresses the defect of *igo1Δ igo2Δ* and *rim15Δ* cells in *HSP26* expression (see Fig. 23 on page 65).

The yeast *protein serine/threonine phosphatase 2A* (PP2A) is a multifunctional enzyme whose trimeric form consists of a scaffolding A subunit, a catalytic C subunit, and one of two regulatory B subunits, namely Cdc55 and Rts1 (Jiang, 2006). The A subunit Tpd3 is the structural subunit that serves as a scaffold to accommodate the other two subunits. The C subunits are the catalytic subunit Pph21 or Pph22, which, in complex with the A subunit, form the dimeric core enzyme. Each of these two catalytic subunits contributes approximately half of the PP2A activity in the cell (Ronne et al., 1991; Sneddon et al., 1990). The B subunit Cdc55 or Rts1 are the regulatory subunits that dictate the substrate specificity and intracellular localization of the AC dimeric core enzyme (Cohen, 1989). Numerous studies showed that PP2A plays roles in cell morphology and cell cycle regulation (Evans and Stark, 1997; Lin and Arndt, 1995; Sneddon et al., 1990).

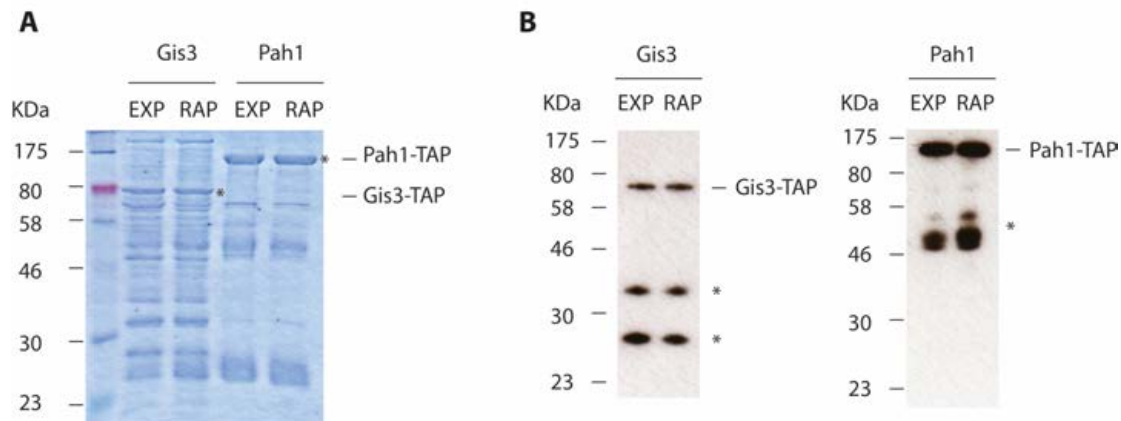


Fig. 42 Gis3-TAP purification. Coomassie blue staining (A) and western blot (B) of Gis3-TAP and Pah1-TAP purified prior to or following rapamycin treatment

gis3Δ mutant cells expressing *GALI-GIS3-TAP* or *GALI-PAH1-TAP* were pregrown in 2% raffinose-containing medium, grown for 4 hr on galactose-containing medium. Cells prior to (EXP) and treated 1 hr with rapamycin (RAP; 0.2 $\mu\text{g ml}^{-1}$) were harvested. Whole cell protein extracts were purified successively with Ni- and IgG-sepharose beads. Purified Gis3-TAP and Pah1-TAP were loaded on coomassie-stained 10% polyacrylamide SDS gel showing the purified proteins (Gis-TAP or Pah1-TAP) (A). Same samples were analyzed by SDS-PAGE, and probed with anti-Protein A antibodies (B). Asterisks in A indicate the corresponding bands of Gis3-TAP and Pah1-TAP, asterisks in B indicate degradation products. Protein size markers (NEB) are indicated in kilodaltons (kDa).

Identified Proteins (271 in total)	Molecular Weight	Fisher's Exact Test P value	Numbers of matched spectra ¹	
			Gis3-TAP	Pah1-TAP
Protein phosphatase PP2A regulatory subunit A : <i>TPD3</i>	71 kDa	95% (0.00026)	21	0
osphatase PP2A regulatory subunit B : <i>CDC55</i>	60 kDa	95% (0.020)	10	0
Serine/threonine-protein phosphatase : <i>PPH21</i>	43 kDa	0% (0.064)	7	0
Serine/threonine-protein phosphatase : <i>PPH21</i>	42 kDa	0% (0.095)	2	0

Table 2. PP2A^{Cdc55} subunits identified as Gis3 specific physical interactors

¹: A certain linearity exists between the number of spectra matched to a certain protein and its concentration. The numbers of matched spectra can thus be used to make semi-quantitative estimates of protein amounts in the sample. See annex 1 for a full list of recovered peptides.

IV. 3. 2. 2 Gis3 interacts with PP2A^{Cdc55} subunits in a yeast two-hybrid system

We next aimed at confirming the interaction between Gis3 and Cdc55, Pph21 and Pph22, using the yeast DUALhunter two-hybrid system that is based on the split-ubiquitin system (Mockli et al., 2007) (Fig. 43).

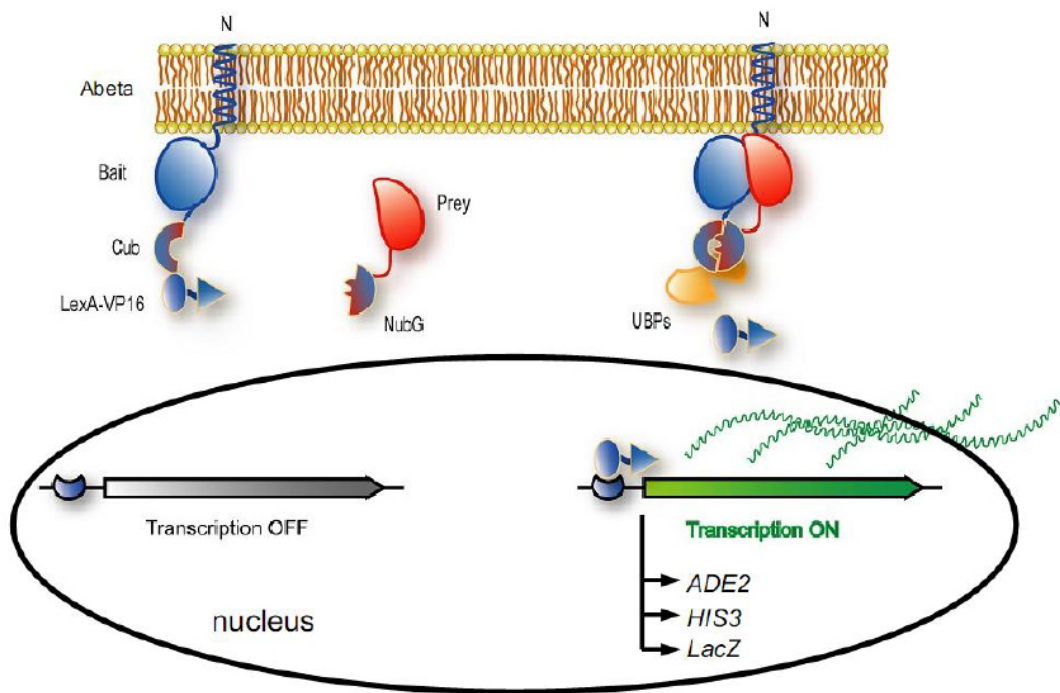


Fig. 43 The DUALhunter system

The bait protein expressed from the pCabWT bait plasmid is fused at its amino-terminus to a membrane anchor (the Abeta transmembrane domain). At its carboxyl-terminus it is fused to a half of ubiquitin (Cub) and to a transcription factor (LexA-VP16). The prey protein expressed from the pPR3 prey plasmid is fused at its amino-terminus to the other half of ubiquitin bearing a mutation (NubG), which abolishes its interaction with Cub. If the bait and the prey interact together, Cub and NubG are close and “split-ubiquitin” is reconstituted. Split-ubiquitin is recognized by ubiquitin-specific proteases of the cytoplasm (UBPs). The polypeptide chain is cleaved between Cub and LexA-VP16. The transcription factor is released, it enters the nucleus, and activates reporter genes, which are in this DUALhunter system *ADE2*, *HIS3*, and *lacZ*. To monitor the interaction between the bait and the prey proteins, growth assays on plates (using medium without adenine and/or histidine) or β -galactosidase assays (on plates or in liquid cultures) can be performed (scheme adapted from the DUALhunter kit user manual from Dualsystems).

GIS3 was cloned in the bait vector, and *CDC55*, *PPH21* and *PPH22* were cloned in the prey vector. We first tested the interaction of Gis3 with Cdc55, Pph21 or Pph22 in wild-type cells. A wild-type Nub (NubI) expressed from the positive control plasmid (pAI-Alg5, annotated Ctl+) constitutively interacted with the Cub that was fused to the bait protein Gis3. As long as the bait protein Gis3 and the NubI were expressed, the *ADE2* reporter gene was induced, rendering cells capable of growing on SD plates without adenine. The negative control plasmid (pDL2-Alg5, annotated Ctl-) expresses the mutated Nub (NubG) fused to an ER protein Alg5. As expected, cells expressing the bait protein Gis3 and NubG-Alg5 (the Ctl-) showed, no growth on SD plates without adenine (Fig. 36A). This suggests that Gis3 is expressed from the bait plasmid and gives no background.

The growth on plates containing adenine-free SD medium was used as readout of the interaction. We observed interaction between Gis3 and Cdc55, Pph21 or Pph22, but not with an unrelated protein Mon1 in diauxic cells (3 days of growth on plate) (Fig. 44A). A liquid β -galactosidase assay was used as another readout of the interaction. As expected, β -galactosidase activity of the controls (*i.e.* negative control and *MON1*) was low. The β -galactosidase activities were similar in exponentially growing, rapamycin-treated and diauxic cells expressing the Gis3 and Cdc55 constructs. Monitored by the β -galactosidase activity, the interaction between Gis3 and Pph21 increased 6- and 10-fold in rapamycin-treated and glucose-limited cells, respectively, when compared to exponentially growing cells. The interaction between Gis3 and Pph22 increased 5- and 9-fold following rapamycin treatment and glucose-limitation, respectively, when compared to the roles in exponentially growing cells (Fig. 44B).

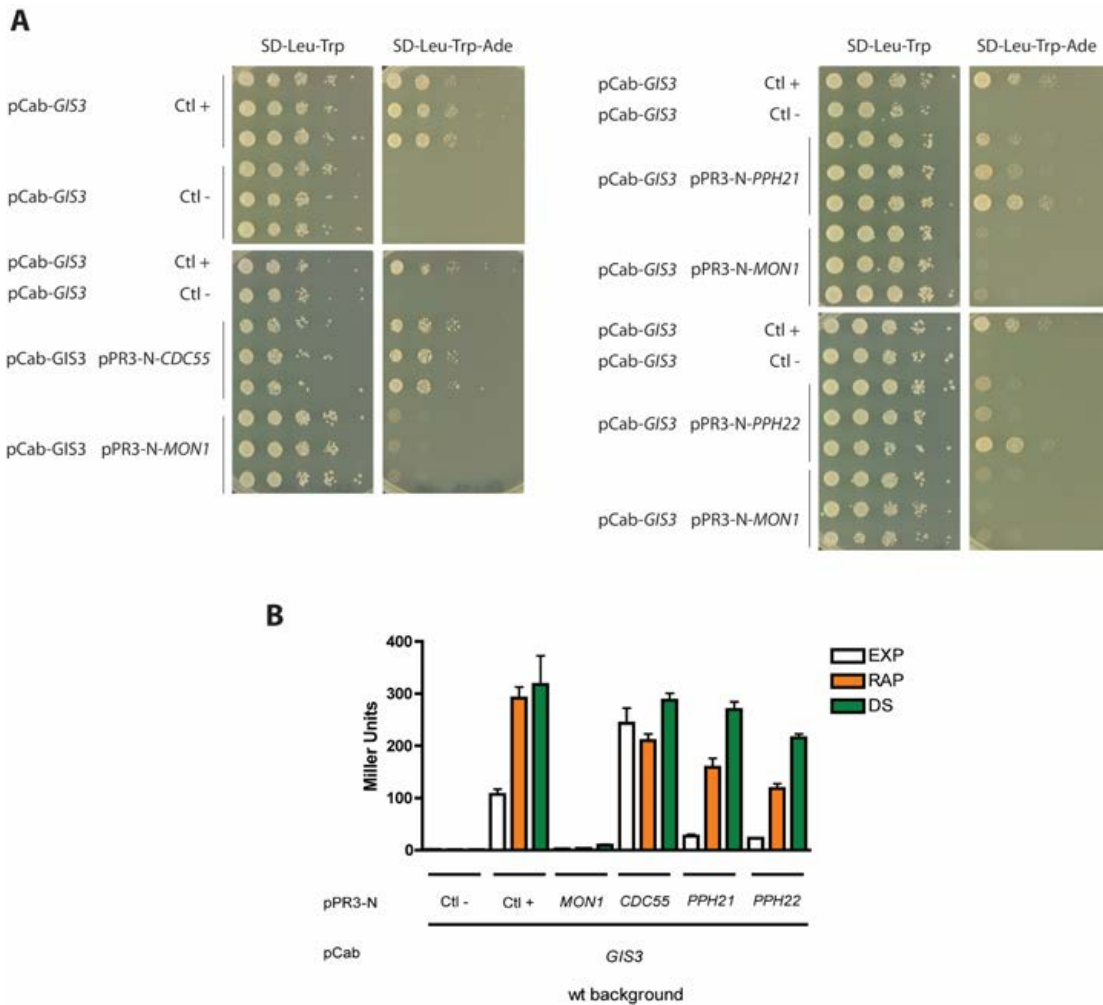


Fig. 44 Gis3 interacts with Cdc55, Pph21 and Pph22 in yeast two-hybrid assays

A. pCab-*GIS3* with positive and negative control plasmids (Ctl+ and Ctl-), pPR3-N-*CDC55*, -*PPH21*, -*PPH22* and -*MON1* were transformed into wild-type NMY51 cells harboring the *ADE2* and *lacZ* reporter genes. 10-fold serial dilutions of each combination were spotted on control medium, SD-Leu-Trp (SD medium without leucine and tryptophan), and on selective medium, SD-Leu-Trp-Ade (SD medium without leucine, tryptophan and adenine). Pictures were taken after 3 days of growth on plates at 30°C.

B. β -galactosidase activities (expressed in Miller units) were measured to monitor the expression of the *lacZ* reporter in strains with indicated genotypes in exponential phase (EXP), following rapamycin treatment (RAP; 0.2 $\mu\text{g ml}^{-1}$; 6 hr) or 24 hr after the exponential phase (DS). Data are reported as averages ($n = 3$), with standard deviations (SDs) indicated by the lines above each bar.

This suggests that Gis3 and Cdc55 constitutively interact with each other, while the interaction between Gis3 and Pph21 or Pph22 is enhanced following rapamycin treatment or glucose limitation. It would be therefore interesting to test whether the rapamycin-induced interaction between Gis3 and Pph21 or Pph22 depends on the presence of Cdc55.

As we observed that the overexpression of Gis3 suppressed the defect of *rim15Δ* in *HSP26* expression, we also tested whether the interaction between Gis3 and Cdc55, Pph21 or Pph22 requires the presence of *RIM15*. Using the yeast DUALhunter two-hybrid system, the interaction between Gis3 and its interactors was tested in a *rim15Δ* cells. A liquid β -galactosidase assay was used as a readout of the interaction. As expected, β -galactosidase activity of the controls (*i.e.* negative control and *MON1*) was low. The β -galactosidase activities were similar in exponentially growing, rapamycin-treated and diauxic wild-type and *rim15Δ* cells expressing Gis3 and Cdc55 constructs. Monitored by the β -galactosidase activity, the interaction between Gis3 and Pph21 or Pph22 in exponentially growing *rim15Δ* cells is 3- or 6-fold higher, respectively, when compared to the values in exponentially growing wild-type cells. The β -galactosidase activities were similar in rapamycin-treated and diauxic wild-type and *rim15Δ* cells expressing Gis3 and Pph21 or Pph22 (Fig. 45).

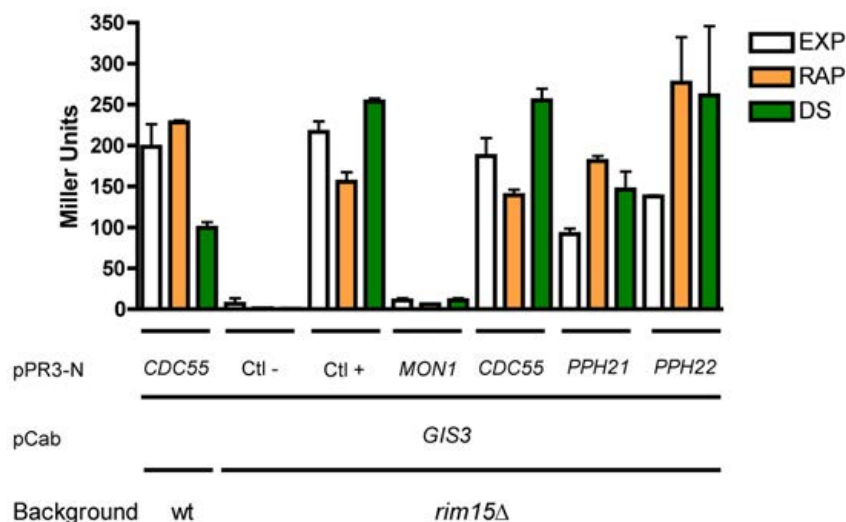


Fig. 45 The interaction of Gis3 and Cdc55, Pph21 and Pph22 is independent of Rim15 in the DUALhunter yeast two-hybrid system

Analyses were performed as described in Fig. 44.

This suggests that Gis3 interacts constitutively with Cdc55 independently of the presence of Rim15, in exponentially growing, rapamycin-treated or glucose-limited cells. Notably, the interaction between Gis3 and Pph21 or Pph22 appears somewhat lower in exponentially growing *rim15Δ* cells than in wild-type cells. However, expression of bait and

prey proteins should be analyzed by immunoblot to confirm that these differences of interactions may not be due to differences in protein expression levels.

IV. 3. 2. 3 Gis3 coimmunoprecipitates with Cdc55 *in vivo*

To confirm the interaction between Gis3 and Cdc55 under physiological conditions, a coimmunoprecipitation experiment was performed. To this end, a strain in which *GIS3* and *CDC55* were genomically tagged with Myc₁₃ and HA₃, respectively, was constructed. Another strain with genomically HA₃-tagged *RCO1* was used as a control to test the specificity of the interaction between Gis3 and Cdc55. Cell lysates were prepared from exponentially growing cells prior to and following 1-hour rapamycin treatment. These lysates were incubated with anti-HA antibodies-coupled sepharose beads, the amount of coimmunoprecipitated Gis3-Myc₁₃ was observed on immunoblot following SDS-PAGE (Fig. 46).

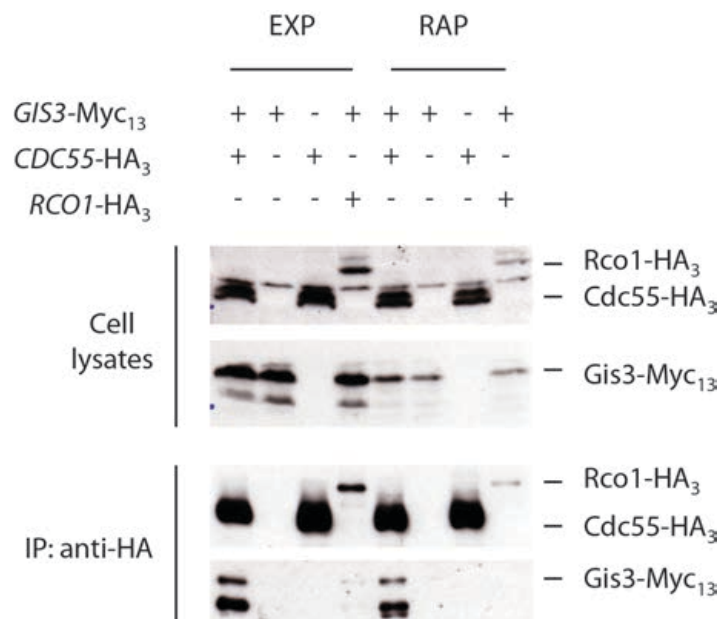


Fig. 46 Gis3 and Cdc55 physically interact with each other prior to and following rapamycin treatment in coimmunoprecipitation experiment

Exponentially growing cells were harvested prior to (EXP) or following rapamycin treatment (RAP; 0.2 $\mu\text{g ml}^{-1}$; 1 hr). Cdc55-HA₃ and Rco1-HA₃ were immunoprecipitated with anti-HA-coated sepharose beads from cell lysates of strains with the indicated genotypes. Cell lysates (Input) and HA immunoprecipitated samples (IP) were subjected to SDS-PAGE, and immunoblots were probed using anti-myc or anti-HA antibodies.

We observed that Gis3 coimmunoprecipitated with Cdc55 both prior to or following rapamycin treatment. However, given the significantly lower expression level of Rco1-HA₃, compared to Cdc55-HA₃, these Co-IP experiments should be repeated with another control protein that is expressed at a similar level as Cdc55-HA₃.

IV. 4 Discussion

We performed a genetic screen for multicopy suppressors of the defect of *igo1Δ igo2Δ* mutant cells in *HSP26* expression. Initially, the suppressors were expected to suppress the defect of *igo1Δ igo2Δ* mutant cells in *HSP26* expression possibly by inhibiting the mRNA decay pathway. Curiously, we identified that overexpression of *GIS3* and *ZDS1* fully suppresses the defect of both *rim15Δ* and *igo1Δ igo2Δ* cells in *HSP26* expression at both mRNA and protein levels following rapamycin treatment (Fig. 35, 36, 38 and 39) or glucose limitation (Fig. 37), while overexpression of *WHI2* only partially suppresses the defect of both *rim15Δ* and *igo1Δ igo2Δ* cells in *HSP26* expression at both mRNA and protein level following rapamycin treatment (Fig. 38 and 40). Since we originally postulated that Rim15 plays two roles, *i.e.* a role in transcriptional activation of quiescence-specific genes and in stabilization of the corresponding mRNA via Igo1/2, we expected that *igo1Δ igo2Δ* high-dosage suppressors would not necessarily suppress the defect in gene expression in *rim15Δ* cells. The results presented in this chapter together with the most recent literature and additional data from the lab, which will be discussed in more detail below, suggest that our original model should be modified as follows. It appears that Igo proteins may actually regulate both transcriptional activation and mRNA stability of quiescence-specific genes primarily by inhibiting the PP2A^{Cdc55} module following their phosphorylation by Rim15 (see Fig. 47). Since we previously observed that the loss of the mRNA decay pathway suppresses the defect of *igo1Δ igo2Δ* cells, but not the one of *rim15Δ* cells in the expression of quiescence-specific genes (Talarek et al., 2010), Rim15 may contribute to full activation of transcription by two different means: namely, by inactivating PP2A^{Cdc55} via phosphorylation of Igo1/2 and by a yet-to-be identified additional, Igo1/2-independent mechanism. This latter mechanism may also impinge on PP2A^{Cdc55} regulation, or act downstream of this module, *e.g.* at the level of the transcription factors Msn2/4 and Gis1, as discussed in the following paragraphs.

IV. 4. 1 Overexpression of *ZDS1* and *WHI2* fully or partially suppress, respectively, respectively the defect of *igo1Δ igo2Δ* and *rim15Δ* cells in *HSP26* expression

Zds1 was found to be involved in maintaining Cdc55 in the cytoplasm (Rossio and Yoshida, 2011). We observed that the deletion of *CDC55* suppresses the defect of *rim15Δ* and *igo1Δ igo2Δ* cells in *HSP26* mRNA accumulation (Bontron, unpublished data). When overexpressed Zds1 may titrate Cdc55 away, phenocopying loss of Cdc55 and hence suppressing the defect of *rim15Δ* and *igo1Δ igo2Δ* cells. Additionally, it has been demonstrated that overexpression of Zds1 leads to increased cytoplasmic localization of the PKA regulatory subunit Bcy1 (Griffioen et al., 2001). It may therefore also be possible that Zds1 may suppress the defect of *rim15Δ* and *igo1Δ igo2Δ* mutant cells in *HSP26* expression by cytoplasmic sequestration of Bcy1, and consequent induction of the G₀ program following PKA inhibition.

Whi2 was found to be required for full activation of the general stress response, possibly by activating Msn2 dephosphorylation (Kaida et al., 2002). We proposed earlier that Rim15 activates the G₀-specific genes via Msn2/4 and Gis1. Overexpression of Whi2 may therefore activate Msn2 and thus allow bypassing the requirement of Rim15.

IV. 4. 2 Gis3: potential inhibitor of PP2A^{Cdc55}

Gis3, the most promising suppressor of the defect of *igo1Δ igo2Δ* mutant cells in *HSP26* expression, has been so far poorly characterized. It was identified as a multicopy suppressor of the Gal- phenotype of *snf1 mig1 srb8/10/11* cells (Balciunas and Ronne, 1999). We found that Gis3 is mainly localized in the nucleus, and did not change its localization following rapamycin treatment (Fig. 41). Moreover, Gis3 physically interacts with the PP2A^{Cdc55} independently of rapamycin treatment or glucose limitation (Fig. 44, 46 and Table 2). Additionally, we observed that the deletion of *CDC55* suppresses the defect of *rim15Δ* and *igo1Δ igo2Δ* cells in *HSP26* mRNA accumulation (Bontron, unpublished data). This suggests that Gis3 when overexpressed suppresses the defect of *rim15Δ* and *igo1Δ igo2Δ* cells in *HSP26* expression by likely inhibiting the nuclear PP2A^{Cdc55} form. Of interest, recent studies

showed that α -endosulfines interact with and inhibit PP2A-B55 δ in higher eukaryotes (Gharbi-Ayachi et al., 2010; Mochida et al., 2010). We observed that the interaction between Igo1 and Cdc55 is enhanced following rapamycin treatment (Bontron, unpublished data). This suggests that the inhibiting role of α -endosulfines on PP2A^{Cdc55} may be conserved throughout evolution. Additionally, Gis3 does not interact with Igo1 (Luo, unpublished data). Consequently, we infer that Gis3 and Igo1/2 may inhibit, in parallel, PP2A^{Cdc55} to regulate the expression of G₀-specific genes. To better characterize Gis3 function, it will be necessary not only to assess Gis3 endogenous protein level prior to and following rapamycin treatment in wild-type, *rim15* Δ and *igo1* Δ *igo2* Δ cells, but also to analyze in detail the phenotype of *gis3* Δ cells.

IV. 4. 3 Working model

To summarize our results, we propose the following working model. In rapamycin treated cells, Rim15 activates Igo1/2 and possibly also Gis3, which both inhibit PP2A phosphatase activity via their interaction with Cdc55 (1 and 2). The PP2A phosphatase inhibits the proper G₀ entry by inhibition of G₀ gene transcription (3) and by favoring the mRNA decay pathway (4). Igo1/2 acts upstream of transcription and post-transcriptional control. Both inhibitors, Igo1 and Gis3 are required to allow full activation of the transcription of G₀-specific genes that are inhibited by PP2A^{Cdc55}. Zds1 may favor G₀-specific transcription by inhibition of PP2A and/or PKA (5), which in turn negatively regulates Msn2. Whi2 may regulate G₀-specific transcription by activating directly the transcription factor Msn2 (6). In addition to its regulation of Igo1/2/Gis3-PP2A branches, Rim15 may activate transcription by directly inhibiting PP2A (7) and/or activating Zds1 (8a), Whi2 (8b) or the transcription factors Msn2/4 and Gis1 (8c) (Fig. 47). This latter suggestion is based on our earlier observation that loss of mRNA decay compounds suppressed the defect of *igo1* Δ *igo2* Δ cells, but not the one of *rim15* Δ cells, in expression of quiescence-specific genes.

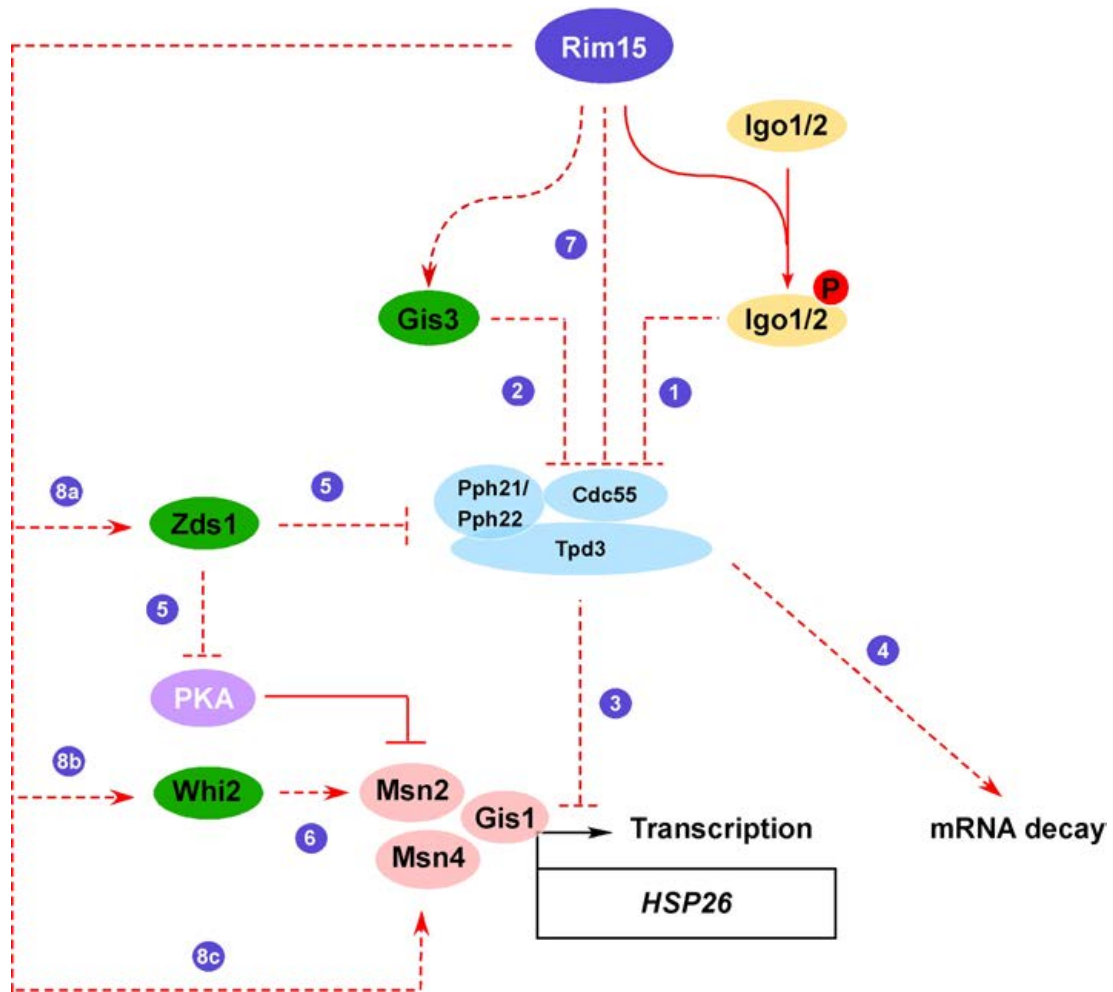


Fig. 47 Model depicting a role for Gis3, Zds1 and Whi2 in suppressing the defect of *igo1Δ igo2Δ* and *rim15Δ* cells in expression of G_0 -specific genes, when overexpressed

Gis3 promotes G_0 entry by inhibiting PP2A phosphatase activity. Zds1 overexpression may suppress *rim15Δ* and *igo1Δ igo2Δ* phenotype by inhibition of PKA and/or PP2A. Whi2 overexpression may suppress the defect of *rim15Δ* and *igo1Δ igo2Δ* mutant cells in *HSP26* expression by activation of Msn2. Dashed lines are proposed regulations, solid lines are experimentally proved regulations.

This model makes several predictions that are testable in the future.

To test whether overexpression of *ZDS1* suppresses the defect of *rim15Δ* and *igo1Δ igo2Δ* cells in *HSP26* expression via its regulation of localization of Cdc55 and/or Bcy1, we could analyze Cdc55-GFP and Bcy1-GFP localization in rapamycin-treated *rim15Δ* and *igo1Δ igo2Δ* cells overexpressing *Zds1*. To test whether Rim15 regulates *Zds1*, we could test whether the localization of *Zds1* is altered by loss of Rim15. We could also test the Msn2 phosphorylation status in rapamycin-treated *rim15Δ* and *igo1Δ igo2Δ* cells overexpressing *Whi2*.

To test the prediction that Gis3 is a PP2A^{Cdc55} inhibitor, an *in vitro* phosphatase assay could be performed. To perform this assay, PP2A^{Cdc55} complex and Gis3 would be purified from yeast and bacteria, respectively. The substrate would be a commercially available phosphopeptide. Following the incubation of PP2A^{Cdc55} with the substrate in presence or not of Gis3, the free phosphate liberated from the substrate could be detected by a colorimetric assay with malachite green. Furthermore, to gain more insight into the structural aspect of the Gis3-PP2A^{Cdc55} interaction, chemical cross-linking combined with mass spectrometric analysis (as described in (Leitner et al., 2010)) of Gis3-Myc₁₃ and Cdc55-3HA, Pph21-3HA, Pph22-3HA, may allow identification of interacting domains of Gis3 and its physical interactors. Additionally, it would be interesting to investigate where the Gis3-PP2A interaction takes place. It has been reported by Gentry and Hallberg that PP2A subunits Cdc55, Tpd3, Pph21 and Pph22 all highly concentrate in the nucleus (Gentry and Hallberg, 2002). Of interest, we found that Gis3 mainly localized in the nucleus (Fig. 41). These observations may suggest that the interaction of Gis3 and its interactors Cdc55, Tpd3, Pph21 and Pph22 highly likely takes place in the nucleus. To confirm this hypothesis, bimolecular fluorescence complementation (Sung and Huh, 2007) could be performed. This experiment consists of fusing the N-terminal and C-terminal parts of YFP with Gis3 and Cdc55, respectively. The reconstitution of YFP occurs when and where the two proteins interact. This could reveal whether Gis3 and PP2A^{Cdc55} interact in the nucleus.

Furthermore, to address the possibility that Igo1 and Gis3 act in parallel to inhibit PP2A, coimmunoprecipitation analyses could be used to test whether Gis3 and Igo1 compete for binding to Cdc55. To this end, a strain with differently genomically tagged Cdc55, Gis3

and Igo1 should be constructed. When Gis3 is immunoprecipitated, Cdc55 should be coimmunoprecipitated, but not Igo1. The result could be confirmed by immunoprecipitating Igo1 and checking whether Gis3 coimmunoprecipitates. In addition, as overexpression of Gis3 suppressed the defect of *igo1Δ igo2Δ* mutant cells in *HSP26* expression, we could speculate that *gis3Δ* should have a defect in the expression of G₀-specific genes. When comparing the levels of *HSP26* mRNA and Hsp26 proteins in *rim15Δ* and *igo1Δ igo2Δ* mutants, we always observe slightly more *HSP26* mRNA and Hsp26 proteins in an *igo1Δ igo2Δ* mutant than in *rim15Δ* mutant (Talarek et al., 2010, Fig. 2C, 2D, 5A, 5B, 6B, 6C). One explanation could be that there would be at least one additional Igo1/2-like protein. This protein could be Gis3. To confirm this hypothesis, we could test whether the levels of *HSP26* mRNA and Hsp26 protein between *rim15Δ* and *igo1Δ igo2Δ gis3Δ* are similar. However, the difference between *rim15Δ* and *igo1Δ igo2Δ* mutants is subtle. It may therefore be easier to use mutants accumulate higher levels of *HSP26* mRNA and proteins. Of interest, loss of Ccr4 suppresses the defect of *igo1Δ igo2Δ* mutants in *HSP26* expression, but not that of *rim15Δ* mutants. We could therefore compare the *HSP26* mRNA and protein levels between *ccr4Δ igo1Δ igo2Δ* and *ccr4Δ igo1Δ igo2Δ gis3Δ* mutants. If the latter mutant accumulates less *HSP26* mRNA and proteins than *ccr4Δ igo1Δ igo2Δ* mutants, this may favor a model in which Gis3 acts in parallel to Igo1/2. To test whether Gis3, like Igo1/2, is downstream of Rim15, we could assess the phosphorylation status and localization of Gis3 in wild-type and *rim15Δ* cells prior to and following rapamycin treatment.

Finally, to further test whether Gis3 overexpression suppresses the defect of *igo1Δ igo2Δ* mutant cells in *HSP26* expression at the transcriptional and/or posttranscriptional level following rapamycin treatment, it would be interesting to use a mRNA stability assay to determine *HSP26* mRNA half-life in *igo1Δ igo2Δ* cells overexpressing *GIS3*. In addition, if Gis3 is an inhibitor of PP2A^{Cdc55}, phosphoproteome analyses of *gis3Δ* mutant cells overexpressing or not *GIS3* prior to or following rapamycin treatment, could possibly reveal downstream substrates of PP2A, whose PP2A-dependent dephosphorylation is inhibited by *GIS3* overexpression. Genetic interactions and deletion phenotype of the candidates and protein interaction studies would reveal how they regulate the initiation of the G₀ program following rapamycin treatment.

V. Concluding remarks

In the second part of my thesis, I confirmed that Igo1/2 promote G_0 program initiation likely by antagonizing the decapping activators Dhh1 and/or Pat1, both component of the 5'-3' decay pathway. In the third part of my thesis, I identified multicopy suppressors, i.e. *GIS3*, *ZDS1* and *WHI2*, which suppressed not only the defect of *igo1Δ igo2Δ* cells, but also the defect in *rim15Δ* cells in *HSP26* expression. This data suggest that Igo1 maybe function as well in the regulation of G_0 entry at the transcriptional level. Taken all of the current data in the literature and the data of the present thesis together, the role of Igo1/2 may be summarized in the following model (Fig. 48).

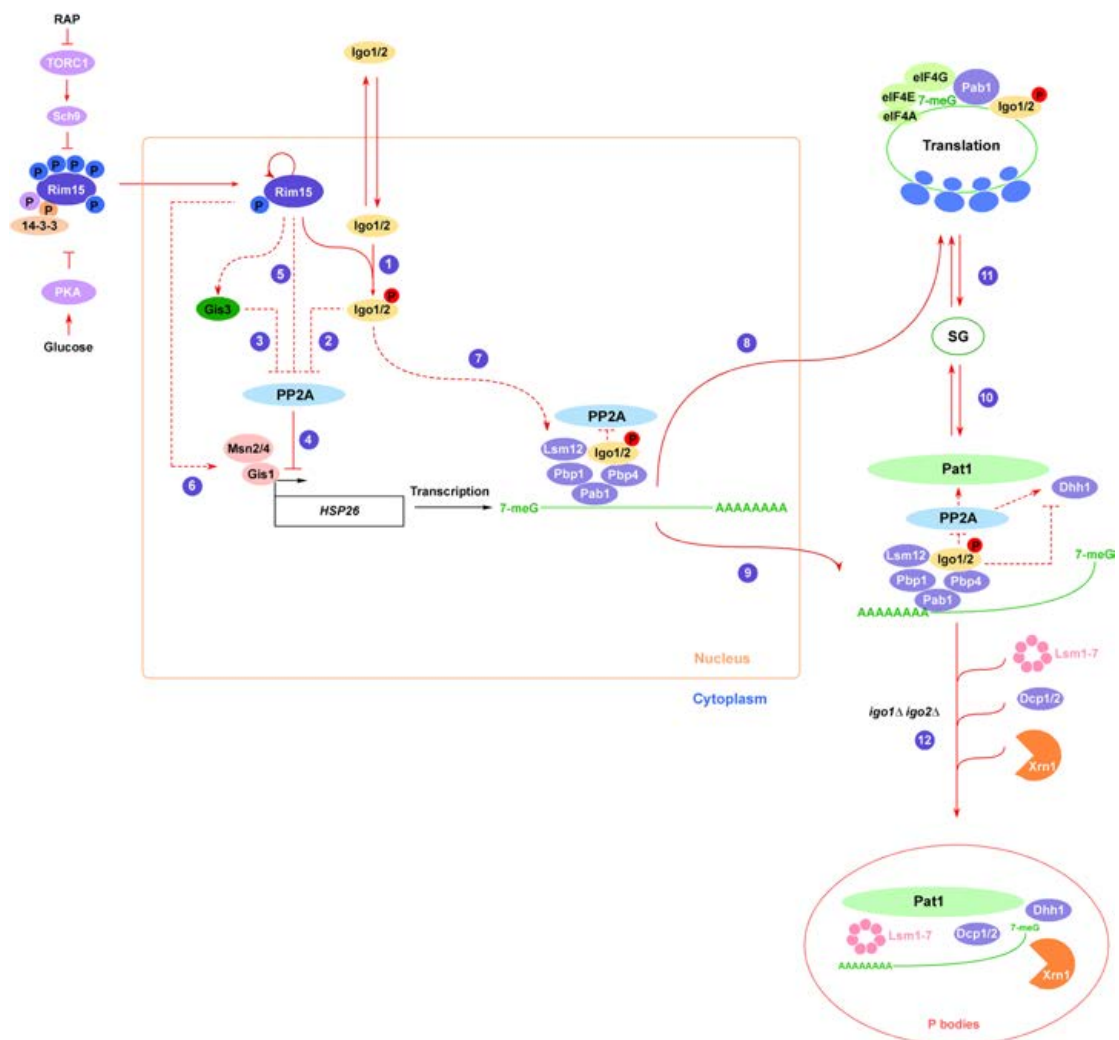


Fig. 48 Model depicting transcriptional and post-transcriptional regulation of G_0 entry by Igo1/2 and Gis3
(See text for detail)

In exponentially growing cells, phosphorylation of Rim15 (on Ser¹⁰⁶¹ by the TORC1 target Sch9 and on Thr¹⁰⁷⁵ by the cyclin-cyclin-dependent kinase complex Pho80-Pho85) mediates tandem 14-3-3 binding to guarantee optimal sequestration of Rim15 in the cytoplasm, where it is kept inactive through additional PKA-mediated phosphorylation events. TORC1 inactivation (e.g., following treatment of cells with rapamycin or following nutrient starvation) causes initiation of the G₀ program in part by abrogating the cytoplasmic retention of Rim15. Nuclear Rim15, presumably released from PKA-mediated inhibition, controls gene expression by different means. Rim15 activates Igo1/2 (via phosphorylation at Ser⁶⁴ in Igo1 and Ser⁶³ in Igo2) (1) and possibly also Gis3, which may both inhibit PP2A phosphatase activity via their interaction with Cdc55 (2 and 3). The PP2A phosphatase inhibits the proper G₀ entry by inhibiting G₀ gene transcription by a yet elusive mechanism (4). Both inhibitors (i.e. Igo1 and Gis3, which likely act in parallel) maybe required for full activation of the transcription of G₀-specific genes that are inhibited by PP2A^{Cdc55}. In addition to the regulation of the Igo1/2-Gis3-PP2A branch, Rim15 may activate transcription by directly inhibiting PP2A (5) and/or activating directly or indirectly the transcription factor Msn2/4 and Gis1 (6). In parallel, Rim15 phosphorylates Igo1 and Igo2, both of which likely shuttle between the cytoplasm and the nucleus. Subsequently, they may assemble to specific messenger ribonucleoprotein (mRNP) complexes (possibly already in the nucleus as depicted or, alternatively, in the cytoplasm). These mRNPs contain at least Igo1/2, Lsm12, the poly(A)-binding protein Pab1 interactor Pbp1, and Pbp4, as well as a nutrient-regulated mRNA (e.g., *HSP26*) that needs to be translated as part of the quiescence program (7). Once in the cytoplasm, the cytoplasmic mRNP complexes likely associate with translation initiation factors and ribosomes for direct translation (8). Alternatively, they may transiently assemble (to some extent in PBs) with 5'-3' decay factors (9). Notably, Dhh1 may either be incorporated into *HSP26* mRNA-containing mRNPs while they reside in the nucleus, or—as depicted in our model—join the corresponding mRNPs in the cytoplasm (e.g., during or following their unloading from ribosomes and disassembly of translation initiation factors). The direct or indirect (via PP2A) inhibition of Dhh1 and/or Pat1 by p-Ser⁶⁴-Igo1 prevents decapping and subsequent 5'-3' degradation of the associated mRNA. This promotes both disassembly of 5'-3' degradation factors from the mRNP and assembly of translation initiation factors (10), leading to the formation of stress granules (SGs). Such mRNP complexes (that may still contain Igo1/2) are thought to exit SGs and to subsequently associate with ribosomes for translation of the corresponding mRNA (11). In the absence of functional Igo1/2, mRNAs

such as the *HSP26* mRNA remain unguarded from Dcp1/2- and Xrn1-mediated decapping and 5'-3' decay (12), respectively, and are therefore prone to degradation.

V. 1 Igo1 may play a role in promoter regulation

To monitor the *HSP26* gene expression in rapamycin-induced or glucose-limited cells, we used two *HSP26* promoter-driven reporters and the endogenous *HSP26* gene as well. The expression of all these readouts are strongly dependent on the presence of Igo1/2. Interestingly, the only common sequence between the 3 readouts is the promoter and the 5'-*untranslated region* (5'-UTR) of *HSP26*. Moreover, an experiment showed that the regulation of *HSP26-lacZ* expression specifically relies on the promoter region rather than the 5'-UTR of *HSP26* (Bontron, unpublished data). This suggests that the promoter region of *HSP26* critically defines the fate of the corresponding mRNA by a process that involves Igo1/2. Of interest, a similar scenario was described in a recently published paper (Bregman et al., 2011), where the authors identified a short *cis* element that is necessary and sufficient to induce enhanced decay of the reporter mRNA. This occurs likely by the binding to the *cis* element within the target promoter of *trans*-acting factors in the nucleus, which subsequently affects the composition of the exported mRNP that in turn regulates mRNA decay in the cytoplasm. A ChIP-seq experiment (Johnson et al., 2007) could help to determine whether Igo1/2 bind to G₀-specific promoters following rapamycin treatment. If it is the case, this experiment would allow us to further define the promoter sequence(s) to which Igo1/2 specifically bind.

V. 2 Igo1 may interact directly or indirectly with G₀ specific mRNAs

Our previous data showed that Igo1 colocalizes with *HSP26-U1A* mRNA in cytoplasmic dots 8 hr following glucose exhaustion (Talarek et al., 2010). One could therefore speculate that Igo1 may interact directly or indirectly with G₀ specific transcripts. However, the fact that Igo1/2-regulated mRNAs do not contain a readily identifiable common sequence motif argues against the possibility that Igo1/2 fulfill their specificity through binding to particular sequences within target mRNAs. Still, it is possible that some specific secondary structure(s) could be recognized by Igo1/2. An electromobility shift assay (EMSA) has been

setup in the lab to assess this possibility. The preliminary results showed that Igo1 interacts with both 5'- and 3'-ends of *HSP26* mRNA (Cameroni, unpublished data). However, since the anti-Igo1 antibodies did not cause a super shift greater than the shift due to the presence of Igo1, the specificity of the interaction still needs to be confirmed by repeating the experiment with an unrelated protein.

V. 3 Igo1 may channel G₀-specific mRNPs to P bodies and stress granules under glucose deprivation conditions

Our data showed that Igo1 physically interacts with Dhh1, Pbp1, Pbp4 and Lsm12 in a rapamycin-inducible manner. Only the rapamycin-induced interaction between Igo1 and Dhh1 and Lsm12 is dependent on the phosphorylation at Ser⁶⁴. We could therefore speculate that following TORC1 inactivation, mRNPs containing at least Igo1/2, Pbp1 and Pbp4 are formed. The recruitment of Dhh1 and Lsm12 would be subsequent to the phosphorylation of Igo1 by Rim15. It has been observed that following glucose deprivation, Dhh1 localizes to both P-bodies and stress granules (Swisher and Parker, 2010), Pbp1, Pbp4 and Lsm12 localize to stress granules (Buchan et al., 2008; Swisher and Parker, 2010). It is possible that the interactions observed only occur in P bodies and/or stress granules. However such granules are not observed following rapamycin treatment suggesting that these mRNPs may form, but may be too small to be detected. It would then be interesting to address when and where the mRNPs comprising Igo1, Pbp1/4, Dhh1 and Lsm12 form. BiFC and FRET experiments between Igo1 and its physical interactors could be developed to address this question. In addition, we could also assess whether Igo1 nuclear accumulation is indispensable for its interaction with its partners by checking the interaction of NLS- or NES-tagged Igo1 and its physical interactors.

V. 4 The Igo1 target PP2A^{Cdc55} may play a role in mRNA stability

We proposed that Igo1 may directly or indirectly regulate mRNA stability in yeast (Talarek et al., 2010). PP2A is inhibited by the Igo1 homologue ARPP-19 and Ensa in *Xenopus* (Gharbi-Ayachi et al., 2010; Mochida et al., 2010). We could therefore ask firstly

whether Igo1 inhibits PP2A and secondly whether this inhibition allows the stabilization of the G₀-specific mRNAs in yeast. Interestingly, it has been reported that in old murine B cells, the increase of the amount and activity of PP2A induces an enhanced dephosphorylation of *tristetraprolin* (TTP). TTP dephosphorylation leads to destabilization of the mRNAs of the transcription factor E47 that regulates the immunoglobulin class switch in murine B cells (Frasca et al., 2010). In addition, TTP has been found to be tightly associated with cytoplasmic deadenylases and promotes rapid deadenylation of target mRNAs in mammalian cells (Clement et al., 2011). These findings may allow us to postulate that in yeast, following rapamycin-induced G₀ entry, Igo1 may play a role in protection of G₀-specific mRNAs by inhibiting PP2A^{Cdc55}, which otherwise favor the deadenylation step of the mRNA decay (See model in Fig. 48).

V. 5 Igo1: a role in mitotic entry?

It has been demonstrated in *Xenopus* that the Rim15 homologue Gwl phosphorylates and activates Igo1 homologues ARPP-19 and Ensa, which in turn inhibits PP2A that negatively regulates mitotic entry (Gharbi-Ayachi et al., 2010; Mochida et al., 2010). Studies in mammalian cells showed that mitotic cyclin mRNA stability and translation derepression is regulated by different stress granule and/or P bodies components, such as *cytoplasmic polyadenylation element binding protein* (CPEB) and HuR (Kim et al., 2011; Wang et al., 2000). mRNA binding protein CPEB is a mammalian P bodies and stress granule component (Eulalio et al., 2007). It has been recently found that in mammalian astrocytes, CPEB1 binds to cyclin B1 mRNA and represses its translation until a proliferation signal phosphorylates CPEB1, resulting in an increase in cyclin B1 protein and progression into mitosis (Kim et al., 2011). Moreover, HuR, a mammalian stress granule component (Eulalio et al., 2007), play a critical role in mammalian cell proliferation at least partially by mediating cell cycle-dependent stabilization of mRNAs encoding cyclin A and B1 (Wang et al., 2000). As HuR shares homology with yeast Pab1, and a recent study in the lab identified Pab1 as Igo1 physical interactor, we could therefore speculate that in yeast, Igo1/2 may play a role in the control of mitotic entry by two means. Igo1/2 may possibly via inhibition of PP2A^{Cdc55} (i) control cyclin B mRNA stability by regulating the phosphorylation status of Pab1, and/or (2) inhibit a yet to be identified the yeast cyclin B translation repressor.

Interestingly, we showed that Igo1/2 protect G₀-specific mRNAs from degradation. Additionally ARPP19 has been shown to protect the GAP43 mRNA from degradation in mice neurons. It is tempting then to speculate that ARPP-19 and Ensa inhibit PP2A to stabilize mitotic-specific mRNAs from degradation, consequently allowing mitotic entry. Such a model in yeast is very attractive but remains speculative based on our current knowledge.

Taken together, Igo1/2 may be involved from the birth to death of the complex lives of mRNAs induced at different stages of cell growth and differentiation. The current thesis provides a basis for future research that should address the molecular details by which Igo1/2 regulate the gene expression program under nutrient-limitation conditions.

Material and methods

Methods

Yeast Experiments and Cloning

Yeast and *Escherichia coli* media were prepared according to standard recipes (Amberg et al., 2005; Sambrook and Russel, 2001) unless otherwise stated. Yeast cells were grown at 30°C in standard rich medium with 2% glucose (YPD) or synthetic defined medium with 2% glucose complemented with the appropriate nutrients for plasmid maintenance. Solid media were prepared as the liquid media, but contained 2% w/v agar in addition. For Kan^R selection, geneticin (Brunshwig, Cat. No. BRP25-011) was added to a final concentration of 200 µg ml⁻¹. To ensure the solubility of G418 in SD medium, glutamate was added to G418-containing SD medium to a final concentration of 1g L⁻¹ as nitrogen source. For Nat^R selection, nourseothricin (WERNER BioAgents, Cat. No. 50000) was added to a final concentration of 100 µg ml⁻¹. For Hgy^R selection, hygromycin (Sigma, Cat. No. H0654) was added to a final concentration of 300 µg ml⁻¹. Thialysine (Sigma, Cat. No. A2636) and L-canavanine (Sigma, Cat. No. C9758) were both added to a final concentration of 50 µg ml⁻¹ to allow the selection of meiotic progeny that carries the *can1Δ* and *lyp1Δ* markers, respectively. For experiments with rapamycin treatment, cell cultures in exponentially growing phase were treated with 200 ng ml⁻¹ rapamycin. The rapamycin stock solution was prepared by dissolving rapamycin powder (LC Labs, Cat. No. R-5000) in an Ethanol:Tween20 (90:10) solution to a final concentration of 1 mg ml⁻¹.

Bacterial cultures were grown at 37°C on LB medium (1% w/v NaCl, 1% w/v Bacto-tryptone, 0.5% w/v yeast extract). Solid medium contained 2% w/v agar in addition. For Amp^R selection, ampicillin was added to a final concentration of 100 µg ml⁻¹. Plasmid manipulations were performed in *E. coli* strain DH5α (Gibco BRL) using standard procedures (Sambrook and Russel, 2001). Standard procedures of yeast genetics and molecular biology were used (Amberg et al., 2005; C, 1991; Sambrook and Russel, 2001).

PCR-based gene deletions of *IGO1*, *IGO2* and *RIM15*, tagging of chromosomal *GIS3*, and standard experimental procedures for cloning were as described (Amberg et al., 2005). Prp20 NLS sequence (----M-V-K-R-T-V-A-T-N-G-D-A-S-G-A-H-R-A-K-K-M-S-K-T-H-A-S-H-I-I-N-A-Q-E-D-Y-K-H-M-Y-----) and its mutated form (underlined K mutated to T) were fused to *IGO1*-GFP. Prp40 NES sequence (-----L-Q-N-K-L-N-E-L-R-L-----) and its mutated form (underlined L mutated to A) were fused to *IGO1*-GFP.

***igo1Δ igo2Δ* phenotype suppressor screen with KO collection**

igo1Δ igo2Δ query strain (XL111; MAT α , *igo1Δ* ::*NatMX4*, *igo2Δ* ::*HphMX4*, *can1Δ* ::*STE2pr-His5*, *lyp1Δ*, *ura3Δ*, *his3Δ1*; derived from strain Y7092; C. Boone lab collection), harboring the *HSP26*-yEmRFP reporter plasmid (pXL026, derived from yEmRFP; Keppler-Ross 2008), was crossed with the Euroscarf collection of 4,857 viable gene deletion mutants essentially as described previously (Tong 2001) using BioMek2000 robot. Diploid cells were selected on SD-Ura+G418 plate, then subjected to sporulation for 10 days. The MAT α haploid cells were selected on SD-His/Arg/Lys/Ura + canavanine (Can) + thialysin (Thia) medium, on which diploid cells were not Can- and Thia-resistant, while only MAT α cells express the *S. pombe HIS5* gene, conferring growth on SD medium without histidine. After a selection of MAT α G418-resistant cells on SD-His/Arg/Lys/Ura + Can/Thia/G418 plates, final MAT α G418-, nourseothricin (Nat)-, hygromycin (Hyg)-resistant triple mutants were selected by two successive replica-pinning on SD-His/Arg/Lys/Ura + Can/Thia/G418/ClonNAT/Hyg medium. The resulting triple mutant collection was screened for purple colonies grown 5 days at 30°C. Candidate mutants were crossed with either *igo1Δ igo2Δ* (XL122; MAT α , *igo1Δ*::*NatMX4*, *igo2Δ*::*HphMX4*, *his3Δ1*, *leu2Δ0*, *lys2Δ0*, *ura3Δ0*) or *rim15Δ* (XL126; MAT α , *rim15Δ*::*NatMX4*, *his3Δ1*, *leu2Δ0*, *lys2Δ0*, *ura3Δ0*) both harboring *HSP26*-yEmRFP reporter plasmid, to screen for purple triple mutants and corresponding white double mutants.

***igo1Δ igo2Δ* multicopy suppressor screen**

igo1Δ igo2Δ cells (XL122; MAT α , *igo1Δ*::*NatMX4*, *igo2Δ*::*HphMX4*, *his3Δ1*, *leu2Δ0*, *lys2Δ0*, *ura3Δ0*) harboring *HSP26*-yEmRFP reporter were transformed with a library of multicopy plasmids containing genomic DNA fragments of about 3.8 kb cloned

downstream of the regulatable *GALI* promoter (Ramer et al., 1992). Transformants were plated on selective medium containing 2% galactose 1% raffinose and 0.1% sucrose to screen for purple colonies. Confirmed galactose-inducible multicopy suppressors were isolated and identified by sequencing.

Preparation of mRNAs for Northern blot analysis

Samples were collected at indicated times, Cells were harvested by centrifugation and washed with DEPC-H₂O. Total RNA was extracted using the Hot Phenol method and prepared as described (Ausubel et al., 1999), 5 μ g RNA were loaded for Northern blot analyses. DNA probes were labeled with [α^{32} P]-CTP using the PRIME-IT II Random Primer labeling kit (Stratagene, Cat. No. 300385). The labeled probes were purified through a spin column by size separation (Bio-Rad, Cat. No. 7326221)

NaOH extraction of proteins for western blot analyses

10 OD units of cells of strains of indicated genotype at different time point were collected and subjected to NaOH/ β -mercaptoethanol protein extraction. The protein extract samples were equilibrated with Ponceau staining and loaded on a 10% SDS-polyacrylamide gel. After the separation, the protein samples were transferred to nitrocellulose membranes (Whatman, Cat. No. GT08123). For PhostagTM gels, 7.5% acrylamide gels containing 25 μ M PhosTagTM (Wako, Cat. No. AAL-107) and 50 μ M MnCl₂ were used. After the separation, gels were treated 10min with transfer buffer with 1mM EDTA then addition 10min with EDTA-free transfer buffer. Protein samples were then transferred to PVDF membrane (Millipore, Cat. No. IPVH00010) (treated 15 sec with methanol, 2 min with H₂O and 15 min with transfer buffer, successively). The membranes were then probed successively with the appropriate primary and secondary antibodies (anti-Hsp26 (kind gift from J. Buchner), anti-GFP (Roche, Cat. No. 11814460001), anti-Rabbit IgG-HRP (Bio-rad, Cat. No. 172-1019), anti-Mouse IgG-HRP (Bio-rad, Cat. No. 172-1011).

Tandem Affinity Purification

Gis3-TAP was purified, using a standard tandem affinity purification (TAP)-tag purification protocol (Gelperin et al., 2005) from *gis3Δ* (BY4741) cells harboring plasmid BG1805-*GIS3*-TAP (that drives expression of His₆-HA₃-Protease 3C-Protein A TAP-tagged *GIS3* from the galactose inducible *GALI* promoter). Prior to protein extraction, cells were pregrown on 2% raffinose-containing medium, grown for 4 hr on galactose-containing medium, and treated for 1 hr with 0.2 mg ml⁻¹ rapamycin. In parallel, Pah1-TAP was purified using the precedent protocol from exponentially growing *gis3Δ* cells that were also treated for 1 hr with 0.2 mg ml⁻¹ rapamycin.

400 OD of cells of each strain at each time point were harvested by centrifugation. The pellets were washed with 50ml cold water, then with 25 ml 1xTAP buffer (0.3 M NaCl, 0.05 M HEPES, pH 7.5 1.5 mM MgCl₂, 0.15% NP40) containing 0.5 mM PMSF and 1 x protease inhibitor (Roche, Cat. No. 05056489001). Cells were homogenized with glass beads in a Precellys 24 homogeniser (Bertin, Cat. No. 03119.200.RD000). Clarified supernatant of cell lysate were incubated with TAP buffer-washed Ni-NTA beads (Qiagen, Cat. No. 1018244) for 1 hr 30 min at 4°C. After a wash with 1ml 1xTAP buffer containing 0.5 mM PMSF, 1 mM DTT, 1 x protease inhibitor and 10 mM Imidazole, purified proteins were eluted twice with 150 μl TAP buffer + 250 mM Imidazole. The eluates were resuspended in 1 ml IPP-150 buffer (10 mM TRIS pH 8.0, 150 mM NaCl, 0.1% NP40) + 0.5 mM PMSF before being loaded on IPP150 buffer-washed IgG beads (GE healthcare, Cat. No. 17-0969-01) and incubated for 1 hr 30 min at 4°C. After washing with 1 ml IPP150 containing 1 mM DTT for 5 min at 4°C, the purified proteins were eluted 3 times with 100 μl 0.1 M glycine pH 3.0 on ice for 5 min.

Purified Igo1-TAP and Pah1 preparations were analyzed with coomassie staining and western blot before being subjected to tandem MS for identification of specific coprecipitating physical interactors of Gis3.

Anti-HA coimmunoprecipitation experiments

GIS3-Myc₁₃ CDC55-HA₃ (XL387), *GIS3-Myc₁₃* (XL386), *CDC33-HA₃* (YSB-4B) and *GIS3-Myc₁₃ RCO1-HA₃* (XL388) cells were grown in YPD. 120 OD of cells of each strain were harvested in exponentially growing phase prior to (EXP) or following 1 hr rapamycin treatment (0.2 $\mu\text{g ml}^{-1}$). The pellets were washed with 1 ml FA buffer (50 mM Hepes pH 7.6, 140 mM NaCl, 1 mM EDTA, 1 mM PMSF, proteases inhibitors cocktail (Roche, Cat. No. 05056489001) and phosphatases inhibitors cocktail (Roche, Cat. No. 04906837001)), before being homogenized with glass beads in a Precellys homogeniser (Precellys, Cat. No. 03119.200.RD000). Clarified supernatant of cell lysate were incubated with FA buffer-washed anti-HA coated agarose beads (Roche, Cat. No. 11815016001) O. N. at 4°C. Pelleted agarose beads were washed with FA320 buffer (FA buffer containing 320 nM NaCl) before being incubated with 50 μl sample buffer and were heat denatured for 5 min at 95°C.

Protein samples (10 μl of HA immunoprecipitated and input samples) for western blotting were separated on 10% SDS-polyacrylamide gels, and transferred to nitrocellulose membranes (Hybond ECL, GE Healthcare). The membranes were then probed successively with the appropriate primary and secondary antibodies (anti-Myc (Roche, Cat. No. 11814460001), anti-HA (kind gift of R. Loewith), anti-Mouse IgG-HRP (172-1011, Bio-rad)).

Microscopy

Cells were imaged using an BX51 microscope (Olympus) equipped with a piezo-positioner (Olympus), a OSRAM 1XHBO 130 W/2 mercury burner (Atlanta Light Bulbs, Inc. GA), 100x 1.45 Plan-Fluar objectives, and a three-position filter sliding rack. Image acquisition was performed with a F-view2 camera (Olympus). The microscope and camera were controlled by CellM software (Olympus). The microscope was equipped with a complete set of filters: U-MWIBA, U-MWIG and U-MNUA2 (Olympus). To ensure that the filters were aligned, we utilized Tetraspeck Fluorescent Microspheres (Molecular Probes, Eugene, OR). Z sections (7–10 each 0.5 μm apart) were projected to two-dimensional images and analyzed with the CellM software (Olympus). Relative level of nuclear Igo1-GFP quantified by comparison of the amount of fluorescence intensity per unit area in the nucleus versus the cytoplasm. All live cell imaging were performed with mid-log phase cells cultured in SD

media supplemented with appropriate nutrients for plasmids maintenance prior to and following rapamycin treatment ($0.2 \mu\text{g ml}^{-1}$) for indicated time. DNA was stained with 4, 6-diamidino-2-phenylindole, which was added to the cultures (4 hr prior to fluorescence microscopy) (Wanke et al., 2005) at a final concentration of $1 \mu\text{g ml}^{-1}$. Cells were harvested by centrifugation at 2000 rpm at room temperature RT for 5 min.

β -galactosidase assays

Classical β -galactosidase assays were performed as previously described (Stern et al., 1984).

Material and Methods

Materials

Yeast strains

Strain name **Back ground** **Mating type** **Genotype** **Reference/Creator** **Figure**

Strains used in Chapter II

BY4741	BY4741	a	<i>his3Δ1 leu2Δ0 met15Δ0 ura3Δ0</i>	EUROSCARF	8, 19
CDV288-12A	BY4741	a	<i>his3Δ1 leu2Δ0 MET15 LYS2 ura3Δ0 igo1Δ::kanMX4 igo2Δ::kanMX2</i>	Talarek et al., 2010/De Virgilio C.	8, 15, 16, 17, 18
Y12055	BY4742	α	<i>his3Δ1 leu2Δ0 lys2Δ0 ura3Δ0 igo1Δ::kanMX4</i>	EUROGENTEC	9, 10, 11, 12, 13
XL051-2C	BY4741	a	<i>igo1Δ::kanMX4 rim15Δ::kanMX4 his3Δ1 leu2Δ0 met15Δ0 ura3Δ0</i>	Talarek et al., 2010/Luo X.	9, 10, 11, 12, 13
YBL003	YBL004	α	<i>trp1Δ63 leu2Δ1 ura3-52 his3Δ200 kap123::HIS3</i>	Seedorf and Silver, 1997/Silver P.	19

Strains used in Chapter III

Y7092	XL111	α	<i>igo1Δ::NatMX4, igo2Δ::HphMX4, can1Δ::STE2pr-His5, lyp1Δ, ura3Δ, his3Δ1</i>	Luo et al., 2010/Luo X.	22
BY4742	BY4742	α	<i>his3Δ1; leu2Δ0; lys2Δ0; ura3Δ0</i>	EUROSCARF	21, 23, 24, 25, 26, 27, 28, 29, 30
BY4742	XL122-16D	α	<i>igo1Δ::Nat igo2Δ::Hph his3Δ1 leu2Δ0 ura3Δ0 LYS2 met15</i>	Luo et al., 2010/Luo X.	21, 23, 24, 25, 26, 27, 28, 29, 30
BY4742	XL126	α	<i>rim15Δ::Nat his3Δ1 leu2Δ0 lys2Δ0 ura3Δ0</i>	Luo et al., 2010/Luo X.	21, 23, 24, 25, 26, 27, 28, 29, 30
BY4741	XL131-9D	a	<i>pat1Δ::Kan his3Δ1 leu2Δ0 ura3Δ0 LYS1 MET15</i>	Luo et al., 2010/Luo X.	23, 26, 27, 28
BY4742	XL136-12B	α	<i>rim15Δ::Nat pat1Δ::Kan his3Δ1 leu2Δ0 ura3Δ0 LYS1 MET15</i>	Luo et al., 2010/Luo X.	23, 26, 27, 28
BY4741	XL131-9B	a	<i>igo1Δ::Nat igo2Δ::Hph pat1Δ::Kan his3Δ1 leu2Δ0 ura3Δ0 LYS1 MET15</i>	Luo et al., 2010/Luo X.	23, 26, 27, 28
BY4742	XL150-5D	α	<i>lsm1Δ::Kan his3Δ1 leu2Δ0 ura3Δ0 LYS1 MET15</i>	Luo X.	23, 29, 30
BY4742	XL155-2B	α	<i>rim15Δ::Nat lsm1Δ::Kan his3Δ1 leu2Δ0 ura3Δ0 LYS1 MET15</i>	Luo X.	23, 29, 30
BY4741	XL150-2B	a	<i>igo1Δ::Nat igo2Δ::Hph lsm1Δ::Kan his3Δ1 leu2Δ0 ura3Δ0 LYS1 MET15</i>	Luo X.	23, 29, 30
BY4741	XL261-1A	a	<i>lsm6Δ::Kan his3Δ1 leu2Δ0 ura3Δ0 LYS1 MET15</i>	Luo X.	23, 29, 30
BY4741	XL261-1D	α	<i>rim15Δ::Nat lsm6Δ::Kan his3Δ1 leu2Δ0 ura3Δ0 LYS1 MET15</i>	Luo X.	23, 29, 30
BY4741	XL260-1A	α	<i>igo1Δ::Nat igo2Δ::Hph lsm6Δ::Kan his3Δ1 leu2Δ0 ura3Δ0 LYS1 MET15</i>	Luo X.	23, 29, 30
BY4741	YKO1C11	a	<i>his3Δ1 leu2Δ0 met15Δ0 ura3Δ0 ccr4Δ::kanMX4</i>	EUROSCARF	23, 24, 25
BY4742	MJA1600-B10	α	<i>rim15Δ::kanMX4 ccr4Δ::kanMX4 his3Δ1 leu2Δ0 LYS2 met15Δ0 ura3Δ0</i>	Talarek et al., 2010/Jaquenoud M.	23, 24, 25
BY4741	MJA1597-4D	a	<i>his3Δ1 leu2Δ0 LYS met ura3Δ0 igo1Δ::kanMX4 igo2Δ::kanMX4 ccr4Δ::kanMX4</i>	Talarek et al., 2010/Jaquenoud M.	23, 24, 25
BY4741	YKO42F10	a	<i>his3Δ1 leu2Δ0 met15Δ0 ura3Δ0 dhh1Δ::kanMX4</i>	EUROSCARF	23, 24, 25
BY4742	MJA1602-3A	α	<i>rim15Δ::kanMX4 dhh1Δ::kanMX4 his3Δ1 leu2Δ0 LYS2 met15Δ0 ura3Δ0</i>	Talarek et al., 2010/Jaquenoud M.	23, 24, 25

Strain name	Back ground	Mating type	Genotype	Reference/ Creator	Figure
BY4741	MJA1621-10B	a	<i>igo1Δ::kanMX4, igo2Δ::kanMX4, dhh1Δ::kanMX4 his3Δ1 leu2Δ0 LYS2 MET15 ura3Δ0</i>	Talarek et al., 2010/ Jaquenoud M.	23, 24, 25
BY4741	XL180-3A	a	<i>igo1Δ::Nat pex18Δ::Kan his3Δ1 leu2Δ0 ura3Δ0 LYS1 MET15</i>	Luo X.	23
BY4741	XL183-2C	α	<i>rim15Δ::Nat pex18Δ::Kan his3Δ1 leu2Δ0 ura3Δ0 LYS1 MET15</i>	Luo X.	23
BY4741	XL180-4B	a	<i>igo1Δ::Nat igo2Δ::Hph pex18Δ::Kan his3Δ1 leu2Δ0 ura3Δ0 LYS1 MET15</i>	Luo X.	23
BY4741	XL172-2D	α	<i>tos9Δ::Kan his3Δ1 leu2Δ0 ura3Δ0 LYS1 MET15</i>	Luo X.	23
BY4741	XL177-2C	a	<i>rim15Δ::Nat tos9Δ::Kan his3Δ1 leu2Δ0 ura3Δ0 LYS1 MET15</i>	Luo X.	23
BY4741	XL172-1D	a	<i>igo1Δ::Nat igo2Δ::Hph tos9Δ::Kan his3Δ1 leu2Δ0 ura3Δ0 LYS1 MET15</i>	Luo X.	23
BY4741	YKO42E6	a	<i>his3Δ1 leu2Δ0 met15Δ0 ura3Δ0 pph21Δ::kanMX4</i>	EUROSCARF	23
BY4741	CDV319-1C	a	<i>his3Δ leu2Δ0 LYS2 met15Δ0 ura3Δ0 rim15Δ::kanMX4 pph21Δ::kanMX4</i>	De Virgilio C.	23
BY4741	CDV321-1D	α	<i>his3Δ leu2Δ0 lys2Δ0 MET15 ura3Δ0 igo1Δ::kanMX4 igo2Δ::kanMX pph21Δ::kanMX4</i>	De Virgilio C.	23

Strains used in Chapter IV

BY4742	BY4742	α	<i>his3Δ1; leu2Δ0; lys2Δ0; ura3Δ0</i>	EUROSCARF	32, 34, 35, 36, 37, 38, 39, 40
XL122-16D	BY4742	α	<i>igo1Δ::Nat igo2Δ::Hph his3Δ1 leu2Δ0 ura3Δ0 LYS2 met15</i>	Luo et al., 2010/ Luo X.	32, 34, 35, 36, 37, 38, 39, 40
XL126	BY4742	α	<i>rim15Δ::Nat his3Δ1 leu2Δ0 lys2Δ0 ura3Δ0</i>	Luo et al., 2010/ Luo X.	32, 34, 35, 36, 37, 38, 39, 40
YKO35F2	BY4742	α	<i>gis3Δ::Kan his3Δ1; leu2Δ0; lys2Δ0; ura3Δ0</i>	EUROSCARF	41, 42
NMY51	w303	a	<i>his3Δ200 trp1-901 leu2-3,112 ade2 LYS::(lexAop)4-HIS3 ura3::(lexAop)8-lacZ ade2::(lexAop)8-ADE2 GAL4</i>	DualHunter	44, 45
BZ001-5AL	w303	a	<i>rim15Δ::Nat his3Δ200 (or his3-11, 15) trp1-901 (or trp1-1) leu2-3,112 ade2 ura3::(lexAop)8-lacZ ade2::(lexAop)8-ADE2 GAL4 LYS::(lexAop)4-HIS3</i>	Zufferey B.	45
YSB-4B	BY4741	a	<i>CDC55-3HA::KanMX6 his3Δ1 leu2Δ0 met15Δ0 ura3Δ0</i>	Bontron S.	46
XL386	BY4741	α	<i>GIS3-Myc13Δ::HIS3MX6 his3Δ1 leu2Δ0 lys2Δ0 ura3Δ0</i>	Luo X.	46
XL387-2A	BY4741	a	<i>GIS3-Myc13Δ::HIS3MX6 CDC55-3HA::KanMX6 his3Δ1; leu2Δ0; ura3Δ0; LYS2, MET15</i>	Luo X.	46
XL388-5B	BY4741	a	<i>GIS3-Myc13Δ::HIS3MX6 RCO1-3HA::HIS3MX6 his3Δ1; leu2Δ0; ura3Δ0; LYS2, MET15</i>	Luo X.	46

Plasmids

Plasmid Name **ORI** **Marker** **Promoter** **Description** **Source** **Figure(s)**

Plasmids used in Chapter II

p101	CEN/ARS	<i>URA3</i>	Null	YCplac33	Gietz R.	8, 16, 17, 18
pCDV1149	CEN/ARS	<i>URA3</i>	Endogenous	YCplac33- <i>IGO1</i>	De Virgilio C.	8
pXL016	CEN/ARS	<i>URA3</i> ; <i>kanMX6</i>	Endogenous	YCplac33- <i>IGO1</i> -EGFP	Luo X.	8, 9, 10, 11, 12, 13, 15, 16, 17, 18
pLC1216	CEN/ARS	<i>URA3</i>	Endogenous	YCplac33- <i>IGO1 S64A</i>	Cameroni L.	8
pXL017	CEN/ARS	<i>URA3</i> ; <i>kanMX6</i>	Endogenous	YCplac33- <i>IGO1 S64A</i> -EGFP	Luo X.	8, 9, 10, 11, 15, 16, 17, 18
pLC1215	CEN/ARS	<i>URA3</i>	Endogenous	YCplac33- <i>IGO1 S64D</i>	Cameroni L.	8
pXL018	CEN/ARS	<i>URA3</i> ; <i>kanMX6</i>	Endogenous	YCplac33- <i>IGO1 S64D</i> -EGFP	Luo X.	8, 11
pLC1218	CEN/ARS	<i>URA3</i>	Endogenous	YCplac33- <i>IGO1 S105A</i>	Cameroni L.	8
pXL019	CEN/ARS	<i>URA3</i> ; <i>kanMX6</i>	Endogenous	YCplac33- <i>IGO1 S105A</i> -EGFP	Luo X.	8, 12
pLC1229	CEN/ARS	<i>URA3</i>	Endogenous	YCplac33- <i>IGO1 S105D</i>	Cameroni L.	8
pXL021	CEN/ARS	<i>URA3</i> ; <i>kanMX6</i>	Endogenous	YCplac33- <i>IGO1 S105D</i> -EGFP	Luo X.	8, 13
pXL026	CEN/ARS	<i>URA3</i> ; <i>kanMX6</i>	Endogenous	YCplac33- <i>IGO1-PRP20NLS</i> -eGFP	Luo X.	15, 16, 17, 18
pXL086	CEN/ARS	<i>URA3</i> ; <i>kanMX6</i>	Endogenous	YCplac33- <i>IGO1-PRP20NLS-19,20KT</i> -GFP	Luo X.	15, 16, 17, 18
pXL092	CEN/ARS	<i>URA3</i> ; <i>kanMX6</i>	Endogenous	YCplac33- <i>IGO1-PRP40NES2</i> -GFP	Luo X.	15, 16, 17, 18
pXL094	CEN/ARS	<i>URA3</i> ; <i>kanMX6</i>	Endogenous	YCplac33- <i>IGO1-PRP40NES2_3LA</i> -GFP	Luo X.	15, 16, 17, 18
p2149	CEN/ARS	<i>HIS3</i>	<i>CYC1</i>	pNP314- <i>HHF2</i> -RFP	Favre V.	15
pXL029	2 μ	<i>URA3</i>	<i>HSP26</i>	<i>HSP26p</i> -yEmRFP	Luo X.	19
pXL051	2 μ	<i>HIS3</i>	<i>HSP26</i>	<i>HSP26p</i> -yEmRFP	Luo X.	8, 16

Plasmids used in Chapter III

pXL029	2 μ	<i>URA3</i>	<i>HSP26</i>	<i>HSP26p</i> -yEmRFP	Luo X.	21, 23
pXL051	2 μ	<i>HIS3</i>	<i>HSP26</i>	<i>HSP26p</i> -yEmRFP	Luo X.	28
pXL060	CEN/ARS	<i>URA3</i>	Endogenous	YCplac33- <i>PAT1</i>	Luo X.	28
p101	CEN/ARS	<i>URA3</i>	Null	YCplac33	Gietz R.	28

Plasmids used in Chapter IV

pXL051	2 μ	<i>HIS3</i>	<i>HSP26</i>	<i>HSP26p</i> -yEmRFP	Luo X.	32
p109	2 μ	<i>URA3</i>	<i>GAL1</i>	pEG-KT	Deschenes R.	32
pXL097	2 μ	<i>URA3</i>	tetO7	ptetO7-HIS ₆ -HA ₃ - <i>IGO1</i>	Luo X.	32, 34
pXL121	2 μ	<i>URA3</i>	tetO7	ptetO7-HIS ₆ -HA ₃ - <i>GIS3</i>	Luo X.	34
pXL104	2 μ	<i>URA3</i>	tetO7	ptetO7-HIS ₆ -HA ₃ - <i>MS11</i>	Luo X.	34, 35, 36, 37
pXL106	2 μ	<i>URA3</i>	tetO7	ptetO7-HIS ₆ -HA ₃ - <i>CDC25</i>	Luo X.	34
pXL098	2 μ	<i>URA3</i>	tetO7	ptetO7-HIS ₆ -HA ₃ - <i>ZDS1</i>	Luo X.	34
pXL103	2 μ	<i>URA3</i>	tetO7	ptetO7-HIS ₆ -HA ₃ - <i>MSN2</i>	Luo X.	34, 38, 39
pXL105	2 μ	<i>URA3</i>	tetO7	ptetO7-HIS ₆ -HA ₃ - <i>WH12</i>	Luo X.	34

Plasmid Name	ORI	Marker	Promoter	Description	Source	Figure(s)
pMPG2	2 μ	<i>URA3</i>	tetO7	ptetO7-HIS ₆ -HA ₃	Peli-Gulli MP.	34, 38, 40
pXL116	CEN/ARS	<i>URA3</i>	Endogenous	pRS416- <i>GIS3p</i> -GFP- <i>GIS3</i>	Luo X.	34, 35, 36, 37, 38, 39, 40
p2149	CEN/ARS	<i>HIS3</i>	<i>CYC1</i>	pNP314- <i>HHF2</i> -RFP	Favre V.	41
p2223	2 μ	<i>URA3</i>	<i>GALI</i>	GAL1p- <i>GIS3</i> -HIS ₆ -HA ₃ -Protease 3C-Protein A	EUROSCARF	41
p2224	2 μ	<i>URA3</i>	<i>GALI</i>	GAL1p-PAH1-HIS ₆ -HA ₃ -Protease 3C-Protein A	EUROSCARF	42
pDL2-Alg5	2 μ	<i>TRP1</i>	<i>ADH1</i>	pDL2-Alg5	Dualhunter	42
pAI-Alg5	2 μ	<i>TRP1</i>	<i>ADH1</i>	pAI-Alg5	Dualhunter	44, 45
pXL125	2 μ	<i>TRP1</i>	<i>CYC1</i>	pCab- <i>GIS3</i>	Luo X.	44, 45
pNT061	2 μ	<i>TRP1</i>	<i>CYC1</i>	pPR3-N- <i>CDC55</i>	Talarek N.	44, 45
pNT059	2 μ	<i>TRP1</i>	<i>CYC1</i>	pPR3-N- <i>PPH21</i>	Talarek N.	44, 45
pNT063	2 μ	<i>TRP1</i>	<i>CYC1</i>	pPR3-N- <i>PPH22</i>	Talarek N.	44, 45
p1860	2 μ	<i>TRP1</i>	<i>CYC1</i>	pPR3-N- <i>MON1</i>	Jaquenoud M.	44, 45

Abbreviation

cAMP	<u>C</u> yclic <u>A</u> MP
CDK	<u>C</u> yclin- <u>d</u> ependent <u>k</u> inase
co-IP	<u>C</u> o- <u>I</u> mmunoprecipitation
DAPI	40,6- <u>d</u> iamidino 2- <u>p</u> henyl <u>i</u> ndole
eIF2	<u>E</u> karyotic <u>t</u> ranslation <u>i</u> nitiation <u>f</u> actor 2
FKBP	<u>F</u> K506- <u>b</u> inding <u>p</u> rotein
FRB	<u>F</u> KBP12- <u>r</u> apamycin <u>b</u> inding
FRET	<u>F</u> luorescence <u>r</u> esonance <u>e</u> nergy <u>t</u> ransfert
GAP	<u>G</u> TPase- <u>a</u> ctivating <u>p</u> rotein
GEF	<u>G</u> uanine nucleotide <u>e</u> xchange <u>f</u> actor
GFP	<u>G</u> reen <u>f</u> luorescent <u>p</u> rotein
IGO	<u>I</u> nitiation of <u>G</u> -zero
NES	<u>N</u> uclear <u>e</u> xport <u>s</u> ignal
NLS	<u>N</u> uclear <u>l</u> ocalization <u>s</u> ignal
MS	<u>M</u> ass <u>s</u> pectrometry
ORF	<u>O</u> pen <u>r</u> eading <u>f</u> rame
Ribi	<u>R</u> ibosome <u>b</u> iogenesis
RP	<u>R</u> ibosomal <u>p</u> rotein
PAGE	<u>P</u> oly <u>a</u> crylamide gel <u>e</u> lectrophoresis
PDS	<u>P</u> ost- <u>d</u> iauxic <u>s</u> hift
PKA	<u>P</u> rotein <u>k</u> inase <u>A</u>
PP2A	<u>P</u> rotein <u>p</u> hosphatase <u>2</u> <u>A</u>
PPase	<u>P</u> hosphatase
TOR	<u>T</u> arget <u>o</u> f <u>r</u> apamycin
TORC1	<u>T</u> OR <u>c</u> omplex 1
SD	<u>S</u> ynthetic <u>d</u> extrose
STREs	<u>S</u> tress <u>r</u> esponse <u>e</u> lements
UTR	<u>U</u> ntranslated <u>r</u> egion
yEmRFP	<u>Y</u> east <u>e</u> nanced <u>m</u> onomeric <u>r</u> ed <u>f</u> luorescent <u>p</u> rotein

Annex 1. Gis3 physical interactors

Identified Proteins (271)	Molecular Weight	Fisher's Exact Test (P-Value)	The numbers of matched spectra ¹	
			Gis3	Pah1
Acetyl CoA synthetase ACS1	79 kDa	95% (0.0000050)	31	0
Translation elongation factor 2 EFT1	93 kDa	95% (0.0000074)	30	0
Vacuolar protein sorting-associated protein 35 VPS35	109 kDa	95% (0.000011)	29	0
Tryptophan synthase SCRG_01033	77 kDa	95% (0.000036)	26	0
RuVB-like protein RVB1	50 kDa	95% (0.000053)	25	0
Heat shock protein 26 HSP26	24 kDa	95% (0.00070)	24	0
Protein phosphatase PP2A regulatory subunit A TPD3	71 kDa	95% (0.00026)	21	0
Vacuolar sorting protein VPS29	31 kDa	95% (0.00026)	21	0
GTPase-activating protein SEC23	85 kDa	95% (0.00038)	20	0
Transcriptional regulator RVB2	52 kDa	95% (0.00057)	19	0
Putative uncharacterized protein SCRG_05618	78 kDa	95% (0.00084)	18	0
Glutamate synthase (NADH) GLT1	238 kDa	95% (0.00084)	18	0
Ribosomal protein L4A RPL4A	39 kDa	95% (0.0013)	17	0
UDP-glucose-starch glucosyltransferase GSY2	80 kDa	95% (0.0027)	15	0
Phosphofructokinase beta subunit SCRG_02099	105 kDa	95% (0.0027)	15	0
Carboxypeptidase Y-deficient PEP8	43 kDa	95% (0.0041)	14	0
Asparagine synthetase [glutamine-hydrolyzing] 2 ASN2	65 kDa	95% (0.0041)	14	0
Autophagy-related protein 18 ATG18	55 kDa	95% (0.0041)	14	0
Glycerol-3-phosphate dehydrogenase (NAD+) GPD2	49 kDa	95% (0.0041)	14	0
Acetyl CoA carboxylase ACC1	250 kDa	95% (0.0060)	13	0
Long chain fatty acyl:CoA synthetase SCRG_01698	78 kDa	95% (0.0060)	13	0
Carnitine acetyltransferase YAT2	103 kDa	95% (0.0060)	13	0
Clustered mitochondria CLU1	145 kDa	95% (0.0060)	13	0
Regulator of ribosome biogenesis RRB1	57 kDa	95% (0.0060)	13	0
Rps0ap GN=EC1118_1G1_5457g	28 kDa	95% (0.044)	12	0
ADP/ATP carrier PET9	34 kDa	95% (0.0090)	12	0
5-aminolevulinate synthase HEM1	59 kDa	95% (0.013)	11	0
Coatomer subunit beta SEC26	109 kDa	95% (0.013)	11	0
Mitochondrial outer membrane protein porin 1 POR1	30 kDa	95% (0.013)	11	0
Protein phosphatase PP2A regulatory subunit B CDC55	60 kDa	95% (0.020)	10	0
AAA ATPase PEX1	117 kDa	95% (0.020)	10	0
Fructose-bisphosphate aldolase FBA1	40 kDa	95% (0.020)	10	0
Hbt1p HBT1	114 kDa	95% (0.020)	10	0
Conserved protein MIR1	33 kDa	95% (0.020)	10	0
Glucosamine-6-phosphate synthase GFA1	80 kDa	95% (0.020)	10	0
Putative uncharacterized protein SCRG_00654	58 kDa	95% (0.029)	9	0
Orotidine 5'-phosphate decarboxylase URA3	29 kDa	95% (0.029)	9	0

60S ribosomal protein L6 RPL6A	20 kDa	0% (0.14)	5	0
Ribosomal protein RPL1B	24 kDa	0% (0.14)	5	0
Fumarase FUM1	53 kDa	0% (0.14)	5	0
Meiotic sister-chromatid recombination protein 3 SCRG_04175	81 kDa	0% (0.14)	5	0
Calmodulin CMD1	16 kDa	0% (0.14)	5	0
Hrk1p HRK1	85 kDa	0% (0.14)	5	0
Replication factor C subunit 5 RFC5	40 kDa	0% (0.14)	5	0
S-adenosylmethionine synthase SAM1	42 kDa	0% (0.21)	4	0
Ribosomal protein L25 RPL25	16 kDa	0% (0.21)	4	0
Putative uncharacterized protein SCRG_02385	138 kDa	0% (0.21)	4	0
Conserved protein ECM14	50 kDa	0% (0.21)	4	0
Polyamine acetyltransferase PAA1	22 kDa	0% (0.21)	4	0
Ribosomal protein L7A RPL7A	28 kDa	0% (0.21)	4	0
Asparagine synthetase ASN1	64 kDa	0% (0.095)	4	0
Heat shock protein 104 HSP104	102 kDa	0% (0.21)	4	0
Conserved protein SCY_2936	38 kDa	0% (0.21)	4	0
Malate dehydrogenase MDH1	36 kDa	0% (0.21)	4	0
Nitrogen permease regulator NPR1	86 kDa	0% (0.21)	4	0
UDP-glucose 4-epimerase GAL10	78 kDa	0% (0.21)	4	0
Phosphorylation inhibited by long chain bases PIL1	38 kDa	0% (0.21)	4	0
Suppressor of los1-1 SOL2	35 kDa	0% (0.21)	4	0
Mps1 binder MOB2	33 kDa	0% (0.21)	4	0
40S ribosomal protein S8 RPS8A	22 kDa	0% (0.21)	4	0
Dasein kinase YCK2	62 kDa	0% (0.21)	4	0
Ribosomal protein L21A RPL21A	18 kDa	0% (0.21)	4	0
Glucose-6-phosphate isomerase PGI1	61 kDa	0% (0.21)	4	0
Alpha-tubulin TUB1	50 kDa	0% (0.21)	4	0
CTPxI TSA1	22 kDa	0% (0.21)	4	0
Glyoxylate reductase SCY_4531	39 kDa	0% (0.21)	4	0
Sit4 suppressor SIS1	38 kDa	0% (0.21)	4	0
4-aminobutyrate aminotransferase UGA1	53 kDa	0% (0.21)	4	0
Putative uncharacterized protein SCRG_02755	57 kDa	0% (0.21)	4	0
Succinate dehydrogenase (Ubiquinone) iron-sulfur protein subunit SDH2	30 kDa	0% (0.21)	4	0
GTP-cyclohydrolase I FOL2	28 kDa	0% (0.21)	4	0
Conserved protein SCY_4498	38 kDa	0% (0.21)	4	0
Conserved protein RPP2A	11 kDa	0% (0.21)	4	0
Nuclear pore complex subunit SEH1	39 kDa	0% (0.21)	4	0
Triosephosphate isomerase TPI1	27 kDa	0% (0.21)	4	0
Ribosomal protein L18 RPL18A	21 kDa	0% (0.21)	4	0
DNA binding protein YHM2	34 kDa	0% (0.21)	4	0
ATP synthase subunit alpha ATP1	59 kDa	0% (0.61)	3	0
DNA-directed RNA polymerase RPO21	192 kDa	0% (0.31)	3	0
Serine/threonine protein kinase YPK1	76 kDa	0% (0.31)	3	0
Conserved protein SFB2	99 kDa	0% (0.31)	3	0
Ribosomal protein L33B RPL33B	12 kDa	0% (0.31)	3	0
Replication factor C subunit 3 RFC3	38 kDa	0% (0.31)	3	0
Conserved protein BBC1	130 kDa	0% (0.31)	3	0

Conserved protein MEU1	38 kDa	0% (0.31)	3	0
General negative regulator of transcription subunit 1 SCRG_05480	240 kDa	0% (0.31)	3	0
Heat shock protein HSP42	43 kDa	0% (0.31)	3	0
6,7-dimethyl-8-ribityllumazine synthase RIB4	19 kDa	0% (0.31)	3	0
Ribosomal protein L24B RPL24B	18 kDa	0% (0.31)	3	0
Acetyl transferase FAS1	229 kDa	0% (0.31)	3	0
Whiskey WHI4	71 kDa	0% (0.31)	3	0
DNA-directed RNA polymerase RPA135	136 kDa	0% (0.31)	3	0
Delta subunit of the coatomer complex (COPI) RET2	61 kDa	0% (0.31)	3	0
Ribosomal protein P2B RPP2B	11 kDa	0% (0.31)	3	0
Serine/threonine-protein phosphatase PPZ1	77 kDa	0% (0.14)	3	0
Endopolyphosphatase PPN1	78 kDa	0% (0.31)	3	0
Conserved protein SCY_5339	29 kDa	0% (0.31)	3	0
60S ribosomal protein L13 RPL13B	23 kDa	0% (0.31)	3	0
UDP-glucose-starch glucosyltransferase GSY1	80 kDa	0% (0.064)	3	0
Ribosomal protein L16B RPL16B	22 kDa	0% (0.31)	3	0
Trehalose-6-phosphate synthase/phosphatase complex 115 kDa regulatory subunit TPS3	119 kDa	0% (0.31)	3	0
DNA-directed RNA polymerase RET1	129 kDa	0% (0.31)	3	0
Citrate synthase CIT1	53 kDa	0% (0.31)	3	0
Serine/threonine protein kinase SCH9	92 kDa	0% (0.31)	3	0
tRNA-His guanylyltransferase THG1	28 kDa	0% (0.31)	3	0
Secretory protein SEC1	83 kDa	0% (0.31)	3	0
Putative uncharacterized protein SCRG_01058	58 kDa	0% (0.31)	3	0
GTPase-activating protein GYP1	73 kDa	0% (0.31)	3	0
Conserved protein SCY_0955	39 kDa	0% (0.31)	3	0
Glutamyl-tRNA synthetase GUS1	81 kDa	0% (0.31)	3	0
Histone deacetylase complex DNA-binding subunit SIN3	175 kDa	0% (0.31)	3	0
Isocitrate dehydrogenase [NADP] IDP2	47 kDa	0% (0.31)	3	0
Vacuolar sorting protein VPS1	79 kDa	0% (0.31)	3	0
Serine/threonine-protein phosphatase CMP2	69 kDa	0% (0.31)	3	0
AMP deaminase AMD1	93 kDa	0% (0.31)	3	0
Amphiphysin-like lipid raft protein RVS161	30 kDa	0% (0.31)	3	0
Ribosomal protein L22A RPL22A	14 kDa	0% (0.31)	3	0
Obg-like ATPase OLA1	44 kDa	0% (0.46)	2	0
Early meiotic induction protein EMI2	56 kDa	0% (0.21)	2	0
Stress-seventy subfamily A ATPase SSA3	71 kDa	95% (0.00000070)	2	0
Conserved protein SFB3	104 kDa	0% (0.46)	2	0
D-lactate dehydrogenase DLD3	55 kDa	0% (0.46)	2	0
Pas domain-containing serine/threonine protein kinase PSK1	152 kDa	0% (0.46)	2	0
Conserved protein SCY_2489	41 kDa	0% (0.46)	2	0
Ribosomal protein L9B RPL9B	22 kDa	0% (0.46)	2	0
Ribosomal protein S9B RPS9B	22 kDa	0% (0.46)	2	0
Ribosomal protein S19A RPS19A	16 kDa	0% (0.69)	2	0
Conserved protein SCY_5659	23 kDa	0% (0.46)	2	0
Conserved protein SCY_4660	41 kDa	0% (0.46)	2	0
Proteasome regulatory particle subunit RPN9	46 kDa	0% (0.46)	2	0

Inositol polyphosphate kinase KCS1	120 kDa	0% (0.46)	2	0
Histone H2A HTA2	14 kDa	0% (0.46)	2	0
Heat shock protein 12 SCRG_05533	12 kDa	0% (0.46)	2	0
Transcriptional activator with GATA-1-type Zn finger DNA-binding motif GAT1	56 kDa	0% (0.46)	2	0
Suppressor of rho3 SRO9	48 kDa	0% (0.46)	2	0
Superoxide dismutase [Cu-Zn] SOD1	16 kDa	0% (0.46)	2	0
Diadenosine 5',5''-P1,P4-tetraphosphate hydrolase DDP1	22 kDa	0% (0.46)	2	0
ADP-ribosylation factor 2 ARF2	21 kDa	0% (0.46)	2	0
Transposon Ty1-JR2 Gag-Pol polyprotein TY1B-JR2	199 kDa	95% (0.000000000077)	2	0
PPIase FPR1	12 kDa	0% (0.46)	2	0
Purine motif triplex-binding protein STM1	30 kDa	0% (0.46)	2	0
Mitochondrial matrix factor MMF1	16 kDa	0% (0.46)	2	0
Mitochondrial outer membrane protein OM14 OM14	15 kDa	0% (0.46)	2	0
Conserved protein SCY_0530	10 kDa	0% (0.46)	2	0
Proteinase inhibitor I2B (PBI2) PBI2	9 kDa	0% (0.46)	2	0
60S ribosomal protein L36 RPL36A	11 kDa	0% (0.46)	2	0
GTP-binding protein GSP2	25 kDa	0% (0.46)	2	0
Cell wall endo-beta-1,3-glucanase BGL2	34 kDa	0% (0.46)	2	0
Conserved protein SCY_1236	55 kDa	0% (0.46)	2	0
Homocitrate synthase LYS20	47 kDa	95% (0.00057)	2	0
Cytochrome c oxidase subunit IV COX4	17 kDa	0% (0.46)	2	0
Ribosomal protein L5 RPL5	34 kDa	0% (0.46)	2	0
Integral membrane protein that along with Pil1p is a primary component of eisosomes LSP1	38 kDa	0% (0.31)	2	0
Serine/threonine-protein phosphatase PPH21	42 kDa	0% (0.095)	2	0
Resistance to o-dinitrobenzene ROD1	92 kDa	0% (0.46)	2	0
Conserved protein MOH1	16 kDa	0% (0.46)	2	0
Malate dehydrogenase MDH2	46 kDa	0% (0.46)	2	0
Profilin PFY1	14 kDa	0% (0.46)	2	0
Ribosomal protein S30B RPS30B	7 kDa	0% (0.46)	2	0
Pyruvate kinase PYK2	55 kDa	0% (0.21)	2	0
Unsaturated phospholipid N-methyltransferase OPI3	23 kDa	0% (0.46)	2	0
Replication factor-A subunit 3 RFA3	14 kDa	0% (0.46)	2	0
Ribosomal protein L34A RPL34A	14 kDa	0% (0.46)	2	0
Carbonic anhydrase NCE103	25 kDa	0% (0.46)	2	0
Conserved protein SCY_2423	47 kDa	0% (0.46)	2	0
Insensitive to killer toxin IKI1	35 kDa	0% (0.46)	2	0
Conserved protein RTS3	29 kDa	0% (0.46)	2	0
Regulatory particle non-ATPase RPN2	104 kDa	0% (0.46)	2	0
Conserved protein SCY_5507	17 kDa	0% (0.46)	2	0
ARF family protein SAR1	21 kDa	0% (0.46)	2	0
Cell division cycle-related protein CDC48	92 kDa	0% (0.46)	2	0
Ubiquitin carrier protein UBC1	24 kDa	0% (0.46)	2	0
Alkaline phosphatase PHO8	63 kDa	0% (0.46)	2	0
Glutaredoxin GRX2	16 kDa	0% (0.46)	2	0
Conserved protein GPB2	99 kDa	0% (0.46)	2	0
Actin binding and severing protein COF1	16 kDa	0% (0.46)	2	0

Conserved protein SCY_3686	56 kDa	0% (0.46)	2	0
Regulatory particle non-ATPase RPN13	18 kDa	0% (0.46)	2	0
Alcohol dehydrogenase II SCRG_02200	37 kDa	95% (0.013)	2	0
Elongation factor 1-gamma 2 SCRG_03939	47 kDa	0% (0.46)	2	0
YOL081Wp-like protein AWRI1631_150770	352 kDa	0% (0.46)	2	0
RNA-binding protein PIN4 PIN4	74 kDa	0% (0.46)	2	0
Respiratory growth induced protein 1 RGI1	19 kDa	0% (0.46)	2	0
Regulatory particle triphosphatase RPT3	48 kDa	0% (0.46)	2	0
AP-2 complex subunit sigma APS2	17 kDa	0% (0.46)	2	0
Sorting nexin SNX3	19 kDa	0% (0.46)	2	0
Histone deacetylase RPD3	49 kDa	0% (0.46)	2	0
Putative uncharacterized protein SCRG_03603	28 kDa	0% (0.46)	2	0
Ribosomal protein S26B RPS26B	13 kDa	0% (0.46)	2	0
Chromatin structure-remodeling complex protein RSC14 LDB7	20 kDa	0% (0.46)	2	0
5,10-methenyltetrahydrofolate synthetase FAU1	24 kDa	0% (0.46)	2	0
DNA-directed RNA polymerase subunit RPB9	14 kDa	0% (0.46)	2	0
Conserved protein SCY_0883	70 kDa	0% (0.68)	1	0
Cell division cycle-related protein CDC54	105 kDa	0% (0.68)	1	0
YBR126Cp-like protein (Fragment) AWRI1631_22080	57 kDa	0% (0.68)	1	0
Ribosomal protein L28 RPL28	17 kDa	0% (0.68)	1	0
Epsilon-COP coatomer subunit SEC28	34 kDa	0% (0.68)	1	0
Serine/threonine protein kinase YAK1	91 kDa	0% (0.68)	1	0
Oxysterol-binding family protein OSH3	114 kDa	0% (0.68)	1	0
Conserved protein SCY_5486	57 kDa	0% (0.68)	1	0
cAMP-dependent protein kinase regulatory subunit BCY1	47 kDa	0% (0.68)	1	0
Aldehyde dehydrogenase ALD6	54 kDa	0% (0.68)	1	0
MAP kinase kinase (MEK) HOG1	49 kDa	0% (0.68)	1	0
Chaperonin subunit epsilon subunit CCT5	62 kDa	0% (0.68)	1	0
Serine/threonine protein kinase SNF1	72 kDa	0% (0.68)	1	0
AC19 RPC19	16 kDa	0% (0.68)	1	0
Conserved protein SCY_2000	57 kDa	0% (0.68)	1	0
Regulatory particle non-ATPase RPN11	34 kDa	0% (0.68)	1	0
Mitosis entry checkpoint MEC1	273 kDa	0% (0.68)	1	0
Histone H2B HTB2	14 kDa	0% (0.68)	1	0
Conserved protein KSP1	117 kDa	0% (0.68)	1	0
Reticulon-like protein 1 RTN1	33 kDa	0% (0.68)	1	0
Nifs-like protein NFS1	54 kDa	0% (0.68)	1	0
Aminoimidazole ribotide synthetase ADE5,7	86 kDa	0% (0.68)	1	0
ADP-ribosylation factor ARF1	21 kDa	0% (0.46)	1	0
Conserved protein SCY_0829	31 kDa	0% (0.68)	1	0
Conserved protein SCY_2408	77 kDa	0% (0.68)	1	0
Ribosomal protein L33A RPL33A	12 kDa	0% (0.31)	1	0
Hsp90 co-chaperone HCH1 SCRG_03408	17 kDa	0% (0.68)	1	0
Exo-1,3-beta-glucanase EXG1	51 kDa	0% (0.68)	1	0
Fatty acid synthase alpha subunit FAS2	207 kDa	0% (0.68)	1	0
Rsp5p E3-ubiquitin ligase complex component BUL2	105 kDa	0% (0.68)	1	0
Partitioning protein REP1 REP1	43 kDa	0% (0.68)	1	0

Nucleoside diphosphate kinase YNK1	17 kDa	0% (0.68)	1	0
Kinesin-related protein KIP2	78 kDa	0% (0.68)	1	0
RNA polymerase II degradation factor 1 DEF1	84 kDa	0% (0.68)	1	0

¹: A certain linearity exists between the number of spectra matched to a certain protein and its concentration. The numbers of matched spectra can thus be used to make semi-quantitative estimates of protein amounts in the sample.

Initiation of the yeast G_0 program requires Igo1 and Igo2, which antagonize activation of decapping of specific nutrient-regulated mRNAs

Xuan Luo,[†] Nicolas Talarek[†] and Claudio De Virgilio*

Department of Medicine; Division of Biochemistry; University of Fribourg; Fribourg, Switzerland

[†]These authors contributed equally to this work.

Growth factors and essential nutrients are key controllers of eukaryotic cell proliferation. In their absence, cells may enter into a quiescent (G_0) state. In yeast, nitrogen and/or carbon limitation causes downregulation of the conserved TORC1 and PKA signaling pathways and consequently activation of Rim15, a member of the PAS protein kinase family. Rim15 orchestrates the initiation of the G_0 program in part by coordinating transcription of *Msn2/4*- and/or *Gis1*-dependent genes with posttranscriptional protection of the corresponding mRNAs via direct phosphorylation of Igo1/2. Here, we show that several factors including Ccr4, the Lsm-Pat1 complex, and Dhh1, which are implicated in mRNA decapping activation, participate in the decay of specific mRNAs during initiation of the G_0 program when Igo1/2 are absent. Accordingly, Igo1/2 likely play a key role in preventing the decapping and subsequent 5'-3' degradation of a set of nutrient-regulated mRNAs that are critical for cell differentiation and chronological life span.

nutrient-, growth factor- and/or hormone-responsive signal transduction pathways. In the yeast *Saccharomyces cerevisiae*, downregulation of the nutrient-regulated kinase activities of the conserved Target Of Rapamycin Complex 1 (TORC1), or the protein kinase A (PKA) had been found to drive cells into a G_0 -like state and to significantly extend chronological life span (CLS).¹⁻⁴ In contrast, loss of the kinase activity of Rim15 prevents access to G_0 and decreases CLS.⁵⁻⁷ TORC1 (via its substrate Sch9) and PKA are thought to signal in parallel pathways to positively regulate ribosome biogenesis and growth and, by maintaining Rim15 in an inactive state in the cytoplasm, to negatively regulate entry into G_0 .⁸⁻¹² The molecular mechanisms linking Rim15 to distal readouts such as the expression of specific nutrient-regulated genes (e.g., *HSP26*; see below), trehalose and glycogen accumulation, and CLS extension involve the stress-response and post-diauxic shift transcription factors *Msn2/4* and *Gis1*,^{7,13,14} respectively, as well as the recently identified paralogous Rim15 target proteins Igo1 and Igo2.¹⁵ Intriguingly, during initiation of the G_0 program, phosphorylation by Rim15 stimulates Igo proteins to associate with both Lsm12, which likely binds to the 3' untranslated region (UTR) of mRNAs in a complex with Pbp1 and Pbp4,^{16,17} as well as with the decapping activator Dhh1. This latter event appears to be key for newly expressed mRNAs to be both sheltered from degradation via the 5'-3' mRNA decay pathway and channeled towards stress granules (SGs) for

Key words: quiescence, TORC1, mRNA stability, 5'-3' mRNA decay pathway, Igo1 and Igo2, yeast

Submitted: 07/13/10

Revised: 08/26/10

Accepted: 08/31/10

DOI: 10.4161/rna.8.1.13483

*Correspondence to: Claudio De Virgilio;
Email: Claudio.DeVirgilio@unifr.ch

Introduction

All living cells appear to be capable of exiting the normal cell cycle and entering a reversible state termed quiescence or G_0 , which is typically characterized by low metabolic activity, including low rates of protein synthesis and transcription. Initiation of the G_0 program is a highly coordinated process, which requires downregulation of conserved

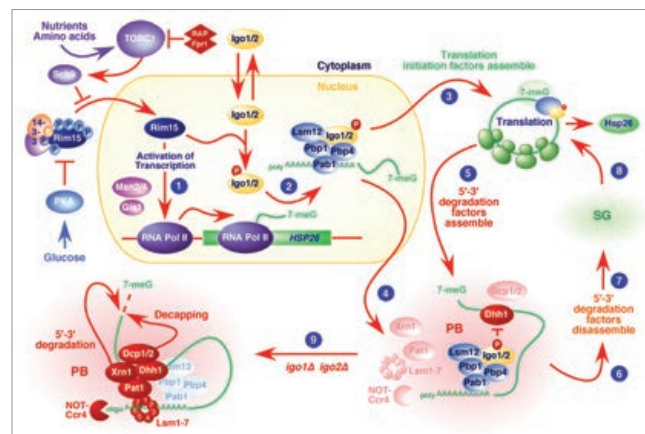


Figure 1. Model depicting a role for Igo1 and Igo2 in protection of specific mRNAs, which are induced during initiation of the G_0 program. In exponentially growing cells, phosphorylation of Rim15 (on Ser⁹⁰¹ by the TORC1 target Sch9 and on Thr¹⁰²⁵ by the cyclin-cyclin-dependent kinase complex Pho80-Pho85)¹⁶ mediates tandem 14-3-3 binding to guarantee optimal sequestration of Rim15 in the cytoplasm, where it is kept inactive through additional PKA-mediated phosphorylation events.^{5,9} TORC1 inactivation (e.g., following treatment of cells with rapamycin or following nutrient starvation) causes initiation of the G_0 program in part by abrogating the cytoplasmic retention of Rim15. Nuclear Rim15, presumably released from PKA-mediated inhibition,²⁶ has a dual role in controlling gene expression by activating transcription of *Msn2/4*- and *Gis1*-dependent genes (1) and protecting the corresponding transcripts from degradation via an Igo1/2-dependent mechanism (2–7).^{13–15} Accordingly, Rim15-dependent phosphorylation of Ser⁶⁴ in Igo1 and Ser⁶³ in Igo2 (both of which likely shuttle between the cytoplasm and the nucleus) leads to the formation of specific messenger ribonucleoprotein (mRNP) complexes (possibly already in the nucleus as depicted or, alternatively, in the cytoplasm) that contain at least Igo1/2, Lsm12, the poly(A)-binding protein Pab1 interactor Pbp1, and Pbp4, as well as a nutrient-regulated mRNA (e.g., *HSP26*) that needs to be translated as part of the quiescence program (2). To this end, the cytoplasmic mRNP complexes likely associate with translation initiation factors and ribosomes for direct translation (3). Alternatively, they may transiently assemble (to some extent in PBs) with 5'-3' degradation factors (4). Notably, Dhh1 may either be incorporated into *HSP26* mRNA-containing mRNPs while they reside in the nucleus, or—as depicted in our model—join the corresponding mRNPs in the cytoplasm (e.g., during or following their unloading from ribosomes and disassembly of translation initiation factors) (5). The interaction of p-Ser⁶⁴-Igo1 with Dhh1 presumably prevents decapping and subsequent 5'-3' degradation of the associated mRNA and promotes both disassembly of 5'-3' degradation factors from the mRNP (6) and reassembly of translation initiation factors (7), a process that may specifically occur in stress granules (SGs). Such mRNP complexes (that may still contain Igo1/2) are thought to exit SGs and to subsequently associate with ribosomes for translation of the corresponding mRNA (8). In the absence of functional Igo1/2, mRNAs such as the *HSP26* mRNA remain unguarded from Dcp1/2- and Xrn1-mediated decapping and 5'-3' decay (9), respectively, and are therefore prone to degradation.

subsequent translation (Fig. 1). Given the conserved nature of Igo proteins,¹⁵ these findings indicate that stabilization of specific mRNAs is a critical determinant of cell differentiation and CLS.

The mRNA Decapping Pathway Targets *HSP26* mRNAs in the Absence of Igo1 and Igo2

To further define the molecular function of Igo1/2, we performed a genome-wide screen for mutations that suppress the defect of *igo1Δ igo2Δ* cells in *HSP26* expression during initiation of the G_0 program. To this end, we constructed an *HSP26*-yEmRFP reporter gene that

expresses, under the control of the yeast *HSP26* promoter, a new yeast enhanced variant of the mCherry monomeric red fluorescent protein (yEmRFP),¹⁸ which confers a vivid purple color to wild-type cells during and following initiation of the G_0 program. As expected, only wild-type cells containing the *HSP26*-yEmRFP reporter plasmid (pXL029), but not corresponding *rim15Δ* or *igo1Δ igo2Δ* cells, were able to form purple colonies when grown for five days on plates containing synthetic defined (SD) medium (Fig. 2A). Next, we crossed an *igo1Δ igo2Δ* strain (XL111; MAT α , *igo1Δ::NatMX4*, *igo2Δ::HphMX4*, *can1Δ::STE2pr-His5*, *hpy1Δ*, *ura3Δ*, *his3Δ1*; derived from

strain Y7092; C. Boone lab collection), harboring the *HSP26*-yEmRFP reporter plasmid, with the Euroscarf collection of 4,857 viable gene deletion mutants essentially as described earlier.¹⁹ The resulting triple mutant collection was screened for mutants that, unlike *igo1Δ igo2Δ* cells, were able to express *HSP26*-yEmRFP and consequently form purple colonies. Notably, since Rim15 controls both activation of transcription (via a still partially understood mechanism that implicates the transcription factors *Msn2/4* and *Gis1*) and posttranscriptional stabilization of mRNAs (by a process that implicates Igo1/2) (Fig. 1), we reasoned that candidate mutations that

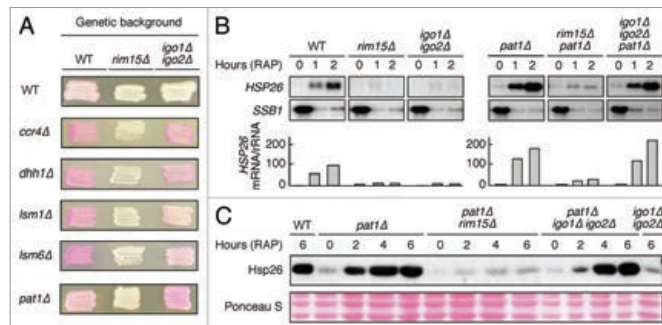


Figure 2. The 5'-3' mRNA degradation pathway targets *HSP26* mRNAs in the absence of Igo1/2. (A) Individual strains were constructed by backcrosses between the single knock-out strains from the Euroscarf collection and isogenic wild-type (BY4742), XL126 (MAT α , *rim15* Δ :*NatMX6*) or XL122-16D (MAT α , *igo1* Δ :*NatMX4*, *igo2* Δ :*HphMX4*) cells, transformed with the *HSP26*-yEmRFP reporter plasmid (pXL029), patched on SD-medium-containing plates, and grown for 5 days at 30°. Expression of yEmRFP under the control of the *HSP26* promoter confers to cells a purple color. (B) Loss of Pat1 suppresses the defect of *igo1* Δ *igo2* Δ , but not that of *rim15* Δ cells in rapamycin-induced *HSP26* mRNA expression. Northern blot analyses of *HSP26* and of rapamycin-repressible *SSB1* were performed with wild-type and indicated mutant strains prior to (0) and following a rapamycin treatment (RAP; 0.2 mg ml⁻¹) of 1 hr or 2 hr. Bar graphs show the relative level of *HSP26* mRNA per rRNA (quantified by Phosphor-Imager analysis and arbitrarily set to 1.0 for exponentially growing wild-type cells). All samples were run on the same gel (identical film exposure time). (C) Loss of Pat1 fully suppresses the defect of *igo1* Δ *igo2* Δ , but not that of *rim15* Δ , in rapamycin-induced Hsp26 protein expression. Cell extracts from the same strains as in (B), treated (2 hr, 4 hr and 6 hr) or not (0 hr) with rapamycin, were analyzed by SDS-PAGE, and immunoblots were probed with specific anti-Hsp26 antibodies. Ponceau S staining of the membranes prior to immunoblot analysis serves as loading control.

suppress the *HSP26*-yEmRFP expression defect in both *rim15* Δ and *igo1* Δ *igo2* Δ cells are very likely to play a role in regulating transcription rather than mRNA stability. To more specifically focus on the role of Igo proteins in posttranscriptional mRNA stability control, such mutations were eliminated in a secondary screen following which we retained a total of five gene deletions that were able to suppress the defect of *igo1* Δ *igo2* Δ cells, but not that of *rim15* Δ cells. In line with and confirming our previous results,¹⁵ our screen identified the *ccr4* Δ and *dbh1* Δ mutations, both of which prevent mRNA decay at early steps of the 5'-3' mRNA decay pathway,²⁰ as *igo1* Δ *igo2* Δ suppressor mutations (Fig. 2A). Interestingly, all three additional, newly identified suppressor mutations (i.e., *lsm1* Δ , *lsm6* Δ and *pat1* Δ) affect genes whose products are constituents of the Lsm1-7/Pat1 (Lsm-Pat1) complex that activates mRNA decapping following deadenylation.²¹ Notably, the other subunits of this complex are either essential (Lsm2-5), or their absence did not significantly suppress (Lsm7) the *igo1* Δ *igo2* Δ phenotype in our assays (data not shown).

To assess further whether loss of Lsm-Pat1 function can also suppress the defect of *igo1* Δ *igo2* Δ cells in *HSP26* expression following TORC1 inactivation, we next measured *HSP26* mRNA and Hsp26 protein levels in rapamycin-treated wild-type, *rim15* Δ , *igo1* Δ *igo2* Δ , *pat1* Δ , *pat1* Δ *rim15* Δ and *pat1* Δ *igo1* Δ *igo2* Δ cells. As expected, loss of Pat1 fully suppressed the defect of *igo1* Δ *igo2* Δ cells, but not that of *rim15* Δ cells, in rapamycin-induced *HSP26* expression (both at the mRNA and protein levels; Fig. 2B and C). These results further support the idea that Rim15 likely has a dual role in controlling gene expression by (1) activating transcription (Fig. 1) and (2) protecting the corresponding transcripts from degradation via an Igo1/2-dependent mechanism that specifically antagonizes the process of mRNA decapping activation. In line with such a model, we previously found that loss of the 5'-3' exonuclease Xrn1, which causes processing bodies (PBs) to increase in number and size due to the entrapping of non-degraded mRNAs,²⁰ allowed *igo1* Δ *igo2* Δ cells, but not *rim15* Δ cells, to accumulate *HSP26*

mRNAs, which then failed to be translated into proteins.¹⁵

mRNA decapping is thought to occur in multiple, sequential steps, which include the partial deadenylation of the poly(A) tail by the NOT-Ccr4 complex, recruitment to the corresponding oligoadenylated mRNAs of the Lsm-Pat1 complex—which, as recently shown in metazoans, serves as a scaffold that binds (via Pat1b) both deadenylation and decapping enzymes^{22,23}—and Dhh1-mediated activation of decapping following remodeling of the 5' structure of the mRNA.^{20,24} Since a defect in any of these steps in the mRNA decapping process can suppress the phenotype of *igo1* Δ *igo2* Δ cells in *HSP26* mRNA (and Hsp26 protein) expression and given the finding that Igo proteins (following phosphorylation by Rim15) interact with Dhh1,¹⁵ Igo proteins are likely to inhibit mRNA decapping at a stage from which mRNAs can still successfully be retrieved for translation (following disassembly of 5'-3' decay factors and assembly of translation initiation factors that may possibly occur within stress granules) (Fig. 1).

Consistent with this view, Igo proteins appear to reach SGs following a transient stopover in PBs in glucose-limited cells.¹⁵

Outlook

While our studies have pinpointed a role for Igo proteins in stabilization of nutrient-regulated mRNAs, which appears to be critical for both initiation of the G₀ program and proper setup of CLS,¹⁵ they also rise a number of interesting issues to be tackled in the future. For instance, rapamycin-induced expression of the *HSP26-LacZ* and *HSP26-γEmRFP* reporter genes, like expression of *HSP26*, was strongly dependent on Igo1/2, indicating that either the promoter region or the 5' UTR of *HSP26* critically defines the fate of the corresponding mRNA by a process that implicates Igo1/2. One attractive model, to be tested in this context, is that Rim15 may be recruited to specific promoter regions to coordinate both temporal and spatial activation of Igo1/2 and ensure timely co-transcriptional loading of activated Igo1/2 onto Lsm12-, Pbp1- and Pbp4-containing messenger ribonucleoprotein (mRNP) complexes. An alternative model that can be experimentally addressed is that activated Igo1/2 may be able to (directly or indirectly) bind to a specific structure or sequence motif within the 5' UTR of nutrient-regulated mRNAs such as the *HSP26* mRNA. Moreover, our present findings suggest that Igo1/2 inhibit 5'-3' mRNA decay of mRNAs by interfering with the mRNA decapping activation system. Future studies that specifically focus on structural/functional aspects of the interaction between Igo1/2 and Dhh1 (and possibly the Lsm-Pat1 complex) are therefore very likely to significantly enhance our general understanding of the mechanisms that control mRNA decay. Finally, the closest homolog of Igo1/2 in mammals, i.e., ARPP-19, has previously been suggested to control axon growth and synaptic plasticity specifically by

stabilizing the growth-associated protein-43 (GAP-43) mRNA in response to nerve growth factor treatment.²⁵ Thus, an exciting challenge will be to test whether the homologs of Igo proteins in higher eukaryotes may have an evolutionarily conserved role in mRNA stability control, which—as observed in yeast—may be critical for cell differentiation and life span.

Acknowledgements

We thank Neta Dean for plasmids, Johannes Buchner and Mick Tuite for antibodies, Charles Boone for yeast strains and Marie-Pierre Péli-Gulli for critically reading the manuscript. This research was supported by the Canton of Fribourg and a grant from the Swiss National Science Foundation (laboratory of C.D.V.).

References

- De Virgilio C, Loewith R. The TOR signalling network from yeast to man. *Int J Biochem Cell Biol* 2006; 38:1476-81.
- De Virgilio C, Loewith R. Cell growth control: little eukaryotes make big contributions. *Oncogene* 2006; 25:6392-415.
- Powers RW, 3rd, Kaeberlein M, Caldwell SD, Kennedy BK, Fields S. Extension of chronological life span in yeast by decreased TOR pathway signaling. *Genes Dev* 2006; 20:174-84.
- Kaeberlein M, Burnner CR, Kennedy BK. Recent developments in yeast aging. *PLoS Genet* 2007; 3:84.
- Reinders A, Bürckert N, Boller T, Wiemken A, De Virgilio C. *Saccharomyces cerevisiae* cAMP-dependent protein kinase controls entry into stationary phase through the Rim15p protein kinase. *Genes Dev* 1998; 12:2943-55.
- Fabrizio P, Pozza F, Pletcher SD, Gendron CM, Longo VD. Regulation of longevity and stress resistance by Sch9 in yeast. *Science* 2001; 292:288-90.
- Wei M, Fabrizio P, Hu J, Ge H, Cheng C, Li L, et al. Life span extension by calorie restriction depends on Rim15 and transcription factors downstream of Ras/PKA, Tor and Sch9. *PLoS Genet* 2008; 4:13.
- Wanke V, Pedruzzi I, Cameroni E, Dubouloz F, De Virgilio C. Regulation of G₀ entry by the Pho80-Pho85 cyclin-CDK complex. *EMBO J* 2005; 24:4271-8.
- Pedruzzi I, Dubouloz F, Cameroni E, Wanke V, Roosen J, Windericks J, et al. TOR and PKA signaling pathways converge on the protein kinase Rim15 to control entry into G₀. *Mol Cell* 2003; 12:1607-13.
- Wanke V, Cameroni E, Uotila A, Piccolis M, Urban J, Loewith R, et al. Caffeine extends yeast lifespan by targeting TORC1. *Mol Microbiol* 2008; 69:277-85.
- Jørgensen P, Rupes I, Sharom JR, Schaefer L, Broach JR, Tyers M. A dynamic transcriptional network communicates growth potential to ribosome synthesis and critical cell size. *Genes Dev* 2004; 18:2491-505.
- Urban J, Souillard A, Huber A, Lippman S, Mukhopadhyay D, Deloche O, et al. Sch9 is a major target of TORC1 in *Saccharomyces cerevisiae*. *Mol Cell* 2007; 26:663-74.
- Pedruzzi I, Bürckert N, Egger P, De Virgilio C. *Saccharomyces cerevisiae* Ras/cAMP pathway controls post-diauxic shift element-dependent transcription through the zinc finger protein Gis1. *EMBO J* 2000; 19:2569-79.
- Cameroni E, Hulo N, Roosen J, Windericks J, De Virgilio C. The novel yeast PAS kinase Rim15 orchestrates G₀-associated antioxidant defense mechanisms. *Cell Cycle* 2004; 3:462-8.
- Talarek N, Cameroni E, Jaquenoud M, Luo X, Bontron S, Lippman S, et al. Initiation of the TORC1-regulated G₀ program requires Igo1/2, which license specific mRNAs to evade degradation via the 5'-3' mRNA decay pathway. *Mol Cell* 2010; 38:345-55.
- Swisher KD, Parker R. Localization to and effects of Pbp1, Pbp4, Lsm12, Dhh1 and Pab1 on stress granules in *Saccharomyces cerevisiae*. *PLoS One* 2010; 5:10006.
- Mangus DA, Smith MM, McSweeney JM, Jacobson A. Identification of factors regulating poly(A) tail synthesis and maturation. *Mol Cell Biol* 2004; 24:4196-206.
- Keppeler-Ross S, Noffz C, Dean N. A new purple fluorescent color marker for genetic studies in *Saccharomyces cerevisiae* and *Candida albicans*. *Genetics* 2008; 179:705-10.
- Tong AH, Evangelista M, Parsons AB, Xu H, Bader GD, Page N, et al. Systematic genetic analysis with ordered arrays of yeast deletion mutants. *Science* 2001; 294:2364-8.
- Parker R, Sheth U. P bodies and the control of mRNA translation and degradation. *Mol Cell* 2007; 25:635-46.
- Franks TM, Lykke-Andersen J. The control of mRNA decapping and P-body formation. *Mol Cell* 2008; 32:605-15.
- Ozgur S, Chekulavaeva M, Stoecklin G. Human Pat1b Connects Deadenylation with mRNA Decapping and Controls the Assembly of Processing-Bodies. *Mol Cell Biol* 2010; 30:4308-23.
- Braun JE, Tritschler F, Haas G, Igraja C, Truffault V, Weichenrieder O, et al. The C-terminal α - α superhelix of Pat1 is required for mRNA decapping in metazoa. *EMBO J* 2010; 29:2368-80.
- Fischer N, Wicz K. The DEAD box protein Dhh1 stimulates the decapping enzyme Dcp1. *EMBO J* 2002; 21:2788-97.
- Irwin N, Chao S, Goritchenko L, Horiuchi A, Greengard P, Nairn AC, et al. Nerve growth factor controls GAP-43 mRNA stability via the phosphoprotein ARPP-19. *Proc Natl Acad Sci USA* 2002; 99:12427-31.
- Griffioen G, Anghileri P, Imre E, Baroni MD, Ruis H. Nutritional control of nucleocytoplasmic localization of cAMP-dependent protein kinase catalytic and regulatory subunits in *Saccharomyces cerevisiae*. *J Biol Chem* 2000; 275:1449-56.

Initiation of the TORC1-Regulated G₀ Program Requires Igo1/2, which License Specific mRNAs to Evade Degradation via the 5'-3' mRNA Decay Pathway

Nicolas Talarek,^{1,4} Elisabetta Cameroni,^{1,4,5} Malika Jaquenoud,¹ Xuan Luo,¹ Séverine Bontron,¹ Soyeon Lippman,² Geeta Devgan,³ Michael Snyder,³ James R. Broach,² and Claudio De Virgilio^{1,*}

¹Department of Medicine, Division of Biochemistry, University of Fribourg, CH-1700 Fribourg, Switzerland

²Department of Molecular Biology, Princeton University, Princeton, NJ 08544, USA

³Department of Molecular, Cellular, and Developmental Biology, Yale University, New Haven, CT 06520, USA

⁴These authors contributed equally to this work

⁵Present address: Institute of Cell Biology, University of Bern, CH-3012, Bern, Switzerland

*Correspondence: claudio.devirgilio@unifr.ch

DOI 10.1016/j.molcel.2010.02.039

SUMMARY

Eukaryotic cell proliferation is controlled by growth factors and essential nutrients, in the absence of which cells may enter into a quiescent (G₀) state. In yeast, nitrogen and/or carbon limitation causes downregulation of the conserved TORC1 and PKA signaling pathways and, consequently, activation of the PAS kinase Rim15, which orchestrates G₀ program initiation and ensures proper life span by controlling distal readouts, including the expression of specific genes. Here, we report that Rim15 coordinates transcription with posttranscriptional mRNA protection by phosphorylating the paralogous Igo1 and Igo2 proteins. This event, which stimulates Igo proteins to associate with the mRNA decapping activator Dhh1, shelters newly expressed mRNAs from degradation via the 5'-3' mRNA decay pathway, thereby enabling their proper translation during initiation of the G₀ program. These results delineate a likely conserved mechanism by which nutrient limitation leads to stabilization of specific mRNAs that are critical for cell differentiation and life span.

INTRODUCTION

Regulation of cell proliferation and growth in response to extracellular cues like growth factors, hormones, and/or nutrients critically affects development and life span in virtually every biological system examined (Gray et al., 2004; Kolter et al., 1993; Malumbres and Barbacid, 2001). In the absence of stimulatory signals, cells may enter into a reversible quiescence (or G₀) state that is typically characterized by low metabolic activity, including low rates of protein synthesis and transcription. Whereas in metazoans quiescence is induced following limitation of growth factors and hormones, in simpler unicellular organisms, quiescence is primarily triggered by nutrient limitation to ensure maximal long-term survival (also referred to as chronological

life span [CLS]). Despite the universal importance of the quiescent state, the mechanisms regulating entry into, survival in, and exit from quiescence remain poorly understood.

Initiation of the quiescence program in yeast includes a general downregulation of protein synthesis, specifically at the level of ribosome biogenesis, mRNA stability, and translation initiation factor activities (De Virgilio and Loewith, 2006). In parallel, activation of autophagy serves to recycle surplus cytoplasmic mass and to turn over ribosomes and mitochondria, thereby contributing to both reduction of cellular energy consumption and cell growth arrest upon G₀ entry (Abeliovich and Klionsky, 2001). Distinct additional hallmarks of quiescent yeast cells include high levels of both the storage carbohydrate glycogen and the stress protectant trehalose and increased expression of specific genes whose products are likely involved in different aspects of stress tolerance and CLS (Gray et al., 2004).

Initiation of the yeast quiescence program requires downregulation of conserved nutrient-responsive signal transduction pathways. Specifically, inhibiting the kinase activities of the target of rapamycin complex 1 (TORC1) or the protein kinase A (PKA) drives cells into a quiescent-like state and significantly extend CLS (Kaeberlein et al., 2007; Powers et al., 2006). In contrast, reducing the kinase activity of Rim15 precludes access to quiescence and decreases CLS (Fabrizio et al., 2001; Reinders et al., 1998; Wei et al., 2008). Whereas TORC1 (via its substrate Sch9) and PKA signal in parallel pathways to positively regulate ribosome biogenesis and growth (Jorgensen et al., 2004; Urban et al., 2007), they negatively regulate quiescence and CLS by maintaining Rim15 in an inactive state in the cytoplasm (Pedruzzi et al., 2003; Wanke et al., 2005, 2008). The molecular elements linking Rim15 to distal readouts, including the expression of specific nutrient-regulated genes, trehalose and glycogen accumulation, extension of CLS, and induction of autophagy, are only partially characterized but involve the stress response and postdiauxic shift transcription factors Msn2/4 and Gis1, respectively (Cameroni et al., 2004; Pedruzzi et al., 2000; Wei et al., 2008; Yorimitsu et al., 2007). Rim15 appears to be conserved among eukaryotes, as it shares homology with the mammalian serine/threonine kinase large tumor suppressor (LATS) (Cameroni et al., 2004; Pedruzzi et al., 2003); PKA, TORC1, and Sch9 have clear orthologs in

mammals: mammalian PKA, mTORC1, and S6K, respectively (Powers, 2007).

A recently discovered facet of the yeast quiescence program is that translating mRNAs on polysomes broadly dissociate from certain translation factors, associate with translational repressors, and accumulate as repressed messenger ribonucleoprotein (mRNP) complexes within cytoplasmic granules, also termed processing bodies (P bodies or PBs) (Brenques et al., 2005; Sheth and Parker, 2003). The possible fate of these mRNAs includes their degradation, repression and/or storage, or dispatch to translation via a transitory stopover in eIF4E-, eIF4G-, and Pab1-containing bodies (EGPBs), which likely correspond to yeast stress granules (SGs) (Buchan et al., 2008; Hoyle et al., 2007; Parker and Sheth, 2007). PBs from yeast to mammals contain a conserved core of proteins consisting of the mRNA decapping machinery, including the decapping enzyme Dcp1/Dcp2, the activators of decapping Dhh1/RCK/DDX6/p54, Pat1, Scd6/RAP55, Edc3, and the heptameric Lsm1–7 complex, and the 5′-3′ exonuclease Xrn1 (Eulalio et al., 2007; Parker and Sheth, 2007). PBs also contain the conserved Ccr4/Pop2/Not1–5 complex that initiates deadenylation of the 3′ poly(A) tail of mRNAs, which, besides allowing 3′-to-5′ degradation of mRNAs by the exosome complex, primarily induces Dcp1/Dcp2-mediated removal of the 5′ end cap structure followed by 5′-to-3′ transcript degradation (Anderson and Kedersha, 2006; Parker and Sheth, 2007). This core of conserved PB components, also coined repression or 5′-3′ mRNA decay machinery, functions in both translation repression and mRNA degradation and competes with the assembly of translational factors (Eulalio et al., 2007; Parker and Sheth, 2007). How nutrient limitation impinges on and regulates this competition remains largely elusive. Moreover, it remains unexplained how specific transcripts can, despite the gradient toward mRNP storage/decay, evade degradation to be translated into proteins during initiation of the G₀ program.

Here, we describe the discovery of the paralogous Igo1 and Igo2 proteins and demonstrate that they play an essential role in ensuring proper initiation of the G-zero (G₀) program, hence their name Igo. We show that inhibition of TORC1 induces Igo1 to associate with the decapping activator Dhh1 and additional proteins that are typically assembled on the 3′ untranslated region (UTR) of mRNAs. Of note, the interaction between Dhh1 and Igo1 requires phosphorylation of Igo1 by Rim15 and is key to preventing degradation of newly expressed mRNAs by the 5′-3′ mRNA decay pathway. In all, our data indicate that protection of specific mRNAs represents a conserved aspect of the cellular response to nutrient deprivation, which critically affects cell differentiation and life span.

RESULTS

Igo1 and Igo2 Are Direct Targets of the TORC1 Downstream Effector Kinase Rim15

To elucidate how Rim15 regulates initiation of the quiescence program, we identified Rim15 target proteins using the proteome chip array technology (Ptacek et al., 2005). The best hit on these arrays was Igo1, which shares 58% identity over its entire length with the putative paralog Igo2. Both proteins have no assigned

function at present but share significant homology with small (16–20 kDa) proteins of the α -endosulfine family in higher eukaryotes (e.g., ENSA and ARPP-16/19) (Dulubova et al., 2001) (Figure 1A), which have been implicated in diverse biological processes, including insulin secretion (Bataille et al., 1999), oocyte meiotic maturation (Von Stetina et al., 2008), neurodegeneration (Woods et al., 2007), and axon growth (Irwin et al., 2002). The molecular function of these proteins, however, remains poorly understood.

In line with and extending our proteome chip data, we found that Rim15 physically and specifically interacted with Igo1 in classical pull-down experiments (Figure 1B) and that Rim15, but not kinase-inactive Rim15^{K823Y} (Rim15^{KD}), phosphorylated bacterially expressed Igo1 and Igo2, as well as human ENSA and ARPP-19, in vitro (Figure 1C). Using a combination of mass spectrometry (MS) and tandem MS analyses on GST-Igo1 samples that had been subjected to in vitro protein kinase assays with Rim15 or Rim15^{KD}, we then identified an evolutionary conserved serine residue (i.e., Ser⁶⁴) in Igo1, which is phosphorylated by Rim15. A mutant version of Igo1 that had Ser⁶⁴ replaced by Ala was no longer phosphorylated by Rim15 (Figure 1C), indicating that Ser⁶⁴ is the only amino acid in Igo1 that is directly phosphorylated by Rim15. To determine whether Ser⁶⁴ is also a target of Rim15 in vivo, we raised antibodies that were highly specific for a pSer⁶⁴-containing peptide, as indicated by their ability to recognize bacterially expressed GST-Igo1 that was phosphorylated in vitro by Rim15, but not GST-Igo1 treated with Rim15^{KD} (Figure 1D). Using these phosphospecific anti-pSer⁶⁴ antibodies, we found that phosphorylation of Ser⁶⁴ in Igo1 within cells largely depended on the presence of Rim15 and was strongly induced following rapamycin-mediated TORC1 inactivation or a shift of cells to low-glucose-containing medium (Figures 1E and 1F), both conditions that expectedly cause Rim15 activation (Pedruzzi et al., 2003; Reinders et al., 1998). Together, these results show that Igo1 is a bona fide Rim15 target and suggest that the corresponding phosphorylation event is evolutionarily conserved.

Igo1 and Igo2 Are Critical for Initiation of the G₀ Program

Rim15 orchestrates various physiological processes associated with the quiescence program, including the accumulation of the storage carbohydrate glycogen, synthesis of trehalose, proper setup of CLS, and the expression of specific nutrient-regulated genes. We therefore evaluated these readouts in cells lacking Igo1 and/or Igo2. Quiescent *rim15Δ* and *igo1Δ igo2Δ* double mutants, but not *igo1Δ* and *igo2Δ* single mutants, had very low glycogen and trehalose levels (both < 10% of wild-type levels; data not shown) and were equally dramatically reduced for CLS (Figure 2A). To investigate whether Igo1/2, like Rim15, are also implicated in gene expression control, we compared the rapamycin response of wild-type with that of *rim15Δ* and *igo1Δ igo2Δ* mutant cells using global transcription analysis. After 180 min of rapamycin treatment, the expression of 478 genes was increased more than 2.8-fold in wild-type cells. Among these, the upregulation of 54 and 103 genes was diminished more than 2-fold in *rim15Δ* and *igo1Δ igo2Δ* cells, respectively. Surprisingly, almost all of the Rim15-dependent genes (which are mainly implicated in stress responses, carbohydrate

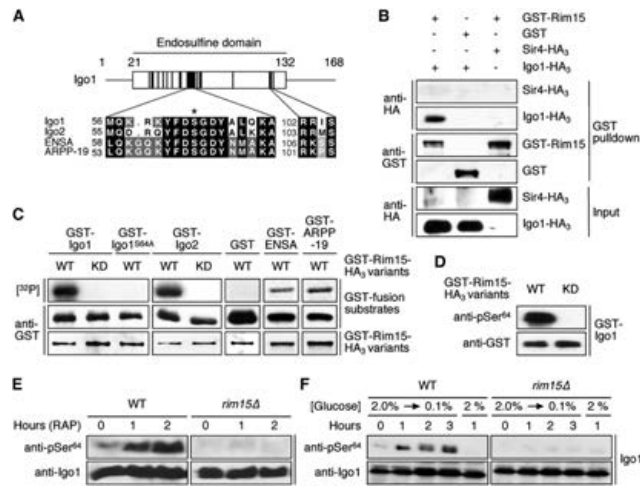


Figure 1. The Protein Kinase Rim15 Directly Phosphorylates Igo1 Both In Vitro and In Vivo
(A) *S. cerevisiae* Igo1 and Igo2 belong to the conserved family of α -endosulfine proteins. The diagram shows the position of the endosulfine domain within Igo1 with highly conserved subdomains indicated by black boxes. Amino acid sequence alignments of yeast Igo1 and Igo2 and of human ENSA (Swiss-Prot: O43768) and ARPP-19 (Swiss-Prot: P56211) are shown for two of these subdomains. The position of the serine targeted by Rim15 (i.e., Ser⁶⁴ and Ser⁶³ in Igo1 and Igo2, respectively) is indicated with an asterisk. A conserved PKA consensus phosphorylation site (RR/KXS) is present in the second subdomain.
(B) Rim15 and Igo1 physically interact. GST-Rim15 or GST were pulled down from lysates of wild-type cells coexpressing Igo1-HA₃ or, as negative control, Sir4-HA₃. Cell lysates (Input) and GST pull-down samples were subjected to SDS-PAGE, and immunoblots were probed using anti-HA or anti-GST antibodies.
(C) Rim15 phosphorylates in vitro GST-Igo1, GST-Igo2, GST-ENSA, and GST-ARPP-19, but not GST-Igo1^{S64A} or GST alone. In control experiments, kinase-inactive Rim15^{KD} neither phosphorylated Igo1 nor Igo2. Levels of indicated GST fusion substrates (purified from *E. coli*) and of GST fusion protein kinase variants (GST-Rim15-HA₃ [WT] or GST-Rim15^{KD}-HA₃ [KD]; purified from yeast) were determined by immunoblot analyses using anti-GST antibodies. [³²P] denotes the autoradiograph.
(D) Rim15 specifically phosphorylates Ser⁶⁴ in Igo1 in vitro. Phosphospecific antibodies directed toward pSer⁶⁴ in Igo1 recognized bacterially expressed GST-Igo1 following in vitro phosphorylation by active GST-Rim15-HA₃ (WT), but not kinase-inactive Rim15^{KD} (KD).
(E and F) In vivo phosphorylation of Ser⁶⁴ in Igo1 requires the presence of Rim15 and is induced by rapamycin (0.2 μ g ml⁻¹) treatment (E) and glucose limitation (F). Levels of Igo1 protein and of Ser⁶⁴ phosphorylation in Igo1 were determined by immunoblot analyses using polyclonal anti-Igo1 and anti-pSer⁶⁴ antibodies, respectively.

metabolism, and respiration) were comprised within the larger set of Igo1/2-dependent genes (Figure 2B). Thus, whereas Igo1/2 are important for expression of a small set of Rim15-independent genes, induction of the entire Rim15-dependent gene expression program requires Igo1/2. Corresponding global transcription analyses of glucose-limited cells (during and following the diauxic shift) essentially confirmed this conclusion (Figure 2B and data not shown). Taken together, the simultaneous loss of Igo1 and Igo2 appears to largely phenocopy the loss of Rim15.

We next assessed quantitatively the role of Igo1/2 in gene expression by studying the induction of *HSP26*, which is most strongly dependent on Rim15 and Igo1/2 for its expression following rapamycin treatment (Figures 2B and 2C), using an *HSP26-lacZ* reporter gene that expresses the bacterial β -galactosidase-encoding *lacZ* gene under the control of the yeast *HSP26* promoter. As expected, rapamycin-induced *HSP26*-

lacZ expression was largely defective in both *rim15 Δ* and *igo1 Δ igo2 Δ* cells. This defect could be cured in *igo1 Δ igo2 Δ* cells by expression of either plasmid-encoded wild-type Igo1 or Igo2, but not by expression of mutant Igo1^{S64A} (Figure 2D), indicating that phosphorylation by Rim15 triggers Igo1 and Igo2 in a redundant manner to ensure proper expression of a specific set of nutrient-regulated genes. Because both human ENSA and ARPP-19 were able to partially replace Igo1/2 function in yeast (Figure 2D), proteins of this family are likely to share an evolutionary conserved role in gene expression.

TORC1 Regulates the Association of Igo1 with Lsm12 and Dhh1 via Rim15

To further elucidate the molecular function of Igo1/2, we purified in parallel experiments Igo1-TAP and Igo1-myc₁₃ from rapamycin-treated yeast cells and identified coprecipitating proteins via tandem MS. Proteins that specifically bound both Igo1-TAP

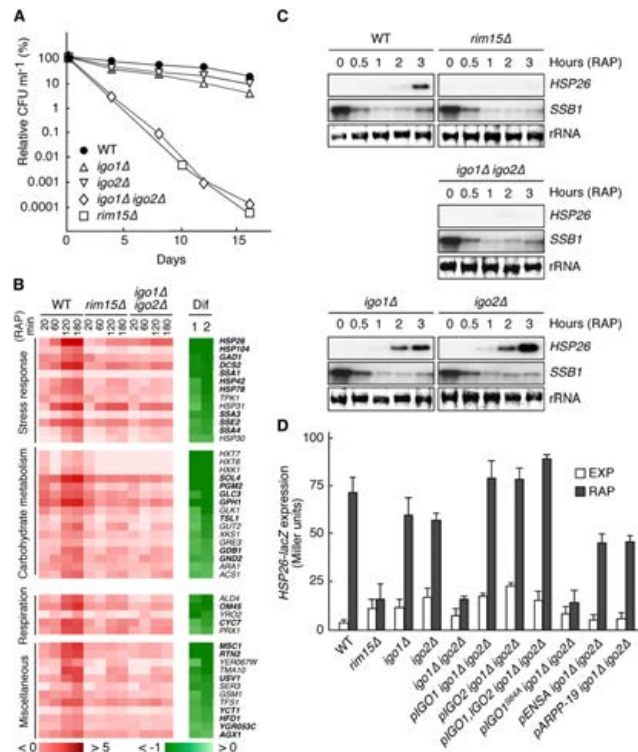


Figure 2. Igo1 and Igo2, Like Rim15, Are Required for TORC1 to Properly Control Gene Expression and Chronological Life Span
 (A) Igo1 and Igo2 are redundant, key determinants of CLS. Survival data (CFU ml⁻¹) are expressed as relative values compared to the values at day 0 (which corresponds to day 4 in early stationary phase cultures). Each data point represents the mean of three samples.
 (B) Rim15 and Igo1/2 play a largely overlapping role in mediating the rapamycin-induced expression of a defined set of genes. Wild-type (WT), *rim15Δ*, and *igo1Δ igo2Δ* cells were treated with rapamycin (0.2 μg ml⁻¹) for the times indicated and were compared by microarray analyses. Genes showing (in wild-type cells) at least a 2.8-fold increase (log₂ ratio > 1.5) in expression following rapamycin treatment (180 min) were classified as rapamycin-induced genes and sorted according to the maximal Igo1/2 dependence of their response (Dif 1 = log₂ [*igo1Δ igo2Δ*]₁₈₀/*igo1Δ igo2Δ*]₀) - log₂ [WT]₁₈₀/WT]₀]; Dif 2 = log₂ [*rim15Δ*]₁₈₀/*rim15Δ*]₀) - log₂ [WT]₁₈₀/WT]₀). Color codes show the log₂ of the expression change relative to untreated cells (red-white) and the corresponding Dif value (green-white). Rim15- and Igo1/2-dependent genes that were (using the same criteria as above) also retrieved in global transcription analyses in glucose-limited (diauxic and post-diauxic) cells are indicated in bold. Northern blot analyses of selected genes confirmed our microarray data (not shown).
 (C) Rapamycin-induced expression of *HSP26* mRNA depends on Rim15 and Igo1/2. Northern blot analyses of *HSP26* and *SSB1* mRNAs were done with exponentially growing WT, *rim15Δ*, *igo1Δ*, *igo2Δ*, and *igo1Δ igo2Δ* cells prior to and following treatment with rapamycin (0.2 μg ml⁻¹) for the times indicated. All samples were run on the same gel (identical film exposure time). The decrease in *SSB1* transcript levels was used as internal control for rapamycin function.
 (D) Both *rim15Δ* and *igo1Δ igo2Δ* mutants are defective in *HSP26-lacZ* expression. β-galactosidase activities (expressed in Miller units) were measured to monitor the expression of an *HSP26-lacZ* fusion gene in exponentially growing cells prior to (EXP) or following rapamycin treatment (RAP; 0.2 μg ml⁻¹; 6 hr). Data are reported as averages (n = 3), with standard deviations (SDs) indicated by the lines above each bar. Relevant genotypes are indicated.

and Igo1-myc₁₃ included members of the Hsp70 family of proteins (i.e., Ssa1/2 and Ssb1/2) as well as Pbp1, Pbp4, and Lsm12 (Table S3 available online). Of interest, the latter three proteins have previously been identified as partners within a ribo-

some-associated protein complex (Fleischer et al., 2006). Pbp1 has originally been characterized as a poly(A)-binding protein Pab1 interactor that is involved in mRNA poly(A) tail length regulation (Mangus et al., 1998). Like its human homolog ataxin 2

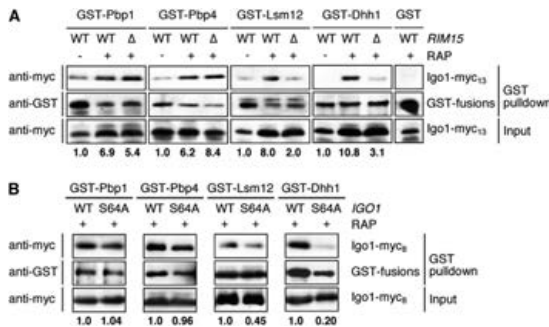


Figure 3. TORC1 Regulates the Association of Igo1 with Pbp1, Pbp4, Lsm12, and Dhh1

(A) Rapamycin-induced Igo1-Lsm12/Dhh1 interactions, but not rapamycin-induced Igo1-Pbp1/Pbp4 interactions, require Rim15. GST-Pbp1, GST-Pbp4, GST-Lsm12, GST-Dhh1, and GST were pulled down from cell lysates of wild-type (WT) or *rim15Δ* (Δ) strains coexpressing Igo1-myc₆. Exponentially growing cells were harvested prior to (–) or following (+) rapamycin treatment (RAP; 0.2 $\mu\text{g ml}^{-1}$; 2 hr). Cell lysates (Input) and GST pull-down samples were subjected to SDS-PAGE, and immunoblots were probed using anti-myc or anti-GST antibodies. Bold numbers below the graph denote the relative level of Igo1-myc₆ coprecipitating per corresponding GST fusion protein (arbitrarily set to 1.0 for each sample derived from exponentially growing cells). For similar experiments with RNase A-treated lysates, see Figure S1.

(B) Mutation of Ser⁶⁴ to Ala in Igo1 strongly reduces the rapamycin-induced Igo1-Lsm12/Dhh1 interactions, but

not the rapamycin-induced Igo1-Pbp1/Pbp4 interactions. GST-Pbp1, GST-Pbp4, GST-Lsm12, and GST-Dhh1 were pulled down from lysates obtained from rapamycin-treated (RAP; 0.2 $\mu\text{g ml}^{-1}$; 2 hr) wild-type strains coexpressing either Igo1-myc₆ (WT) or Igo1^{S64A}-myc₆ (S64A). Cell lysates and GST pull-down samples were treated as in (A). Bold numbers below the graph denote the relative level of Igo1-myc₆ or Igo1^{S64A}-myc₆ coprecipitating per corresponding GST fusion protein (arbitrarily set to 1.0 for each sample derived from rapamycin-treated Igo1-myc₆-expressing cells).

(Raiser et al., 2005), Pbp1 is a member of the Like Sm (Lsm) proteins, which are predicted to function as mRNA-binding proteins that modulate biogenesis, translation, and/or degradation of mRNAs (He and Parker, 2000). Pbp4, which has no clear homolog in higher eukaryotes, was originally identified as a Pbp1-interacting protein, but its function remains presently unknown (Mangus et al., 2004). Finally, Lsm12 is an evolutionarily conserved protein of also unknown function, which, like Pbp1, contains an N-terminal Lsm domain (Albrecht and Lengauer, 2004).

We next tried to confirm the interactions between Igo1 and Pbp1, Pbp4, or Lsm12 in pull-down experiments. Because yeast interactome studies indicated that Pbp1 and Lsm12 may share an additional partner, namely the DEAD/H box RNA helicase Dhh1 (Tarassov et al., 2008), and because the association between Pbp1/ataxin 2 and Dhh1/DDX6 appears to be evolutionary conserved (Nonhoff et al., 2007), we also included Dhh1 in these experiments. In extracts from exponentially growing wild-type cells, Igo1-myc interacted weakly with GST-Pbp1, GST-Pbp4, GST-Lsm12, and GST-Dhh1, but not with GST alone (Figure 3A). Rapamycin treatment strongly increased (6.2- to 10.2-fold) the affinity of Igo1-myc for GST-Pbp1, GST-Pbp4, GST-Lsm12, and GST-Dhh1. Of note, whereas none of these interactions appeared to be sensitive to RNase treatment (Figure S1), the rapamycin-induced Igo1-myc - GST-Lsm12/Dhh1 interactions, but not the corresponding Igo1-myc - GST-Pbp1/Pbp4 interactions, were strongly reduced in the absence of Rim15 or if Igo1-myc harbored the S64A mutation (Figures 3A and 3B). Thus, TORC1 inactivation likely results in the recruitment of Igo1 to Pbp1/Pbp4-containing mRNA-protein complexes, where it may, following phosphorylation by Rim15, associate with Lsm12 and Dhh1.

TORC1 Regulates mRNA Stability via Igo1 and Igo2

Because both Pbp1, by controlling mRNA polyadenylation (Mangus et al., 1998), and Dhh1, by promoting mRNA decapping

(Parker and Sheth, 2007), are implicated in regulation of mRNA stability, we hypothesized that Igo1/2 may play a role in stabilizing the substantial subset of rapamycin-induced, Igo1/2-dependent mRNA species (Figure 2B). In line with this assumption, loss of Igo1/2 reduced, on average by 35%, the half-lives of newly transcribed poly(A)⁺ RNAs in rapamycin-treated, but not in exponentially growing, cells (Figure 4). Considering the fact that the bulk of poly(A)⁺ RNAs isolated from rapamycin-treated cells contained both Igo1/2-dependent and Igo1/2-independent mRNA species, this calculated average mRNA half-life reduction likely underestimates the actual effect of Igo proteins on specific mRNAs. In support of this notion, loss of Igo1/2 reduced the half-life of a specific *HSP26-lacZ* mRNA by 65% in rapamycin-treated cells (Figure S2).

Igo1 and Igo2 Shelter HSP26 mRNAs from Degradation via the 5'-3' mRNA Decay Pathway

To explore the possibility that Igo1/2 may prevent degradation of mRNAs via the 5'-3' mRNA decay pathway, we determined whether loss of Dhh1 or Ccr4, which prevents mRNA turnover at early steps of PB formation and traps mRNAs in polysomes (Parker and Sheth, 2007), may suppress the defect of *igo1Δ* *igo2Δ* and *rim15Δ* cells in *HSP26* expression. Following rapamycin treatment, Dhh1- or Ccr4-deficient cells expressed *HSP26* (both at the mRNA and protein levels) to higher levels than wild-type cells, indicating the existence of a futile cycle in which mRNA turnover operates to some extent on newly synthesized mRNAs (Figures 5A and 5B). Remarkably, loss of either Dhh1 or Ccr4 suppressed the defect of *igo1Δ* *igo2Δ* cells, but not that of *rim15Δ* cells, in rapamycin-induced *HSP26* expression (again both at the mRNA and protein levels) (Figures 5A and 5B). From these results, we infer that Rim15 likely has a dual role in controlling gene expression by (1) activating transcription (via a still partially understood mechanism) and (2) protecting the corresponding transcripts from degradation via an Igo1/2-dependent mechanism. In line with such a model, loss of the

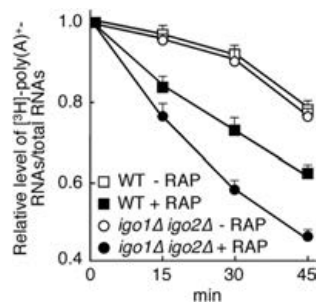


Figure 4. Igo1 and Igo2 Stabilize mRNAs following Inactivation of TORC1

The half-life of total poly(A)⁺ RNAs was determined in exponentially growing (open symbols) and rapamycin-treated (solid symbols) wild-type (□, ■) and *igo1Δ igo2Δ* (○, ●) cells using a classical [³H]-uracil pulse-chase labeling protocol. Exponentially growing cells were either treated or not with 0.2 μg ml⁻¹ rapamycin for 90 min, subjected to a 30 min [³H]-uracil pulse (in the continuous presence or absence of rapamycin), and chased with an excess of cold uracil at time 0. The radioactivity in poly(A)⁺ RNAs, isolated in each case from 100 μg of [³H]-uracil pulse-labeled total RNAs, was determined by liquid scintillation counting, normalized by the counts in the corresponding total RNA sample, and expressed as relative level of total [³H]-poly(A)⁺ RNAs/total RNAs (arbitrarily set to 1.0 for each sample at the beginning of the chase period). Data are reported as averages (n = 3), with SDs indicated by the lines above each data point. A nonlinear least squares model was fit to determine the half-life of total poly(A)⁺ RNAs. The calculated average half-life of total poly(A)⁺ RNAs was 103 min (±8 SD) and 98 min (±7 SD) in exponentially growing wild-type and *igo1Δ igo2Δ* cells, respectively, and 60 min (±1 SD) and 39 min (±1 SD) in rapamycin-treated wild-type and *igo1Δ igo2Δ* cells, respectively. Igo1/2 also stabilize a specific *HSP26-lacZ* mRNA following TORC1 inactivation (Figure S2).

5'-3' exonuclease Xrn1, which, in contrast to loss of Dhh1 or Ccr4, causes PBs to increase in number and size due to the entrapping of nondegraded mRNAs (Parker and Sheth, 2007), allowed *igo1Δ igo2Δ* cells, but not *rim15Δ* cells, to accumulate *HSP26* mRNAs, which then failed to be translated into proteins (Figures 5A and 5B). We confirmed these results independently by using the chimeric *HSP26-LacZ* gene, the expression pattern of which (measured by northern blot and β-galactosidase activity assays) was comparable to that of the endogenous *HSP26* gene in various strains (Figures S3B and 5C). Taken together, our data indicate that Igo1/2 are required to prevent degradation of *HSP26* mRNAs via the 5'-3' mRNA decay pathway, but—as also supported by standard polysome analyses (Figure S4)—are dispensable for translation per se.

Igo1 May Escort *HSP26* mRNAs during Their Transit through PBs to Reach EGPBs/SGs

To study whether Igo proteins may colocalize with *HSP26* mRNAs, we used a strategy that enables specific mRNAs to be followed in live cells (Brodsky and Silver, 2000). Accordingly, we constructed a modified *HSP26* gene that encodes an mRNA harboring multiple U1A-binding sites in its 3'UTR. Binding

of plasmid-expressed U1A-GFP allows visualization of this specific mRNA by fluorescence microscopy (Figure 6A). In control northern blot experiments, *HSP26-U1A* expression mirrored the expression of the endogenous *HSP26* gene in all of the conditions and strains tested. Using this system, we found *HSP26* mRNAs to form distinct cytoplasmic GFP foci in rapamycin-treated wild-type cells or, more abundantly, in cells subjected to glucose limitation (following growth in batch cultures for 48 hr), which also induced *HSP26* expression in a strongly Rim15- and Igo1/2-dependent manner (Figures 6A, 6B, and 6C). Up to 60% of these cytoplasmic foci precisely colocalized with the PB marker Dcp2-RFP, indicating that a fraction of *HSP26* mRNAs, instead of being translated at ribosomes, is targeted to PBs following rapamycin treatment or glucose limitation. During glucose limitation, the relative number of *HSP26* mRNA-containing, Dcp2-RFP-positive foci steadily increased in wild-type cells, whereas corresponding foci were almost entirely absent in *rim15Δ* cells, which was expected given the low level of *HSP26* expression in these cells (Figure 6D). Intriguingly, *igo1Δ igo2Δ* cells contained a slightly elevated relative number of *HSP26* mRNA-containing, Dcp2-RFP-positive foci during an early phase of glucose limitation, which, in contrast to wild-type cells, decreased considerably during later phases of glucose limitation. Given the particular concentration of the 5'-3' mRNA decay machinery in PBs, these results can be most simply interpreted with a primary role of Igo1/2 in preventing degradation of mRNAs within PBs. In line with such a model, we also observed that loss of Xrn1 enabled glucose-limited *igo1Δ igo2Δ* cells, but not *rim15Δ* cells, to regain their ability to normally accumulate *HSP26* mRNAs and to form *HSP26* mRNA containing foci that colocalized with PBs (Figures 6B and 6D).

To test whether Igo1 is also present in PBs, we analyzed the subcellular localization of a functional Igo1-GFP fusion protein prior to and following glucose limitation. During exponential growth, Igo1-GFP had a diffuse appearance in both the cytoplasm and the nucleus (Figure 7A). Remarkably, Igo1-GFP, like GFP-Rim15 (Pedruzzi et al., 2003), started to accumulate in the nuclei of cells when ~50% of the initial amount of glucose in the culture had been consumed. While Igo1-GFP started to fade away from nuclei following glucose exhaustion, we observed a transient increase of Igo1-GFP foci that colocalized with the PB marker protein Dcp2-RFP and, in parallel, an increase of Igo1-GFP foci colocalizing with RFP-tagged Pab1 (Figures 7A and 7B), which, albeit also present in some PBs, represents a key constituent of EGPBs/SGs in yeast (Buchan et al., 2008; Hoyle et al., 2007). Because EGPBs/SGs assemble on pre-existing PBs in glucose-deprived yeast cells (Buchan et al., 2008), our data suggest that Igo1 may escort mRNAs to primarily prevent their degradation via the 5'-3' mRNA decay pathway to ultimately ensure their presence in EGPBs/SGs, from where they may return to translation. In support of this model, a significant fraction of *HSP26* mRNA-containing foci colocalized with Igo1-RFP as well as with Pab1-RFP-containing EGPBs/SGs in glucose-limited cells (Figures 7C and 7D). Moreover, loss of Igo1/2 strongly shifted, in a Dhh1-dependent manner, the relative distribution of *HSP26* mRNAs among cytoplasmic foci toward Dcp2-RFP-positive PBs (Figures S5A and S5B).

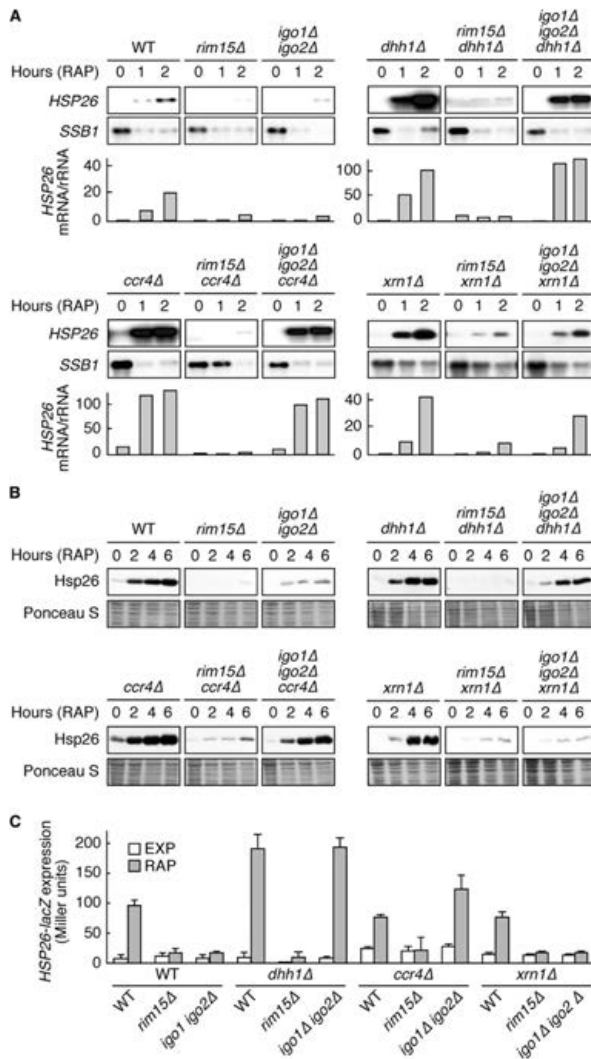


Figure 5. The 5'-3' mRNA Decay Pathway Targets HSP26 mRNAs in *igo1Δ igo2Δ* Mutants

(A) Loss of Dhh1, Ccr4, or Xrn1 suppresses the defect of *igo1Δ igo2Δ*, but not that of *rim15Δ* cells, in rapamycin-induced HSP26 mRNA expression. Northern blot analyses of HSP26 and of rapamycin-repressible *SSB1* were done with wild-type and indicated mutant strains prior to (0) and following a rapamycin treatment (RAP; $0.2 \mu\text{g ml}^{-1}$) of 1 hr or 2 hr. Bar graphs show the relative level of HSP26 mRNA per rRNA (quantified by PhosphorImager analysis and arbitrarily set to 1.0 for exponentially growing wild-type cells). All samples were run on the same gel (identical film exposure time). Similar results were obtained for other genes (e.g., *SOL4* and *DCS2*) (Figure S3A). (B and C) Loss of Dhh1 or Ccr4, but not loss of Xrn1, suppresses the defect of *igo1Δ igo2Δ* in rapamycin-induced Hsp26 protein expression. (B) Cell extracts from the same strains as in (A), treated (2 hr, 4 hr, and 6 hr) or not (0 hr) with rapamycin, were analyzed by SDS-PAGE, and immunoblots were probed with specific anti-Hsp26 antibodies. Ponceau S staining of the membranes prior to immunoblot analysis served as loading control. (C) HSP26-lacZ expression was monitored (as in Figure 2D) in exponentially growing cells prior to (EXP) and following a 6 hr rapamycin treatment (RAP). Data are reported as averages ($n = 3$), with SDs indicated by the lines above each bar. Strains were as in (A). Please see Figure S3B for northern blot analyses.

inhibit initiation of the G₀ program, CLS, and, as recently reported, autophagy (Pedruzzi et al., 2003; Reininders et al., 1998; Wanke et al., 2008; Yorimitsu et al., 2007). Here, we describe the discovery of two bona fide Rim15 targets, namely the paralogous Igo1 and Igo2 proteins. We also provide evidence that these proteins play an essential role in initiation of the G₀ program by preventing the degradation of specific nutrient-regulated mRNAs via the 5'-3' mRNA decay pathway. Thus, our data not only identify a key aspect of the cellular response to nutrient deprivation (i.e., posttranscriptional stabilization of specific mRNAs), but also provide a molecular mechanism, which supports the idea that untranslated mRNAs assemble into mRNPs, the fate of which (i.e., translation or decay) is critically regulated by the nature of associated proteins.

DISCUSSION

Previous work has documented that the conserved TORC1 and PKA nutrient signaling pathways converge on Rim15 to

How may Igo1/2 protect mRNAs from degradation? TORC1 inhibition broadly shifts translating mRNAs on polysomes toward a repressing mRNP state within PBs and accelerates the deadenylation-dependent decapping pathway (Albig and Decker,

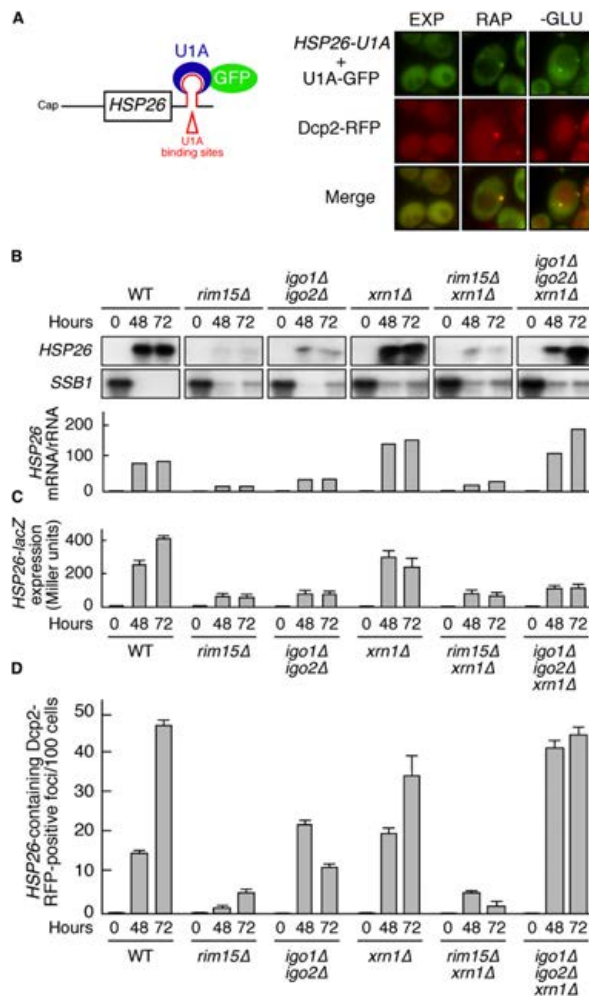


Figure 6. Stable Presence of HSP26 mRNAs within PBs Requires Igo1 and Igo2

(A) HSP26 mRNAs colocalize with the PB marker Dcp2-RFP. Binding of U1A-GFP to an HSP26 mRNA harboring multiple (16 in total) U1A-binding sites in its 3'UTR allows analysis of HSP26 mRNA localization. Wild-type cells coexpressing Dcp2-RFP, as well as HSP26-U1A mRNA and U1A-GFP, were harvested prior to (EXP) or following rapamycin treatment (RAP; 0.2 $\mu\text{g ml}^{-1}$; 2 hr) or glucose limitation (i.e., following growth for 24 hr in batch cultures; -GLU) and analyzed by fluorescence microscopy. GFP foci were absent in control cells expressing either the HSP26 reporter or the U1A-GFP fusion plasmid solely (Hoyle et al., 2007 and data not shown).

(B) Loss of Xrm1 suppresses the defect of *igo1Δ igo2Δ*, but not that of *rim15Δ* cells, in HSP26 mRNA expression following glucose limitation. Northern blot analyses of HSP26 and SSB1 in wild-type and indicated mutant strains harvested in exponential growth phase (0) and following glucose limitation (i.e., following growth for 48 hr or 72 hr in batch cultures). All samples were run on the same gel (identical film exposure time). Bar graphs show the relative levels of HSP26 mRNA per rRNA (arbitrarily set to 1.0 for exponentially growing wild-type cells).

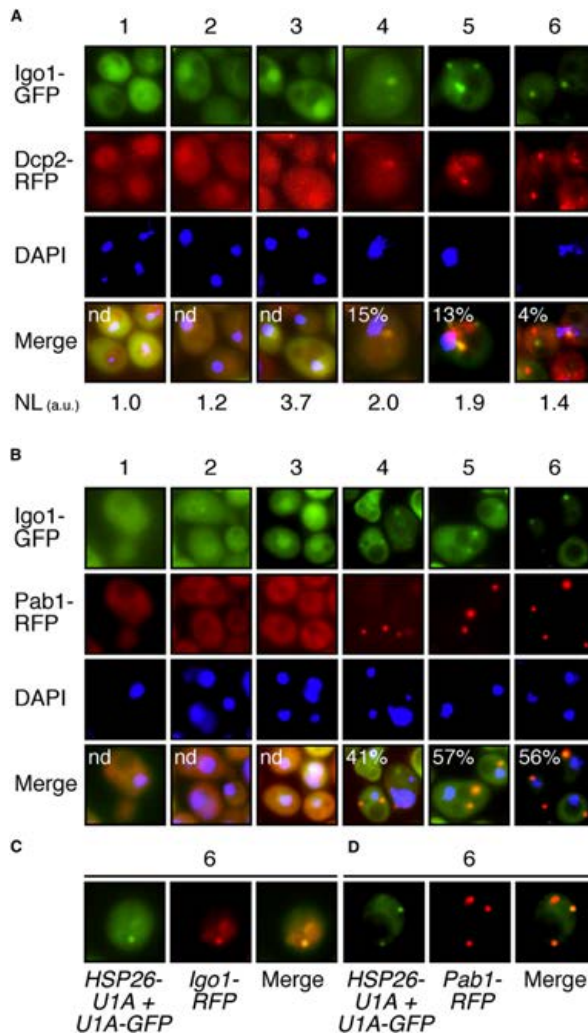
(C) Loss of Xrm1 does not suppress the defect of *igo1Δ igo2Δ* in HSP26-lacZ expression following glucose limitation. HSP26-lacZ expression was monitored (as in Figure 2D) in wild-type and indicated mutant strains that were grown as in (B). In control experiments, HSP26-lacZ mRNA accumulation patterns were found to be comparable to the ones of the endogenous HSP26 gene for all strains studied (data not shown). Data are reported as averages (n = 3), with SD indicated by the lines above each bar.

(D) Igo1/2 ensure survival of HSP26 mRNAs within PBs. The number of HSP26 mRNA-containing, Dcp2-RFP-positive cytoplasmic foci per 100 cells was determined (as in A) in wild-type and indicated mutant strains that were harvested in exponential growth phase (0) and following glucose limitation (i.e., following growth for 48 hr or 72 hr in batch cultures). Data are reported as averages (n = 3), with SDs indicated by the lines above the bars. Please note that Igo1/2 are dispensable for translation per se (Figure S4).

assembling specific repressors or activators of translation into different mRNP complexes, which may be structurally reorganized due to ATPase/helicase-

driven displacement of regulatory proteins from the core mRNAs (Minshall et al., 2009; Weston and Sommerville, 2006). An attractive model to be addressed in future studies therefore posits that activated Igo1, by interacting with Dhh1, interferes with the ability of Dhh1 to assemble translational repressors and/or with its role in remodeling translationally active mRNP complexes into a repression/decay state.

2001), which is normally stimulated by Dhh1 and the Lsm-Pat1 complex (Parker and Sheth, 2007). Of interest, studies of yeast Dhh1 and the orthologous DDX6-like RNA helicases in higher eukaryotes revealed a general role for these proteins in remodeling of mRNP complexes for entry into translation, storage, or decay pathways (Weston and Sommerville, 2006). As recently proposed, DDX6-like helicases may execute their function by



Diverse processes, such as degradation of mRNAs with aberrant translation termination codons by a quality control process termed nonsense-mediated decay (NMD), rapid turnover of mRNAs containing AU-rich destabilizing elements (AREs) in their 3'UTRs, or micro-RNA (miRNA)-mediated translation repression

Figure 7. Igo1 Colocalizes with PBs, EGPBs, and HSP26 mRNAs in Glucose-Limited Cells

(A and B) Igo1 dynamically colocalizes with PBs and EGPBs. Wild-type cells coexpressing Igo1-GFP and the PB marker Dcp2-RFP (A) or the EGPB/SG marker Pab1-RFP (B) were grown in batch cultures and visualized by fluorescence microscopy at the following stages of the growth curve: exponential growth phase (1); time point at which 50% of the initial glucose was consumed (2); time point of glucose exhaustion (3); and 2 hr (4), 5 hr (5), and 8 hr (6) following glucose exhaustion. Relative levels of nuclear Igo1-GFP were quantified (in A) by comparison of the fluorescence intensity per unit area in the nucleus versus cytoplasm, expressed in arbitrary units (au), and indicated at the bottom of the images (NL). DNA was stained with 4',6-diamidino-2-phenylindole (DAPI). The percentage of cytoplasmic Igo1-GFP foci colocalizing with Dcp2-RFP (A) or Pab1-RFP (B) was assessed and indicated (in %) in the corresponding merged pictures.

(C and D) HSP26 mRNAs colocalize with Igo1 and EGPBs. Wild-type cells expressing HSP26-U1A mRNA and U1A-GFP together with Igo1-RFP (C) or Pab1-RFP (D) were harvested 8 hr (6) following glucose exhaustion and analyzed by fluorescence microscopy. For the assessment of the relative distribution of HSP26 mRNAs between PBs and EGPBs/SG, see also Figure S5.

in mammalian cells, all implicate mRNA-specific regulators, which deliver mRNAs to the repression/decay machinery (Eulalio et al., 2007). Although it is, in principle, possible that Igo1/2 may exert their specificity through binding of particular sequence signatures within target mRNAs, the fact that the Igo1/2-controlled mRNAs do not contain a readily identifiable common sequence motif argues against such a mechanism. More likely, specificity of Igo1/2 is brought about, at least in part, by their temporal activation via Rim15 during initiation of the G₀ program. In this context, it is worth noting that RNA polymerase II transcription units can influence the posttranscriptional fate of mRNAs by affecting the composition of mRNP particles (Jensen et al., 2003). Future studies should therefore also address the intriguing possibility that Rim15 may be recruited to specific promoter regions, which could ensure timely

cotranscriptional activation of the Igo1-Dhh1-/Lsm12 associations within newly forming mRNP complexes. Such a scenario, in which Igo1/2 may serve as a "molecular memory" of a gene's transcriptional activity by assembling into corresponding mRNP complexes, could also provide a mechanistic basis for the

previously observed homodirectional changes in transcriptome composition and mRNA translation in rapamycin-treated cells (Preiss et al., 2003).

Igo1, as well as its interacting partners Dhh1, Lsm12, and Pbp1, have clear orthologs in mammals: mammalian ENSA/ARPP-16/19, RCK/p54, Q3MHD2, and ataxin 2, respectively (Albrecht and Lengauer, 2004; Dulubova et al., 2001; Ralsler et al., 2005; Weston and Sommerville, 2006). Of these, both RCK/p54 and ataxin 2 have been described to occur within SGs and proposed to be involved in mRNA metabolism. Thus, together with our finding that human ENSA/ARPP-19 partially complement the gene expression defect in an *igo1Δ igo2Δ* mutant, these observations indicate that Igo1/2 may have an evolutionarily conserved role in mRNA stability control. Intriguingly, ARPP-19 has previously been suggested to control axon growth and synaptic plasticity specifically by stabilizing the growth-associated protein-43 (GAP-43) mRNA in response to nerve growth factor treatment (Irwin et al., 2002). Our study, which identifies a biological function of Igo1/2, may therefore have far-reaching implications for understanding how extracellular, growth-related cues impinge on posttranscriptional gene expression to control eukaryotic differentiation programs.

EXPERIMENTAL PROCEDURES

Cloning and Yeast Experiments

Yeast strains and plasmids used in this study are listed in Tables S1 and S2. Strains were grown at 30°C in standard rich medium with 2% glucose (YPD) or synthetic defined medium with 2% glucose complemented with the appropriate nutrients for plasmid maintenance. PCR-based gene deletions, tagging of chromosomal *IGO1*, and standard experimental procedures for cloning were as described (Amberg et al., 2005).

Mass Spectrometry and Phosphospecific Antibodies

To identify phosphorylation sites in Igo1, purified, bacterially expressed GST-Igo1 was subjected to protein kinase assays using nonradioactive ATP and wild-type or kinase-inactive Rim15^{KD} as described (Wanke et al., 2005). Following separation of the reaction mixtures by SDS-PAGE, the bands corresponding to GST-Igo1 were excised, digested with trypsin, loaded onto a microcapillary liquid chromatography system (OD-SAQ, C18, 5 μm 300 Å, 75 μm ID × 10 cm), and eluted directly into a tandem mass spectrometer (Voyager Super STR) with electrospray ionization. A 1306.6-D peptide (corresponding to the theoretical peptide Y-F-D-S-G-D-Y-A-L-Q-K) appeared to be phosphorylated at the serine residue (which corresponds to Ser⁶⁴ in Igo1) specifically in the GST-Igo1 sample that was treated with wild-type Rim15. Phosphospecific antibodies were raised against the phosphorylated synthetic peptide K-R-K-Y-F-D-pS-G-D-Y-A-L-Q-C (in which pS represents phospho-Ser⁶⁴ of Igo1). The serum was pre-adsorbed with the nonphosphorylated form of the peptide and affinity purified with the phosphorylated peptide by Eurogentec.

Tandem Affinity Purification and Immunoprecipitation Experiments

Igo1-TAP was purified, using a standard tandem affinity purification (TAP)-tag purification protocol (Gelperin et al., 2005) from wild-type (BY4741) cells harboring plasmid BG1805-*IGO1-TAP* (that drives expression of Igo1-TAP from the galactose-inducible *GAL1* promoter). Prior to protein extraction, cells were pregrown on 2% raffinose-containing medium, grown for 4 hr on galactose-containing medium, and treated for 1 hr with 0.2 μg ml⁻¹ rapamycin. In parallel, Igo1-myc₁₃ was purified using a classical immunoprecipitation (IP) protocol from exponentially growing LC54 cells (expressing a chromosomally tagged Igo1-myc₁₃ under the control of the endogenous *IGO1* promoter) that were also treated for 1 hr with 0.2 μg ml⁻¹ rapamycin. Purified Igo1-TAP and

Igo1-myc₁₃ preparations were analyzed for coprecipitating partner proteins using standard MS.

Miscellaneous

Analyses of global transcription changes (including RNA extraction, cRNA synthesis, microarray hybridization, and data analyses) were carried out as published (Urban et al., 2007). Northern blot analyses, β-galactosidase measurements, and aging assays were also performed as described (Reinders et al., 1998; Wanke et al., 2008). Cells were imaged using an Olympus BX54 microscope equipped with a piezo-positioner (Olympus). Z sections (7–10 each 0.5 μm apart) were projected to two-dimensional images and analyzed with the CellM software (Olympus). Details of proteome chip and polysome analyses are described in the Supplemental Information.

ACCESSION NUMBERS

Microarray data have been deposited at the Gene Expression Omnibus (<http://www.ncbi.nlm.nih.gov/geo/>) with the accession number GSE20539. The microarray data set is available at http://puma.princeton.edu/cgi-bin/publication/viewPublication.pl?pub_no=531.

SUPPLEMENTAL INFORMATION

Supplemental Information includes Supplemental Experimental Procedures, three tables, and five figures and is available with this article online at doi: 10.1016/j.molcel.2010.02.039.

ACKNOWLEDGMENTS

We thank Pamela Silver, Roy Parker, and Mark Ashe for strains and plasmids; Manfredo Quadroni for MS analyses; Johannes Buchner and Mick Tuite for antibodies; Patrick Linder and Monique Doere for help with polysome analyses; and Marie-Pierre Péli-Gulli for critical comments on the manuscript. This research was supported by the Canton of Fribourg and grants from the Swiss National Science Foundation (laboratory of C.D.V.), the Marie Heim-Vögtlin program (to S.B.), and the NIH (laboratories of M.S. and J.R.B.).

Received: July 18, 2009

Revised: October 7, 2009

Accepted: February 16, 2010

Published: May 13, 2010

REFERENCES

- Abeliovich, H., and Klionsky, D.J. (2001). Autophagy in yeast: mechanistic insights and physiological function. *Microbiol. Mol. Biol. Rev.* 65, 463–479.
- Albig, A.R., and Decker, C.J. (2001). The target of rapamycin signaling pathway regulates mRNA turnover in the yeast *Saccharomyces cerevisiae*. *Mol. Biol. Cell* 12, 3428–3438.
- Albrecht, M., and Lengauer, T. (2004). Novel Sm-like proteins with long C-terminal tails and associated methyltransferases. *FEBS Lett.* 569, 18–26.
- Amberg, D.C., Burke, D.J., and Strathern, J.N. (2005). *Methods in Yeast Genetics* (Cold Spring Harbor: Cold Spring Harbor Laboratory Press).
- Anderson, P., and Kedersha, N. (2006). RNA granules. *J. Cell Biol.* 172, 803–808.
- Bataille, D., Héron, L., Virsolvy, A., Peyrolier, K., LeCam, A., Gros, L., and Blache, P. (1999). α-Endosulfine, a new entity in the control of insulin secretion. *Cell. Mol. Life Sci.* 56, 78–84.
- Bregues, M., Teixeira, D., and Parker, R. (2005). Movement of eukaryotic mRNAs between polysomes and cytoplasmic processing bodies. *Science* 310, 486–489.
- Brodsky, A.S., and Silver, P.A. (2000). Pre-mRNA processing factors are required for nuclear export. *RNA* 6, 1737–1749.
- Buchan, J.R., Muhlrad, D., and Parker, R. (2008). P bodies promote stress granule assembly in *Saccharomyces cerevisiae*. *J. Cell Biol.* 183, 441–455.

- Cameroni, E., Hulo, N., Roosen, J., Winderickx, J., and De Virgilio, C. (2004). The novel yeast PAS kinase Rim 15 orchestrates G₀-associated antioxidant defense mechanisms. *Cell Cycle* 3, 462–468.
- De Virgilio, C., and Loewith, R. (2006). The TOR signalling network from yeast to man. *Int. J. Biochem. Cell Biol.* 38, 1476–1481.
- Dulubova, I., Horiuchi, A., Snyder, G.L., Girault, J.A., Czernik, A.J., Shao, L., Ramabhadran, R., Greengard, P., and Nairn, A.C. (2001). ARPP-16/ARPP-19: a highly conserved family of cAMP-regulated phosphoproteins. *J. Neurochem.* 77, 229–238.
- Eulalio, A., Behm-Ansmant, I., and Izaurralde, E. (2007). P bodies: at the crossroads of post-transcriptional pathways. *Nat. Rev. Mol. Cell Biol.* 8, 9–22.
- Fabrizio, P., Pozza, F., Pletcher, S.D., Gendron, C.M., and Longo, V.D. (2001). Regulation of longevity and stress resistance by Sch9 in yeast. *Science* 292, 288–290.
- Fleischer, T.C., Weaver, C.M., McAfee, K.J., Jennings, J.L., and Link, A.J. (2006). Systematic identification and functional screens of uncharacterized proteins associated with eukaryotic ribosomal complexes. *Genes Dev.* 20, 1294–1307.
- Gelperin, D.M., White, M.A., Wilkinson, M.L., Kon, Y., Kung, L.A., Wise, K.J., Lopez-Hoyo, N., Jiang, L., Piccirillo, S., Yu, H., et al. (2005). Biochemical and genetic analysis of the yeast proteome with a movable ORF collection. *Genes Dev.* 19, 2816–2826.
- Gray, J.V., Petsko, G.A., Johnston, G.C., Ringe, D., Singer, R.A., and Werner-Washburne, M. (2004). “Sleeping beauty”: quiescence in *Saccharomyces cerevisiae*. *Microbiol. Mol. Biol. Rev.* 68, 187–206.
- He, W., and Parker, R. (2000). Functions of Lsm proteins in mRNA degradation and splicing. *Curr. Opin. Cell Biol.* 12, 346–350.
- Hoyle, N.P., Castelli, L.M., Campbell, S.G., Holmes, L.E., and Ashe, M.P. (2007). Stress-dependent relocalization of translationally primed mRNPs to cytoplasmic granules that are kinetically and spatially distinct from P-bodies. *J. Cell Biol.* 179, 65–74.
- Irwin, N., Chao, S., Goritschenko, L., Horiuchi, A., Greengard, P., Nairn, A.C., and Benowitz, L.I. (2002). Nerve growth factor controls GAP-43 mRNA stability via the phosphoprotein ARPP-19. *Proc. Natl. Acad. Sci. USA* 99, 12427–12431.
- Jensen, T.H., Dower, K., Libri, D., and Rosbash, M. (2003). Early formation of mRNP: license for export or quality control? *Mol. Cell* 11, 1129–1138.
- Jorgensen, P., Rupes, I., Sharom, J.R., Schnepfer, L., Broach, J.R., and Tyers, M. (2004). A dynamic transcriptional network communicates growth potential to ribosome synthesis and critical cell size. *Genes Dev.* 18, 2491–2505.
- Kaeberlein, M., Burtner, C.R., and Kennedy, B.K. (2007). Recent developments in yeast aging. *PLoS Genet.* 3, e84.
- Kolter, R., Siegle, D.A., and Tormo, A. (1993). The stationary phase of the bacterial life cycle. *Annu. Rev. Microbiol.* 47, 855–874.
- Malumbres, M., and Barbacid, M. (2001). To cycle or not to cycle: a critical decision in cancer. *Nat. Rev. Cancer* 1, 222–231.
- Mangus, D.A., Amrani, N., and Jacobson, A. (1998). Pbp1p, a factor interacting with *Saccharomyces cerevisiae* poly(A)-binding protein, regulates polyadenylation. *Mol. Cell Biol.* 18, 7383–7396.
- Mangus, D.A., Smith, M.M., McSweeney, J.M., and Jacobson, A. (2004). Identification of factors regulating poly(A) tail synthesis and maturation. *Mol. Cell Biol.* 24, 4196–4206.
- Minshall, N., Kress, M., Weil, D., and Standart, N. (2009). Role of p54 RNA helicase activity and its C-terminal domain in translational repression, P-body localization and assembly. *Mol. Biol. Cell* 20, 2464–2472.
- Nonhoff, U., Raiser, M., Welzel, F., Piccini, I., Balzereit, D., Yaspo, M.L., Lehraich, H., and Krobitsch, S. (2007). Ataxin-2 interacts with the DEAD/H-box RNA helicase DDX6 and interferes with P-bodies and stress granules. *Mol. Biol. Cell* 18, 1385–1396.
- Parker, R., and Sheth, U. (2007). P bodies and the control of mRNA translation and degradation. *Mol. Cell* 25, 635–646.
- Pedrucci, I., Bürckert, N., Egger, P., and De Virgilio, C. (2000). *Saccharomyces cerevisiae* Ras/cAMP pathway controls post-diauxic shift element-dependent transcription through the zinc finger protein Gis1. *EMBO J.* 19, 2569–2579.
- Pedrucci, I., Dubouloz, F., Cameroni, E., Wanke, V., Roosen, J., Winderickx, J., and De Virgilio, C. (2003). TOR and PKA signaling pathways converge on the protein kinase Rim15 to control entry into G₀. *Mol. Cell* 12, 1607–1613.
- Powers, R.W., III, Kaeberlein, M., Caldwell, S.D., Kennedy, B.K., and Fields, S. (2006). Extension of chronological life span in yeast by decreased TOR pathway signaling. *Genes Dev.* 20, 174–184.
- Powers, T. (2007). TOR signaling and S6 kinase 1: Yeast catches up. *Cell Metab.* 6, 1–2.
- Preiss, T., Baron-Benhamou, J., Ansorge, W., and Hentze, M.W. (2003). Homodirectional changes in transcriptome composition and mRNA translation induced by rapamycin and heat shock. *Nat. Struct. Biol.* 10, 1039–1047.
- Placek, J., Devgan, G., Michaud, G., Zhu, H., Zhu, X., Fasolo, J., Guo, H., Jona, G., Breitkreutz, A., Sopko, R., et al. (2005). Global analysis of protein phosphorylation in yeast. *Nature* 438, 679–684.
- Raiser, M., Albrecht, M., Nonhoff, U., Lengauer, T., Lehraich, H., and Krobitsch, S. (2005). An integrative approach to gain insights into the cellular function of human ataxin-2. *J. Mol. Biol.* 346, 203–214.
- Reinders, A., Bürckert, N., Boller, T., Wiemken, A., and De Virgilio, C. (1998). *Saccharomyces cerevisiae* cAMP-dependent protein kinase controls entry into stationary phase through the Rim15p protein kinase. *Genes Dev.* 12, 2943–2955.
- Sheth, U., and Parker, R. (2003). Decapping and decay of messenger RNA occur in cytoplasmic processing bodies. *Science* 300, 805–808.
- Tarassov, K., Messier, V., Landry, C.R., Radinovic, S., Serna Molina, M.M., Shames, I., Malitskaya, Y., Vogel, J., Bussey, H., and Michnick, S.W. (2008). An in vivo map of the yeast protein interactome. *Science* 320, 1465–1470.
- Urban, J., Soulard, A., Huber, A., Lippman, S., Mukhopadhyay, D., Deloche, O., Wanke, V., Anrather, D., Ammerer, G., Riezman, H., et al. (2007). Sch9 is a major target of TORC1 in *Saccharomyces cerevisiae*. *Mol. Cell* 26, 663–674.
- Von Stetina, J.R., Tranguch, S., Dey, S.K., Lee, L.A., Cha, B., and Drummond-Barbosa, D. (2008). α -Endosulfine is a conserved protein required for oocyte meiotic maturation in *Drosophila*. *Development* 135, 3697–3706.
- Wanke, V., Cameroni, E., Uotila, A., Piccolis, M., Urban, J., Loewith, R., and De Virgilio, C. (2008). Caffeine extends yeast lifespan by targeting TORC1. *Mol. Microbiol.* 69, 277–285.
- Wanke, V., Pedrucci, I., Cameroni, E., Dubouloz, F., and De Virgilio, C. (2005). Regulation of G₀ entry by the Pho80-Pho85 cyclin-CDK complex. *EMBO J.* 24, 4271–4278.
- Wei, M., Fabrizio, P., Hu, J., Ge, H., Cheng, C., Li, L., and Longo, V.D. (2008). Life span extension by calorie restriction depends on Rim15 and transcription factors downstream of Ras/PKA, Tor, and Sch9. *PLoS Genet.* 4, e13.
- Weston, A., and Sommerville, J. (2006). Xp54 and related (DDX6-like) RNA helicases: roles in messenger RNP assembly, translation regulation and RNA degradation. *Nucleic Acids Res.* 34, 3082–3094.
- Woods, W.S., Boettcher, J.M., Zhou, D.H., Kloepper, K.D., Hartman, K.L., Lador, D.T., Oi, Z., Rienstra, C.M., and George, J.M. (2007). Conformation-specific binding of α -synuclein to novel protein partners detected by phage display and NMR spectroscopy. *J. Biol. Chem.* 282, 34555–34567.
- Yorimitsu, T., Zaman, S., Broach, J.R., and Klionsky, D.J. (2007). Protein kinase A and Sch9 cooperatively regulate induction of autophagy in *Saccharomyces cerevisiae*. *Mol. Biol. Cell* 18, 4180–4189.

Supplemental Figures

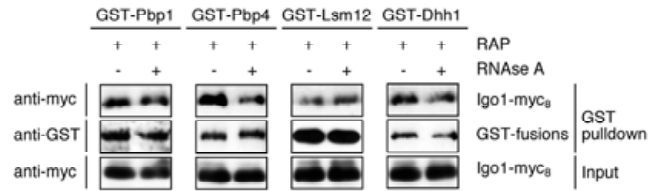


Figure S1, related to Figure 3. Associations of Igo1 with Pbp1, Pbp4, Lsm12, and Dhh1 are Insensitive to RNase A Treatment

GST-Pbp1, GST-Pbp4, GST-Lsm12, GST-Dhh1, and GST were pulled down from lysates obtained from rapamycin-treated (+ RAP; 0.2 $\mu\text{g ml}^{-1}$; 2 hr) wild-type strains co-expressing Igo1-myc₈. Lysates were either treated (+) or not treated (-) with RNase A prior to the pull-down experiments. Cell lysates and GST pull-down samples were subjected to SDS-PAGE and immunoblots were probed with anti-myc or anti-GST antibodies.

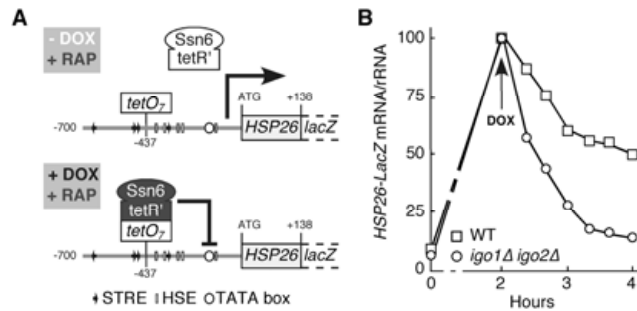


Figure S2, related to Figure 4. Igo1 and Igo2 Stabilize *HSP26-lacZ* mRNAs following Inactivation of TORC1

(A) Schematic view of the *HSP26-lacZ* reporter gene (used in B) illustrating 700 nucleotides of the *HSP26* promoter region including the positions of the stress-response elements (STREs), the heat-shock-elements (HSEs; Chen and Pederson, 1993), and the inserted seven doxycycline-responsive *tetO* elements (*tetO*₇). Nucleotide +138 of *HSP26* is fused to the *lacZ* gene. Doxycycline treatment triggers binding of the chimeric tetR⁺-Ssn6 fusion protein to the *tetO*₇ region and consequently mediates transcriptional repression of the reporter gene.

(B) Exponentially growing wild-type (□) and *igo1Δ igo2Δ* (○) cells harboring the doxycycline-repressible reporter and expressing the chimeric tetR⁺-Ssn6 protein were treated with rapamycin (0.2 μg ml⁻¹) at time 0. After 2 hr, cells were treated with doxycycline (DOX; 15 μg ml⁻¹) and grown for additional 2 hr in the continuous presence of rapamycin. *HSP26-lacZ* transcript levels were determined via northern blot analysis, quantified by PhosphorImager analysis, and expressed as relative level of *HSP26-lacZ* mRNA per rRNA (arbitrarily set to 100% for both strains for the values at the 2 hr time point of the rapamycin treatment; the relative *HSP26-lacZ* transcript levels were 3-fold higher in wild-type than in *igo1Δ igo2Δ* cells at this time point). In control experiments, addition of doxycycline prior to the rapamycin treatment fully abolished the *HSP26-lacZ* induction in wild-type and *igo1Δ igo2Δ* cells (not shown). The calculated half live of the *HSP26-lacZ* mRNA was 104 min (± 7 SD; n = 3) and 36 min (± 4 SD; n = 3) in rapamycin-treated wild-type and *igo1Δ igo2Δ* cells, respectively.

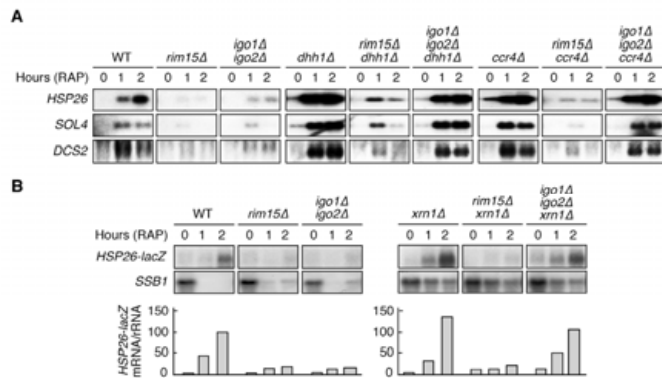


Figure S3, related to Figure 5. The 5'-3' mRNA Decay Pathway Targets Specific mRNAs in *igo1Δ igo2Δ* Mutants

(A) Loss of Dhh1 or Ccr4 suppresses the defect of *igo1Δ igo2Δ*, but not that of *rim15Δ* cells, in rapamycin-induced *HSP26*, *SOL4*, and *DCS2* mRNA expression. Transcript levels were determined by northern blot analysis in wild-type (WT) and mutant strains prior to (0) and following a 1-hr or 2-hr rapamycin treatment (RAP; 0.2 $\mu\text{g ml}^{-1}$).

(B) *HSP26-LacZ* transcript levels prior to and following rapamycin treatment. Transcript levels of *HSP26-lacZ* and *SSB1* were determined by northern blot analysis in wild-type (WT) and indicated mutant strains prior to (0) and following a rapamycin treatment (RAP; 0.2 $\mu\text{g ml}^{-1}$) of 1 hr or 2 hr. Bar graphs show the relative level of *HSP26-lacZ* mRNA per rRNA (arbitrarily set to 1.0 for exponentially growing wild-type cells).

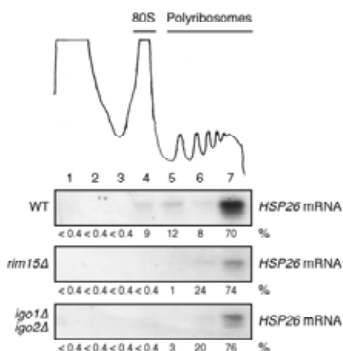


Figure S4, related to Figure 6. *HSP26* mRNA Fractionates with Polyribosomes on Sucrose Gradients in the Absence of Igo1/2

The top trace shows the UV absorbance profile at 254 nm of a cell extract of rapamycin-treated (2 hr; $0.2 \mu\text{g ml}^{-1}$) wild-type yeast after sedimentation on a 7 to 50 % linear sucrose gradient. Nearly identical profiles were obtained from *rim15Δ* and *igo1Δ igo2Δ* cell extracts (not shown). Aligned below are northern blots performed on total RNA isolated from the indicated (1-7) sucrose gradient fractions of wild-type (WT), *rim15Δ*, and *igo1Δ igo2Δ* cell extracts (all harvested after a 2-hr rapamycin treatment). The relative levels of *HSP26* input mRNA (set to 100% for wild-type cells) were 18% and 32% for *rim15Δ* and *igo1Δ igo2Δ* cells, respectively. The positions of the 80S monosomes and polyribosomes are indicated. *HSP26* mRNA was quantified by PhosphorImager analysis and the percentage of *HSP26* mRNA in the indicated sucrose gradient fractions is indicated at the bottom of each panel.

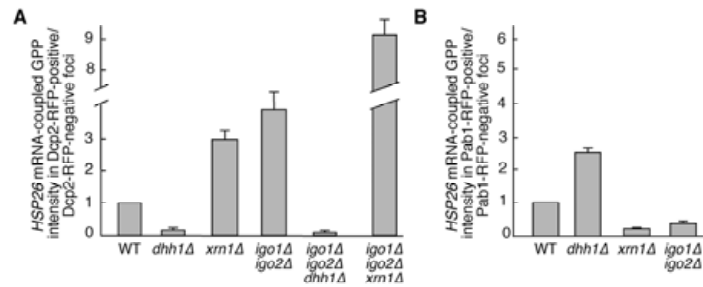


Figure S5, related to Figure 7. Relative Distribution of *HSP26* mRNAs among Cytoplasmic Foci

(A, B) Wild-type (WT) and indicated mutant strains co-expressing the PB-marker protein Dcp2-RFP (A) or the EGPB/SG-marker protein Pab1-RFP (B), as well as *HSP26-U1A* mRNA and the U1A-GFP binding protein were harvested following glucose limitation (*i.e.* following growth for 48 hr in batch cultures). Bars represent (in a total of 100 cells) the ratio between the intensity of *HSP26* mRNA-coupled GFP signal in cytoplasmic foci that co-stained with Dcp2-RFP (A) or Pab1-RFP (B) and that detected in foci devoid of the corresponding RFP signal. This ratio was set to 1.0 for wild-type cells. Data represent averages ($n = 3$), with SDs indicated by the lines above each bar. The GFP signal in each *HSP26* mRNA-containing cytoplasmic focus was calculated as the mean intensity within the region of the focus multiplied by its area, after subtraction of the mean background intensity of a nearby area of comparable size. Within an experiment, exposure settings were identical. Notably, loss of Xrn1, like loss of Igo1/2, strongly shifted the relative distribution of *HSP26* mRNAs among cytoplasmic foci towards Dcp2-RFP-positive PBs and the effects of loss of both Igo1/2 and of Xrn1 appeared to be additive (A). As expected, loss of Dhh1 enhanced, while loss of Xrn1 or of Igo1/2 reduced, the relative amount of *HSP26* mRNAs in Pab1-RFP-positive EGPs/SGs (B).

Supplemental Tables

Table S1. Strains Used in This Study

Strain	Genotype	Source	Figure/Table
BY4741	MATa; <i>his3Δ1, leu2Δ0, met15Δ0, ura3Δ0</i>	Euroscarf	1B, E, F, 2A, C, D, 4, 5A-C, 6A-D, S3, S4, S5A, Table3
BY4742	MATa; <i>his3Δ1, leu2Δ0, lys2Δ0, ura3Δ0</i>	Euroscarf	
YFL033C	MATa; <i>rim15Δ::kanMX4</i> [BY4741]	Euroscarf	1E, F, 2A, C, D, 5A-C, 6B-D, S3, S4
YNL157W	MATa; <i>igo1Δ::kanMX4</i> [BY4741]	Euroscarf	2A, C, D, 3B, 7A, C, S1
YHR132W-A	MATa; <i>igo2Δ::kanMX4</i> [BY4741]	Euroscarf	2A, C, D
CDV288-12A	MATa; <i>igo1Δ::kanMX4, igo2Δ::kanMX4</i> [BY4741]	This study	2A, C, D, 4, 5A-C, 6B-D, S3, S4, S5A
LC54	MATa; <i>IGO1-myc₁₃::kanMX4</i> [BY4741]	This study	3A, Table 3
MJA1709-8B	MATa; <i>rim15Δ::kanMX4 IGO1-myc₁₃::kanMX4</i> [BY4741]	This study	3A
NT255-1B	MATa; <i>leu2Δ0::LEU2-TetR'-SSN6</i> [BY4741/2]	This study	S2B
NT280-12D	MATa; <i>leu2Δ0::LEU2-TetR'-SSN6 igo1Δ::kanMX4, igo2Δ::kanMX4</i> [BY4741/2]	This study	S2B
YDL160C	MATa; <i>dhh1Δ::kanMX4</i> [BY4741]	Euroscarf	5A-C, S3A, S5A
YAL021C	MATa; <i>ccr4Δ::kanMX4</i> [BY4741]	Euroscarf	5A-C, S3A
NT205-1B	MATa; <i>xrn1Δ::kanMX4</i> [BY4741/2]	This study	5A-C, 6B-D, S3B, S5A
MJA1602-3A	MATa; <i>rim15Δ::kanMX4, dhh1Δ::kanMX4</i> [BY4741/2]	This study	5A-C, S3A
MJA1600-10B	MATa; <i>rim15Δ::kanMX4, ccr4Δ::kanMX4</i> [BY4741/2]	This study	5A-C, S3A
MJA1621-10B	MATa; <i>igo1Δ::kanMX4, igo2Δ::kanMX4, dhh1Δ::kanMX4</i> [BY4741/2]	This study	5A-C, S3A, S5A
MJA1597-4D	MATa; <i>igo1Δ::kanMX4, igo2Δ::kanMX4, ccr4Δ::kanMX4</i> [BY4741/2]	This study	5A-C, S3A
NT205-1A	MATa; <i>rim15Δ::kanMX4, xrn1Δ::kanMX4</i> [BY4741/2]	This study	5A-C, 6B-D, S3B
NT206-7A	MATa; <i>igo1Δ::kanMX4, igo2Δ::kanMX4, xrn1Δ::kanMX4</i> [BY4741/2]	This study	5A-C, 6B-D, S3B, S5A
Y2864	MATa; <i>gal1Δ::HIS3, ade2-1, his3-11,15, leu2-3,112, trp1-1, ura3-1, can1-100</i>	Wang <i>et al.</i> , 2004	2B
CDV314	MATa; <i>rim15Δ::kanMX4</i> [Y2864]	This study	2B
CDV308-1B	MATa; <i>igo1Δ::kanMX4, igo2Δ::kanMX4</i> [Y2864]	This study	2B
yMK1344	MATa; <i>his3-11, 15, leu2-3, 112, trp1-1, ura3-1, DCPI-GFP::G418, PAB1-RFP::NAT</i>	Hoyle <i>et al.</i> , 2007	
NT253-13B	MATa; <i>igo1Δ::kanMX4, PAB1-RFP::NAT</i> [BY4741/2]	This study	7B
NT169-9C	MATa; <i>PAB1-RFP::NAT</i> [BY4741/2]	This study	7D, S5B
NT255-6B	MATa; <i>igo1Δ::kanMX4, igo2Δ::kanMX4, PAB1-RFP::NAT</i> [BY4741/2]	This study	S5B
NT298	MATa; <i>dhh1Δ::kanMX4, PAB1-RFP::NAT</i> [BY4741/2]	This study	S5B
NT301	MATa; <i>xrn1Δ::kanMX4, PAB1-RFP::NAT</i> [BY4741/2]	This study	S5B

Table S2. Plasmids Used in This Study

Plasmid	Description	Source	Figure/Table
YEplac181	2 μ , <i>LEU2</i>	Gietz and Sugino, 1988	
pCDV1157	[YEPlac181] <i>TDH3p-IGO1-HA₃</i>	This study	1B
pCDV1159	[YEPlac181] <i>TDH3p-SIR4-HA₃</i>	This study	1B
YEplac195	2 μ , <i>URA3</i>	Gietz and Sugino, 1988	
pNB566	[YEPlac195] <i>GAL1p-GST-RIM15</i>	Wanke <i>et al.</i> , 2005	1B
pLC803	[YEPlac195] <i>GAL1p-GST</i>	This study	1B
pCDV487	[YEPlac195] <i>GAL1p-GST-RIM15-HA₃</i>	Pedruzzi <i>et al.</i> , 2003	1B,C, D
pIP779	[YEPlac195] <i>GAL1p-GST-RIM15^{K823Y}-HA₃</i>	This study	1C, D
pGEX3	<i>GST</i>	Smith and Johnson, 1988	1C
pLC1092	[pGEX3] <i>GST-IGO1</i>	This study	1C, D
pLC1134	[pGEX3] <i>GST-IGO1^{S64A}</i>	This study	1C
pVW1109	[pGEX3] <i>GST-IGO2</i>	This study	1C
MJA1497	[pGEX3] <i>GST-ENSA</i>	This study	1C
MJA1498	[pGEX3] <i>GST-ARPP-19</i>	This study	1C
YCplac33	CEN, <i>URA3</i>	Gietz and Sugino, 1988	2D
pBG1805-IGO1-TAP	<i>GAL1p-IGO1-HA-6HIS-3C-ZZ</i>	Gelperin <i>et al.</i> , 2005	Table 3
pLC1427	[YCplac33] <i>IGO1-myc₈</i>	This study	2D, 3B, S1
pLC1430	[YCplac33] <i>IGO1^{S64A}-myc₈</i>	This study	2D, 3B
pLC1429	[YCplac33] <i>IGO2-myc₈</i>	This study	2D
pMJA1481	[YEplac195] <i>IGO1p-ENSA-myc₈</i>	This study	2D
pMJA1482	[YEplac195] <i>IGO1p-ARPP-19-myc₈</i>	This study	2D
pUKC414	CEN, <i>URA3, HSP26-lacZ</i>	Ferreira <i>et al.</i> , 2001	5C, 6C
pXL1633	CEN, <i>HIS3, HSP26-lacZ</i>	This study	2D
pCDV1082	YCpIF2- <i>ADH1p-GST</i>	This study	3A, B, S1
pMJA1655	YCpIF2- <i>ADH1p-GST-PBP4</i>	This study	3A, B, S1
pMJA1654	YCpIF2- <i>ADH1p-GST-PBP1</i>	This study	3A, B, S1
pMJA1656	YCpIF2- <i>ADH1p-GST-DHH1</i>	This study	3A, B, S1
pMJA1657	YCpIF2- <i>ADH1p-GST-LSM12</i>	This study	3A, B, S1
pCM242	CMVp(<i>tetR'-SSN6</i>):- <i>LEU2</i>	Belli <i>et al.</i> , 1998	S2B
pNT012	CEN, <i>URA3, HSP26p::tetO-HSP26-LacZ</i>	This study	S2A, B
pTG003	PRS315- <i>DCP2-RFP</i>	Gill <i>et al.</i> , 2006	6A, D, 7A, S5A
pPS2037	PRS416- <i>PGK1p-PGK1-U1A-PGK1</i> 3'UTR	Brodsky and Silver, 2000	
pNT003	PRS416- <i>HSP26p-HSP26-U1A-HSP26</i> 3'UTR	This study	6A, D, 7C, D, S5
pPS2045	PRS313- <i>GALp-U1A(1-94)-GFP</i>	Brodsky and Silver, 2000	
pNT004	PRS413- <i>ADH1p-U1A(1-94)-GFP</i>	This study	6A, D, 7C, D, S5
pXL1632	[YCplac33] <i>IGO1-GFP</i>	This study	7A, B
pNT005	[YCplac33] <i>IGO1-RFP</i>	This study	7C

Table S3. Proteins Identified in Igo1-TAP and Igo1-myc₁₃ Pull-Down Experiments

Protein ¹	Igo1-TAP	Igo1-myc ₁₃	MW	Function/Description
Act1		✓	41.7	Actin
Ate1	✓		57.9	Arginyl-tRNA-protein transferase
Clu1	✓		145.2	Component of eIF3
Hhfl1/2		✓	11.4	Histone H4
Hrk1	✓		85.7	Protein kinase implicated in activation of Pma1
Hsc82		✓	80.9	Cytoplasmic chaperone of the Hsp90 family
Htb1		✓	14.3	Histone H2B
Igo1	✓	✓	18.0	Required for initiation of G ₀ ; target of Rim15 protein kinase
Ilv6	✓		34.0	Regulatory subunit of acetolactate synthase
Lsm12	✓	✓	21.3	Sm-like protein; interacts with Pbp1/4; associates with ribosomes
Mot2	✓		65.4	Subunit of the CCR4-NOT complex
Pbp1	✓	✓	78.8	Interacts with Pab1 to regulate mRNA polyadenylation
Pbp4	✓	✓	19.9	Pbp1p binding protein 4; interacts with Lsm12
Por1		✓	30.4	Mitochondrial porin, outer membrane protein
Psp2	✓		65.6	Possible role in mitochondrial mRNA splicing
Rim1		✓	15.4	Role in mitochondrial DNA replication; binds single-stranded DNA
Rps18A		✓	17.0	Protein component of the small (40S) ribosomal subunit
Rsp5	✓		91.8	E3 ubiquitin-protein ligase
Sec23	✓		85.4	GTPase-activating protein; involved in ER to Golgi transport
Sfp1	✓		74.8	Transcription factor controlling expression of Ribi genes
Ssa1/2	✓	✓	69.6	Hsp70 family member
Ssa4		✓	69.7	Hsp70 family member
Ssb1/2	✓	✓	66.6	Hsp70 family member; ribosome-associated molecular chaperone
Ssc1	✓		70.6	Hsp70 family member; role in mitochondrial protein import
Tef1		✓	50.0	Translational elongation factor EF-1 α

¹Proteins were identified by LC-MS-MS analysis of polypeptides in purified Igo1-TAP and Igo1-myc₁₃ preparations (see Experimental Procedures). Only proteins for which at least four peptides were identified and, in the case of Igo1-TAP, for which the number of identified peptides was also at least four times higher than the number of peptides recovered with an unrelated control (Gtr1-TAP) were included in the list. The preparations (*i.e.* Igo1-TAP and/or Igo1-myc₁₃) in which corresponding peptides were identified are indicated (✓). Proteins for which peptides were recovered in both Igo1-TAP and Igo1-myc₁₃ preparations are highlighted in bold.

Supplemental Experimental Procedures

Proteome Chip Analyses

Yeast proteome microarrays were prepared as previously described (Ptacek et al., 2005). Approximately 4400 GST::His-tagged yeast proteins were overexpressed and purified by affinity chromatography and spotted in duplicate on a surface-modified microscope slide. The autophosphorylating kinases Pka2, Pkc-a and Cmk1 were added at defined locations to serve as both positive controls and landmarks for the identification of phosphorylation signals on the array. Common kinase substrates, such as myelin basic protein (MBP), histone H1, casein, polyGlu-Tyr, and a carboxyterminal domain (CTD) peptide containing three copies of the acidic CTD of RNA polymerase II were also included to exhibit the addition of kinase activity on the array.

To determine the optimal amount of kinase to use for probing the proteome arrays, a dilution series (1:1, 1:2, 1:5, 1:10, and 1:20) of wild-type Rim15 and kinase-inactive Rim15^{KD} was made in a total volume of 200 μ l kinase buffer containing 2 μ l [γ -³³P] ATP and added to test arrays containing positive controls and common kinase substrates as described (Ptacek et al., 2005). Using the optimized conditions, proteome arrays were probed in duplicate with wild-type Rim15 and Rim15^{KD} in 200 μ l kinase buffer containing 2 μ l [γ -³³P]ATP in a humidified chamber at 30°C for 1 hr. Arrays were then exposed to X-ray film for 1, 3 and 7 days. Data analysis was performed as described previously (Ptacek et al., 2005). In short, substrate proteins that displayed reproducible signals higher than those of neighboring spots in at least three of the four spots were identified and then compared to the autophosphorylation control. Only those spots that were specifically phosphorylated in the presence of wild-type Rim15 were scored as positive substrates. The proteome arrays probed with Rim15^{KD} exhibited signals identical to those obtained in the absence of protein kinase.

Polysome Analyses

Strains were grown in synthetic defined medium to mid-log phase and either treated, or not, with rapamycin for 2 hr. Cycloheximide (0.1 mg ml⁻¹ final concentration) was added just prior to harvesting. Extracts (of 150 OD₆₀₀ of yeast cultures) were layered onto 7-50% linear sucrose gradients and centrifuged at 35'000 rpm at 4°C for 210 min. Gradient analysis was performed using an ISCO UA-6 collector with continuous monitoring at A_{254nm}. Manually collected fractions were used for RNA extraction as described (Gaillard and Aguilera, 2008).

Supplemental References

- Belli, G., Gari, E., Piedrafita, L., Aldea, M., and Herrero, E. (1998). An activator/repressor dual system allows tight tetracycline-regulated gene expression in budding yeast. *Nucleic. Acids Res.* *26*, 942-947.
- Brodsky, A.S., and Silver, P.A. (2000). Pre-mRNA processing factors are required for nuclear export. *RNA* *6*, 1737-1749.
- Chen, J., and Pederson, D.S. (1993). A distal heat shock element promotes the rapid response to heat shock of the *HSP26* gene in the yeast *Saccharomyces cerevisiae*. *J. Biol. Chem.* *268*, 7442-7448.
- Ferreira, P.C., Ness, F., Edwards, S.R., Cox, B.S., and Tuite, M.F. (2001). The elimination of the yeast [*PSI*⁺] prion by guanidine hydrochloride is the result of Hsp104 inactivation. *Mol. Microbiol.* *40*, 1357-1369.
- Gaillard, H., and Aguilera, A. (2008). A novel class of mRNA-containing cytoplasmic granules are produced in response to UV-irradiation. *Mol. Biol. Cell* *19*, 4980-4992.
- Gietz, R.D., and Sugino, A. (1988). New yeast-*Escherichia coli* shuttle vectors constructed with *in vitro* mutagenized yeast genes lacking six-base pair restriction sites. *Gene* *74*, 527-534.
- Gill, T., Aulds, J., and Schmitt, M.E. (2006). A specialized processing body that is temporally and asymmetrically regulated during the cell cycle in *Saccharomyces cerevisiae*. *J. Cell Biol.* *173*, 35-45.
- Hoyle, N.P., Castelli, L.M., Campbell, S.G., Holmes, L.E., and Ashe, M.P. (2007). Stress-dependent relocation of translationally primed mRNPs to cytoplasmic granules that are kinetically and spatially distinct from P-bodies. *J. Cell Biol.* *179*, 65-74.
- Pedrucci, I., Dubouloz, F., Cameroni, E., Wanke, V., Roosen, J., Winderickx, J., and De Virgilio, C. (2003). TOR and PKA signaling pathways converge on the protein kinase Rim15 to control entry into G₀. *Mol. Cell* *12*, 1607-1613.
- Ptacek, J., Devgan, G., Michaud, G., Zhu, H., Zhu, X., Fasolo, J., Guo, H., Jona, G., Breitkreutz, A., Sopko, R., et al. (2005). Global analysis of protein phosphorylation in yeast. *Nature* *438*, 679-684.
- Smith, D.B., and Johnson, K.S. (1988). Single-step purification of polypeptides expressed in *Escherichia coli* as fusions with glutathione *S*-transferase. *Gene* *67*, 31-40.
- Wang, Y., Pierce, M., Schneper, L., Guldal, C.G., Zhang, X., Tavazoie, S., and Broach, J.R. (2004). Ras and Gpa2 mediate one branch of a redundant glucose signaling pathway in yeast. *PLoS Biol.* *2*, E128.
- Wanke, V., Pedrucci, I., Cameroni, E., Dubouloz, F., and De Virgilio, C. (2005). Regulation of G₀ entry by the Pho80-Pho85 cyclin-CDK complex. *EMBO J.* *24*, 4271-4278.

References

- Albig, A.R., and Decker, C.J. (2001). The target of rapamycin signaling pathway regulates mRNA turnover in the yeast *Saccharomyces cerevisiae*. *Mol Biol Cell* *12*, 3428-3438.
- Albrecht, M., and Lengauer, T. (2004). Novel Sm-like proteins with long C-terminal tails and associated methyltransferases. *FEBS Lett* *569*, 18-26.
- Allen, T.D., Cronshaw, J.M., Bagley, S., Kiseleva, E., and Goldberg, M.W. (2000). The nuclear pore complex: mediator of translocation between nucleus and cytoplasm. *J Cell Sci* *113 (Pt 10)*, 1651-1659.
- Amberg, D.C., Burke, D.J., and Strathern, J.N. (2005). *Methods in Yeast Genetics* (Cold Spring Harbor, Cold Spring Harbor Laboratory Press).
- Araki, T., Uesono, Y., Oguchi, T., and Toh, E.A. (2005). LAS24/KOG1, a component of the TOR complex 1 (TORC1), is needed for resistance to local anesthetic tetracaine and normal distribution of actin cytoskeleton in yeast. *Genes Genet Syst* *80*, 325-343.
- Arribere, J.A., Doudna, J.A., and Gilbert, W.V. (2011). Reconsidering movement of eukaryotic mRNAs between polysomes and P bodies. *Mol Cell* *44*, 745-758.
- Ausubel, M., Brent, R., Kingston, R.E., Moore, D.D., Seidman, J.G., Smith, J.A., and Struhl, K. (1999). *Current protocols in molecular biology* (John Wiley & Sons, Inc., Media).
- Avruch, J., Long, X., Ortiz-Vega, S., Rapley, J., Papageorgiou, A., and Dai, N. (2009). Amino acid regulation of TOR complex 1. *Am J Physiol Endocrinol Metab* *296*, E592-602.
- Balagopal, V., Fluch, L., and Nissan, T. (2012). Ways and means of eukaryotic mRNA decay. *Biochim Biophys Acta*.
- Balciunas, D., and Ronne, H. (1999). Yeast genes GIS1-4: multicopy suppressors of the Gal- phenotype of *snf1 mig1 srb8/10/11* cells. *Mol Gen Genet* *262*, 589-599.
- Bataille, D., Heron, L., Virsolvy, A., Peyrollier, K., LeCam, A., Gros, L., and Blache, P. (1999). alpha-Endosulfine, a new entity in the control of insulin secretion. *Cell Mol Life Sci* *56*, 78-84.
- Beck, T., and Hall, M.N. (1999). The TOR signalling pathway controls nuclear localization of nutrient-regulated transcription factors. *Nature* *402*, 689-692.
- Bell, W., Klaassen, P., Ohnacker, M., Boller, T., Herweijer, M., Schoppink, P., Van der Zee, P., and Wiemken, A. (1992). Characterization of the 56-kDa subunit of yeast trehalose-6-phosphate synthase and cloning of its gene reveal its identity with the product of CIF1, a regulator of carbon catabolite inactivation. *Eur J Biochem* *209*, 951-959.
- Berchtold, D., and Walther, T.C. (2009). TORC2 plasma membrane localization is essential for cell viability and restricted to a distinct domain. *Mol Biol Cell* *20*, 1565-1575.
- Berger, A.B., Decourty, L., Badis, G., Nehrass, U., Jacquier, A., and Gadal, O. (2007). Hmo1 is required for TOR-dependent regulation of ribosomal protein gene transcription. *Mol Cell Biol* *27*, 8015-8026.
- Berset, C., Trachsel, H., and Altmann, M. (1998). The TOR (target of rapamycin) signal transduction pathway regulates the stability of translation initiation factor eIF4G in the yeast *Saccharomyces cerevisiae*. *Proc Natl Acad Sci U S A* *95*, 4264-4269.
- Bertram, P.G., Choi, J.H., Carvalho, J., Ai, W., Zeng, C., Chan, T.F., and Zheng, X.F. (2000). Tripartite regulation of Gln3p by TOR, Ure2p, and phosphatases. *J Biol Chem* *275*, 35727-35733.

- Beugnet, A., Tee, A.R., Taylor, P.M., and Proud, C.G. (2003). Regulation of targets of mTOR (mammalian target of rapamycin) signalling by intracellular amino acid availability. *Biochem J* 372, 555-566.
- Binda, M., Peli-Gulli, M.P., Bonfils, G., Panchaud, N., Urban, J., Sturgill, T.W., Loewith, R., and De Virgilio, C. (2009). The Vam6 GEF controls TORC1 by activating the EGO complex. *Mol Cell* 35, 563-573.
- Blewett, N., Collier, J., and Goldstrohm, A. (2011). A quantitative assay for measuring mRNA decapping by splinted ligation reverse transcription polymerase chain reaction: qSL-RT-PCR. *Rna* 17, 535-543.
- Boer, V.M., Amini, S., and Botstein, D. (2008). Influence of genotype and nutrition on survival and metabolism of starving yeast. *Proc Natl Acad Sci U S A* 105, 6930-6935.
- Bonfils, G., Jaquenoud, M., Bontron, S., Ostrowicz, C., Ungermann, C., and De Virgilio, C. (2012). Leucyl-tRNA Synthetase Controls TORC1 via the EGO Complex. *Mol Cell* 46, 105-110.
- Bonnerot, C., Boeck, R., and Lapeyre, B. (2000). The two proteins Pat1p (Mrt1p) and Spb8p interact in vivo, are required for mRNA decay, and are functionally linked to Pab1p. *Mol Cell Biol* 20, 5939-5946.
- Borggreffe, T., Davis, R., Erdjument-Bromage, H., Tempst, P., and Kornberg, R.D. (2002). A complex of the Srb8, -9, -10, and -11 transcriptional regulatory proteins from yeast. *J Biol Chem* 277, 44202-44207.
- Boucherie, H. (1985). Protein synthesis during transition and stationary phases under glucose limitation in *Saccharomyces cerevisiae*. *J Bacteriol* 161, 385-392.
- Bouveret, E., Rigaut, G., Shevchenko, A., Wilm, M., and Seraphin, B. (2000). A Sm-like protein complex that participates in mRNA degradation. *Embo J* 19, 1661-1671.
- Bregman, A., Avraham-Kelbert, M., Barkai, O., Duek, L., Guterman, A., and Choder, M. (2011). Promoter elements regulate cytoplasmic mRNA decay. *Cell* 147, 1473-1483.
- Breitkreutz, A., Choi, H., Sharom, J.R., Boucher, L., Neduva, V., Larsen, B., Lin, Z.Y., Breitkreutz, B.J., Stark, C., Liu, G., *et al.* (2010). A global protein kinase and phosphatase interaction network in yeast. *Science* 328, 1043-1046.
- Broek, D., Toda, T., Michaeli, T., Levin, L., Birchmeier, C., Zoller, M., Powers, S., and Wigler, M. (1987). The *S. cerevisiae* CDC25 gene product regulates the RAS/adenylyate cyclase pathway. *Cell* 48, 789-799.
- Brown, C.E., and Sachs, A.B. (1998). Poly(A) tail length control in *Saccharomyces cerevisiae* occurs by message-specific deadenylation. *Mol Cell Biol* 18, 6548-6559.
- Buchan, J.R., Muhlrad, D., and Parker, R. (2008). P bodies promote stress granule assembly in *Saccharomyces cerevisiae*. *J Cell Biol* 183, 441-455.
- Buchan, J.R., and Parker, R. (2009). Eukaryotic stress granules: the ins and outs of translation. *Mol Cell* 36, 932-941.
- Budhwar, R., Lu, A., and Hirsch, J.P. (2010). Nutrient control of yeast PKA activity involves opposing effects on phosphorylation of the Bcy1 regulatory subunit. *Mol Biol Cell* 21, 3749-3758.
- Budovskaya, Y.V., Stephan, J.S., Deminoff, S.J., and Herman, P.K. (2005). An evolutionary proteomics approach identifies substrates of the cAMP-dependent protein kinase. *Proc Natl Acad Sci U S A* 102, 13933-13938.
- Budovskaya, Y.V., Stephan, J.S., Reggiori, F., Klionsky, D.J., and Herman, P.K. (2004). The Ras/cAMP-dependent protein kinase signaling pathway regulates an early step of the autophagy process in *Saccharomyces cerevisiae*. *J Biol Chem* 279, 20663-20671.
- Guitherie, C. (1991). Guide to yeast genetics and molecular biology. *Methods Enzymol* 194, 1-863.

- Cameroni, E., Hulo, N., Roosen, J., Winderickx, J., and De Virgilio, C. (2004). The novel yeast PAS kinase Rim 15 orchestrates G0-associated antioxidant defense mechanisms. *Cell Cycle* 3, 462-468.
- Cardenas, M.E., Cutler, N.S., Lorenz, M.C., Di Como, C.J., and Heitman, J. (1999). The TOR signaling cascade regulates gene expression in response to nutrients. *Genes Dev* 13, 3271-3279.
- Carlson, M. (1997). Genetics of transcriptional regulation in yeast: connections to the RNA polymerase II CTD. *Annu Rev Cell Dev Biol* 13, 1-23.
- Carroll, A.S., Bishop, A.C., DeRisi, J.L., Shokat, K.M., and O'Shea, E.K. (2001). Chemical inhibition of the Pho85 cyclin-dependent kinase reveals a role in the environmental stress response. *Proc Natl Acad Sci U S A* 98, 12578-12583.
- Carroll, A.S., and O'Shea, E.K. (2002). Pho85 and signaling environmental conditions. *Trends Biochem Sci* 27, 87-93.
- Castilho, P.V., Williams, B.C., Mochida, S., Zhao, Y., and Goldberg, M.L. (2009). The M phase kinase Greatwall (Gwl) promotes inactivation of PP2A/B55delta, a phosphatase directed against CDK phosphosites. *Mol Biol Cell* 20, 4777-4789.
- Chang, Y.W., Howard, S.C., Budovskaya, Y.V., Rine, J., and Herman, P.K. (2001). The rye mutants identify a role for Ssn/Srb proteins of the RNA polymerase II holoenzyme during stationary phase entry in *Saccharomyces cerevisiae*. *Genetics* 157, 17-26.
- Chang, Y.W., Howard, S.C., and Herman, P.K. (2004). The Ras/PKA signaling pathway directly targets the Srb9 protein, a component of the general RNA polymerase II transcription apparatus. *Mol Cell* 15, 107-116.
- Chen, J.C., and Powers, T. (2006). Coordinate regulation of multiple and distinct biosynthetic pathways by TOR and PKA kinases in *S. cerevisiae*. *Curr Genet* 49, 281-293.
- Cherkasova, V., Qiu, H., and Hinnebusch, A.G. (2010). Snf1 promotes phosphorylation of the alpha subunit of eukaryotic translation initiation factor 2 by activating Gcn2 and inhibiting phosphatases Glc7 and Sit4. *Mol Cell Biol* 30, 2862-2873.
- Cherkasova, V.A., and Hinnebusch, A.G. (2003). Translational control by TOR and TAP42 through dephosphorylation of eIF2alpha kinase GCN2. *Genes Dev* 17, 859-872.
- Choder, M. (1991). A general topoisomerase I-dependent transcriptional repression in the stationary phase in yeast. *Genes Dev* 5, 2315-2326.
- Choder, M. (1993). A growth rate-limiting process in the last growth phase of the yeast life cycle involves RPB4, a subunit of RNA polymerase II. *J Bacteriol* 175, 6358-6363.
- Choder, M., and Young, R.A. (1993). A portion of RNA polymerase II molecules has a component essential for stress responses and stress survival. *Mol Cell Biol* 13, 6984-6991.
- Chowdhury, A., Raju, K.K., Kalurupalle, S., and Tharun, S. (2012). Both Sm-domain and C-terminal extension of Lsm1 are important for the RNA-binding activity of the Lsm1-7-Pat1 complex. *Rna* 18, 936-944.
- Cipollina, C., van den Brink, J., Daran-Lapujade, P., Pronk, J.T., Porro, D., and de Winde, J.H. (2008a). *Saccharomyces cerevisiae* SFP1: at the crossroads of central metabolism and ribosome biogenesis. *Microbiology* 154, 1686-1699.
- Cipollina, C., van den Brink, J., Daran-Lapujade, P., Pronk, J.T., Vai, M., and de Winde, J.H. (2008b). Revisiting the role of yeast Sfp1 in ribosome biogenesis and cell size control: a chemostat study. *Microbiology* 154, 337-346.
- Claypool, J.A., French, S.L., Johzuka, K., Eliason, K., Vu, L., Dodd, J.A., Beyer, A.L., and Nomura, M. (2004). Tor pathway regulates Rrn3p-dependent recruitment of yeast RNA polymerase I to the promoter but does not participate in alteration of the number of active genes. *Mol Biol Cell* 15, 946-956.

- Clement, S.L., Scheckel, C., Stoecklin, G., and Lykke-Andersen, J. (2011). Phosphorylation of tristetraprolin by MK2 impairs AU-rich element mRNA decay by preventing deadenylase recruitment. *Mol Cell Biol* 31, 256-266.
- Cohen, P. (1989). The structure and regulation of protein phosphatases. *Annu Rev Biochem* 58, 453-508.
- Coller, J., and Parker, R. (2005). General translational repression by activators of mRNA decapping. *Cell* 122, 875-886.
- Coller, J.M., Tucker, M., Sheth, U., Valencia-Sanchez, M.A., and Parker, R. (2001). The DEAD box helicase, Dhh1p, functions in mRNA decapping and interacts with both the decapping and deadenylase complexes. *Rna* 7, 1717-1727.
- Colombo, S., Ma, P., Cauwenberg, L., Winderickx, J., Crauwels, M., Teunissen, A., Nauwelaers, D., de Winde, J.H., Gorwa, M.F., Colavizza, D., *et al.* (1998). Involvement of distinct G-proteins, Gpa2 and Ras, in glucose- and intracellular acidification-induced cAMP signalling in the yeast *Saccharomyces cerevisiae*. *Embo J* 17, 3326-3341.
- Colombo, S., Ronchetti, D., Thevelein, J.M., Winderickx, J., and Martegani, E. (2004). Activation state of the Ras2 protein and glucose-induced signaling in *Saccharomyces cerevisiae*. *J Biol Chem* 279, 46715-46722.
- Corden, J.L. (1990). Tails of RNA polymerase II. *Trends Biochem Sci* 15, 383-387.
- Cosentino, G.P., Schmelzle, T., Haghghat, A., Helliwell, S.B., Hall, M.N., and Sonenberg, N. (2000). Eap1p, a novel eukaryotic translation initiation factor 4E-associated protein in *Saccharomyces cerevisiae*. *Mol Cell Biol* 20, 4604-4613.
- Costa, V., and Moradas-Ferreira, P. (2001). Oxidative stress and signal transduction in *Saccharomyces cerevisiae*: insights into ageing, apoptosis and diseases. *Mol Aspects Med* 22, 217-246.
- Cougot, N., Cavalier, A., Thomas, D., and Gillet, R. (2012). The Dual Organization of P-bodies Revealed by Immunoelectron Microscopy and Electron Tomography. *J Mol Biol*.
- Cytrynska, M., Frajnt, M., and Jakubowicz, T. (2001). *Saccharomyces cerevisiae* pyruvate kinase Pyk1 is PKA phosphorylation substrate in vitro. *FEMS Microbiol Lett* 203, 223-227.
- Dahmus, M.E. (1996). Reversible phosphorylation of the C-terminal domain of RNA polymerase II. *J Biol Chem* 271, 19009-19012.
- Dazert, E., and Hall, M.N. (2011). mTOR signaling in disease. *Curr Opin Cell Biol* 23, 744-755.
- De Craene, J.O., Soetens, O., and Andre, B. (2001). The Npr1 kinase controls biosynthetic and endocytic sorting of the yeast Gap1 permease. *J Biol Chem* 276, 43939-43948.
- De Virgilio, C. (2012). The essence of yeast quiescence. *FEMS Microbiol Rev* 36, 306-339.
- De Virgilio, C., Burckert, N., Bell, W., Jenö, P., Boller, T., and Wiemken, A. (1993). Disruption of TPS2, the gene encoding the 100-kDa subunit of the trehalose-6-phosphate synthase/phosphatase complex in *Saccharomyces cerevisiae*, causes accumulation of trehalose-6-phosphate and loss of trehalose-6-phosphate phosphatase activity. *Eur J Biochem* 212, 315-323.
- De Virgilio, C., and Loewith, R. (2006). Cell growth control: little eukaryotes make big contributions. *Oncogene* 25, 6392-6415.
- Decker, C.J., and Parker, R. (1993). A turnover pathway for both stable and unstable mRNAs in yeast: evidence for a requirement for deadenylation. *Genes Dev* 7, 1632-1643.
- DeRisi, J.L., Iyer, V.R., and Brown, P.O. (1997). Exploring the metabolic and genetic control of gene expression on a genomic scale. *Science* 278, 680-686.

- Deshmukh, M.V., Jones, B.N., Quang-Dang, D.U., Flinders, J., Floor, S.N., Kim, C., Jemielity, J., Kalek, M., Darzynkiewicz, E., and Gross, J.D. (2008). mRNA decapping is promoted by an RNA-binding channel in Dcp2. *Mol Cell* 29, 324-336.
- Di Como, C.J., and Arndt, K.T. (1996). Nutrients, via the Tor proteins, stimulate the association of Tap42 with type 2A phosphatases. *Genes Dev* 10, 1904-1916.
- Dickson, L.M., and Brown, A.J. (1998). mRNA translation in yeast during entry into stationary phase. *Mol Gen Genet* 259, 282-293.
- Dihazi, H., Kessler, R., and Eschrich, K. (2003). Glucose-induced stimulation of the Ras-cAMP pathway in yeast leads to multiple phosphorylations and activation of 6-phosphofructo-2-kinase. *Biochemistry* 42, 6275-6282.
- Dilova, I., Aronova, S., Chen, J.C., and Powers, T. (2004). Tor signaling and nutrient-based signals converge on Mks1p phosphorylation to regulate expression of Rtg1.Rtg3p-dependent target genes. *J Biol Chem* 279, 46527-46535.
- Dokudovskaya, S., Waharte, F., Schlessinger, A., Pieper, U., Devos, D.P., Cristea, I.M., Williams, R., Salamero, J., Chait, B.T., Sali, A., *et al.* (2011). A conserved coatomer-related complex containing Sec13 and Seh1 dynamically associates with the vacuole in *Saccharomyces cerevisiae*. *Mol Cell Proteomics* 10, M110 006478.
- Dubouloz, F., Deloche, O., Wanke, V., Cameroni, E., and De Virgilio, C. (2005). The TOR and EGO protein complexes orchestrate microautophagy in yeast. *Mol Cell* 19, 15-26.
- Dulubova, I., Horiuchi, A., Snyder, G.L., Girault, J.A., Czernik, A.J., Shao, L., Ramabhadran, R., Greengard, P., and Nairn, A.C. (2001). ARPP-16/ARPP-19: a highly conserved family of cAMP-regulated phosphoproteins. *J Neurochem* 77, 229-238.
- Dunckley, T., and Parker, R. (1999). The DCP2 protein is required for mRNA decapping in *Saccharomyces cerevisiae* and contains a functional MutT motif. *Embo J* 18, 5411-5422.
- Duvel, K., and Broach, J.R. (2004). The role of phosphatases in TOR signaling in yeast. *Curr Top Microbiol Immunol* 279, 19-38.
- Duvel, K., Santhanam, A., Garrett, S., Schneper, L., and Broach, J.R. (2003). Multiple roles of Tap42 in mediating rapamycin-induced transcriptional changes in yeast. *Mol Cell* 11, 1467-1478.
- Eulalio, A., Behm-Ansmant, I., and Izaurralde, E. (2007). P bodies: at the crossroads of post-transcriptional pathways. *Nat Rev Mol Cell Biol* 8, 9-22.
- Evans, D.R., and Stark, M.J. (1997). Mutations in the *Saccharomyces cerevisiae* type 2A protein phosphatase catalytic subunit reveal roles in cell wall integrity, actin cytoskeleton organization and mitosis. *Genetics* 145, 227-241.
- Fischer, N., and Weis, K. (2002). The DEAD box protein Dhh1 stimulates the decapping enzyme Dcp1. *Embo J* 21, 2788-2797.
- Fleischer, T.C., Weaver, C.M., McAfee, K.J., Jennings, J.L., and Link, A.J. (2006). Systematic identification and functional screens of uncharacterized proteins associated with eukaryotic ribosomal complexes. *Genes Dev* 20, 1294-1307.
- Floor, S.N., Jones, B.N., and Gross, J.D. (2008). Control of mRNA decapping by Dcp2: An open and shut case? *RNA Biol* 5, 189-192.
- Floor, S.N., Jones, B.N., Hernandez, G.A., and Gross, J.D. (2010). A split active site couples cap recognition by Dcp2 to activation. *Nat Struct Mol Biol* 17, 1096-1101.
- Fornerod, M., Ohno, M., Yoshida, M., and Mattaj, I.W. (1997). CRM1 is an export receptor for leucine-rich nuclear export signals. *Cell* 90, 1051-1060.

- Francois, J., and Parrou, J.L. (2001). Reserve carbohydrates metabolism in the yeast *Saccharomyces cerevisiae*. *FEMS Microbiol Rev* 25, 125-145.
- Frasca, D., Romero, M., Landin, A.M., Diaz, A., Riley, R.L., and Blomberg, B.B. (2010). Protein phosphatase 2A (PP2A) is increased in old murine B cells and mediates p38 MAPK/tristetraprolin dephosphorylation and E47 mRNA instability. *Mech Ageing Dev* 131, 306-314.
- Freckleton, G., Lippman, S.I., Broach, J.R., and Tavazoie, S. (2009). Microarray profiling of phage-display selections for rapid mapping of transcription factor-DNA interactions. *PLoS Genet* 5, e1000449.
- Fried, H., and Kutay, U. (2003). Nucleocytoplasmic transport: taking an inventory. *Cell Mol Life Sci* 60, 1659-1688.
- Fuge, E.K., Braun, E.L., and Werner-Washburne, M. (1994). Protein synthesis in long-term stationary-phase cultures of *Saccharomyces cerevisiae*. *J Bacteriol* 176, 5802-5813.
- Funakoshi, T., Matsuura, A., Noda, T., and Ohsumi, Y. (1997). Analyses of APG13 gene involved in autophagy in yeast, *Saccharomyces cerevisiae*. *Gene* 192, 207-213.
- Gallelo, F., Portela, P., Moreno, S., and Rossi, S. (2010). Characterization of substrates that have a differential effect on *Saccharomyces cerevisiae* protein kinase A holoenzyme activation. *J Biol Chem* 285, 29770-29779.
- Gancedo, J.M., Mazon, M.J., and Gancedo, C. (1983). Fructose 2,6-bisphosphate activates the cAMP-dependent phosphorylation of yeast fructose-1,6-bisphosphatase in vitro. *J Biol Chem* 258, 5998-5999.
- Gao, M., and Kaiser, C.A. (2006). A conserved GTPase-containing complex is required for intracellular sorting of the general amino-acid permease in yeast. *Nat Cell Biol* 8, 657-667.
- Garneau, N.L., Wilusz, J., and Wilusz, C.J. (2007). The highways and byways of mRNA decay. *Nat Rev Mol Cell Biol* 8, 113-126.
- Garreau, H., Hasan, R.N., Renault, G., Estruch, F., Boy-Marcotte, E., and Jacquet, M. (2000). Hyperphosphorylation of Msn2p and Msn4p in response to heat shock and the diauxic shift is inhibited by cAMP in *Saccharomyces cerevisiae*. *Microbiology* 146 (Pt 9), 2113-2120.
- Gasch, A.P., Spellman, P.T., Kao, C.M., Carmel-Harel, O., Eisen, M.B., Storz, G., Botstein, D., and Brown, P.O. (2000). Genomic expression programs in the response of yeast cells to environmental changes. *Mol Biol Cell* 11, 4241-4257.
- Gasch, A.P., and Werner-Washburne, M. (2002). The genomics of yeast responses to environmental stress and starvation. *Funct Integr Genomics* 2, 181-192.
- Gelperin, D.M., White, M.A., Wilkinson, M.L., Kon, Y., Kung, L.A., Wise, K.J., Lopez-Hoyo, N., Jiang, L., Piccirillo, S., Yu, H., *et al.* (2005). Biochemical and genetic analysis of the yeast proteome with a movable ORF collection. *Genes Dev* 19, 2816-2826.
- Gentry, M.S., and Hallberg, R.L. (2002). Localization of *Saccharomyces cerevisiae* protein phosphatase 2A subunits throughout mitotic cell cycle. *Mol Biol Cell* 13, 3477-3492.
- Georis, I., Feller, A., Tate, J.J., Cooper, T.G., and Dubois, E. (2009). Nitrogen catabolite repression-sensitive transcription as a readout of Tor pathway regulation: the genetic background, reporter gene and GATA factor assayed determine the outcomes. *Genetics* 181, 861-874.
- Georis, I., Tate, J.J., Feller, A., Cooper, T.G., and Dubois, E. (2011). Intranuclear function for protein phosphatase 2A: Pph21 and Pph22 are required for rapamycin-induced GATA factor binding to the DAL5 promoter in yeast. *Mol Cell Biol* 31, 92-104.
- Gharbi-Ayachi, A., Labbe, J.C., Burgess, A., Vigneron, S., Strub, J.M., Brioude, E., Van-Dorselaer, A., Castro, A., and Lorca, T. (2010). The substrate of Greatwall kinase, Arpp19, controls mitosis by inhibiting protein phosphatase 2A. *Science* 330, 1673-1677.

- Girault, J.A., Horiuchi, A., Gustafson, E.L., Rosen, N.L., and Greengard, P. (1990). Differential expression of ARPP-16 and ARPP-19, two highly related cAMP-regulated phosphoproteins, one of which is specifically associated with dopamine-innervated brain regions. *J Neurosci* *10*, 1124-1133.
- Gong, R., Li, L., Liu, Y., Wang, P., Yang, H., Wang, L., Cheng, J., Guan, K.L., and Xu, Y. (2011). Crystal structure of the Gtr1p-Gtr2p complex reveals new insights into the amino acid-induced TORC1 activation. *Genes Dev* *25*, 1668-1673.
- Gorner, W., Durchschlag, E., Martinez-Pastor, M.T., Estruch, F., Ammerer, G., Hamilton, B., Ruis, H., and Schuller, C. (1998). Nuclear localization of the C2H2 zinc finger protein Msn2p is regulated by stress and protein kinase A activity. *Genes Dev* *12*, 586-597.
- Gorner, W., Durchschlag, E., Wolf, J., Brown, E.L., Ammerer, G., Ruis, H., and Schuller, C. (2002). Acute glucose starvation activates the nuclear localization signal of a stress-specific yeast transcription factor. *Embo J* *21*, 135-144.
- Griffioen, G., Anghileri, P., Imre, E., Baroni, M.D., and Ruis, H. (2000). Nutritional control of nucleocytoplasmic localization of cAMP-dependent protein kinase catalytic and regulatory subunits in *Saccharomyces cerevisiae*. *J Biol Chem* *275*, 1449-1456.
- Griffioen, G., Branduardi, P., Ballarini, A., Anghileri, P., Norbeck, J., Baroni, M.D., and Ruis, H. (2001). Nucleocytoplasmic distribution of budding yeast protein kinase A regulatory subunit Bcy1 requires Zds1 and is regulated by Yak1-dependent phosphorylation of its targeting domain. *Mol Cell Biol* *21*, 511-523.
- Gross, A., Winograd, S., Marbach, I., and Levitzki, A. (1999). The N-terminal half of Cdc25 is essential for processing glucose signaling in *Saccharomyces cerevisiae*. *Biochemistry* *38*, 13252-13262.
- Gross, E., Goldberg, D., and Levitzki, A. (1992). Phosphorylation of the *S. cerevisiae* Cdc25 in response to glucose results in its dissociation from Ras. *Nature* *360*, 762-765.
- Hahn, S., Maurer, P., Caesar, S., and Schlenstedt, G. (2008). Classical NLS proteins from *Saccharomyces cerevisiae*. *J Mol Biol* *379*, 678-694.
- Hall, D.B., Wade, J.T., and Struhl, K. (2006). An HMG protein, Hmo1, associates with promoters of many ribosomal protein genes and throughout the rRNA gene locus in *Saccharomyces cerevisiae*. *Mol Cell Biol* *26*, 3672-3679.
- Hall, D.D., Markwardt, D.D., Parviz, F., and Heideman, W. (1998). Regulation of the Cln3-Cdc28 kinase by cAMP in *Saccharomyces cerevisiae*. *Embo J* *17*, 4370-4378.
- Han, J.M., Jeong, S.J., Park, M.C., Kim, G., Kwon, N.H., Kim, H.K., Ha, S.H., Ryu, S.H., and Kim, S. (2012). Leucyl-tRNA Synthetase Is an Intracellular Leucine Sensor for the mTORC1-Signaling Pathway. *Cell* *149*, 410-424.
- Hardwick, J.S., Kuruvilla, F.G., Tong, J.K., Shamji, A.F., and Schreiber, S.L. (1999). Rapamycin-modulated transcription defines the subset of nutrient-sensitive signaling pathways directly controlled by the Tor proteins. *Proc Natl Acad Sci U S A* *96*, 14866-14870.
- Hardy, T.A., and Roach, P.J. (1993). Control of yeast glycogen synthase-2 by COOH-terminal phosphorylation. *J Biol Chem* *268*, 23799-23805.
- Hartwell, L.H. (1974). *Saccharomyces cerevisiae* cell cycle. *Bacteriol Rev* *38*, 164-198.
- Haruki, H., Nishikawa, J., and Laemmli, U.K. (2008). The anchor-away technique: rapid, conditional establishment of yeast mutant phenotypes. *Mol Cell* *31*, 925-932.
- Heitman, J., Movva, N.R., and Hall, M.N. (1991). Targets for cell cycle arrest by the immunosuppressant rapamycin in yeast. *Science* *253*, 905-909.

- Hinnebusch, A.G. (2005). Translational regulation of GCN4 and the general amino acid control of yeast. *Annu Rev Microbiol* 59, 407-450.
- Holstege, F.C., Jennings, E.G., Wyrick, J.J., Lee, T.I., Hengartner, C.J., Green, M.R., Golub, T.R., Lander, E.S., and Young, R.A. (1998). Dissecting the regulatory circuitry of a eukaryotic genome. *Cell* 95, 717-728.
- Howard, S.C., Budovskaya, Y.V., Chang, Y.W., and Herman, P.K. (2002). The C-terminal domain of the largest subunit of RNA polymerase II is required for stationary phase entry and functionally interacts with the Ras/PKA signaling pathway. *J Biol Chem* 277, 19488-19497.
- Howard, S.C., Hester, A., and Herman, P.K. (2003). The Ras/PKA signaling pathway may control RNA polymerase II elongation via the Spt4p/Spt5p complex in *Saccharomyces cerevisiae*. *Genetics* 165, 1059-1070.
- Hoyle, N.P., Castelli, L.M., Campbell, S.G., Holmes, L.E., and Ashe, M.P. (2007). Stress-dependent relocalization of translationally primed mRNPs to cytoplasmic granules that are kinetically and spatially distinct from P-bodies. *J Cell Biol* 179, 65-74.
- Hsu, C.L., and Stevens, A. (1993). Yeast cells lacking 5'→3' exoribonuclease 1 contain mRNA species that are poly(A) deficient and partially lack the 5' cap structure. *Mol Cell Biol* 13, 4826-4835.
- Hu, W., Sweet, T.J., Chamnongpol, S., Baker, K.E., and Collier, J. (2009). Co-translational mRNA decay in *Saccharomyces cerevisiae*. *Nature* 461, 225-229.
- Hu, Y., Liu, E., Bai, X., and Zhang, A. (2010). The localization and concentration of the PDE2-encoded high-affinity cAMP phosphodiesterase is regulated by cAMP-dependent protein kinase A in the yeast *Saccharomyces cerevisiae*. *FEMS Yeast Res* 10, 177-187.
- Huang, D., Friesen, H., and Andrews, B. (2007). Pho85, a multifunctional cyclin-dependent protein kinase in budding yeast. *Mol Microbiol* 66, 303-314.
- Huang, D., Moffat, J., Wilson, W.A., Moore, L., Cheng, C., Roach, P.J., and Andrews, B. (1998). Cyclin partners determine Pho85 protein kinase substrate specificity in vitro and in vivo: control of glycogen biosynthesis by Pcl8 and Pcl10. *Mol Cell Biol* 18, 3289-3299.
- Huber, A., Bodenmiller, B., Uotila, A., Stahl, M., Wanka, S., Gerrits, B., Aebersold, R., and Loewith, R. (2009). Characterization of the rapamycin-sensitive phosphoproteome reveals that Sch9 is a central coordinator of protein synthesis. *Genes Dev* 23, 1929-1943.
- Humphrey, E.L., Shamji, A.F., Bernstein, B.E., and Schreiber, S.L. (2004). Rpd3p relocation mediates a transcriptional response to rapamycin in yeast. *Chem Biol* 11, 295-299.
- Irwin, N., Chao, S., Goritchenko, L., Horiuchi, A., Greengard, P., Nairn, A.C., and Benowitz, L.I. (2002). Nerve growth factor controls GAP-43 mRNA stability via the phosphoprotein ARPP-19. *Proc Natl Acad Sci U S A* 99, 12427-12431.
- Jacinto, E., Guo, B., Arndt, K.T., Schmelzle, T., and Hall, M.N. (2001). TIP41 interacts with TAP42 and negatively regulates the TOR signaling pathway. *Mol Cell* 8, 1017-1026.
- Jamieson, D.J. (1992). *Saccharomyces cerevisiae* has distinct adaptive responses to both hydrogen peroxide and menadione. *J Bacteriol* 174, 6678-6681.
- Jiang, Y. (2006). Regulation of the cell cycle by protein phosphatase 2A in *Saccharomyces cerevisiae*. *Microbiol Mol Biol Rev* 70, 440-449.
- Jiang, Y., and Broach, J.R. (1999). Tor proteins and protein phosphatase 2A reciprocally regulate Tap42 in controlling cell growth in yeast. *Embo J* 18, 2782-2792.
- Jinek, M., Coyle, S.M., and Doudna, J.A. (2011). Coupled 5' nucleotide recognition and processivity in Xrm1-mediated mRNA decay. *Mol Cell* 41, 600-608.

- Johnson, D.S., Mortazavi, A., Myers, R.M., and Wold, B. (2007). Genome-wide mapping of in vivo protein-DNA interactions. *Science* *316*, 1497-1502.
- Johnston, S.D., Enomoto, S., Schneper, L., McClellan, M.C., Twu, F., Montgomery, N.D., Haney, S.A., Broach, J.R., and Berman, J. (2001). CAC3(MSI1) suppression of RAS2(G19V) is independent of chromatin assembly factor I and mediated by NPR1. *Mol Cell Biol* *21*, 1784-1794.
- Ju, Q., and Warner, J.R. (1994). Ribosome synthesis during the growth cycle of *Saccharomyces cerevisiae*. *Yeast* *10*, 151-157.
- Kafadar, K.A., and Cyert, M.S. (2004). Integration of stress responses: modulation of calcineurin signaling in *Saccharomyces cerevisiae* by protein kinase A. *Eukaryot Cell* *3*, 1147-1153.
- Kaffman, A., Herskowitz, I., Tjian, R., and O'Shea, E.K. (1994). Phosphorylation of the transcription factor PHO4 by a cyclin-CDK complex, PHO80-PHO85. *Science* *263*, 1153-1156.
- Kaida, D., Yashiroda, H., Toh-e, A., and Kikuchi, Y. (2002). Yeast Whi2 and Psr1-phosphatase form a complex and regulate STRE-mediated gene expression. *Genes Cells* *7*, 543-552.
- Kaldis, P., Pitluk, Z.W., Bany, I.A., Enke, D.A., Wagner, M., Winter, E., and Solomon, M.J. (1998). Localization and regulation of the cdk-activating kinase (Cak1p) from budding yeast. *J Cell Sci* *111* (Pt 24), 3585-3596.
- Kamada, Y., Funakoshi, T., Shintani, T., Nagano, K., Ohsumi, M., and Ohsumi, Y. (2000). Tor-mediated induction of autophagy via an Apg1 protein kinase complex. *J Cell Biol* *150*, 1507-1513.
- Kamada, Y., Yoshino, K., Kondo, C., Kawamata, T., Oshiro, N., Yonezawa, K., and Ohsumi, Y. (2010). Tor directly controls the Atg1 kinase complex to regulate autophagy. *Mol Cell Biol* *30*, 1049-1058.
- Kedersha, N., Stoecklin, G., Ayodele, M., Yacono, P., Lykke-Andersen, J., Fritzler, M.J., Scheuner, D., Kaufman, R.J., Golan, D.E., and Anderson, P. (2005). Stress granules and processing bodies are dynamically linked sites of mRNP remodeling. *J Cell Biol* *169*, 871-884.
- Kepler-Ross, S., Noffz, C., and Dean, N. (2008). A new purple fluorescent color marker for genetic studies in *Saccharomyces cerevisiae* and *Candida albicans*. *Genetics* *179*, 705-710.
- Kim, E., Goraksha-Hicks, P., Li, L., Neufeld, T.P., and Guan, K.L. (2008). Regulation of TORC1 by Rag GTPases in nutrient response. *Nat Cell Biol* *10*, 935-945.
- Kim, J.H., and Johnston, M. (2006). Two glucose-sensing pathways converge on Rgt1 to regulate expression of glucose transporter genes in *Saccharomyces cerevisiae*. *J Biol Chem* *281*, 26144-26149.
- Kim, K.C., Oh, W.J., Ko, K.H., Shin, C.Y., and Wells, D.G. (2011). Cyclin B1 expression regulated by cytoplasmic polyadenylation element binding protein in astrocytes. *J Neurosci* *31*, 12118-12128.
- Klein, C., and Struhl, K. (1994). Protein kinase A mediates growth-regulated expression of yeast ribosomal protein genes by modulating RAPI transcriptional activity. *Mol Cell Biol* *14*, 1920-1928.
- Klosinska, M.M., Crutchfield, C.A., Bradley, P.H., Rabinowitz, J.D., and Broach, J.R. (2011). Yeast cells can access distinct quiescent states. *Genes Dev* *25*, 336-349.
- Kogan, K., Spear, E.D., Kaiser, C.A., and Fass, D. (2010). Structural conservation of components in the amino acid sensing branch of the TOR pathway in yeast and mammals. *J Mol Biol* *402*, 388-398.
- Komarnitsky, P., Cho, E.J., and Buratowski, S. (2000). Different phosphorylated forms of RNA polymerase II and associated mRNA processing factors during transcription. *Genes Dev* *14*, 2452-2460.
- Komeili, A., and O'Shea, E.K. (2000). Nuclear transport and transcription. *Curr Opin Cell Biol* *12*, 355-360.

- Komeili, A., Wedaman, K.P., O'Shea, E.K., and Powers, T. (2000). Mechanism of metabolic control. Target of rapamycin signaling links nitrogen quality to the activity of the Rtg1 and Rtg3 transcription factors. *J Cell Biol* *151*, 863-878.
- Kuret, J., Johnson, K.E., Nicolette, C., and Zoller, M.J. (1988). Mutagenesis of the regulatory subunit of yeast cAMP-dependent protein kinase. Isolation of site-directed mutants with altered binding affinity for catalytic subunit. *J Biol Chem* *263*, 9149-9154.
- Lange, A., Mills, R.E., Lange, C.J., Stewart, M., Devine, S.E., and Corbett, A.H. (2007). Classical nuclear localization signals: definition, function, and interaction with importin alpha. *J Biol Chem* *282*, 5101-5105.
- Laporte, D., Lebaudy, A., Sahin, A., Pinson, B., Ceschin, J., Daignan-Fornier, B., and Sagot, I. (2011). Metabolic status rather than cell cycle signals control quiescence entry and exit. *J Cell Biol* *192*, 949-957.
- Lee, J., Moir, R.D., McIntosh, K.B., and Willis, I.M. (2012). TOR Signaling Regulates Ribosome and tRNA Synthesis via LAMMER/Clk and GSK-3 Family Kinases. *Mol Cell* *45*, 836-843.
- Lee, P., Cho, B.R., Joo, H.S., and Hahn, J.S. (2008). Yeast Yak1 kinase, a bridge between PKA and stress-responsive transcription factors, Hsf1 and Msn2/Msn4. *Mol Microbiol* *70*, 882-895.
- Lee, P., Paik, S.M., Shin, C.S., Huh, W.K., and Hahn, J.S. (2011). Regulation of yeast Yak1 kinase by PKA and autophosphorylation-dependent 14-3-3 binding. *Mol Microbiol* *79*, 633-646.
- Leitner, A., Walzthoeni, T., Kahraman, A., Herzog, F., Rinner, O., Beck, M., and Aebersold, R. (2010). Probing native protein structures by chemical cross-linking, mass spectrometry, and bioinformatics. *Mol Cell Proteomics* *9*, 1634-1649.
- Lempiainen, H., and Shore, D. (2009). Growth control and ribosome biogenesis. *Curr Opin Cell Biol* *21*, 855-863.
- Lempiainen, H., Uotila, A., Urban, J., Dohnal, I., Ammerer, G., Loewith, R., and Shore, D. (2009). Sfp1 interaction with TORC1 and Mrs6 reveals feedback regulation on TOR signaling. *Mol Cell* *33*, 704-716.
- Li, H., Tsang, C.K., Watkins, M., Bertram, P.G., and Zheng, X.F. (2006). Nutrient regulates Tor1 nuclear localization and association with rDNA promoter. *Nature* *442*, 1058-1061.
- Li, Z., Vizeacoumar, F.J., Bahr, S., Li, J., Warringer, J., Vizeacoumar, F.S., Min, R., Vandersluis, B., Bellay, J., Devit, M., *et al.* (2011). Systematic exploration of essential yeast gene function with temperature-sensitive mutants. *Nat Biotechnol* *29*, 361-367.
- Liko, D., Slattery, M.G., and Heideman, W. (2007). Stb3 binds to ribosomal RNA processing element motifs that control transcriptional responses to growth in *Saccharomyces cerevisiae*. *J Biol Chem* *282*, 26623-26628.
- Lillie, S.H., and Pringle, J.R. (1980). Reserve carbohydrate metabolism in *Saccharomyces cerevisiae*: responses to nutrient limitation. *J Bacteriol* *143*, 1384-1394.
- Lin, F.C., and Arndt, K.T. (1995). The role of *Saccharomyces cerevisiae* type 2A phosphatase in the actin cytoskeleton and in entry into mitosis. *Embo J* *14*, 2745-2759.
- Lin, K., Rath, V.L., Dai, S.C., Fletterick, R.J., and Hwang, P.K. (1996). A protein phosphorylation switch at the conserved allosteric site in GP. *Science* *273*, 1539-1542.
- Lippman, S.I., and Broach, J.R. (2009). Protein kinase A and TORC1 activate genes for ribosomal biogenesis by inactivating repressors encoded by Dot6 and its homolog Tod6. *Proc Natl Acad Sci U S A* *106*, 19928-19933.
- Liu, H., Rodgers, N.D., Jiao, X., and Kiledjian, M. (2002). The scavenger mRNA decapping enzyme DcpS is a member of the HIT family of pyrophosphatases. *Embo J* *21*, 4699-4708.
- Liu, Z., and Butow, R.A. (2006). Mitochondrial retrograde signaling. *Annu Rev Genet* *40*, 159-185.

- Loewith, R., and Hall, M.N. (2011). Target of rapamycin (TOR) in nutrient signaling and growth control. *Genetics* *189*, 1177-1201.
- Loewith, R., Jacinto, E., Wullschleger, S., Lorberg, A., Crespo, J.L., Bonenfant, D., Oppliger, W., Jenoe, P., and Hall, M.N. (2002). Two TOR complexes, only one of which is rapamycin sensitive, have distinct roles in cell growth control. *Mol Cell* *10*, 457-468.
- Ma, P., Wera, S., Van Dijck, P., and Thevelein, J.M. (1999). The PDE1-encoded low-affinity phosphodiesterase in the yeast *Saccharomyces cerevisiae* has a specific function in controlling agonist-induced cAMP signaling. *Mol Biol Cell* *10*, 91-104.
- MacGurn, J.A., Hsu, P.C., Smolka, M.B., and Emr, S.D. (2011). TORC1 regulates endocytosis via Npr1-mediated phosphoinhibition of a ubiquitin ligase adaptor. *Cell* *147*, 1104-1117.
- Malys, N., Carroll, K., Miyan, J., Tollervy, D., and McCarthy, J.E. (2004). The 'scavenger' m7GpppX pyrophosphatase activity of Dcs1 modulates nutrient-induced responses in yeast. *Nucleic Acids Res* *32*, 3590-3600.
- Mangus, D.A., Amrani, N., and Jacobson, A. (1998). Pbp1p, a factor interacting with *Saccharomyces cerevisiae* poly(A)-binding protein, regulates polyadenylation. *Mol Cell Biol* *18*, 7383-7396.
- Mangus, D.A., Evans, M.C., Agrin, N.S., Smith, M., Gongidi, P., and Jacobson, A. (2004a). Positive and negative regulation of poly(A) nuclease. *Mol Cell Biol* *24*, 5521-5533.
- Mangus, D.A., Smith, M.M., McSweeney, J.M., and Jacobson, A. (2004b). Identification of factors regulating poly(A) tail synthesis and maturation. *Mol Cell Biol* *24*, 4196-4206.
- Marion, R.M., Regev, A., Segal, E., Barash, Y., Koller, D., Friedman, N., and O'Shea, E.K. (2004). Sfp1 is a stress- and nutrient-sensitive regulator of ribosomal protein gene expression. *Proc Natl Acad Sci U S A* *101*, 14315-14322.
- Marnef, A., and Standart, N. (2010). Pat1 proteins: a life in translation, translation repression and mRNA decay. *Biochem Soc Trans* *38*, 1602-1607.
- Martin, D.E., Soulard, A., and Hall, M.N. (2004). TOR regulates ribosomal protein gene expression via PKA and the Forkhead transcription factor FHL1. *Cell* *119*, 969-979.
- Mazur, P., Morin, N., Baginsky, W., el-Sherbeini, M., Clemas, J.A., Nielsen, J.B., and Foor, F. (1995). Differential expression and function of two homologous subunits of yeast 1,3-beta-D-glucan synthase. *Mol Cell Biol* *15*, 5671-5681.
- Measday, V., Moore, L., Retnakaran, R., Lee, J., Donoviel, M., Neiman, A.M., and Andrews, B. (1997). A family of cyclin-like proteins that interact with the Pho85 cyclin-dependent kinase. *Mol Cell Biol* *17*, 1212-1223.
- Miller, J.E., and Reese, J.C. (2012). Ccr4-Not complex: the control freak of eukaryotic cells. *Crit Rev Biochem Mol Biol*.
- Mochida, S., and Hunt, T. (2012). Protein phosphatases and their regulation in the control of mitosis. *EMBO Rep*.
- Mochida, S., Maslen, S.L., Skehel, M., and Hunt, T. (2010). Greatwall phosphorylates an inhibitor of protein phosphatase 2A that is essential for mitosis. *Science* *330*, 1670-1673.
- Mockli, N., Deplazes, A., Hassa, P.O., Zhang, Z., Peter, M., Hottiger, M.O., Stagljar, I., and Auerbach, D. (2007). Yeast split-ubiquitin-based cytosolic screening system to detect interactions between transcriptionally active proteins. *Biotechniques* *42*, 725-730.
- Moir, R.D., Lee, J., Haeusler, R.A., Desai, N., Engelke, D.R., and Willis, I.M. (2006). Protein kinase A regulates RNA polymerase III transcription through the nuclear localization of Maf1. *Proc Natl Acad Sci U S A* *103*, 15044-15049.

- Moriya, H., Shimizu-Yoshida, Y., Omori, A., Iwashita, S., Katoh, M., and Sakai, A. (2001). Yak1p, a DYRK family kinase, translocates to the nucleus and phosphorylates yeast Pop2p in response to a glucose signal. *Genes Dev* 15, 1217-1228.
- Muhlrad, D., Decker, C.J., and Parker, R. (1994). Deadenylation of the unstable mRNA encoded by the yeast MFA2 gene leads to decapping followed by 5'→3' digestion of the transcript. *Genes Dev* 8, 855-866.
- Muhlrad, D., Decker, C.J., and Parker, R. (1995). Turnover mechanisms of the stable yeast PGK1 mRNA. *Mol Cell Biol* 15, 2145-2156.
- Murphy, M.W., Olson, B.L., and Siliciano, P.G. (2004). The yeast splicing factor Prp40p contains functional leucine-rich nuclear export signals that are essential for splicing. *Genetics* 166, 53-65.
- Neklesa, T.K., and Davis, R.W. (2009). A genome-wide screen for regulators of TORC1 in response to amino acid starvation reveals a conserved Npr2/3 complex. *PLoS Genet* 5, e1000515.
- Neuman-Silberberg, F.S., Bhattacharya, S., and Broach, J.R. (1995). Nutrient availability and the RAS/cyclic AMP pathway both induce expression of ribosomal protein genes in *Saccharomyces cerevisiae* but by different mechanisms. *Mol Cell Biol* 15, 3187-3196.
- Nishizawa, M., Katou, Y., Shirahige, K., and Toh-e, A. (2004). Yeast Pho85 kinase is required for proper gene expression during the diauxic shift. *Yeast* 21, 903-918.
- Nissan, T., Rajyaguru, P., She, M., Song, H., and Parker, R. (2010). Decapping activators in *Saccharomyces cerevisiae* act by multiple mechanisms. *Mol Cell* 39, 773-783.
- O'Donnell, A.F., Apffel, A., Gardner, R.G., and Cyert, M.S. (2010). Alpha-arrestins Aly1 and Aly2 regulate intracellular trafficking in response to nutrient signaling. *Mol Biol Cell* 21, 3552-3566.
- O'Neill, E.M., Kaffman, A., Jolly, E.R., and O'Shea, E.K. (1996). Regulation of PHO4 nuclear localization by the PHO80-PHO85 cyclin-CDK complex. *Science* 271, 209-212.
- Oficjalska-Pham, D., Harismendy, O., Smagowicz, W.J., Gonzalez de Peredo, A., Boguta, M., Sentenac, A., and Lefebvre, O. (2006). General repression of RNA polymerase III transcription is triggered by protein phosphatase type 2A-mediated dephosphorylation of Maf1. *Mol Cell* 22, 623-632.
- Ostapenko, D., and Solomon, M.J. (2005). Phosphorylation by Cak1 regulates the C-terminal domain kinase Ctk1 in *Saccharomyces cerevisiae*. *Mol Cell Biol* 25, 3906-3913.
- Padilla, P.A., Fuge, E.K., Crawford, M.E., Errett, A., and Werner-Washburne, M. (1998). The highly conserved, coregulated SNO and SNZ gene families in *Saccharomyces cerevisiae* respond to nutrient limitation. *J Bacteriol* 180, 5718-5726.
- Panni, S., Landgraf, C., Volkmer-Engert, R., Cesareni, G., and Castagnoli, L. (2008). Role of 14-3-3 proteins in the regulation of neutral trehalase in the yeast *Saccharomyces cerevisiae*. *FEMS Yeast Res* 8, 53-63.
- Parker, R., and Sheth, U. (2007). P bodies and the control of mRNA translation and degradation. *Mol Cell* 25, 635-646.
- Paz, I., and Choder, M. (2001). Eukaryotic translation initiation factor 4E-dependent translation is not essential for survival of starved yeast cells. *J Bacteriol* 183, 4477-4483.
- Pedruzzi, I., Burckert, N., Egger, P., and De Virgilio, C. (2000). *Saccharomyces cerevisiae* Ras/cAMP pathway controls post-diauxic shift element-dependent transcription through the zinc finger protein Gis1. *Embo J* 19, 2569-2579.
- Pedruzzi, I., Dubouloz, F., Cameroni, E., Wanke, V., Roosen, J., Winderickx, J., and De Virgilio, C. (2003). TOR and PKA signaling pathways converge on the protein kinase Rim15 to control entry into G0. *Mol Cell* 12, 1607-1613.

- Peeters, T., Louwet, W., Gelade, R., Nauwelaers, D., Thevelein, J.M., and Versele, M. (2006). Kelch-repeat proteins interacting with the Galpha protein Gpa2 bypass adenylate cyclase for direct regulation of protein kinase A in yeast. *Proc Natl Acad Sci U S A* *103*, 13034-13039.
- Peeters, T., Versele, M., and Thevelein, J.M. (2007). Directly from Galpha to protein kinase A: the kelch repeat protein bypass of adenylate cyclase. *Trends Biochem Sci* *32*, 547-554.
- Pereira, M.D., Eleutherio, E.C., and Panek, A.D. (2001). Acquisition of tolerance against oxidative damage in *Saccharomyces cerevisiae*. *BMC Microbiol* *1*, 11.
- Pestov, D.G., and Shcherbik, N. (2012). Rapid cytoplasmic turnover of yeast ribosomes in response to rapamycin inhibition of TOR. *Mol Cell Biol*.
- Pilkington, G.R., and Parker, R. (2008). Pat1 contains distinct functional domains that promote P-body assembly and activation of decapping. *Mol Cell Biol* *28*, 1298-1312.
- Portela, P., Howell, S., Moreno, S., and Rossi, S. (2002). In vivo and in vitro phosphorylation of two isoforms of yeast pyruvate kinase by protein kinase A. *J Biol Chem* *277*, 30477-30487.
- Portela, P., Moreno, S., and Rossi, S. (2006). Characterization of yeast pyruvate kinase 1 as a protein kinase A substrate, and specificity of the phosphorylation site sequence in the whole protein. *Biochem J* *396*, 117-126.
- Powers, T., and Walter, P. (1999). Regulation of ribosome biogenesis by the rapamycin-sensitive TOR-signaling pathway in *Saccharomyces cerevisiae*. *Mol Biol Cell* *10*, 987-1000.
- Ptacek, J., Devgan, G., Michaud, G., Zhu, H., Zhu, X., Fasolo, J., Guo, H., Jona, G., Breitkreutz, A., Sopko, R., *et al.* (2005). Global analysis of protein phosphorylation in yeast. *Nature* *438*, 679-684.
- Radonjic, M., Andrau, J.C., Lijnzaad, P., Kemmeren, P., Kockelkorn, T.T., van Leenen, D., van Berkum, N.L., and Holstege, F.C. (2005). Genome-wide analyses reveal RNA polymerase II located upstream of genes poised for rapid response upon *S. cerevisiae* stationary phase exit. *Mol Cell* *18*, 171-183.
- Ramachandran, V., and Herman, P.K. (2011). Antagonistic interactions between the cAMP-dependent protein kinase and Tor signaling pathways modulate cell growth in *Saccharomyces cerevisiae*. *Genetics* *187*, 441-454.
- Ramachandran, V., Shah, K.H., and Herman, P.K. (2011). The cAMP-dependent protein kinase signaling pathway is a key regulator of P body foci formation. *Mol Cell* *43*, 973-981.
- Ramer, S.W., Elledge, S.J., and Davis, R.W. (1992). Dominant genetics using a yeast genomic library under the control of a strong inducible promoter. *Proc Natl Acad Sci U S A* *89*, 11589-11593.
- Reid, J.L., Iyer, V.R., Brown, P.O., and Struhl, K. (2000). Coordinate regulation of yeast ribosomal protein genes is associated with targeted recruitment of Esa1 histone acetylase. *Mol Cell* *6*, 1297-1307.
- Reinders, A., Burckert, N., Boller, T., Wiemken, A., and De Virgilio, C. (1998). *Saccharomyces cerevisiae* cAMP-dependent protein kinase controls entry into stationary phase through the Rim15p protein kinase. *Genes Dev* *12*, 2943-2955.
- Reinke, A., Anderson, S., McCaffery, J.M., Yates, J., 3rd, Aronova, S., Chu, S., Fairclough, S., Iverson, C., Wedaman, K.P., and Powers, T. (2004). TOR complex 1 includes a novel component, Tco89p (YPL180w), and cooperates with Ssd1p to maintain cellular integrity in *Saccharomyces cerevisiae*. *J Biol Chem* *279*, 14752-14762.
- Rittenhouse, J., Moberly, L., and Marcus, F. (1987). Phosphorylation in vivo of yeast (*Saccharomyces cerevisiae*) fructose-1,6-bisphosphatase at the cyclic AMP-dependent site. *J Biol Chem* *262*, 10114-10119.
- Roberts, D.N., Wilson, B., Huff, J.T., Stewart, A.J., and Cairns, B.R. (2006). Dephosphorylation and genome-wide association of Maf1 with Pol III-transcribed genes during repression. *Mol Cell* *22*, 633-644.

- Robertson, L.S., and Fink, G.R. (1998). The three yeast A kinases have specific signaling functions in pseudohyphal growth. *Proc Natl Acad Sci U S A* 95, 13783-13787.
- Rohde, J.R., and Cardenas, M.E. (2003). The tor pathway regulates gene expression by linking nutrient sensing to histone acetylation. *Mol Cell Biol* 23, 629-635.
- Rolland, F., Wanke, V., Cauwenberg, L., Ma, P., Boles, E., Vanoni, M., de Winder, J.H., Thevelein, J.M., and Winderickx, J. (2001). The role of hexose transport and phosphorylation in cAMP signalling in the yeast *Saccharomyces cerevisiae*. *FEMS Yeast Res* 1, 33-45.
- Romano, P.R., Garcia-Barrio, M.T., Zhang, X., Wang, Q., Taylor, D.R., Zhang, F., Herring, C., Mathews, M.B., Qin, J., and Hinnebusch, A.G. (1998). Autophosphorylation in the activation loop is required for full kinase activity in vivo of human and yeast eukaryotic initiation factor 2alpha kinases PKR and GCN2. *Mol Cell Biol* 18, 2282-2297.
- Ronne, H., Carlberg, M., Hu, G.Z., and Nehlin, J.O. (1991). Protein phosphatase 2A in *Saccharomyces cerevisiae*: effects on cell growth and bud morphogenesis. *Mol Cell Biol* 11, 4876-4884.
- Rossio, V., and Yoshida, S. (2011). Spatial regulation of Cdc55-PP2A by Zds1/Zds2 controls mitotic entry and mitotic exit in budding yeast. *J Cell Biol* 193, 445-454.
- Rudra, D., Zhao, Y., and Warner, J.R. (2005). Central role of Ifh1p-Fhl1p interaction in the synthesis of yeast ribosomal proteins. *Embo J* 24, 533-542.
- Ruggieri, R., Tanaka, K., Nakafuku, M., Kaziro, Y., Toh-e, A., and Matsumoto, K. (1989). MS11, a negative regulator of the RAS-cAMP pathway in *Saccharomyces cerevisiae*. *Proc Natl Acad Sci U S A* 86, 8778-8782.
- Saldanha, A.J., Brauer, M.J., and Botstein, D. (2004). Nutritional homeostasis in batch and steady-state culture of yeast. *Mol Biol Cell* 15, 4089-4104.
- Sambrook, J., and Russel, D.W. (2001). *Molecular cloning: a laboratory manual* (Cold Spring Harbor, Cold Spring Harbor Laboratory Press).
- Sancak, Y., Peterson, T.R., Shaul, Y.D., Lindquist, R.A., Thoreen, C.C., Bar-Peled, L., and Sabatini, D.M. (2008). The Rag GTPases bind raptor and mediate amino acid signaling to mTORC1. *Science* 320, 1496-1501.
- Santhanam, A., Hartley, A., Duvel, K., Broach, J.R., and Garrett, S. (2004). PP2A phosphatase activity is required for stress and Tor kinase regulation of yeast stress response factor Msn2p. *Eukaryot Cell* 3, 1261-1271.
- Schawalder, S.B., Kabani, M., Howald, I., Choudhury, U., Werner, M., and Shore, D. (2004). Growth-regulated recruitment of the essential yeast ribosomal protein gene activator Ifh1. *Nature* 432, 1058-1061.
- Schlenstedt, G., Smirnova, E., Deane, R., Solsbacher, J., Kutay, U., Gorlich, D., Ponstingl, H., and Bischoff, F.R. (1997). Yrb4p, a yeast ran-GTP-binding protein involved in import of ribosomal protein L25 into the nucleus. *Embo J* 16, 6237-6249.
- Schmidt, A., Beck, T., Koller, A., Kunz, J., and Hall, M.N. (1998). The TOR nutrient signalling pathway phosphorylates NPR1 and inhibits turnover of the tryptophan permease. *Embo J* 17, 6924-6931.
- Segev, N., and Hay, N. (2012). Hijacking Leucyl-tRNA Synthetase for Amino Acid-Dependent Regulation of TORC1. *Mol Cell* 46, 4-6.
- Sekito, T., Liu, Z., Thornton, J., and Butow, R.A. (2002). RTG-dependent mitochondria-to-nucleus signaling is regulated by MKS1 and is linked to formation of yeast prion [URE3]. *Mol Biol Cell* 13, 795-804.
- Shamji, A.F., Kuruvilla, F.G., and Schreiber, S.L. (2000). Partitioning the transcriptional program induced by rapamycin among the effectors of the Tor proteins. *Curr Biol* 10, 1574-1581.
- Shenhar, G., and Kassir, Y. (2001). A positive regulator of mitosis, Sok2, functions as a negative regulator of meiosis in *Saccharomyces cerevisiae*. *Mol Cell Biol* 21, 1603-1612.

- Sherlock, G., and Rosamond, J. (1993). Starting to cycle: G1 controls regulating cell division in budding yeast. *J Gen Microbiol* *139*, 2531-2541.
- Sheth, U., and Parker, R. (2003). Decapping and decay of messenger RNA occur in cytoplasmic processing bodies. *Science* *300*, 805-808.
- Shi, L., Sutter, B.M., Ye, X., and Tu, B.P. (2010). Trehalose is a key determinant of the quiescent metabolic state that fuels cell cycle progression upon return to growth. *Mol Biol Cell* *21*, 1982-1990.
- Singer, M.A., and Lindquist, S. (1998). Multiple effects of trehalose on protein folding in vitro and in vivo. *Mol Cell* *1*, 639-648.
- Smets, B., Ghillebert, R., De Snijder, P., Binda, M., Swinnen, E., De Virgilio, C., and Winderickx, J. (2010). Life in the midst of scarcity: adaptations to nutrient availability in *Saccharomyces cerevisiae*. *Curr Genet* *56*, 1-32.
- Sneddon, A.A., Cohen, P.T., and Stark, M.J. (1990). *Saccharomyces cerevisiae* protein phosphatase 2A performs an essential cellular function and is encoded by two genes. *Embo J* *9*, 4339-4346.
- Sopko, R., Huang, D., Preston, N., Chua, G., Papp, B., Kafadar, K., Snyder, M., Oliver, S.G., Cyert, M., Hughes, T.R., *et al.* (2006). Mapping pathways and phenotypes by systematic gene overexpression. *Mol Cell* *21*, 319-330.
- Soulard, A., Cremonesi, A., Moes, S., Schutz, F., Jenö, P., and Hall, M.N. (2010). The rapamycin-sensitive phosphoproteome reveals that TOR controls protein kinase A toward some but not all substrates. *Mol Biol Cell* *21*, 3475-3486.
- Stade, K., Ford, C.S., Guthrie, C., and Weis, K. (1997). Exportin 1 (Crm1p) is an essential nuclear export factor. *Cell* *90*, 1041-1050.
- Stathopoulos, A.M., and Cyert, M.S. (1997). Calcineurin acts through the CRZ1/TCN1-encoded transcription factor to regulate gene expression in yeast. *Genes Dev* *11*, 3432-3444.
- Steiger, M., Carr-Schmid, A., Schwartz, D.C., Kiledjian, M., and Parker, R. (2003). Analysis of recombinant yeast decapping enzyme. *Rna* *9*, 231-238.
- Stephan, J.S., Yeh, Y.Y., Ramachandran, V., Deminoff, S.J., and Herman, P.K. (2009). The Tor and PKA signaling pathways independently target the Atg1/Atg13 protein kinase complex to control autophagy. *Proc Natl Acad Sci U S A* *106*, 17049-17054.
- Stern, M., Jensen, R., and Herskowitz, I. (1984). Five SWI genes are required for expression of the HO gene in yeast. *J Mol Biol* *178*, 853-868.
- Sturgill, T.W., Cohen, A., Diefenbacher, M., Trautwein, M., Martin, D.E., and Hall, M.N. (2008). TOR1 and TOR2 have distinct locations in live cells. *Eukaryot Cell* *7*, 1819-1830.
- Su, S.S., and Mitchell, A.P. (1993). Identification of functionally related genes that stimulate early meiotic gene expression in yeast. *Genetics* *133*, 67-77.
- Sung, M.K., and Huh, W.K. (2007). Bimolecular fluorescence complementation analysis system for in vivo detection of protein-protein interaction in *Saccharomyces cerevisiae*. *Yeast* *24*, 767-775.
- Swisher, K.D., and Parker, R. (2010). Localization to, and effects of Pbp1, Pbp4, Lsm12, Dhh1, and Pab1 on stress granules in *Saccharomyces cerevisiae*. *PLoS One* *5*, e10006.
- Talarek, N., Cameroni, E., Jaquenoud, M., Luo, X., Bontron, S., Lippman, S., Devgan, G., Snyder, M., Broach, J.R., and De Virgilio, C. (2010). Initiation of the TORC1-regulated G0 program requires Igo1/2, which license specific mRNAs to evade degradation via the 5'-3' mRNA decay pathway. *Mol Cell* *38*, 345-355.
- Tamaskovic, R., Bichsel, S.J., and Hemmings, B.A. (2003). NDR family of AGC kinases--essential regulators of the cell cycle and morphogenesis. *FEBS Lett* *546*, 73-80.

- Tanaka, K., Matsumoto, K., and Toh, E.A. (1989). IRA1, an inhibitory regulator of the RAS-cyclic AMP pathway in *Saccharomyces cerevisiae*. *Mol Cell Biol* 9, 757-768.
- Tanaka, K., Nakafuku, M., Tamanoi, F., Kaziro, Y., Matsumoto, K., and Toh-e, A. (1990). IRA2, a second gene of *Saccharomyces cerevisiae* that encodes a protein with a domain homologous to mammalian ras GTPase-activating protein. *Mol Cell Biol* 10, 4303-4313.
- Tate, J.J., Georis, I., Dubois, E., and Cooper, T.G. (2010). Distinct phosphatase requirements and GATA factor responses to nitrogen catabolite repression and rapamycin treatment in *Saccharomyces cerevisiae*. *J Biol Chem* 285, 17880-17895.
- Tate, J.J., Georis, I., Feller, A., Dubois, E., and Cooper, T.G. (2009). Rapamycin-induced Gln3 dephosphorylation is insufficient for nuclear localization: Sit4 and PP2A phosphatases are regulated and function differently. *J Biol Chem* 284, 2522-2534.
- Tharun, S., He, W., Mayes, A.E., Lennertz, P., Beggs, J.D., and Parker, R. (2000). Yeast Sm-like proteins function in mRNA decapping and decay. *Nature* 404, 515-518.
- Tharun, S., and Parker, R. (2001). Targeting an mRNA for decapping: displacement of translation factors and association of the Lsm1p-7p complex on deadenylated yeast mRNAs. *Mol Cell* 8, 1075-1083.
- Thevelein, J.M., and de Winde, J.H. (1999). Novel sensing mechanisms and targets for the cAMP-protein kinase A pathway in the yeast *Saccharomyces cerevisiae*. *Mol Microbiol* 33, 904-918.
- Timblin, B.K., and Bergman, L.W. (1997). Elevated expression of stress response genes resulting from deletion of the PHO85 gene. *Mol Microbiol* 26, 981-990.
- Toda, T., Uno, I., Ishikawa, T., Powers, S., Kataoka, T., Broek, D., Cameron, S., Broach, J., Matsumoto, K., and Wigler, M. (1985). In yeast, RAS proteins are controlling elements of adenylate cyclase. *Cell* 40, 27-36.
- Tong, A.H.Y., and Boone, C. (2007). High-Throughput Strain Construction and Systematic Synthetic Lethal Screening in *Saccharomyces cerevisiae*, Vol Yeast Gene Analysis, Second Edition. edn (Elsevier Ltd.).
- Urban, J., Soulard, A., Huber, A., Lippman, S., Mukhopadhyay, D., Deloche, O., Wanke, V., Anrather, D., Ammerer, G., Riezman, H., *et al.* (2007). Sch9 is a major target of TORC1 in *Saccharomyces cerevisiae*. *Mol Cell* 26, 663-674.
- Van Hoof, C., Martens, E., Longin, S., Jordens, J., Stevens, I., Janssens, V., and Goris, J. (2005). Specific interactions of PP2A and PP2A-like phosphatases with the yeast PTPA homologues, Ypa1 and Ypa2. *Biochem J* 386, 93-102.
- Vaseghi, S., Macherhammer, F., Zibek, S., and Reuss, M. (2001). Signal transduction dynamics of the protein kinase-A/phosphofruktokinase-2 system in *Saccharomyces cerevisiae*. *Metab Eng* 3, 163-172.
- Vigneron, S., Brioudes, E., Burgess, A., Labbe, J.C., Lorca, T., and Castro, A. (2009). Greatwall maintains mitosis through regulation of PP2A. *Embo J* 28, 2786-2793.
- Virsolvoy-Vergine, A., Leray, H., Kuroki, S., Lupo, B., Dufour, M., and Bataille, D. (1992). Endosulfine, an endogenous peptidic ligand for the sulfonyleurea receptor: purification and partial characterization from ovine brain. *Proc Natl Acad Sci U S A* 89, 6629-6633.
- Von Stetina, J.R., Tranguich, S., Dey, S.K., Lee, L.A., Cha, B., and Drummond-Barbosa, D. (2008). alpha-Endosulfine is a conserved protein required for oocyte meiotic maturation in *Drosophila*. *Development* 135, 3697-3706.
- Vuorio, O.E., Kalkkinen, N., and Londesborough, J. (1993). Cloning of two related genes encoding the 56-kDa and 123-kDa subunits of trehalose synthase from the yeast *Saccharomyces cerevisiae*. *Eur J Biochem* 216, 849-861.

- Wade, J.T., Hall, D.B., and Struhl, K. (2004). The transcription factor Ifh1 is a key regulator of yeast ribosomal protein genes. *Nature* *432*, 1054-1058.
- Walker, S.S., Shen, W.C., Reese, J.C., Apone, L.M., and Green, M.R. (1997). Yeast TAF(II)145 required for transcription of G1/S cyclin genes and regulated by the cellular growth state. *Cell* *90*, 607-614.
- Wang, W., Caldwell, M.C., Lin, S., Furneaux, H., and Gorospe, M. (2000). HuR regulates cyclin A and cyclin B1 mRNA stability during cell proliferation. *Embo J* *19*, 2340-2350.
- Wanke, V., Cameroni, E., Uotila, A., Piccolis, M., Urban, J., Loewith, R., and De Virgilio, C. (2008). Caffeine extends yeast lifespan by targeting TORC1. *Mol Microbiol* *69*, 277-285.
- Wanke, V., Pedruzzi, I., Cameroni, E., Dubouloz, F., and De Virgilio, C. (2005). Regulation of G0 entry by the Pho80-Pho85 cyclin-CDK complex. *Embo J* *24*, 4271-4278.
- Ward, M.P., Gimeno, C.J., Fink, G.R., and Garrett, S. (1995). SOK2 may regulate cyclic AMP-dependent protein kinase-stimulated growth and pseudohyphal development by repressing transcription. *Mol Cell Biol* *15*, 6854-6863.
- Wedaman, K.P., Reinke, A., Anderson, S., Yates, J., 3rd, McCaffery, J.M., and Powers, T. (2003). Tor kinases are in distinct membrane-associated protein complexes in *Saccharomyces cerevisiae*. *Mol Biol Cell* *14*, 1204-1220.
- Wei, W., Nurse, P., and Broek, D. (1993). Yeast cells can enter a quiescent state through G1, S, G2, or M phase of the cell cycle. *Cancer Res* *53*, 1867-1870.
- Wek, R.C., Cannon, J.F., Dever, T.E., and Hinnebusch, A.G. (1992). Truncated protein phosphatase GLC7 restores translational activation of GCN4 expression in yeast mutants defective for the eIF-2 alpha kinase GCN2. *Mol Cell Biol* *12*, 5700-5710.
- Wera, S., De Schrijver, E., Geyskens, I., Nwaka, S., and Thevelein, J.M. (1999). Opposite roles of trehalase activity in heat-shock recovery and heat-shock survival in *Saccharomyces cerevisiae*. *Biochem J* *343 Pt 3*, 621-626.
- Werner-Washburne, M., Braun, E., Johnston, G.C., and Singer, R.A. (1993). Stationary phase in the yeast *Saccharomyces cerevisiae*. *Microbiol Rev* *57*, 383-401.
- Werner-Washburne, M., Brown, D., and Braun, E. (1991). Bcy1, the regulatory subunit of cAMP-dependent protein kinase in yeast, is differentially modified in response to the physiological status of the cell. *J Biol Chem* *266*, 19704-19709.
- Wiedenmann, J., Ivanchenko, S., Oswald, F., Schmitt, F., Rocker, C., Salih, A., Spindler, K.D., and Nienhaus, G.U. (2004). EosFP, a fluorescent marker protein with UV-inducible green-to-red fluorescence conversion. *Proc Natl Acad Sci U S A* *101*, 15905-15910.
- Wilson, W.A., Mahrenholz, A.M., and Roach, P.J. (1999). Substrate targeting of the yeast cyclin-dependent kinase Pho85p by the cyclin Pcl10p. *Mol Cell Biol* *19*, 7020-7030.
- Wilson, W.A., Roach, P.J., Montero, M., Baroja-Fernandez, E., Munoz, F.J., Eydallin, G., Viale, A.M., and Pozueta-Romero, J. (2010). Regulation of glycogen metabolism in yeast and bacteria. *FEMS Microbiol Rev* *34*, 952-985.
- Woods, W.S., Boettcher, J.M., Zhou, D.H., Kloepper, K.D., Hartman, K.L., Lador, D.T., Qi, Z., Rienstra, C.M., and George, J.M. (2007). Conformation-specific binding of alpha-synuclein to novel protein partners detected by phage display and NMR spectroscopy. *J Biol Chem* *282*, 34555-34567.
- Yan, G., Lai, Y., and Jiang, Y. (2012). The TOR Complex 1 Is a Direct Target of Rho1 GTPase. *Mol Cell* *45*, 743-753.

- Yan, G., Shen, X., and Jiang, Y. (2006). Rapamycin activates Tap42-associated phosphatases by abrogating their association with Tor complex 1. *Embo J* 25, 3546-3555.
- Yoon, J.H., Choi, E.J., and Parker, R. (2010). Dcp2 phosphorylation by Ste20 modulates stress granule assembly and mRNA decay in *Saccharomyces cerevisiae*. *J Cell Biol* 189, 813-827.
- Yorimitsu, T., He, C., Wang, K., and Klionsky, D.J. (2009). Tap42-associated protein phosphatase type 2A negatively regulates induction of autophagy. *Autophagy* 5, 616-624.
- Yoshimoto, H., Saltsman, K., Gasch, A.P., Li, H.X., Ogawa, N., Botstein, D., Brown, P.O., and Cyert, M.S. (2002). Genome-wide analysis of gene expression regulated by the calcineurin/Crz1p signaling pathway in *Saccharomyces cerevisiae*. *J Biol Chem* 277, 31079-31088.
- Yu, J., Zhao, Y., Li, Z., Galas, S., and Goldberg, M.L. (2006). Greatwall kinase participates in the Cdc2 autoregulatory loop in *Xenopus* egg extracts. *Mol Cell* 22, 83-91.
- Zappacosta, F., Huddleston, M.J., Karcher, R.L., Gelfand, V.I., Carr, S.A., and Annan, R.S. (2002). Improved sensitivity for phosphopeptide mapping using capillary column HPLC and microionspray mass spectrometry: comparative phosphorylation site mapping from gel-derived proteins. *Anal Chem* 74, 3221-3231.
- Zaragoza, D., Ghavidel, A., Heitman, J., and Schultz, M.C. (1998). Rapamycin induces the G0 program of transcriptional repression in yeast by interfering with the TOR signaling pathway. *Mol Cell Biol* 18, 4463-4470.
- Zhao, Y., McIntosh, K.B., Rudra, D., Schawaldner, S., Shore, D., and Warner, J.R. (2006). Fine-structure analysis of ribosomal protein gene transcription. *Mol Cell Biol* 26, 4853-4862.
- Zheng, Y., and Jiang, Y. (2005). The yeast phosphotyrosyl phosphatase activator is part of the Tap42-phosphatase complexes. *Mol Biol Cell* 16, 2119-2127.
- Zoncu, R., Bar-Peled, L., Efeyan, A., Wang, S., Sancak, Y., and Sabatini, D.M. (2011). mTORC1 senses lysosomal amino acids through an inside-out mechanism that requires the vacuolar H(+)-ATPase. *Science* 334, 678-683.